FUNCTIONAL EVALUATION OF MEMBERS OF THE LIV-1 FAMILY OF PROTEINS AND THEIR ROLE IN BREAST CANCER

by

NORMAWATI MOHAMAD ZAHARI

A thesis

presented to the Cardiff University

in fulfillment of the

thesis requirement for the degree of

Doctor of Philosophy

Welsh School of Pharmacy

Cardiff, Wales, United Kingdom, 2008

ProQuest LLC
789 East Eisenhower Parkway
P.O. Box 1346
Ann Arbor, MI 48106-1346

DECLARATION

This work has not previously been accepted in substance for any degree and is not concurrently submitted in candidature for any degree.

Signed.....(candidate) Date.....

STATEMENT 1

This thesis is being submitted in partial fulfillment of the requirements for the degree of .....(insert MCh, MD, MPhil, PhD etc, as appropriate)

Signed.....(candidate) Date.....

STATEMENT 2

This thesis is the result of my own independent work/investigation, except where otherwise stated. Other sources are acknowledged by explicit references.

Signed.....(candidate) Date.....

STATEMENT 3

I hereby give consent for my thesis, if accepted, to be available for photocopying and for inter-library loan, and for the title and summary to be made available to outside organizations.

Signed.....(candidate) Date.....

Abstract

All nine members of the LZT subfamily have similarities to members of the ZIP superfamily, especially in the region associated with their ability to transport zinc intracellular. Computer analysis of the nine sequences suggests that they are all members of this subfamily, however, in phylogenetic tree some members group separately, suggesting differences in function. The LZT-Hs7, LZT-Hs8 and LZT-Hs9 were cloned into a vector suitable for expression of recombinant proteins in mammalian cells. For the first time, this demonstration showed, a plasma membrane location for LZT-Hs7 and LZT-Hs8 which similar finding to LIV-1, and an intracellular location for LZT-Hs9, similar to that observed previously for LZT-Hs1. In addition, zinc transport capability was investigated. Affymetrix U133A analysis of LZT-Hs1, LIV-1, LZT-Hs4, LZT-Hs5 and pS2 confirmed that LZT-Hs1, LIV-1 and LZT-Hs4 were regulated by estradiol. This study was extended to investigate the expression of all nine family members in breast cancer cells treated with oestradiol, anti-oestrogens and additionally in tamoxifen and faslodex resistant cells, using semi-quantitative PCR. Differential expression of these family members was seen with some members constitutively expressed whilst others either elevated or reduced in the different conditions. This analysis demonstrated that LZT-Hs1 was considerably elevated in tamoxifen resistance. In an effort to investigate a possible role for LZT-Hs1 in tamoxifen resistant cells, it was reduced by siRNA. Interestingly, in the presence of siRNA for LZT-Hs1, it was not possible to demonstrate the activation of EGFR or Src as previously observered in the tamoxifen resistant phenotype using Western blotting analysis. This is an exciting result, which suggests a role for LZT-Hs1 in driving the growth of tamoxifen resistant breast cancer cells.

Acknowledgements

Bismillah

I simply want to say that both Professor Robert I. Nicholson and Dr Kathryn M. Taylor had done a terrific job. Both of my supervisors have put forth extra effort in guiding me and I really appreciate being the **ONE** who benefits this time. Thank you for being such a great spot and helping me through many difficult times.

I have learned more from the Tenovus Centre for Cancer Research and the Welsh School of Pharmacy than from any schools or universities that I have ever had been. Denise Barrow, Lynne Farrow and Dr Claire Simons are three lovely and special people to me.Thanks guys!

If it had not been from a strong support of Professor Amru Nasrul Haq Boyce and Universiti Malaya, Malaysia, I would not have the chance to do a PhD.

Lastly, to my dear family whom never make me worry over anything at all in the world. 'Thank you Family'to Mrs Habibah Zahari, Dr Nor Aliah, Sohaimi, Ana, Fauziah, Zulkifli, Siti Rokiah, Zainah, Zainal, Amirul Arif Wong, Hamid, Zarina, Mahmud Marzuki, Roziah, my 3 dearest aunties Aunty Kalimah, Zainabon and Aunty Ngah, nieces and nephews: Fatihah, Aiman, Nabila, Nesrin, Nadia, Elya, Alif, Qistina, Amir, Amani and Aishah, and not forgetting my cousins.

Dedication

Solely for those who seek for strength to continue when confusion, inefficiency and demoralization creep-in.

Mrs (Dr) Sophie Buchaillard-Davies and I,

we turn blood into rose!

How kewl is that?

12th November 2007 to 12th November 2008

Table of Contents

List of Figures

List of Tables

Chapter 1

Introduction

1.1 Breast cancer

Breast cancer is a commonly encountered cancer in the United Kingdom (UK) and it is now the third most associated cause of cancer deaths after cancers of the lung and large bowel. The observed incidence of breast cancer in 2000 was 40,710 new cases in the UK. It is predominantly a disease associated with women, with only 1% of breast cancers occurring in men. A report by the cancer statistics division of the constitutive countries of the UK showed that a lifetime risk of women developing breast cancer is one in nine. Importantly, the survival rate for breast cancer patients has shown recent improvements, where the relative five-year survival rate for women diagnosed in England and Wales has increased to 77% during the period 1996 to 1999 compared to only 52% in 1971 to 1975. This has lead to an obvious reduction in mortality caused by breast cancer in the UK with for example breast cancer deaths falling from 15,625 in 1989 to 12,838 in 2002. It is thought that breast cancer mortality has declined because of several reasons, including the successful initiation of te breast screening program, the increased specialisation of care for patients and finally, the wide spread adoption of tamoxifen as an adjuvant therapy in the treatment of primary breast cancer and the above information was obtained from the CancerStats Monograph 2004 publication.

1.2 Oestrogens and breast cancer

Although a relative contribution of multiple risk factors to the development of breast cancer may explain its high incidence and our failure to fully eradicate the disease, reproductive history and hormone exposure are believed to play a pivotal role in the origins and growth of the disease (Booth et al. 1989; Gwinn et al. 1990; Jordan et al. 2003). One of the most pertinent observations relevant to the treatment and understanding of breast cancer aetiology was the demonstration by Beatson in 1895 that ovariectomy performed on premenopausal patients with advanced breast cancer was able to cause a significant regression of their disease (Love and Philips 2002). This empirical observation has laid the foundation for the discovery of ovarian oestrogens as an important driving force for the growth of premenopausal breast cancer (Aebi et al. 2000; Kristensen and Børresen-Dale 2000; Miller et al. 1985), and also, the realisation that following the menopause oestrogens could be derived from non-ovarian sources, most notably adrenal androgens by peripheral aromatization (Burger 1996; Hutton et al. 1979; Lucisano et al. 1984; Nyholm et al. 1993). Importantly, since it was later discovered that some breast tumours possess the aromatase enzyme, it is now thought that a proportion of breast cancers assume a degree of autonomous growth control (Dowsett et al. 1996a; Macaulay et al. 1994; Reed and Purohit 1996; Sasano and Ozaki 1997).

1.2.1 Mechanism of action of oestrogens

Evidençe accumulated over several decades has provided a significant level of understanding of the cellular actions of steroid hormones in their target tissues (Liao 1975; McDonnell et al. 1993; Sluyser and Kassenaar 1975). Early experiments using radio-labelled oestrogens showed that while these lipophic molecules penetrated all cells, they were retained only in classical oestrogen responsive tissues (Larionov et al. 2002; Marsigliante et al. 1992). This capacity to retain oestrogens was subsequently shown to be due to the presence of receptor proteins in target tissues, termed oestrogen receptors (Braunsberg 1977; McClelland et al. 1998; Poortman et al. 1983). Such receptors were initially found in the rat uterus (Bergink 1980; Leake 1997; Sutherland et al. 1980) and vagina (Miller and Sharpe 1998; Prat et al. 2007) and some experimental and clinical breast cancers (Michalides et al. 1996; Patterson et al. 1982).

Using the titration method (Girdler et al. 2001; Wilson et al. 1984), and a sub-cellular fractionation technique (Marsigliante et al. 1995; Smith and Schwartz 1979; Wilkinson et al. 1983), experiments showed that the oestrogen receptor proteins were cytoplasmic and nuclear in origin and that they bound oestrogens with high affinity (Attardi et al. 1980; Lazier and Haggarty 1979; Smith and Schwartz 1979). Upon oestrogen binding to the receptor protein, the resulting steroid-receptor complex undergoes a conformational change and dimerises with another oestrogen receptor subunit. As a result of this activation, the oestrogen receptor binds to chromosomal DNA at oestrogen response elements (EREs) in the

promoter regions of oestrogen responsive genes (Parker 1990; Sabbah et al. 1996). Such promoters are normally localised upstream of the translated regions of oestrogen responsive genes.

To stimulate DNA transcription, a transcription unit is formed which is composed of coactivator (CoA) molecules and oestrogen receptor complexes, which subsequently engage with the transcription apparatus (e.g. RNA polymerases). Separately, corepressor (CoR) molecules, which normally prevent transcription are loss from the ERE sites (Hagen et al. 2004; Shibata et al. 1997). It is a combination of these events which allows nuclear RNAs derived from oestrogen responsive genes to be specifically transcribed (Westley and May 1988). Ultimately, the nuclear RNA is processed to produce messenger RNA (mRNA) species which are transported to the cytoplasm for subsequent translation by ribosomes into new protein products (Keir 1980; Knecht and Luck 1977).

The oestrogen receptor possesses two transcriptional activator functions, AF-1, which is present in the A/B domain of the receptor and is regulated in a ligand independent manner through growth factor promoted phosphorylation (Kato et al. 2000), and AF-2, which is present in the E domain of the receptor and is ligand dependent (Flőtotto et al. 2001). Frequently, in order that the receptor is maximally active, both AF-1 and AF-2 are required to be synergistically involved (Parker 1998).

The diagram below is showing a representation of estrogen receptor (ER) and the structural domains of ER (A-F) with their amino acid numbers below the figure corresponding to the domain boundaries. Under the structural figure indicates the functional domain of the estrogen receptor and the far left describes the functions.

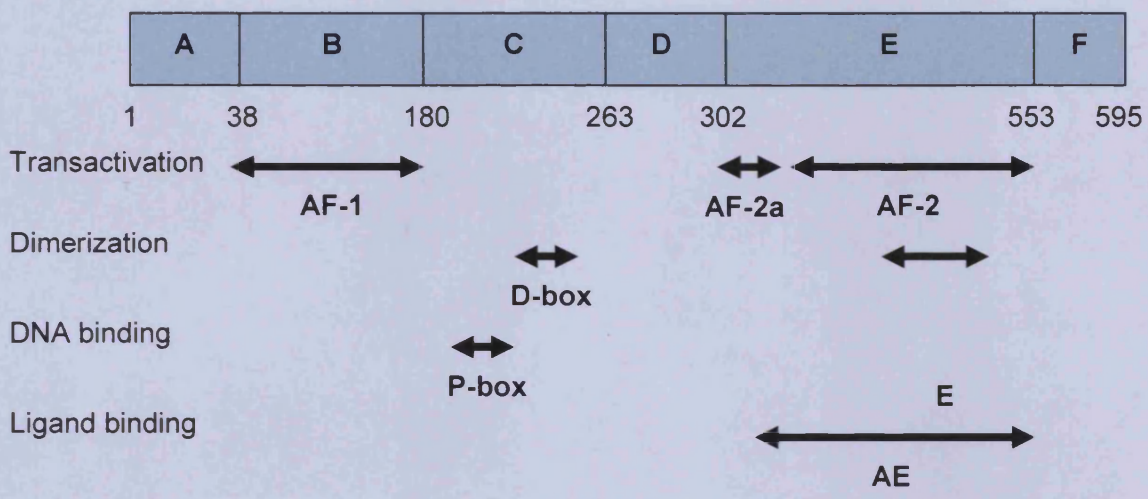

Adapt from Anne M. Bowcock, et al. 1999. *The Breast Cancer, Molecular Genetics, Pathogenesis, and Therapeutics*. Humana Press, Totowa, New Jersey.

Genetically, there are two subtypes of oestrogen receptors, α and β, which are able to form homo- and heterodimers in cells (Marsigliante et al. 1996; Schwabe et al. 1993). It is believed that the α α and β β subtypes, and the α β subtype, are able to promote different responses within target cells, although it is believed that the a subtype predominates in the classical oestrogen target tissues such as the breast (Chappell et al. 2000; Keeling et al. 2000; Scobie et al. 2002). Interestingly, various oestrogenic molecules bind to the ER subtypes with different affinities (Katzenellenbogen et al. 2000). Thus while 17β oestradiol, the most potent oestrogen produced in women, binds to both α and β receptors with high affinity, oestrone, a

less potent oestrogen, binds predominantly to the α subtype, while oestriol, a weak oestrogen, binds primarily to the β subtype (Benassayag et al. 1999; Koga et al. 1990; Kuiper et al. 1997; Platet et al. 2004).

The diagram below shows the mechanism of action of the estrogen where the estrogen receptor (ER) bound to the estrogen (E) and then act to bind to an estrogen responsive element (ERE). Subsequently, the transcription is activated by direct interaction with the components such as the RNA polymerase II transcription complex, and basal transcription factors (RNA Pol II/ Basal Txn Factors), sequence specific transcription factors (Txn Factors), and/or additional co-activator protein (CoA).

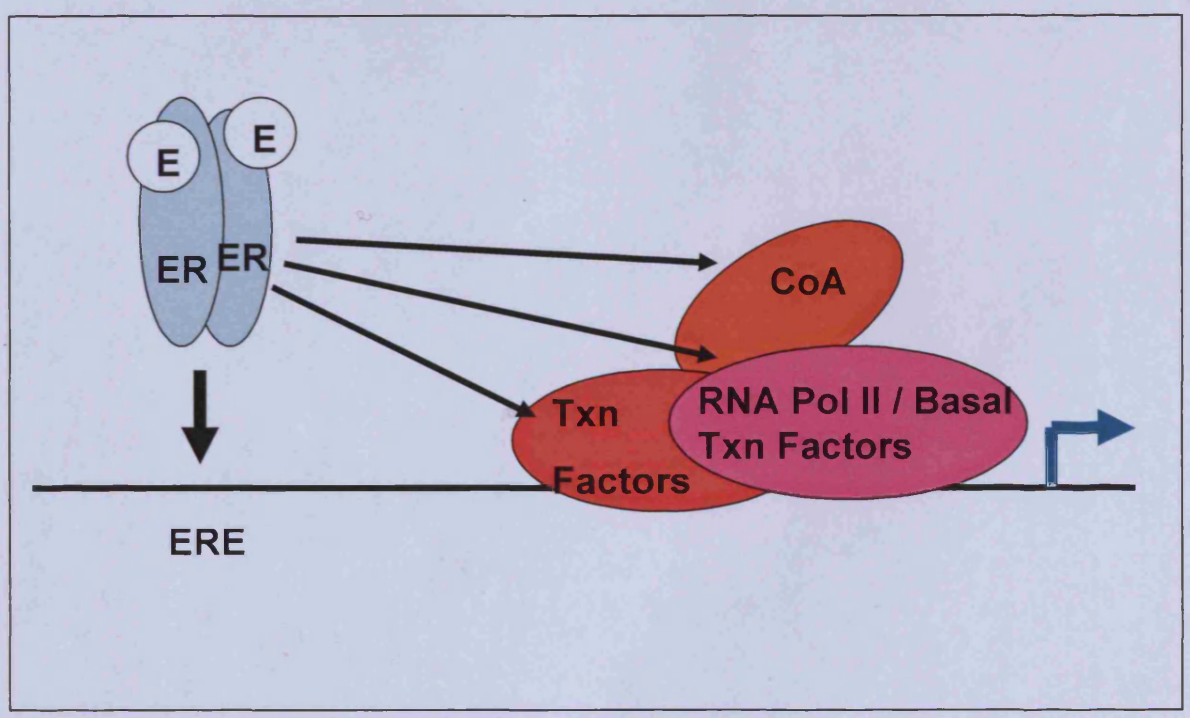

Adapt from Anne M. Bowcock, et al. 1999. *The Breast Cancer, Molecular Genetics, Pathogenesis, and Therapeutics*. Humana Press, Totowa, New Jersey.

In addition to the direct actions of oestrogen receptors on EREs, they have also been shown to modulate the transcription of genes that do not contain an ERE. This is facilitated by direct protein interactions between the oestrogen receptor and other nuclear transcription factors (Beato and Klug 2000; Koohi et al. 2005; Salmi et al. 1998; Song et al. 1998). These include Activator Protein-1 (AP-1) (Cerillo et al. 1998; Gee et al. 2000; Kushner et al. 2000) and Sp-1 (Marino et al. 2006; Tanaka et al. 2000).

1.2.2 Membrane actions of the oestrogen receptor

In addition to the nuclear actions of oestrogens, it has recently been demonstrated that some oestrogen receptors may also be present in the cell membrane, and interact with caveolin-1 (Kiss et al. 2006; Spies et al. 2006), additionally, G coupled proteins (Boonyaratanakornkit and Edwards 2004; Hart et al. 2005), several tyrosine kinase receptors, including the epidermal growth factor receptor (EGFR) (Godden et al. 1992; Sainsbury et al. 1985), and Insulin-like growth factor receptor-1 (IGF-1R) (Happerfield et al. 1997; Nardon et al. 2003), and a non-receptor tyrosine kinase, c-src (Hart et al. 2005; Kiss et al. 2006).

Through the G coupled proteins and tyrosine kinases, oestrogens are able to directly activate signals to the nucleus via phosphorylation cascades involving mitogen activated protein kinase (MAPK) (Luttrell et al. 1996) and phosphoinositide 3-kinase (PI 3K/AKT) (Müller and Frick 1999). Since signalling through these molecules is able to target and activate nuclear transcription factors, including ER and AP-1 (Gee et al. 2000; Rochefort 1995), the activation of membrane ER by oestrogens represents another way of effecting gene transcription (Sormunen et al. 1999).

1.2.3 Oestrogen receptors and breast cancer

Multiple studies have shown that oestrogen receptors (ERα) are expressed in approximately 70 to 80% of breast cancers (Girdler et al. 2001). Their presence has been linked to several good prognostic features (Leygue et al. 1999), including low histological grade (Chappell et al. 2000; Umekita et al. 1992), low mitotic activity, tubular diffentiation (Knowlden et al. 2000), and response to endocrine measures which will be discussed further in the thesis finding.

It is now standard practice to measure ERα in all primary breast cancers in the UK, where they are used to select patients for adjuvant endocrine therapy (Friedlander and Thewes 2003; Howell et al. 1998; Jarzabek et al. 2005). According to a number of meta-analyses, oestrogen receptor positivity predicts for a disease free and survival benefit to anti-hormone therapy (principally, tamoxifen, see below), with patients with oestrogen receptor positive disease receiving tamoxifen enjoying a 25% 10-year survival advantage over those who do not receive the drug (Krulik 1994; Y. Nio 1999). In advanced disease, oestrogen receptor measurements, similarly predict for endocrine responsive disease, although it is evident that about 40% of oestrogen receptor positive tumours now fail endocrine treatments (Dowsett 1996; Nicholson et al. 1989). Significantly, in advanced disease it is also clear that therapeutic benefit to endocrine measures is of a finite duration, with median response times being measured in months rather than years (Andersen 1992; Dowsett et al. 1996a; McGuire et al. 1975). Clearly, the majority of breast cancer are ultimately able to escape the beneficial

actions of anti-hormonal therapy and gain a de novo or acquired resistant phenotype (Dowsett et al. 1996b; Iino et al. 1997).

ERβ has also been measured in breast cancer specimens (Jirstrőm et al. 2005; Knowlden et al. 2000). Although there is much debate as to their clinical significance (Piquer et al. 1991), in one study their expression in ERα positive disease has been linked to endocrine response (Murphy and Watson 2006; Skliris et al. 2006).

1.3 Endocrine therapies

In light of the importance of oestrogens in breast cancer growth, several classes of drugs have been synthesised that are in clinical practice or development. These include antioestrogens (e.g. tamoxifen and fulvestrant) (Elkak and Mokbel 2001; Howell et al. 1996), aromatase inhibitors (Harris et al. 1983; Macaskill and Dixon 2007)and LH-RH agonists (Schally et al. 1984; Tan and Wolff 2007; Zidan et al. 2002).

1.3.1 Tamoxifen, a Selective Estrogen Receptor Modulator (SERM)

The antioestrogenic drug tamoxifen is the most commonly used anti-cancer agent in breast cancer (Legha and Blumenschein 1982; Pritchard and Sutherland 1989). It was first developed in the mid 1960's and entered clinical trials in the early 1970's. Like previous ablative and additive endocrine measures, tamoxifen promotes tumour remissions in approximately one-third of unselected women with advanced disease and in about 60% of patients with oestrogen receptor (α) positive tumours (Davis and Carbone 1978; Kimmick and Muss 1995; Pritchard and Sutherland 1989). Because of its relatively low incidence of

side effects, tamoxifen usage was quickly extended to earlier stages of breast cancer where it has been shown to extend 10 year survival rates of primary breast cancer patients by approximately 25% (Espie 1998).

Significantly, the mode of action of tamoxifen involves its binding to oestrogen receptors where it produces a complex that can possess both oestrogen agonistic and antagonistic activity (Favoni and De Cupis 1998; Rochefort and Borgna 1981). The diagram below shows the model for the mechanism of action of anti-estrogens where the non-steroidal anti-estrogen Tamoxifen binds to estrogen receptor (ER) results in an altered conformation which subsequently interferes with the ER's interaction with the transcription factors.

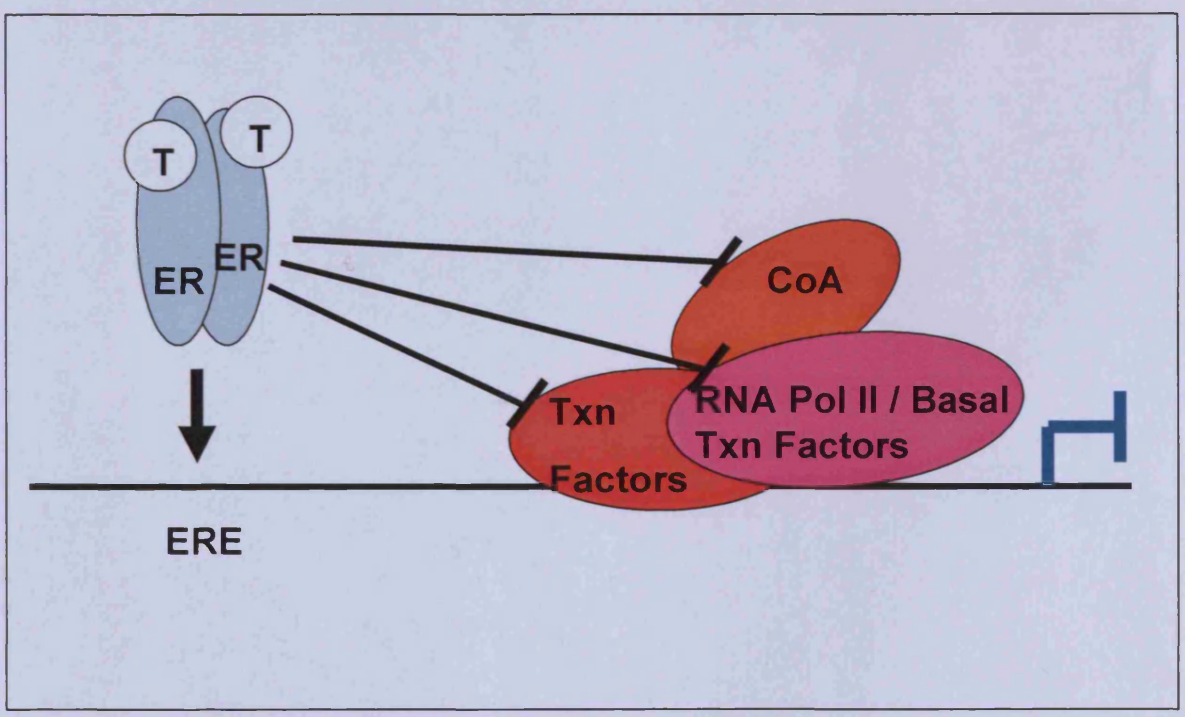

Adapt from Anne M. Bowcock, et al. 1999. *The Breast Cancer, Molecular Genetics, Pathogenesis, and Therapeutics*. Humana Press, Totowa, New Jersey.

It is thought that in breast cancer cells, its antagonistic activity prevails and thus oestrogen responsive events are reduced leading to an inhibition of tumour growth (Howell 2006). This may however, be a time dependent event since tamoxifen has been shown to induce an initial tumour flare that precedes the growth inhibition. In molecular terms, while tamoxifen is believed to be a full antagonist of the AF-2 activity of the oestrogen receptor, it often possesses some AF-1 activity (Mahfoudi et al. 1995). It is thought that its ability to maintain AF-1 responses associates with its agonistic properties (McInerney and Katzenellenbogen 1996).

Although the majority of effects promoted by tamoxifen are clearly beneficial to the patient, tumour model systems suggest that it is a poor inducer of apoptosis (cell death) and surviving tumour cells invariably develop resistance (Johnston 1997). This phenomenon is also seen in the clinic with tumour remissions in patients with advanced disease on average only lasting 6 to 18 months before disease progression is evident (Michlmayr et al. 1981). Increases in tumour EGFR activity have been reported in some tumour models as a mechanism to promote tamoxifen resistant growth and in MCF-7 human breast cancer cells (the model system used in the present thesis), it has been shown that membrane associated EGFR is raised as much as 40-fold on the acquisition of tamoxifen resistance (Knowlden et al. 2003; Miller 1987; Nicholson et al. 1994). In such cells, there is also evidence for the up-regulation of HER2, an EGFR family member, increased heterodimerisation of EGFR and HER2 and increased activity of several of their downstream signal transduction pathways, including MAPK and PI3K/AKT (Hutcheson et al. 2003; Leary and Dowsett 2006).

Indeed, in such resistant cells it has been suggested that some of the EGFR/HER2 induced kinases are able to phosphorylate and activate oestrogen receptors, adding to their AF-1 activity (Britton et al. 2006). Significantly, in human breast cancers increased EGFR and HER2 have been linked to poor patient outlook (Eccles 2001) and failure to respond to various endocrine measures, including tamoxifen (Knoop et al. 2001). Interestingly, increased AP-1 activity has also been linked to tamoxifen resistance and increased growth factor signaling, where the oestrogen receptor may bind directly to AP-1 to promote transcription of genes involved in growth regulation (Cui et al. 2006).

1.3.2 Faslodex, a Selective Estrogen Receptor Down-regulator (SERD)

The anti-oestrogenic drug faslodex is termed a pure anti-oestrogen in that it possesses no obvious oestrogenic activity (Addo et al. 2002; Hermenegildo and Cano 2000; Horne et al. 1988; Howell 2006; Sainsbury et al. 1987). In model systems this property produces a more complete inhibition of tumour growth than is achieved with tamoxifen (Dowsett et al. 2005; Long et al. 1998). Clinically, faslodex has been shown to produce tumour remissions in advanced breast cancer patients with a response rate that is slightly superior to tamoxifen (Howell et al. 2004; McKeage et al. 2004). Despite its favourable clinical profile, faslodex is at present most commonly used as a second or third line endocrine therapy after tamoxifen or aromatase inhibitors (Mauriac et al. 2003).

In molecular terms, although faslodex, like tamoxifen, binds to the oestrogen receptor, it is biologically inert and destabilises the oestrogen receptor protein leading to rapid ER degradation (Osborne et al. 2004).

The diagram below shows the mechanisms of action of anti-estrogens where the steroidal anti-estrogens Faslodex may act by increasing the turnover rate of estrogen receptor (ER) or by decreasing the stability of the estrogen receptor (ER). They may also interfere with DNA binding or interactions of the estrogen receptor (ER) with components of the RNA PolII/ Basal Txn Factor complex.

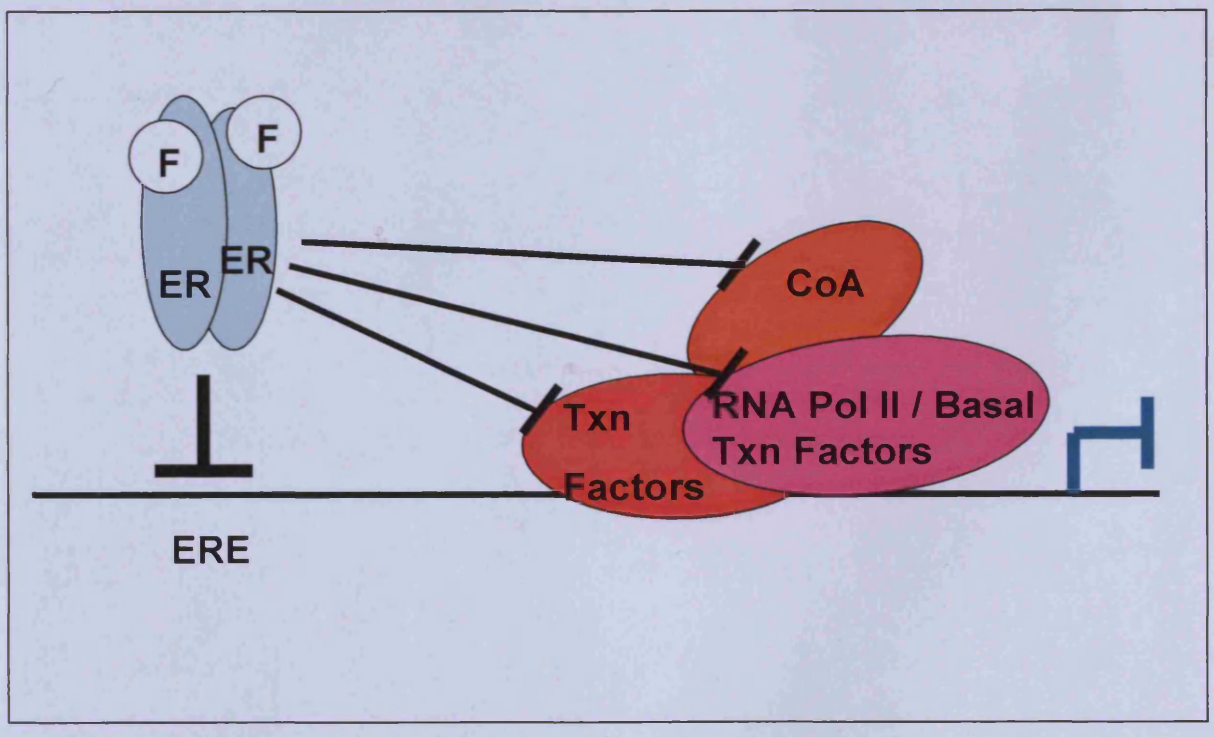

Adapt from Anne M. Bowcock, et al. 1999. *The Breast Cancer, Molecular Genetics, Pathogenesis, and Therapeutics*. Humana Press, Totowa, New Jersey.

Indeed, within hours of exposing breast cancer cells to faslodex in vitro oestrogen receptor levels dramatically fall. Such activity has also been recorded in clinical breast cancer specimens removed 3 weeks after the initiation of faslodex treatment (Robertson et al. 2007). Despite this interesting property, resistance develops in all advanced breast cancer patients treated with the drug and is present de novo in approximately 50% of women (Dowsett et al. 2005). In experimental models of faslodex resistance, increased EGFR has once again been linked to the development of this state, although less is known about the downstream consequences of altered EGFR signaling (McClelland et al. 2001).

1.3.3 Oestrogen deprivation using aromatase inhibitors

Alternative strategies to directly targeting breast cancer oestrogen receptors with anti-oestrogenic drugs in post-menopausal women primarily involve the use of aromatase inhibitors (Combs 1995; Harris et al. 1983). These inhibitors prevent the aromatisation of androgens to oestrogens and may be divided into two types based on their mechanism of action. Steroidal aromatase inhibitors bind to the substrate pocket of the aromatase enzyme causing an irreversible inhibition, while non-steroidal inhibitors competitively and reversibly inhibit the P450 domain of the aromatase protein (Bossche et al. 1994).

The current, so called, third generation of aromatase inhibitors (among are exemestane, anastrozole and letrozole) show a high degree of selectivity for the aromatase enzyme and inhibit whole body aromatisation by 97 to 99% (Dowsett 1998). They have been shown to be effective in both advanced (Santen et al. 1982) and primary (Evans 1994) breast cancer and the latter instance to be superior to tamoxifen. Despite this, however, they are not spared the

phenomenon of de novo and acquired resistance, where model systems suggest that tumour cells, in some instances, may become hyper-sensitive to very low levels of oestrogens (Chen et al. 2006). Although the precise mechanisms involved in resistance to oestrogen deprivation are still under investigation, several studies have once again suggested a role for increased growth factor signalling involving both membrane (Miller et al. 2005) and nuclear (Shin et al. 2006) oestrogen receptors.

1.4 Endocrine resistance and tumour progression

In general terms, two characteristics of tumour cells dictate long-term patient prognosis, their growth rate and their invasiveness, where rapid growth and high invasive potential are invariably associated with poor outlook (Nicholson et al. 1993; Parr et al. 2004). Significantly, recent studies from the Tenovus Centre for Cancer Research laboratories have suggested that the development of acquired resistance to tamoxifen, faslodex and the EGFR inhibitor gefitinib is associated with these characteristics (Hiscox et al. 2004) and has accelerated research to identify the signalling molecules involved.

Several pathways have to date been linked to the increased invasiveness of anti-hormone resistant cells, including increased levels and activity of c-src, a non-receptor tyrosine kinase able to effect cell:cell and cell:matrix interactions (Knowlden et al. 2005) and c-met, a receptor tyrosine kinase, previously strongly implicated in tumour metastasis (Sonobe et al. 1998). Interestingly, a recent link between breast cancer cell's growth and invasion and the activation of such tyrosine kinases has been forged by the observations that firstly. zinc can activate several tyrosine kinases, including the EGFR (Samet et al. 2003), IGF-1R

(Knowlden et al. 2005) and c-Src (Wu et al. 2002). Secondly, zinc levels are increased in some anti-hormone resistant cells and finally, the cellular levels of zinc are regulated, in part, by the LIV1 family of zinc transporters, where LIV1 levels in clinical breast cancer specimens has been associated to tumour cell spread to the regional lymph nodes (Manning et al. 1994).

1.5 LIV-1 and LZT subfamily of zinc transporters

Zinc transporter families

Zinc is an essential ion in cells, without it, cells die. Zinc is a co-factor for more than 300 enzymes and is involved in protein, nucleic acid, carbohydrate and lipid metabolism, as well a in the control of gene transcription (Wu et al. 1977), differentiation (Krishna Murthy et al. 1973), development and growth (Nakamura 1965). Zinc deficiency can be detrimental, causing stunted growth (Bierich et al. 1982) and serious metabolic disorders (Pfeiffer et al. 1974), while excess zinc can be toxic to cells (Suh et al. 2000). It is therefore important that levels of zinc within cells be constantly controlled. In stress cells, zinc does not pass through cellular membranes and relies on two families of zinc transporters for its transport.

The ZnT family, which is previously termed CDF for cation diffusion facilitators, of zinc transporters (Paulsen and Saier Jr 1997), transport zinc out of cells or into intracellular compartments from the cytoplasm (now termed SLC30A). Whereas the ZIP family (for Zrt-, Irt-like Proteins, SLC39A) of zinc transporters (Eide 2004), transport zinc into the cell cytoplasm from either outside the cell or from intracellular compartments. The ZnT family

contains 9 human sequences and the ZIP family contains 14 human sequences (Liuzzi and Cousins 2004).

The ZIP family of zinc transporters is reported to have approximately 86 members, which can be further divided into four separate subfamilies. The first subfamily is the fungal and plant sequences (subfamily I), second is the mammalian, nematode and insect genes (subfamily II), thirdly, the gufA gene of Myxococcus xanthus with unknown function (gufA subfamily) and finally, the LIV-1 subfamily related to the oestrogen-regulated gene, LIV-1 (Taylor and Nicholson 2003). The role of each of these subgroups is suggested to be transport of metal ions especially zinc across cellular membranes and into the cytoplasm (Gaither and Eide 2001; Guerinot 2000).

The LZT subfamily members and the ZIP superfamily have eight conserved transmembrane domains. The LZT subfamily has a long and variable extracellular N-terminus region whilst the C-terminus is very short, as also found in the ZIP superfamily. Additionally, there are special motifs such as the HEXPHE motif found in transmembrane domain V and an HNF motif in transmembrane domain IV. This motif is placed within the pore formed in the transmembrane domains that it is able to form a metal binding site for the ZIP transporters. Furthermore the sequences contain histidine-rich repeat motifs throughout the LZT subfamily sequences, on the N-terminus and extracellular loop between transmembrane domains II and III, which are also suggested to enable zinc transport. Another region between

transmembrane III and IV is an area with mixed charge and a number of polarity residues which may also play a role in zinc transport (Taylor and Nicholson 2003).

The 14 human members of the SLC39A family fall into four groups: subfamily I (ZIP 9), subfamily II (ZIP 1, 2 and 3), gufA subfamily (ZIP 11) and the LZT subfamily (LZT-Hs1 to LZT-Hs9). The LZT subfamily represents the LIV-1 family of Zinc Transporters as LIV-1 was the first member to be discovered (Manning et al. 1994) and for the 9 members of the LZT subfamily, in this thesis they will be referred as 'LZT-Hs( )', where the bracket contains the number assigned to each of the LZT members and Hs refers to homo sapiens. However, in this thesis, the original LIV-1 gene nomenclature remains.

Some of the family members have been studied and do have a role in progressing diseases and additionally, LIV-1 gene that has been linked to oestrogen regulation and breast cancer metastasis (Manning et al. 1994). A defect in the LZT-Hs5 gene produces the zinc deficiency disease, acrodermatitis enteropathica caused by a defective uptake of zinc in the intestine (Nakano et al. 2003). One member of the LZT subfamily called the LZT-Hs6 or BigM103 has been suggested to inhibit cancer cell growth and is induced by Bcg and retinoic acid (Begum et al. 2002) and LZT-Hs4 increases intracellular zinc and it is regulated by IL-6 (Liuzzi et al. 2005). It is known that HKE4 increases intracellular zinc whilst present in endoplasmic reticulum (Taylor et al. 2004) or the Golgi body (Huang et al. 2005). The functional significance of the various members of the LZT family of zinc transporters is so far largely undetermined. Although data is slowly emerging on the role of the individual

family members in individual tissues, the expression of all 9 members of the LZT family has not been attempted yet in any tissues. Furthermore, the functional significance of individual members in a disease state such as breast cancer has not been examined.

The hypothesis of this study is to observe whether any members of the LZT subfamily besides LIV-1 show significant level of expression in breast cancer disease.

Thesis aims:

1. To compare and examine the structures of the LIV1 family members whether they have similarities/dissimilarities, and finally observe their potential functional motifs.
2. To clone the LZT-Hs7, LZT-Hs8 and LZT-Hs9 genes subsequently, investigate their protein sub-cellular distribution, and capacity to transport zinc.
3. To assess the oestrogen/anti-oestrogen regulation of the nine LIV1 family members in MCF-7 human breast cancer cells and make comparison this to a computer prediction of the presence of EREs within the oestrogen receptor α promoter.
4. To determine the expression of the nine LIV1 family members in endocrine responsive and resistant MCF-7 breast cancer cells to assess their likely contribution to the increased tumour cell growth and invasiveness seen in resistant cells.
5. To reduce the expression of a LIV1 family member using siRNA technology, subsequently assess its impact on EGFR signalling because it is a major effecter of endocrine resistance.

Chapter 2
Materials and Methods

2.1 Materials

2.1.1 Plasticware

The plasticware used in this study were: 50ml Falcon tubes were purchased from Becton Dickinson Ltd, Cowley, Oxfordshire, UK; 10cm bacteria plates were obtained from Fisher Scientific UK Ltd, Loughborough, Leicestershire, UK; 250ml polypropylene centrifuge bottles used in the large scale preparation of DNA were bought from Kendro Laboratory Products Ltd, Bishops Stortford, Herfordshire, UK; microcentrifuge tubes were supplied from Elkay Laboratory Products (UK) Ltd, Basingstoke, Hampshire UK; Disposable pipette tips were bought from Greiner Labortechnik Ltd, Stonehouse, Gloucestershire, UK. The plasticware used were T25 and T75 tissue culture flasks, 35mm, 60mm and 150mm tissue culture dishes, 12- and 24- well tissue culture plates and Cryovials manufactured by Nunc, Roskilde, Denmark and supplied by Fisher Scientific UK Ltd, Loughborough, Leicestershire, UK. The filtered 12.5 cm tissue culture flasks were manufactured by Falson Plastics obtained from BD Biosciences Clontech UK, Cowley, Oxford, UK.

2.1.2 Enzymes and inhibitors

The molecular biology enzymes which were used in the PCR and RT-PCR study were: RNAsin™ RNase Inhibitor were purchased from Promega UK, Southampton, UK; MMLV Reverse Transcriptase and Vent® Proofreading Taq polymerase enzymes were purchased

from Invitrogen, Paisley, UK; Biotaq™ DNA polymerase enzyme is bought from Bioline Ltd, London, UK.

2.1.3 Chemical, media and buffers

All molecular biology grade chemicals and media was purchased from Sigma-Aldrich Company Ltd, Poole, Dorset, UK; general laboratory grade chemicals and solvents were obtained from Fisher Scientific UK Ltd, Loughborough.

2.1.4 Molecular weight markers

DNA molecular weight markers used to estimate size of the nucleic, namely the 1kb DNA ladder was bought from Promega UK, Southampton, UK; the HyperLadderIV was supplied from Bioline Ltd, Humber Road, London, UK., as listed in Appendix C.

2.1.5 Antibiotic

The antibiotic ampicillin was purchased from Sigma-Aldrich Company Ltd, Poole, Dorset, UK. To prepare the ampicillin stock solution of 1000X concentration, 100mg of ampicillin was diluted in 1ml of sterile nuclease free water and then sterilized by filtration through a 0.2μM filter which was purchased from Millipore Inc., Harrow Middlesex, UK and aliquots were stored in -20^0C.

2.1.6 Oligonucleotides

Primers for all PCR procedures were synthesized by MWG-Biotech AG, Anzinger Str. 7, D-85560 Ebersberg, and Germany.

2.1.7 Equipment

The UV transilluminator, namely Fotodyne Inc. 3-3002 UV transilluminator used to visualize all ethidium bromide stained gels was bought from Flowgen Instruments Ltd, Maidstone, Kent, UK. The UV spectrophotometer, namely the Cecil CE2041 2000 series UV spec, used to determine the concentrations of both nucleic acid and proteins in solution, was purchased from Cecil Instruments Ltd, Cambridge, UK. Gel electrophoresis equipment was purchased from Invitrogen, Paisley, UK. The power supply was using the Bio-Rad Power Pac p1000 which was purchased from Bio-Rad Laboratories Ltd, Hemel Hempstead, Hertfordshire, UK. Two systems used to photograph the EtBr gels, namely the Polaroid® Hand Held DS-34 Camera and secondly, AlphaDigiDoc Imaging System with Olympus C-5060 Wide zoom camera. The former system was purchased from the Polaroid® Corporation, Cambridge UK, and the Hypercassettes™ used autoradiography was bought from Amersham Biosciences UK Ltd, Little Chalfont, Buckinghamshire, UK. The latter system was purchased from Alpha Innotech Corporation, San Leandro, California, attached with a Canon-Pixma iP400 printer. The micro centrifugation steps were carried out using refrigerated microcentrifuge, namely IEC Micromax RF 3593, which was purchased from Thermo Life Sciences, Basingstoke, Hampshire, UK. The Sorval RS6000 centrifuge model RC5B with the SLA600TC and SLA1500 rotors were bought from Kendro Laboratory Products Ltd, Bishops Stortford, Hertfordshire, UK. The Beckman TL-100 and L-80 ultracentrifuges were bought from Beckman Coulter UK Ltd, High Wycombe, Buckinghamshire, UK.

2.1.8 Computer searches

The computer software packages were used to access information of the LZT subfamily members to determine their similarities and dissimilarities of their sequences/genes and secondary structure proteins and to investigate their potential functional motifs. The computer software packages were used to verify the positive LZT-Hs7, LZT-Hs8 and LZT-Hs9 recombinants (Table 2-1).

2.1.9 Protein biochemistry

For the purpose of SDS PAGE procedure, the resolving and stacking gel buffers were purchased from Bio-Rad Laboratories Ltd, Hemel Hempstead, Hertfordshire, UK. Other chemicals used were 40% acrylamide/bis-acrylamide solution, Trizma® base, glycine, KCl, HEPES, sodium azide, Tween 20, TEMED, DTT the reducing agent and finally, for the protease inhibitors were leupeptin, bacitracin, PMSF, pepstatin A and aprotinin; all were purchased from Sigma-Aldrich Company Ltd, Poole, Dorset, UK. As for the general laboratory reagents used including glycerol, formaldehyde, NaCl, NaH_2PO4 and Na_2HPO4 all were bought from Fisher Scientific Ltd, Loughborough, Leicestershire, UK. The recipes for the buffers are in Appendix B.

For the blotting materials, nitrocellulose transfer membranes with pore size of 0.45μm were purchased from Sigma-Aldrich Company Ltd, Poole, Dorset, UK. The Whatman No3 filter paper was obtained from Whatman International Ltd, Maidstone, Kent, UK.

The chemiluminescent substrates used for the detection of immunostained Western blotted membranes (Supersignal® West Dura Extended Duration Chemiluminescent Substrate, the Supersignal® West Femto Maximum Sensitivity Substrate and the Supersignal® West Pico Substrate) were bought from Pierce and Warriner Ltd., Cheshire, UK. The Alexa Fluor 488-conjugated antimouse and Alexa Fluor 594-conjugated antirabbit antibodies and Texas Red Phalloidin were bought from Molecular Probes, Europe BV, Leiden, The Netherlands. The Rainbow™ coloured protein molecular weight marker for protein size estimation on SDA-PAGE gels was purchased from Amersham Biosciences UK Ltd, Little Chalfont, Buckinghamshire, UK. For the purpose of SDS-PAGE and Western Blotting procedures, the Bio-Rad Mini-Trans Blot™ and Power Pac 300 were purchased from Bio-Rad Laboratories Ltd, Hemel Hempstead, Hertfordshire, UK; while the Leica RPE automatic microscope used for fluorescence microscopy was purchased from Leica Microsystems Ltd, Milton Keynes, UK.

2.2 Cloning

2.2.1 Vector choice

To facilitate the cloning of LZT-Hs7, LZT-Hs8 and LZT-Hs9 the plasmid vector, pcDNA5/FRT/V5-His-TOPO® TA (Invitrogen) was used throughout. This vector has a CMV promoter upstream of multiple cloning sites, which enable its expression in mammalian cells. The downstream region includes a V5 epitope that enables its detection. The vector also contains an ampicillin resistance gene for positive recombinant selection.

2.2.2 TA cloning

To facilitate the cloning the plasmid vector, pcDNA5/FRT/V5-His-TOPO® TA, possess a single 3' thymidine (T) overhangs for the TA Cloning technique and by adding 3' adenines (A) overhangs are used to clone the blunt-ended fragments of PCR products. Cloning by DNA amplification by Vent® Proofreading Taq polymerase produces blunt-ended products following the 3' to 5' exonuclease activity.

Additionally, the vector has Topoismerase covalently bound to the vector. This bond between the vector and the Topoisomerase enzyme is the phosphor-tyrosyl (Try-274) bond subsequently attacked by the 5' hydroxyl of the PCR product hence releasing the enzyme and efficiently cloning the PCR products.

2.2.3 Design of oligonucleotides

For genes of interest, the forward primers were designed to include the Kozak translation initiation sequence (G/A) NN ATG, which allow a proper initiation of translation, followed by the ATG start codon. The reverse primer of LZT-Hs9 comprised a region that matched the 3' side of the specified target regions of the genes of interest followed by the V5 epitope sequence and ending with a stop codon, TAA. The V5 epitope enables the detection of the recombinant protein by the anti-V5 antibody (Table 2-2).

2.2.4 Amplification conditions for cloning

The 25µl of PCR mixture consisted of 0.5µl of the DNA template i.e 0.5µl of LZT-Hs7, LZT-Hs8 and LZT-Hs9 plasmids, 24µl of the PCR master mix which contains of 0.25mM of

dNTP's, 0.5μM of 3' and 5' primers, 0.1 Weiss units/μl of Vent® Proofreading Taq polymerase, 1X PCR buffer (10mM Tris-HCl pH 8.3, 50mM KCl, 1.5mM $MgCl_2$, 0.001 w/v gelatine) and 0.5μl nuclease free water. In the thermal cycler, to separate the double stranded DNA, the plasmid was heated to 94^0C for a minute. Following this, the Vent® Proofreading Taq polymerase synthesizes new double-stranded DNA molecules by catalyzing the template. The polymerase operates at a temperature called the annealing temperature, which is 57^0C and this was performed for 1 minute. To allow the successful synthesis of the new DNA strands, a further incubation was carried out at 72^0C for 1 minute. This procedure was repeated for 26 cycles which enables the DNA to replicates exponentially in the automated thermal cycler. Additionally, further 10 minutes incubation period was added enable the cycle to complete.

To facilitate the cloning of the PCR products after amplification with Vent® Proofreading Taq polymerase, the vial containing these products was place on ice and 1 μl or unit of Bioline *Taq* polymerase was added per tube. After mixing, tubes were incubated at 72^0C for 10 minutes and then quickly placed on ice back to the cloning procedure.

2.2.4.1 Cloning reaction

The TOPO® Cloning solution was prepared by adding together 4 μl of fresh PCR product, 1 μl of Salt Solution, 1 μl of TOPO® vector and 1 μl of sterile water which were supplied by the manufacturer. The mixture was mixed gently and incubated for 30 minutes at room temperature.

The cloning procedure was completed by adding 6 µl of the TOPO® Cloning mixture to a vial of One Shot® TOP10 Chemically Competent *E. coli* followed by gentle mixing. Subsequently, the mixture was placed on ice was for 30 minutes, followed by 30 seconds period of heat-shock at 42^0C before being once again transferred on ice. 250 µl of SOC medium at room temperature was added into the transformation mixture and the tube capped tightly before being rotated horizontally at 200 rpm at 37^0C for 1 hour. This transformation mixture was spread on a prewarmed antibiotic ampicillin selective plate and incubated overnight at 37^0C before the colonies were picked and tested for positivity using PCR.

PCR cocktail was prepared without the DNA addition in a final reaction volume of 25 µl. A colony was subsequently picked and part of it was resuspended in the PCR cocktail. The remaining part of the colony was preserved on another ampicillin selective agar plate for further analysis. This procedure was repeated for multiple colonies if required.

2.2.4.2 Testing of colonies

A PCR procedure was used to analyze positive recombinants. In the study we chose to test for the positive colonies using an orientation analysis only which confirms that the bacteria have the construct inserted in the correct orientation. Two sets of primers pair were used in the PCR cocktail. Firstly, forward primer (T7) for the vector that was included in the kit and a reverse primer that hybridizes within the inserted gene. Secondly, a reverse primer (BGH) which was included in the kit and a forward primer that hybridizes within the inserted gene. The primers used in the PCR to confirm positive recombinants for LZT-Hs7, LZT-Hs8 and LZT-Hs9 (Table 2-3).

Positive transformed bacteria cultures were stored at -70C in a solution containing 15 – 20% glycerol. In each instance, the suspension of bacteria for storage was taken from logarithmically growing cultures in ampicillin selective Luria Bertani broth (0.85ml) and added to 0.15ml of autoclaved sterile glycerol solution.

2.2.4.3 Agarose gel electrophoresis

Agarose gel electrophoresis is a procedure for analyzing the PCR products by size fractionation. For the purpose of preparing 3v/v agarose gel multipurpose agarose (Bioline Ltd, London, UK) was dissolved in 1X TAE buffer by heating until boiling in a microwave oven. The solution was then cooled to room temperature and 1µl of 10mg/ml stock solution of EtBr was added to 50ml and the solution was poured into a casting tray and positioned the well comb at one end of the gel. Following this, the gel was left to set for about 40 minutes on a level surface and then submerged in an electrophoresis tank containing 1X TAE buffer.

The DNA molecular weight marker and the PCR products were loaded into the formed wells using Gilson pipette. For the PCR product mixture, each mixture contained 1 volume of the DNA loading buffer to 5 volumes of the PCR products. The DNA molecular weight marker solution was made up of equal volumes of DNA loading buffer and the DNA molecular weight marker. A constant voltage of 95 volts was applied across the gel until the leading dye front had migrated to the desired distance from the positive electrode. The DNA molecular weight marker to determine the DNA size is in Appendix C.

The DNA was visualized using an ultraviolet transilluminator and photographed using either a DS34 direct screen instant Polaroid® camera with Polaroid® type 667 black and white film or a AlphaDigiDoc Imaging System attached to Olympus C-5060 Wide Zoom camera. In the latter instance, a print out of the gel was made using a Canon-Pixma iP400 printer.

2.2.4.4 Verification of sequences

Sequencing of the plasmid was carried in the Molecular Biology Support Unit within School of Biosciences, Cardiff University, using an ABI377 Automated DNA Sequencer. The DNA sequences generated from the cycle sequencing of the positive recombinant clones were analysed using a BLAST computer software package (Table 2-1). In all instances, this confirmed that the recombinants clones examined were fully homologous to their relevant cDNAs and had not mutated during the PCR procedure.

2.2.5 Plasmid purification

The molecular biology kits used for harvesting the plasmids were the QIAprep Spin Miniprep kit and the EndoFree Plasmid Maxi kit, which were bought from Qiagen Ltd, Crawley, West Sussex, UK.

2.2.5.1 Mini preparations of the plasmids

Plasmid purification was carried out using a commercially available QIAprep Spin Miniprep kit, which uses the anion exchange resin method. This method which allows about 10 – 30 μg of plasmid to be prepared. Firstly, a 2ml aliquot of L-broth containing 50μg/ml concentration of ampicillin in a capped Falcon 2059 polypropylene tube, was inoculated with a single colony of transformed bacteria and incubated overnight at room temperature in a

shaking incubator. Following this, 1.5ml of the culture was transferred into a sterile microcentrifuge tube and centrifugated at room temperature at 3,000 rpm for 5 minutes to produce a bacteria pellet. The plasmid was isolated from the bacteria pellet according to manufacturer instructions while using the QIAprep Spin Miniprep kit. The plasmid integrity was checked by loading a 1 μg aliquot of the isolated plasmid DNA on an agarose gel followed by its electrophores. The plasmid stocks were aliquoted for sequencing verification of the sequences and stored at -20^{0}C.

2.2.5.2 Maxi preparations of plasmids

Large scale preparation of highly purified plasmid DNA generates material suitable for the transfection of mammalian cells. This was achieved by EndoFree Plasmid Maxi kit. Firstly, glycerol stocks were inoculated with a positive recombinant clones using an inoculating loop, which were then streaked on selective Luria Bertani agar plates containing 50μg/ml of ampicillin. The plates were subsequently incubated overnight at 37^{0}C and single bacteria colonies were obtained and used to re-inoculate 2 – 5 ml of selective Luria Bertani broth. These bacterial starter cultures were incubated at 37^{0}C with continuous agitation for 12 hours at 37^{0}C until the cultures entered the late logarithmic phase of growth.

A 250 ml aliquot of sterile Luria Bertani broth in a 1 L conical flask supplemented with 50 μg/ml of ampicillin was inoculated with 2.5 ml of the overnight starter culture and the mixture was incubated at 37^{0}C for 1 hour. The culture was transferred into a 250 ml polypropylene centrifugation bottle and placed into a SLA1500 rotor that was spun at 4^{0}C for 10 minutes at 5,000 rpm in a Sorvall RS6000 centrifuge. After discarding the supernatant, the

cell pellets were resuspended in a cell resuspension buffer appropriate to the method instructed by the EndoFree Plasmid Maxi kit supplied protocol.

The plasmid integrity was check by loading a 1 μg aliquot of the isolated plasmid DNA on the agarose gel followed by electrophoresis. The plasmid stocks were aliquoted for sequencing verification of the sequences, cell transfection and stored at -20^{0}C.

2.3 Cell culture

All cell lines, including CHO cells, were routinely maintained in their respective propagation media and the media was replenished twice during 7 day of culture periods. All monolayer cell lines were routinely cultured in a monitored flow CO_2 gassed incubator. The ambient temperature of the incubator was 37^{0}C and it had a humidified atmosphere of 5% CO_2.

2.3.1 Cell passage

On reaching confluence, cells were passaged. This involved a washing step at room temperature PBS buffer then incubation with 2ml of trypsin/EDTA solution (0.05%/0.025% w/v) at 37^{0}C for 5 minutes, followed by the trypsin/EDTA inactivation by the addition of 10ml of their respective propagation media. Using a fixed angle rotor in a Jouan C312 centrifuge, the cells were pelleted at 1,000 rpm for 5 minutes. The media was then aspirated and the cell pellet resuspended in 10ml of propagation media. Finally, the cells were aliquoted into tissue culture flasks containing their propagation media using a dilution factor suitable to the cell lines.

2.3.2 CHO cells

Chinese Hamster Ovary (CHO) cells were used for transient transfection of the LZT-Hs7, LZT-Hs8 and LZT-Hs9 recombinants for subsequent protein and immunofluorescence studies. Throughout the investigations, the experiments used cells cultured in 35 mm and 15 cm dishes.

CHO cells were routinely cultured and passaged in complete Minimal Essential (α-MEM). The complete formula contains 10% FCS, 4mM L-glutamine, 10μg/ml penicillin/streptomycin and 2.5μg/ml of fungizone-Amphotericin B. To propagate the CHO cells, the cells were plated out at a 30-fold dilution into $15cm^2$ tissue culture flasks.

For recombinant protein analysis, which requires relatively large numbers of CHO cells, 17-hour or 24-hour transfected cells were grown in incubator until 80% confluent before harvesting the cells. Transfected cells for immunofluorescence for protein localization study, CHO cells were grown on 0.17mm thick coverslips placed in 35mm dishes and then post-harvest the cells after 17-hour incubation. Transfected cells for protein molecular weight study, the cells were grown on 35 mm dishes and then post-harvest the cells after 24-hour incubation. In all instances, cells were incubated at 37^0C in 5% CO_2.

2.3.3 LZT-Hs7, LZT-Hs8 and LZT-Hs9 transient transfections

Prior to commencing the transfection, two types of medium were prepared; firstly, a transfection medium containing the lipid and DNA mixture in α-MEM with 2% glutamine, and secondly, a replenishing medium containing 2% glutamine and 10% serum in α-MEM.

The latter was used to wash the confluent cells before the transfection. In each instance the above medium were produced asceptically.

Once the appropriate solutions were prepared, the cells normal growth medium was removed and the cells were washed for three times with PBS buffer at room temperature. Following this, 1.5 ml of the replenishing media was added into the dish.

The lipid and DNA complex mixture was produced according to (Taylor et al. 2003) using 4.4μg of DNA to 13.8μl of Lipofectamine2000™. This was sufficient for a transfection in either a well of six-well plate or one 35mm tissue culture dish. The lipid mixture was made by adding 13.8μl of Lipofectamine2000™ into 250μl of serum free medium in a marked microcentrifuge tube. The DNA mixture was made by adding 4.4μg of Qiagen® Maxi-Prep purified recombinant DNA to 250μl of the serum free medium in a second marked microcentrifuge tube. These steps are termed as the diluting procedure. Subsequently, the diluted Lipofectamine2000™ and DNA were added together and this was performed within 5 minutes of the dilution step. The resulting transfection mixture was then gently mixed and incubated at room temperature for 20 minutes. Once the incubation was completed, the lipid and DNA mixture was gently overlayed onto the earlier replenished cell dishes. The dishes were again placed into the humidified atmosphere incubator at 370C in 5% CO2. The transfection mixture was not removed, until the cells were harvested accordingly.

2.3.4 MCF-7 cells and its sub-lines

A variety of MCF-7 sub-lines were used to assess the expression of the LZT family of genes using mRNA analysis. In the Tissue Culture Laboratory, at Tenovus Centre for Cancer Research, their MCF-7 cells which are the ER human positive breast cancer cell line which has been exposed to variety hormonal and anti-hormonal agents. This has lead to the development of several sub-lines which have become resistant to anti-oestrogen and oestrogen withdrawal. Parental MCF-7 cells were originally obtained from Aztra-Zeneca Pharmaceuticals Division, Macclesfield, UK.

The MCF-7 cell line was routinely cultured and passage in complete RPMI 1640 medium, whilst the anti-hormonal resistant cells were grown in in complete RPMI 1640 supplemented with a maintenance concentration of the specified agent. The concentrations of hormones and anti-hormones routinely used were 10^{-9}M 17-β oestradiol and 10^{-7}M tamoxifen or faslodex. The complete RPMI 1640 media was supplemented with 4mM L-glutamine, 5% charcoal stripped Foetal Calf Serum (FCS), 10μg/ml of penicillin/streptomycin and 2.5μg/ml fungizone-Amphotericin B. The culture medium was changed twice a week.

All stock solutions of 17-β estradiol, tamoxifen and faslodex are prepared in ethanol and stored at -20^{0}C. The 17-β estradiol and tamoxifen were purchased from the Sigma-Aldrich Company Ltd, Dorset, UK, while the faslodex is supplied by Astra-Zeneca, Pharmaceuticals Division, Macclesfield, UK.

In total seven MCF-7 sub-lines were used to isolate mRNA and these were :

1) Parental MCF-7 cells:

2) MCF-7 cells treated with 10^{-9}M oestradiol for 10 days

3) MCF-7 cells treated with 10^{-7}M tamoxifen for 10 days

4) MCF-7 cells treated with 10^{-7}M faslodex for 10 days

5) MCF-7 cells grown in heat inactivated charcoal stripped serum for 10 days (X-medium).

6) Tamoxifen resistant MCF-7 cells grown semi-confluence

7) Early faslodex resistant MCF-7 cells grown semi-confluence Early resistance involved growing the cells for 70 passages. Late faslodex resistant MCF-7 cells grown semi-confluence Late resistance involved growing the cells for 140 passages

8) MCF-7 cells resistant to X medium grown to semi-confluence (X-cells)

Cells for the above were seeded in six-well plates or or 35 mm tissue culture dishes for the RNA and protein studies respectively. In each instance 3 x 10^5 cells were seeded and they were incubated at 37^0C in a humidified atmosphere containing 5% CO_2 incubator until they are 80% confluent.

2.3.4.1 Preparation of RNA for PCR

All the RNA samples described in this study were isolated using the TRI® reagent (Sigma-Aldrich, Dorset, UK) RNA kit.

2.3.4.2 Preparation of mRNA

In order to prepare a small amount of mRNA (30 - 50 μg) for the following RT-PCR study, approximately 1.5 X 10^6 cells of sub-confluent adherent cultured cells were harvested from a

60mm tissue culture dish. The media was discarded by aspiration and after that tissue culture dishes were washed with room temperature PBS buffer for three times. In order to lyse the cells, 1 ml of the TRI reagent was added directly on a culture dish. The dish was swirled around to enable the lysate to form and the mixture appeared viscous. The resulting lysate was scraped of the dish using a cell scraper. Prior to this the cell scraper was washed with ethanol and PBS buffer to aovid contamination. The cell lysate was subjected to repeated suction and reversed using pipette to make them homogeneous. The lysate was transferred into a microcentrifuge tube and placed on ice.

To separate RNA from DNA and protein, 0.2ml of chloroform was added into the lysate. The microcentrifuge tube was capped and was shaken vigorously using a vortex and following this, the lysate was set at room temperature for five minutes to allow the formation of three layers of solution in the lysate. The TRI reagent dissolves the RNA into the aqueous phase layer. The aqueous layer containing the RNA was aspirated and aliquoted to a new microcentrifuge tube. In an attempt to isolate the total RNA, 0.5ml of isopropanol was added into the RNA in the aqueous layer. The microcentrifuge tube was capped and the solution was mixed gently. Following this, the solution was set at room temperature for 10 minutes. The microcentrifuge tube was cemtrifuged at 13,000X rpm for 10 minutes and the RNA pellet was obtained at the bottom of the microcentrifuge tube. By avoiding the debris pellet, the solution was aspirated and leaving the pellet behind. 1 ml 75% ethanol was added into the microcentrifuge tube to wash the RNA pellet. The capped microcentrifuge tube was shaken vigorously but briefly, using vortex. Once the RNA pellet was floated in the ethanol, the

microcentrifuge tube was centrifuged at 13,000X rpm for 5 minutes period was carried out. By avoiding the RNA pellet, the ethanol solution was aspirated as much as possible and the pellet was left to set at the bottom of the microcentrifuge tube.

For the purpose of air-drying the RNA pellet, as little as possible, ethanol solution was left with the pellet. To recover the pellet, the microcentrifuge tube was uncapped and about ten minutes period at room temperature would allow the ethanol solution to dry completely. Finally, the RNA pellet was dissolved in 10 to 50ul nuclease-free water (Invitrogen, UK,) and stored at -80^{0}C refrigerator for avoiding degradation of the RNA. The quality of the RNA was evaluated by Cecil CE 2041UV Spectrophotometer and electrophoresis in 3% agarose and by PCR-based technique, or RT-PCR. The RNA concentration was estimated using the Cecil CF2041 UV spectrophotometer. This was performed by reading the optical density of 4 µl of RNA diluted to a final volume of 1 ml in sterile nuclease free water and was read at 260nm. The RNA concentration was calculated from a RNA calibration curve. The RNA purity was determined by calculation of the ratio of absorbance at 260nm to absorbance at 280nm and the pure RNA has a ratio of 1.8-2.2.

2.3.4.3 RT-PCR

RT-PCR is a PCR technique which used the reverse transcriptase enzyme to transcribe mRNA sequences into a double stranded cDNA template. This method was to synthesize and extend the first strand of DNA using random hexamer oligonucleotides (Knowlden et al. 1997).

20µl of RT-PCR solution was used, containing 1µg total cellular RNA, 10µM random hexamer oligonucleotide mixture, 0.156mM dNTP mixture, 0.01M dithiothreitol and 1X concentrated PCR buffer.

To denature the secondary structure of the RNA, the resulting solution was denatured at 95^0C for five minutes on the thermal cycler (PTC-100™ Programmable Thermal Controller, MJ Research, Inc). Once the denaturing process was completed, the microcentrifuge tube was removed from the thermal cycler and quickly placed on ice for five minutes. After this period, the mixture was spun in a centrifuge for 1 minute. For the purpose of obtaining good quality PCR products, 0.5µl of RNase inhibitor (equivalent to 25 Weiss units) and 1µl of MMLV-Reverse Transcriptase were added into the resulting RT-PCR solution on ice. These molecules were added into the solution to prevent any RNA degradation and prime DNA synthesis from the RNA templates, respectively. Following this addition, the microcentrifuge tube was capped to prevent dehydration during the reverse transcription process process. In the thermal cycler the reversed transcription program incubation uses 40 minutes at 42^0C. The temperature was then raised to 95^0C for five minutes to allow denaturing of the cDNA and RNA complexes and the inactivation of the MMLV-Reverse Transcriptase molecules in the samples.

The resulting cDNA mixtures from the reverse transcriptase reaction were used in at standard Polymerase Chain Reaction, which used gene-specific primers to the various LZT family members. Experiments involving the RNA profiling of the LZT family of genes used the

primers listed in Table 2-4. Along side the LZT family of genes, the expression of pS2, β-actin and α-actin was also examined. The primer sets for these genes are listed in Table 2-5. The assigned annealing temperature, the number of cycles used for the amplification and the expected band size for the LZT family of genes, together with the control genes (pS2, α- and β- actin) are also shown in Table 2-4 and Table 2-5, respectively.

2.3.5 siRNA to LZT-Hs1 transient transfection

Small interfering RNA, siRNA, molecules were synthetically developed to knockdown mRNA of genes of interest. In order to characterize LZT-Hs1 gene functions in the tamoxifen resistant cell line, transient transfection was performed using a commercially available siRNA to LZT-Hs1. The siRNA to LZT-Hs1 kit that was bought from Dharmacon, Thermo Fisher Scientific Inc, UK.

The procedure involved the addition of 0.2 nmol of the siRNA molecule is diluted in 250μl of serum free medium to 4μl of Lipofectamine2000™ reagent is diluted to 250 μl in serum free medium. These solutions must be mixed together within 5 minutes of making and must be incubated with the cells within 60 minutes. As such, the mixture was spread over the tamoxifen resistant cells in a 35mm tissue culture dish for either 24 or 48 hours incubation at 37^0C in 5% CO_2. The controls for the siRNA study were tamoxifen resistant cells without siRNA treatment, tamoxifen resistant cells with Lipofectamine2000™ only and tamoxifen resistant cells with siC scrambled control treatment. Following the siRNA and control treatments, preparations were made for two studies; in mRNA study, cells were harvested 24

hours after the transient transfection and in the second study, the cells were harvested at 48 hours.

Table 2-4 and Table 2-5 are showing the details of the primers and parameters for PCR programme for analysis in the RNA expression study.

2.3.6 Detection of proteins by Western blots

2.3.6.1 Lysis solution

In order to avoid protein degradation, the cell harvesting procedure was always carried out on ice. The lysis buffer, Triton-X-100, contained 50mM Tris of pH 7.5, 5mM EGTA, 150mM NaCl, 1% Triton X-100, 2nM sodium orthovanadate, 50mM sodium fluoride, 10mM sodium molybdate, 20μM phenylarsine oxide, 1mM phenyl-methylsulfonyl fluoride, 10μg/ml leupeptin and 10μg/ml aprotinin.

After washing the cells in room temperature PBS, 30μl of the lysis solution was added to each dish. Then using a scraper the protein lysates were collected into labeled microcentrifuge tubes. The cell debris was pelleted by centrifugation at 13,000 rpm for 20 minutes at 4^0C and the supernatant, which contained the protein of interest, was aliquoted into new microcentrifuge tubes and stored at -70^0C until used.

2.3.6.2 Protein concentration determination

To determine the concentration of protein in the whole cell lysate, a small sample was removed and used in a colorimetric protein assay kit (Bio-Rad DC Protein Assay Kit). The

method is based on the folin phenol method of Lowry and colleagues which allows rapid determination of protein concentrations following their solubilisation by a detergent. All the samples were read for their absorbance at 750nm measurement in a Cecil CE2041 spectrophotometer relative to a standard protein curve generated from a series of known concentration of BSA.

2.3.6.3 Protein preparation

A small sample containing 40-80µg of protein was aliquoted into an equivalent volume of 2X concentrated Laemmli sample buffer and the resultant mixtures was denatured at 100^0C for ten minutes in dry heating block (Techne DB-2A Dri-Block). After a brief pulse spin on the microcentrifuge, the denatured protein samples were used for SDS-Page and Western blotting.

2.4 SDS-Page and Western Blot

The discontinuous polyacrylamide gel electrophoresis method for protein separation was used here. The protein marker scale to determine the protein molecular weight is in Appendix C.

2.4.1 SDS-Page

For the purpose of separation, two types of gels were used, the stacking gel and a resolving gel. In the former gel of the concentration of acrylamide was 4%, whereas the resolving gel was 7.5%. All western blots were carried out using the Bio-Rad Blot™ apparatus. The resolving gel buffer used was 1.5M Tris-HCl pH 8.8 (Bio-Rad) and the stacking gel buffer

was 0.5M Tris-HCl pH 6.8 (Bio-Rad). The stock acrylamide solution comprised of 30% Acrylamide and 0.8% N,N'-methylene-bis-acrylamide.

Using the resolving gel mixture, appropriate Bio-Rad gel formers with 1mm spacers and 10cm back plates were set-up. Immediately, after pouring the resolving gel, a thin layer of water was discharged on top of the gel. The resolving gel was then left to solidify for about 30 minutes. Once the gel was solidified, the water was removed using a piece of Whatmann 3MM filter paper. Following this, the stacking gel solution was poured onto the resolving gel and appropriate gel combs put in place. The gel combs used were10mm and each of the formed wells has a capacity to hold a total of 50µl protein sample. Finally, after the stacking gel solidified, the wells were rinsed out and flooded with electrophoresis (0.05M Tris, 0.384M glycine, 0.1% SDS). As routine, one track of the gel was loaded with 10 µl of standard Rainbow Markers™ (Amersham BioSciences) while the other tracks were used to load the protein samples. The gels were subject toelectrophoresis at 150V for about an hour, which allowed the dye front to migrate the desired distance down the gel.

2.4.2 Western Blot

The term western blotting is commonly used to describe both the transfer of protein from an acrylamide gel to a nitrocellulose membrane and then the subsequent immunoblotting procedure using specific antibodies. Using specific antibody probing it is possible to identify a protein of interest from other protein of similar.

Following the gel electrophoresis, the polyacrylamide gels were transferred to an immobilised membrane using a Bio-Rad Blot™ electrophoresis cell. In the assembly of one unit of the transfer apparatus, two 10cm X 8cm sheets of nitrocellulose membrane (nitrocellulose membrane pore size 0.45μM, Sigma-Aldrich) were cut for each gel. Prior to the transferring procedure, a transfer buffer was prepared (25mM Trizma® base , 191mM glycine, 20% v/v methanol and 0.1% SDS). The buffer was then filled into a tray, temporarily, and in the electrophoresis transfer tank. Using the buffer in the tray, the filter paper, the fiber pads supplied with the transfer apparatus and the nitrocellulose membrane were pre-soaked. In addition, the gels were removed from the glass backing plates and immersed in the tray. In the electrophoresis transfer tank, the blotting insert, a small magnetic stirrer and an ice pack were placed in the tank.

The procedure of western blotting, there are several sources of error have been identified and trapped air bubbles in the blotting cassette must be avoided. The assembly of the blotting cassette therefore is always done whilst everything else is submerged in the transfer buffer in the tray. To set up the western blot, the blotting cassette was opened and the black side placed down in the tray. A single fiber pad was then placed in the black side of the cassette followed by a single sheet of filter paper that was placed next to the gel. Following this, the nitrocellulose membrane was placed on the gel and a single sheet of filter paper was positioned on top of it and lastly followed by another single fiber pad. The blotting cassette was then carefully closed and pressed gently under the transfer buffer to expel any trapped air bubbles. Once the cassette is ready, it was then positioned in the blotting insert with the

membrane nearest the positive electrode of the electrophoresis unit. An ice block was inserted in the transfer tank before the lid was placed on the transfer tank. The buffer was gently stirred while the current was applied at 150V across the electrodes for an hour at room temperature.

2.4.3 Immunoblotting

Immunoblotting allows characterization of protein of interest using monoclonal or polyclonal antibodies. The membrane was first incubated with 5% w/v substitute of 2.5g Marvel milk reconstituted in 50ml of TBS Tween. The blocking was done in a 50ml Falcon tube whilst it was on a rotatory mixer at room temperature for 1 hour. The blocking solution was then decanted into a waste container and the blots incubated with a primary antibody in 1% w/v of the blocking solution. The antibody incubation step was also performed on a rotatory mixer at room temperature for 1 hour. Prior to the secondary antibody incubation, the membranes were washed 3 times for a total of 15 minutes with a TBS Tween solution. Following this, the secondary antibody was applied to the membrane and once again incubated for 1 hour on a rotatory mixer at room temperaturefollowed by 9 washes in a total of 45 minutes. The membranes was then placed in a fresh plastic sleeve.

2.4.4 Protein detection

On completion of the immunoblotting process, the membranes were incubated with 1 ml of a chemiluminescent detection mixture at room temperature for five minutes and then transferred to another fresh plastic sleeve. This was then exposed to an X-ray film (Hyperfilm-ECL) in a closed cassette. The first film was normally exposed for 30 to 60 seconds in order to judge the correct subsequent exposure time.

2.4.5 Antibodies

The anti-V5 antibody that detects the 14 amino acid epitope at the C-terminal fusion proteins expressed using pcDNA5/FRT/V5-His-TOPO® TA vector was bought from Invitrogen, Paisley, UK and used at a dilution of 1:1000. The Y^{1068}, phosphorylated EGFR and Y^{1178} phosphorylated EGFR antibodies were purchase from Cell Signalling, Technology, Hertfordshire, UK, whilst phosphor c-Src 418 antibody was purchased from Biosource International, Nivelles, Belgium and in each instance they were used at a dilution of 1:2000. Rabbit-antimouse antibodies were obtained from Dako, High Wycombe, Buckinghamshire, UK, and the donkey-antirabbit antibodies were purchased from Amersham Biosciences UK Ltd., Little Chalfont, Buckinghamshire, UK), and used at a dilution of 1:2000. The β-actin mouse monoclonal antibody which recognizes an N-terminal epitope of the β-isoform of actin was bought from Sigma-Aldrich Company Ltd, Poole, Dorset, UK, and was used at a dilution of 1:10,000. The LZT-Hs1 polyclonal antibody was 'in-house' generated antibody and the serum was used at dilution of 1:750.

2.5 Fluorescent microscopy

2.5.1 Coverslip procedure

2.2 X 10^5 CHO cells were grown on a 0.17 mm thick coverslips prior to transfection for 24 hours. Following this, the cells were fixed with 4% v/v formaldehyde for 15 minutes then incubated either with permeabilising or non-permeabilising buffer. Permeabilising buffer was prepare from 0.4% w/v Saponin and 1% w/v bovine serum albumin in PBS buffer, whilst the non permeabilising buffer lacks Saponin. Subsequently, the cells were incubated in 10% v/v normal goat serum, and followed by an 1 hour incubation at room temperature with anti-V5

antibody. After washing Alexa Fluor 488-conjugated anti-mouse antibody was added followed by 1 hour incubation at room temperature. F-actin was stained using Texas Red®-X for 15 minutes. After the incubations the coverslips were assembled on to slides using Vectorshield containing 1.5 µg/ml of DAPI to counterstain the cell nuclei. All the coverslips are visualized using the imaging system.

2.5.2 Detection of zinc using Newport Green™ diacetate

Tamoxifen resistant cells were grown on coverslips for 24 hours following the transient transfection procedure and then were rinsed with warm PBS. 50µM of Newport Green dye was then discharged directly onto the coverslips and incubated in the dark for 30 minutes at 37^0C.

2.5.3 Imaging system

2.5.3.1 AlphaDigiDoc Innotech Imaging

The AlphaDigiDoc Innotech Imaging system was used to scan all gel electrophoresis and X-ray images and was linked to Olympus C-5060 Wide zoom camera. An ultra violet light box and a white light box were used for the gel electrophoresis and X-ray images, respectively. The images densities and statistics data were generated by using Spot Density Measurement function and an Excel Microsoft, statistical package respectively.

2.5.3.2 Fluorescent microscope

The fluorescent microscope used was an inverted LEICA DM IRE2 microscope with an oil immersion 63X objective and a Hammamatsu camera. The images were taken using a mercury-lamp-base system, which was supported by Openlab Modular computer software

package. Fluorescent superimposed images were acquired using multiple band-pass filters that were set for DAPI, fluorescein and Texas Red Phalloidin.

It is important to note, for stringent analysis, all experiments done in triplicates and repeated at least three times. This applies to the recombinant study (Chapter 3), the RNA expression study (Chapter 5), also in the procedures involved in the computer searches (Chapter 3 and Chapter 5). The only exception to this is in the LZT-Hs1 small interfering RNA study where the RNA expression experiments were done in triplicates and repeated three times while the protein analysis was done once and pooled the triplicates protein samples used for a Western blotting procedure. The MCF-7 cells treated with Tamoxifen for the small interfering RNA study were prepared immediately upon request, by the Tissue Culture Laboratory, in Tenovus Centre for Cancer Research, while the RNA collections were prepared prior to storage in the -80^{0}C refrigerator until the respective study started.

Table 2-1: Computer softwares packages used for LZT subfamily to gather information

Databases	WWW-Address	Description
DRAGON ERE FINDER	http://research.i2r.a-star.edu.sg/DRAGON/ERE-V2/	System for Identification and Interactive Analyses of Estrogen Response Elements in DNA Sequences
EMBL	Http://www.ebi.ac.uk/embl/	European Molecular Biology Laboratory nucleotide sequence database at EBI, Hinxton, UK
GenBank	Http://www.ncbi.nlm.nih.gov/Genbank/GenbankOverview.html	DNA Genome Sequence Database at National Center for Biotechnology information, NCBI, Bethesda, MD, USA
SWISS-PROT/TrEMBL	Http://www.expasy.ch/	PIR-International Protein Sequence Database, annotated protein database by PIR, MIPS and JIPID at NBRF, Georgetown University, USA
Fasta3	Http://www.ebi.ac.uk/fasta3/	Sequence similarity and homology searching against nucleotide and protein database using Fasta3 (Global Alignment)
BLAST2	Http://www.ebi.ac.uk/blastall/	NCBI blast2 (blastall) program (Local Alignment)
TMPRED	http://www.ch.embnet.org/software/TMPRED_form.html	Tool to prediction of transmembrane regions and protein orientation
TreeView	http://taxonomy.zoology.	Tool to build phylogenetic analysis of protein and

	gla.ac.uk/rod/rod.html	DNA sequences
ELM	http://elm.eu.org/	Tool to search of functional sites in proteins
NetNGlyc	http://www.cbs.dtu.dk/services/NetNGlyc/	Tool to predict N-glycosylation sites in human proteins

Table 2-2: Forward and reverse primers of LZT-Hs7, LZT-Hs8 and LZT-Hs9 for cloning

LZT subfamily gene and the sequence accession number	Forward primer	Reverse primer	Nucleotide size (Base pairs)
LZT-Hs7 NM_173596	5'- CCC ATC ACC **ATG GGG TCC CCA GTG** -3'	5'- **TTC TCA GCC CTC AGT GGT** C-3'	1686
LZT-Hs8 NM_152725	5'- CCC ATC ACC **ATG TGC TTC CGG ACA AAG** -3'	5'- **TAT TTT AAT ATT TTG CTC** -3'	1962
LZT-Hs9 NM_152264	5'- CCC ATC ACC **ATG TCC CTG CCC TGG** -3'	5'- TAA **CGT AGA ATC GAG ACC GAG GAG AGG GTT AGG GAT AGG CTT ACC GTT ACT CGG GAG** -3'	1094

Underlined nucleotides in the forward primer are located on the 5'end of the sequence whilst in the reverse primer the underlined nucleotides are complementary to the 3' end of the sequence. The red is the complementary sequence of V5 tag.

Table 2-3: Forward and reverse primers for LZT-Hs7, LZT-Hs8, and LZT-Hs9 for orientation analysis by PCR

LZT family of gene	Forward primer	Orientation analysis using BGH primer	Nucleotide size (Base pairs)
LZT-Hs7	5'- CCC ATC ACC ATG GGG TCC CCA GTG -3'	5' - CCC ATC ACC ATG GGG TCC CCA GTG – 3'	1827
LZT-Hs8	5'- CCC ATC ACC ATG TGC TTC CGG ACA AAG -3'	5' - CCC ATC ACC ATG GGG TCC CCA GTG – 3'	2103
LZT-Hs9	5'- CCC ATC ACC ATG TCC CTG CCC TGG -3'	5' - CCC ATC ACC ATG GGG TCC CCA GTG – 3'	1295

Table 2-4: Primers set, annealing temperature, cycle number and expected band size for the LZT subfamily of genes in RNA profiling study

LZT subfamily	Forward primer	Reverse primer	Annealing ^{0}C	Cycle	Expected size (Base pairs)
LZT-Hs1	5'- ATC GCT CTC TAC TTC AGA TC -3'	5'- CTC TTC TGA ACC CCT CTT G -3'	57^{0}C		392
LZT-Hs2	5'- TTG GCA GTT CAA GAG GGA AAG -3'	5'- CGA TTA TGC TCA TAC TGT -3'	55^{0}C	31	451
LIV-1	5'- GTC TAA CAG CTC TAG GAG GC -3'	5'- CAC CAA TTG CTA GGC CAT CG -3'	55^{0}C	35	576
LZT-Hs4	5'- TGC TTG GCT TAT GGA GAA CC -3'	5'-GAG ATG ACG GTC ACA CAG AGG -3'	55^{0}C	29	425

LZT-Hs5	5'- CCC ATC ACC ATG GCG TCC CTG G -3'	5'-GGT GCC CTC GGG GTT GCT GAG G -3'	55^{0}C	29	330
LZT-Hs6	5'- CCC ATC ACC ATG GCC CCG GGT CGC GCG -3'	5'- CCC ATC ACC ATG GCC CCG GGT CGC GCG -3'	55^{0}C	29	335
LZT-Hs7	5'- GGG TGA CCT GGA AGA GTC AA -3'	5'- CAG CAA GGG CCG TAG TAG AC -3'	57^{0}C	33	388
LZT-Hs8	5'- AAA CTT GCC TTC CCC AGA CT -3'	5'- TGA GTG AGA GGC CCT TCT GT -3'	57^{0}C	31	297
LZT-Hs9	5'- CCC ATC ACC ATG GCG GGC CCA AG -3'	5'-GGG AAT GAC AAG CAA CGG GAA-3'	59^{0}C	29	242

Table 2-5: Primers set, annealing temperature, cycle number and expected band size for the control genes for mRNA profiling study

Control genes	Forward primer	Reverse primer	Annealing ^0C	Cycle	Predicted size(Base pairs)
α-actin	5'- CTA CGT CGC CCT GGA CTT CGA GC -3'	5'- GAT GGA GCC GCC GAT CCA CAC GG -3'	55^0C	29	204
β-actin	5'- GGA GCA ATG ATC TTG ATC TT -3'	5'- CCT TCC TGG GCA TGG GGT CCT -3'	55^0C	29	336
pS2	5'- CAT GGA GAA CAA GGT GAT CTG -3	5'- CAG AAG CGT GTC TGA GGT GTC -3'	55^0C	29	336

Chapter 3

Computer Search

This chapter describes the scientific classification of the LIV-1 family of genes used in this thesis in comparison to other literatures. The study of the family protein secondary-structure is important to show the similarities and differences among the LZT family members themselves and between the LZT subfamily and the ZIP superfamily. The secondary motifs study also predicts the protein functional sites that arise because of particular requirements on the secondary-structure of specific region or more than one. This region or regions may be important for their binding properties or importantly, their enzymatic activity. Subsequently, as an introductory study, the post-translation modification such as the phosphorylation sites in the LIV-1 family of proteins were investigated that possibly contributes to regulation of enzyme for example in the MAPK pathways for carcinogenesis. The aim of the work presented in this chapter was to establish whether there were recogniseable motifs, which were relevant to the function of LIV-1 subfamily.

3.1 Gene nomenclature

ZIP transporters consist of a superfamily of zinc transporters that are divided into 4 subfamilies. One subfamily (LIV-1 subfamily) consists of genes that share similarities to the LIV-1 gene, which is an oestrogen-regulated gene and it has been implicated in metastatic breast cancer disease (Manning et al. 1994), This superfamily is also known as the SLC39A family of metal transporters, which play a role in zinc homeostasis. The ZIP superfamily acronym stands for Zrt-, Irt-like proteins and the LIV-1 subfamily has been termed LZT,

which stands for LIV-1 family of ZIP Transporters. Table 3-1 shows the gene nomenclature across the 9 members of the LZT subfamily and in this thesis they will be referred as 'LZT-Hs ( )', where the bracket contains the number assigned to each of the LZT members and Hs refers to homo sapiens. However, in this thesis, the original LIV-1 gene nomenclature remains.

3.2 Protein secondary-structure prediction

ClustalW (Eddy 1995) computer software package allows the sequences of all 9 members of the LZT subfamily to be aligned in order to observe any differences in secondary-structure protein among the LZT subfamily. As we know, the ZIP superfamily play a role in zinc homeostasis, and alignment of the full distribution of the LZT subfamily by ClustalW will help prediction of any interesting structural properties within the LZT subfamily. The BOXSHADE3.2 computer software package was used to shade the residues. Identical residues shown by black color and complementary residues were identified in grey, using a cut-off value of 50% homology as shown in Figure 3-1. There are four main areas within the LZT subfamily that show a large proportion of identical residues, among there are the CPALLY region, transmembrane domains (TM), ZIP consensus sequence and H E X P H E motif.

This alignment of the LZT subfamily using ClustalW could be represented as a phylogenetic tree shown in Figure 3-2. As can be seen, LZT-Hs4 and LZT-Hs6 are clustered together, LZT-Hs1 clustered with LZT-Hs9, and finally, LZT-Hs2 clustered with the LIV-1 gene. These patterns shown in the phylogenetic/dendogram representation, suggests the possibility

of these clustered genes sharing similar properties of either secondary-structure and/or protein functionality.

3.3 Uniqueness of LZT subfamily members

Within the LZT subfamily, the individual family members probably share properties predicted to be involved in zinc transport and this section discuss the similarities among the LZT subfamily, which are not found in the ZIP superfamily.

3.3.1 N- terminus

The N-terminus is the sequence immediately after the translation start site, and predicted to reside extracellularly in those family members that reside on the plasma membrane. There are 133 residues in the N- terminus of LZT-Hs1 gene and 405 residues in the LZT-Hs2 gene. 317 residues in the LIV-1 gene, 152 residues in the LZT-Hs4 gene, 325 residues in the LZT-Hs5 gene, 127 residues in the LZT-Hs6 gene, 212 residues in the LZT-Hs7 gene, 365 residues in the LZT-Hs8 gene and 66 residues in the LZT-Hs9 gene (Figure 3-1).

3.3.2 C- terminus

C- terminus of the LZT subfamily is very short and is situated immediately after transmembrane domains 8. It was observed, 6 residues in the C- terminus of LZT-Hs2 gene, 6 residues in the LIV-1 gene, 3 residues in the LZT-Hs4 gene, 2 residues in the LZT-Hs5 gene, 3 residues in the LZT-Hs6 gene, 7 residues in the LZT-Hs7 gene and 2 residues in the LZT-Hs8 gene. Neither LZT-Hs1 nor LZT-Hs9 has any residues beyond transmembrane domain 8 (Figure 3-1). Since LZT-Hs1 is known to reside in the endoplasmic reticulum may

suggests a similar location for LZT-Hs9 (Taylor et al. 2004). This trait of very short and extracellular C- terminus predictions are similar to the attributes of the ZIP superfamily zinc transporters (Guerinot 2000).

3.3.3 HNF motif unique to LZT subfamily

As seen in Figure 3-3, another interesting feature in transmembrane domain IV is that it holds a conserved motif H N F, where H is histidine, N for asparagine and F is for phenylalanine residues. The ZIP superfamily of zinc transporters have conserved residues in a similar region however they have H S residues (S, serine), instead of the H N F in LZT subfamily, however both of the conserved regions are predicted to be part of an intramembrane heavy metal binding site despite having differences in the motif between these two families.

3.3.4 CPALLY motif unique to LZT subfamily

There is a motif in 7 out of 9 LZT subfamily members that contains 3 conserved cysteine and 1 proline residue. This has been termed the CPALLY motif (Figure 3-4). Cysteine residues are known to have a role in protein tertiary structure and this motif may thus have an important role in the control of zinc transport. Interestingly LZT Hs1 and LZT Hs9 do not contain the CPALLY motif. LZT-Hs1 resides on intracellular membranes (Huang et al. 2005; Taylor et al. 2004) and this may suggest a role for the CPALLY motif in regulating zinc influx into the cell. Furthermore, neither LZT-Hs1 nor LZT-Hs9 contains the cysteine residue preceding the HEXXH motif in transmembrane domain V. This may suggest that 1 of the 3 cysteine in the CPALLY motif binds to the cysteine in transmembrane V to control the zinc influx.

3.3.5 HEXPHE motif unique to LZT subfamily

As seen in Figure 3-.5, a conserved motif in the LZT subfamily located in transmembrane domain V is the H E X P H E motif, where H is for Histidine, E is Glutamic acid, P is Proline and 'X' is any amino acid. In contrast, the ZIP superfamily have a motif H X X X E instead of H E X P H E which it was predicted to form a pore region providing a transport mechanism for zinc ions. Interestingly, within the LZT subfamily members, LZT-Hs4 and LZT-Hs6 genes have lost their initial H, histidine residue of the HEXPHE motif sequence and replaced by glutamic acid (E) residue. Changes in this amino acid of these sequences suggest that these genes may prefer to transport metal ions other than zinc (Liuzzi et al. 2005).

3.3.6 PEST motif unique to LZT subfamily

Strong PEST motifs consists of amino acid proline (P), glutamic acid (E), serine (S) and threonine (T) and when present, PEST motifs are able to reduce the half-lives of proteins dramatically as they target proteins for proteolytic degradation allowing the protein to exert various different cellular functions (Rechsteiner and Rogers 1996). The PEST site analysis achieved using the PESTfind software package is shown in Figure 3-5, indicated by red arrows. There are only 2 genes of the LZT subfamily identified with a PEST motif and they are: LZT-Hs2, in the sequence at position 206 with RGEPSNEPSTETN residues and at position 575 with RLN**ETELTGLEQQESPP**, whilst the second gene is LIV-1, PEST site at position 209 with KDV**SSSTPPSVTS** residues.

3.4 The compilation of information from the various computer searches describing each of members of the LZT subfamily.

3.4.1 LZT-Hs1

LZT-Hs1 sequence contains 469 residues (Figure 3-5), and it has a close relationship with LZT-Hs9 sequence with both sequences sharing a high similarity of residues (Figure 3-2). The LZT-Hs1 gene has one predicted N-linked glycosylation site that is located intracellularly (Table 3-6). Interestingly, LZT-Hs1 does not contain the CPALLY motif and it resides on the ER membrane. This may suggest an important role of the motif for control of zinc influx at the plasma membrane or intracellular organelles. The LZT-Hs1 gene has 9 histidine residues in between transmembrane III and IV which may play a role in zinc transport (Figure 3-5). The protein resides in the endoplasmic reticulum, Golgi body and membrane fractions (Table 3-5).

3.4.2 LZT-Hs2

The total amino acids in LZT-Hs2 sequence is 831 residues (Figure 3-5) and it has the greatest homology with LIV-1 of all the family members (Figure 3-2). There are five predicted N-linked glycosylation sites, which are located extracellularly suggesting that the protein resides on the plasma membrane and the protein could potentially be glycosylated (Table 3-6). There are two strong potential PEST sites, one of which is situated extracellularly in the N-terminus and the other is located intracellularly (Figure 3-5). The PEST regions suggest that LZT-Hs2 may be post-translationally modified by proteolytic cleavage. Recently, work in the Tenovus Centre for Cancer Researh laboratories has shown,

LIV-1 has been observed to be cleaved in the endoplasmic reticulum region before relocation to the plasma membrane (Taylor, personal communication) and the presence of the PEST sites may suggest proteolytic processing of LZT-Hs2 (Figure 3-5). The protein is suggested to be found on the plasma membrane (Table 3-5).

3.4.3 LIV-1

The LIV-1 sequence is 749 residues (Figure 3-5), and it shares similarities with the LZT-Hs2 and LZT-Hs7 sequences based on homology of residues (Figure 3-2). Four predicted N-linked glycosylation sites are located extracellularly, suggesting that the protein resides on the plasma membrane and the protein is potentially glycosylated (Table 3-6). One strong potential PEST site is located extracellularly in the N-terminus suggesting proteolytic processing using a similar mechanism to LZT-Hs2 sequence. Finally, the LIV-1 protein has been located on the plasma membrane and in lamellipodiae (Table 3-5), suggestive of involvement in proliferation process by the latter (Table 3-5).

3.4.4 LZT-Hs4

The LZT-Hs4 sequence contains 492 residues (Figure 3-5), and it has a close relationship with the LZT-Hs6 sequence because both sequences share a high similarity (Figure 3-2). The LZT-Hs4 gene has three predicted N-linked glycosylation sites that are located extracellularly suggesting that the protein resides on the plasma membrane (Table 3-6) and that LZT-Hs4 protein is likely to be glycosylated. Interestingly, the first histidine residue of the HEXPHE motif is replaced by a glutamic acid residue suggesting that this gene may preferentially transport metal ions other than zinc.

3.4.5 LZT-Hs5

The total amino acids in the LZT-Hs5 sequence is 647 residues (Figure 3-5) and it shares residues homologous with LZT-Hs1, LZT-Hs2, LIV-1, LZT-Hs7 and LZT-Hs9 (Figure 3-2). There is one predicted N-linked glycosylation site, which is located intracellularly (Table 3-6). There is no strong potential PEST site and the LZT-Hs5 protein is suggested to be located on the plasma membrane (Table 3-6).

3.4.6 LZT-Hs6

LZT-Hs6 sequence contains 460 residues (Figure 3-5) and it has a close relationship with LZT-Hs4 (Figure 3-2). The LZT-Hs6 protein has two predicted N-linked glycosylation sites (Table 3-6), which are located extracellularly suggesting that the protein may be glycosylated and reside on the plasma membrane (Table 3-5). Interestingly, the first histidine residue of the H E X P H E conserved motif in the LZT-Hs6 protein in replaced with a glutamic acid residue suggesting that the LZT-Hs6 gene may transport other metal ions to zinc. The LZT-Hs6 protein is suggested to be located in vesicles (Table 3-5).

3.4.7 LZT-Hs7

The total amino acids of the LZT-Hs7 sequence is 540 residues (Figure 3-5) and it has a high homology of residues with the LZT-Hs2 and LIV-1 sequences as shown in the phylogenetic tree (Figure 3-2). Three predicted N-linked glycosylation sites are located extracellularly suggesting that the protein resides on the plasma membrane of cells and the protein is potentially glycosylated.

3.4.8 LZT-Hs8

The total amino acids in the LZT-Hs8 sequence is 654 residues (Figure 3-5) and it is present on a separate arm of the phylogenetic tree suggesting no close homology to other family member (Figure 3-2). Interestingly, there is no histidine residue identified in between transmembrane domains III and IV (Figure 3-5). Results from the study have found that the LZT-Hs8 protein resides on the plasma membrane (Table 3-5).

3.4.9 LZT-Hs9

The LZT-Hs9 sequence contains 364 residues (Figure 3-5) and it shows a close relationship with the LZT-Hs1 sequence (Figure 3-2). The LZT-Hs9 protein does not contain any glycosylation site suggesting that it may be located intracellularly. Interestingly, like LZT-Hs1 protein, the CPALLY motif is absent in LZT-Hs9 protein suggesting a similar function of subcellular location or function (Figure 3-5). Results from the study have found that the LZT-Hs9 protein resides intracellularly suggestive of the endoplasmic reticulum (Table 3-5).

3.5 Characterization of LZT subfamily and ZIP superfamily

The aim of the following discussion is to understand the role of the LZT subfamily by comparing the similarities and differences between the LZT subfamily and ZIP superfamily.

3.5.1 Similarity of transmembrane domains LZT subfamily to ZIP superfamily

One of the features of ZIP superfamily proteins includes sharing a similar membrane topology in which case the amino- and carboxy-terminal ends of the protein are located on

the outside surface of the plasma membrane and the superfamily are predicted to have 8 transmembrane domains (Guerinot 2000).

There are many transmembrane prediction methods available however only 2 computer packages were used for the transmembrane domains. These were TMpred and DAS software packages (Table 2-1), that were based on a hidden Markov model, which is a similar method to that used in ClustalW. A study has revealed that in transmembrane topology predictions, the accuracies of prediction were lower among eukaryotic sequences as compared to those obtained for prokaryote counterparts (Ikeda et al. 2002).

It appears that LZT-Hs1 possessed 8 transmembrane domains instead of 7 as predicted in Table 3-2. This may be because there is a proline residue located in transmembrane domain V of the protein sequence, which has a less hydrophobic feature, and may bias the TMpred software package prediction (Hofmann and Stoffel 1993). Nevertheless, the LZT-Hs1 has been characterized with 8 transmembrane domains due to its close homology with other family members (Figure 3-1).

Table 3-2 shows results for TMpred computer packages search indicating LZT-Hs8 and LZT-Hs9 N- terminus ends are located outside the transmembrane domains. This is unexpected as the other family members have an internal N-terminus, that includes a transmembrane domain and after cleavage in the cell, this would render the N-terminus end of the protein to be located extracellularly. A possible explanation for the discrepancy of

LZT-Hs8 and LZT-Hs9 could be that the apparent but weak detection of a shorter transmembrane domain within the N-terminus (Table 3-2).

Table 3-3 shows the results of a SignalP search for cleavage sites for all the members of LZT subfamily, and they each contain a single signal peptide cleavage site predicted to be located at the N-terminus (Emanuelsson et al. 2007). The cleavage process will remove this initial transmembrane domain and allow the remaining N-terminal sequence to be located outside the cell. This process is also observed within the ZIP superfamily sequences and this explains why the usual prediction of transmembrane domains is nine.

In general, this shows that the LZT subfamily members have 8 transmembrane domains as observed in the ZIP superfamily of zinc transporters with an additional signal peptide transmembrane domain. Figure 3-1 shows an alignment of the LZT subfamily encompassing eight transmembrane domains indicated with red color lines and roman numerals written underneath for each transmembrane domain (TM).

3.5.2 Similarity between LZT subfamily and ZIP superfamily

The protein secondary structure analysis of LZT subfamily members has provided sufficient proof that it belongs to ZIP superfamily zinc transporters. Firstly, the ZIP superfamily is predicted to contain eight transmembrane domains, an extracellular N- and C- termini region and containing a long variable region in the cytoplasmic loop between transmembrane

domains III and IV, and the discussion above has proved that the LZT subfamily sequences share the same attributes.

.

Additionally, one main character of the ZIP superfamily is the ability to transport zinc that is also shared by the LZT subfamily members. Previously, it has been shown that LIV-1 (Taylor et al. 2003) and HKE4 (Taylor et al. 2004) genes transport zinc ion despite the fact that the latter has the first histidine, H, residue of the H E X P H E motif replaced by glutamic acid, E, hence suggesting the gene might able to transport other ions. Among other family members that transport zinc or other metal ions are LZT-Hs4(Tominaga et al. 2005), LZT-Hs5 (Dufner-Beattie et al. 2003), LZT-Hs6 (Dalton et al. 2005) and LZT- Hs7 (Dufner-Beattie et al. 2004; Huang et al. 2005; Wang et al. 2004).

3.5.3 Differences of histidine rich region between LZT subfamily and ZIP superfamily

The ZIP superfamily contain a histidine rich region of H X H X H where H is for histidine residue and X refers to any substitute residue, which is present on the loop between transmembrane domain III and IV. This region is thought to be important for zinc transport. In other words, this cytoplasmic histidine region is predicted to be a metal binding domain for the ZIP superfamily of zinc transporters (Guerinot 2000).

Interestingly, in the LZT subfamily, the histidine repeats occur throughout the sequence, mainly in the extracellular N terminus, between transmembrane II and III, and between

transmembrane IV and V (Figure 3-5). It is observed that the LZT-Hs2 and the LIV-1 proteins contain the highest number of histidine repeats within the LZT subfamily, in contrast to LZT-Hs9, which contains only 1 histidine residue.

The total number of histidine residues in the variable loop between transmembrane III and IV for LZT-Hs1 protein is 9 histidine residues. LZT-Hs2 contains 20 histidine, LIV-1 contains 21 histidine, LZT-Hs4 contains 7 histidine, LZT-Hs5 contains 6 histidine, LZT-Hs6 contains 5 histidine, LZT-Hs7 contains 6 histidine, LZT-Hs8 has none, and finally, LZT-Hs9 contains only 1 histidine residue in this region. Obviously, all members except LZT-Hs8 (none), a high number of histidine residues and this raised the question if LZT-Hs8 gene functions differently to others or for example, it may not preferentially transport zinc but other metal ions.

Another important feature of the region between transmembrane domains III and IV it contains a mixed charge region. In the ZIP superfamily, it is predicted that the zinc ion is taken up as a divalent cation that has a strong tendency to form tetrahedral complexes to exert its function (Guerinot 2000). Importantly, the LZT subfamily possess a mixed charge region in the same place as the ZIP superfamily variable region is, which the latter is predicted as a binding region for metal ion, for example, zinc ion.

The mixed charge region prediction for the LIV-1 family was achieved by using the SOSUI (Hirokawa et al. 1998) software package revealing the location and presence of charged residues in the variable loop between transmembrane domains III and IV (Table 3-4). The

mixed charge region is a region of unbalanced quantity of charge in the variable loop and may play a role in binding and transport divalent cations such as zinc. Among the negative charged amino acids are D, aspartic acid residue and E, glutamic acid residue, in contrast, the positive charged amino acids are K, lysine residue and R, arginine residue. Molecules that add polarity to the region are the N, asparagine residue, Q, glutamine, S, serine and Y, tyrosine residues. Importantly, this region possesses a mixed charge region and also contain many high polarity molecules suggesting that the region may be important for metal ion transport for the LZT subfamily.

All the LZT subfamily members have less residues with negative charges compared to the number of residues with positive charges (Table 3-4), however, even with weak negative surface potential such as this, divalent cations could still be attracted through the membrane. There were equal number of positive and negative charges for LZT-Hs1, and in contrast, LZT-Hs2 has only 2 residues with negative charges and 7 residues with positive charges. LIV-1 has 4 residues with negative charges but 10 residues of positive charges. Interestingly, LZT-Hs4 has an equal number of positive and negative residues in this mixed charged region, and LZT-Hs5 has 9 residues with negative charges and only 4 residues with positive charges. Overall, LZT-Hs6, LZT-Hs7, LZT-Hs8 and LZT-Hs9 hold only 3, 1, 4 and 1 negative residues, respectively, as compared to 5, 4, 5 and 1 positive residues.

The polarity of the protein may be important for helping the divalent zinc ions pass through the transmembrane domains. In Table 3-4 it is shown that in total LZT-Hs1 have 6 residues

with polarity, LZT-Hs2 has 9, LIV-1 has 11 residues, LZT-Hs4 has 12 residues and LZT-Hs5 has only 4 residues that could add polarity to the mixed charged region. LZT-Hs6, LZT-Hs7, LZT-Hs8 and LZT-Hs9 has 6, 5, 7 and 3 residues with polarity, respectively.

3.5.4 Differences between LZT subfamily and ZIP superfamily

There are four differences between the LZT subfamily and the ZIP superfamily zinc transporters; firstly, there are sevenfold more histidine rich repeats in the LZT subfamily than in the ZIP superfamily of zinc transporters. Secondly, the conserved region of H E X P H E X in the LZT subfamily is a unique motif with a potential metalloprotease ability that is not found in the ZIP superfamily of zinc transporters. Thirdly, the LZT subfamily members have a long N-termini compare to the ZIP superfamily of zinc transporters and finally, the possibility of a pore structure formation between transmembrane III and IV, which includes with transmembrane II, and the conserved mixed charge region may suggest a mechanism of zinc transport.

3.6 Predicted functional site in members of LZT subfamily

The Eukaryotic Linear Motif (ELM) software packages predict small functional sites of proteins from the sequences. The computer software package also predicts the protein-protein interaction, regulation of the protein by phosphorylation, acetylation or other post-translational modification or the proteins' cell compartment targeting (Puntervoll et al. 2003).

Table 3-7 shows the summary of the predicted functional sites for the LZT subfamily.

3.6.1 Proline-Directed Kinase phosphorylation site: ([S/T])P motif

One motif that is shared by all 9 of the LZT subfamily members is the proline-directed kinase site with the sequence formula of **([S / T]) P** , where S is serine, T is threonine and P is proline residue. This motif consists of a serine/threonine residue preceding a proline residue that is required to activate the kinase enzymatic function such as phosphorylation process.

3.6.2 MAPK interacting molecule

A large family of MAP and CDK-like kinases recognize this motif. The MAPK kinase and the extracellular-signal-regulated kinases (ERK) are responsible for sending proliferation and mitogenic signals. Generally, the mechanism involves sending signals from the cellular surface to the nucleus by activation of transcription factors. This motif is observed on proteins present in the nucleus and cytosol of the cell suggesting the proteins may be involved in cell proliferation. As can be seen in Table 3-7, within the LZT subfamily, most of the respective members are found to possess one of these motifs.

Table 3-1: LZT subfamily gene nomenclature

LIV-1 family gene	Protein name	Human gene name	Sequence Accession number
LZT-Hs1	HKE4	SLC39A7	NM_006979
LZT-Hs2	ZIP10	SLC39A10	NM_020342
LIV-1	LIV-1	SLC39A6	NM_012319
LZT-Hs4	ZIP14	SLC39A14	NM_015359
LZT-Hs5	ZIP4	SLC39A4	NM_173596
LZT-Hs6	BIGM103	SLC39A8	NM_022154
LZT-Hs7	ZIP5	SLC39A5	NM_173596
LZT-Hs8	ZIP12	SLC39A12	NM_152725
LZT-Hs9	ZIP13	SLC39A13	NM_152264

The information gathered from text-based search using National Center for Biotechnology Information (NCBI) for the nucleotide and protein sequences information.

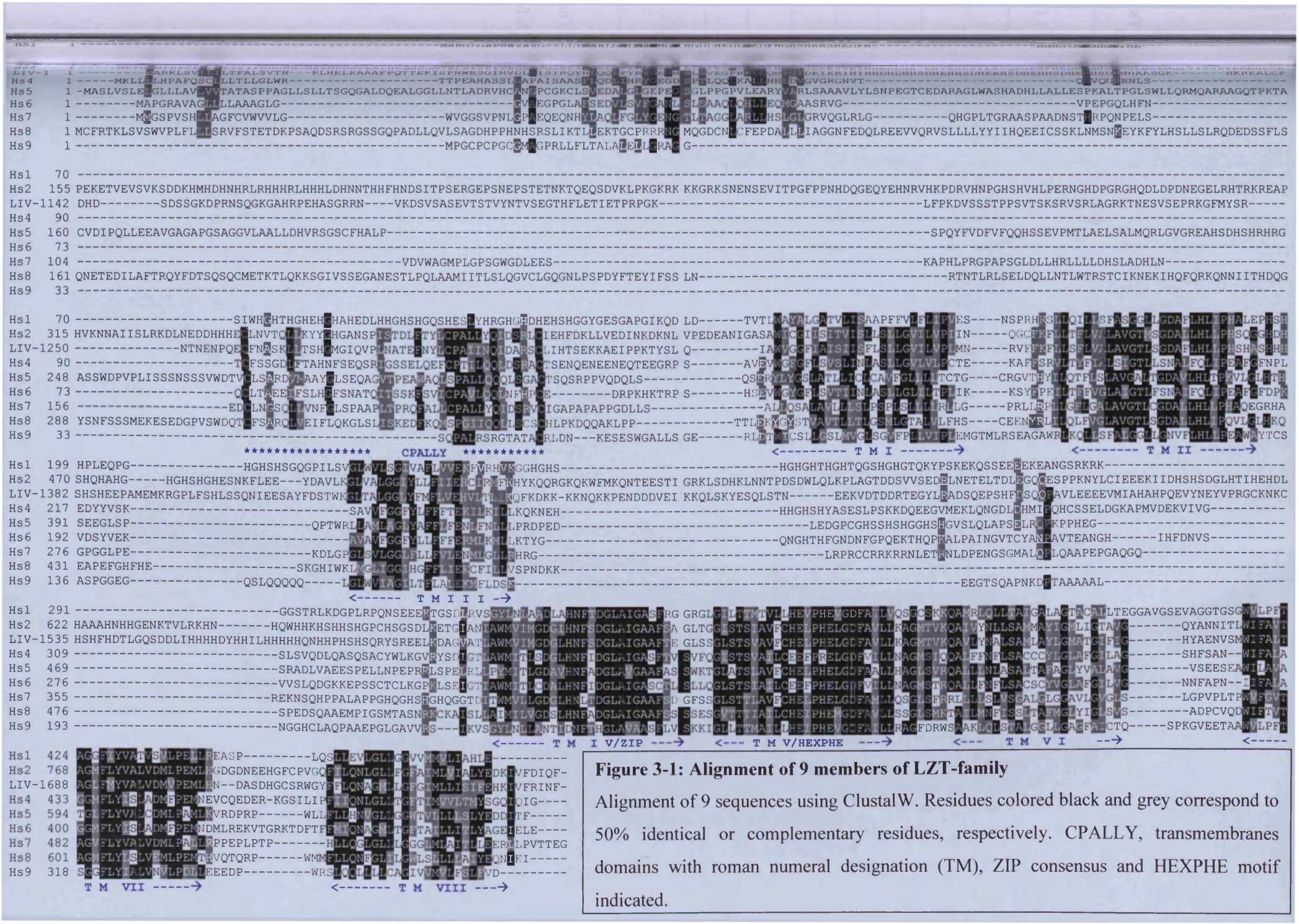

Figure 3-1: Alignment of 9 members of LZT-family

Alignment of 9 sequences using ClustalW. Residues colored black and grey correspond to 50% identical or complementary residues, respectively. CPALLY, transmembranes domains with roman numeral designation (TM), ZIP consensus and HEXPHE motif indicated.

Figure 3-2: Phylogenetic tree representing LZT subfamily

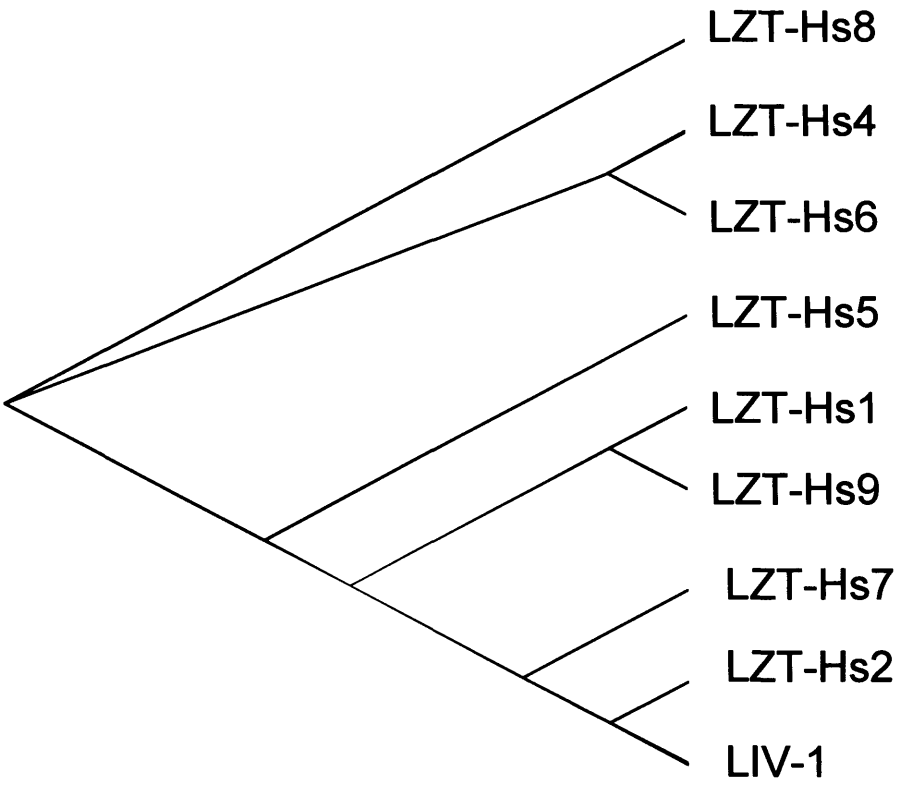

Alignment of the multiple sequences of the LZT subfamily genes analysis result converted into the phylogenetic tree presentation by using TreeView software. The tree shows three main clusters within the LIV-1 family indicating the relationship within the LZT subfamily.

Table 3-2: Prediction of LZT subfamily transmembrane (TM) domains topology

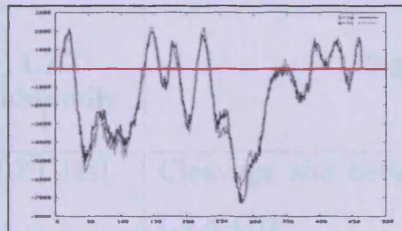 LZT-Hs1 protein has N-terminus inside and 7 strong transmembrane helices.	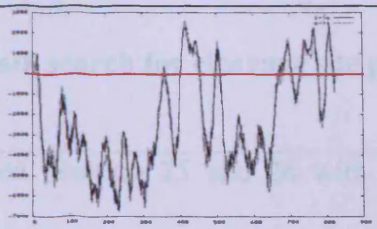 LZT-Hs2 protein has the N-terminus inside and 8 strong transmembrane helices.	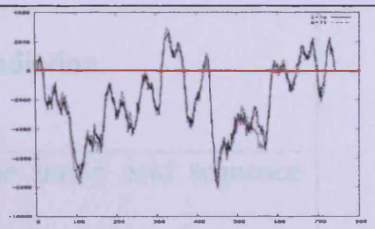 LIV-1 protein has the N-terminus inside and 9 strong transmembrane helices.
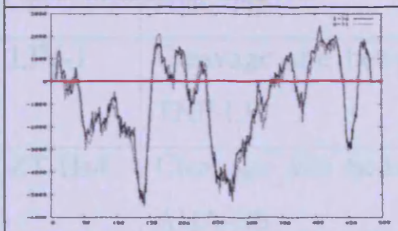 LZT-Hs4 protein has the N-terminus inside and 9 strong transmembrane helices.	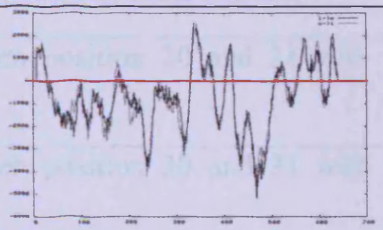 LZT-Hs5 protein has the N-terminus inside and 9 strong transmembrane helices.	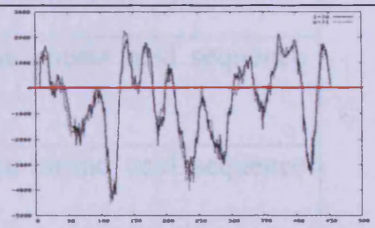 LZT-Hs6 protein has the N-terminus inside and 9 strong transmembrane helices.
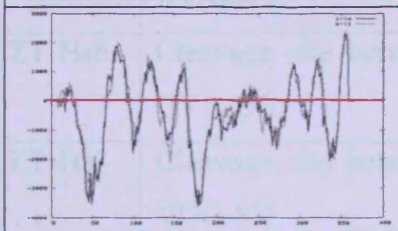 LZT-Hs7 has the N-terminus inside and 9 strong transmembrane helices.	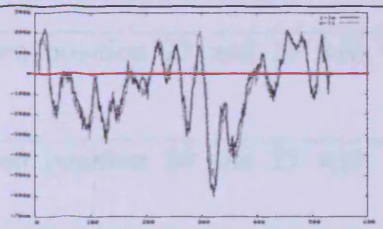 LZT-Hs8 protein has the N-terminus outside and 10 strong transmembrane helices.	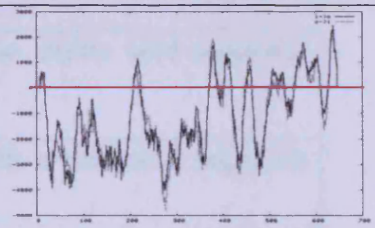 LZT-Hs9 protein has the N-terminus outside and 8 strong transmembrane helices.

The information of transmembrane domains topology gathered from TMpred software packages. The red line is the basal score for the weight-matrices values of the protein and the plot above the score is the prediction topology of the protein.

Table 3-3: Predicted cleavage sites for LZT subfamily

LZT subfamily	SignalP search for cleavage site prediction
LZT-Hs1	Cleavage site between position 25 and 26 with the amino acid sequence LVA-GH
LZT-Hs2	Cleavage site between position 25 and 26 with the amino acid sequence NHC-HE
LIV-1	Cleavage site between position 20 and 21 with the amino acid sequence TNP-LH
LZT-Hs4	Cleavage site between position 30 and 31 with the amino acid sequence AHA-SS
LZT-Hs5	Cleavage site between position 22 and 23 with the amino acid sequence ATA-SP
LZT-Hs6	Cleavage site between position 22 and 23 with the amino acid sequence GVA-EG
LZT-Hs7	Cleavage site between position 24 and 25 with the amino acid sequence VGG-SV
LZT-Hs8	Cleavage site between position 23 and 24 with the amino acid sequence VFS-TE
LZT-Hs9	Cleavage site between position 32 and 33 with the amino acid sequence AGG-SQ

The location of signal peptide cleavage sites in amino acid sequences obtained from SignalP 3.0 software packages.

Table 3-4: Predicted polarity and charge residues between transmembrane III and IV

LZT subfamily members	D	E	K	R	N	Q	S	Y
LZT-Hs1	2	3	3	2	1	1	4	-
LZT-Hs2	1	1	6	1	-	4	4	1
LIV-1	2	2	8	2	2	4	3	2
LZT-Hs4	2	1	3	1	1	4	5	2
LZT-Hs5	3	6	-	4	1	-	3	-
LZT-Hs6	1	2	5	-	-	1	4	1
LZT-Hs7	-	1	1	3	1	2	2	-
LZT-Hs8	2	2	4	1	2	1	4	-
LZT-Hs9	-	1	-	1	1	1	1	-

The site of charge residues were obtained from SOSUI software package, (+) indicates the positive charges and, (-) for negative charges. The residues involved are D for aspartic acid, E for glutamic acid, K for lysine, R for arginine, N for asparagine, Q for glutamine, S for serine, and Y for tyrosine. Residues D and E represents the negative charges, whilst K and R are the positive charges, and N, Q, S, Y are residues of polarity.

Figure 3-3: Two conserved motif of HNF and HEXPHE in transmembrane IV and V

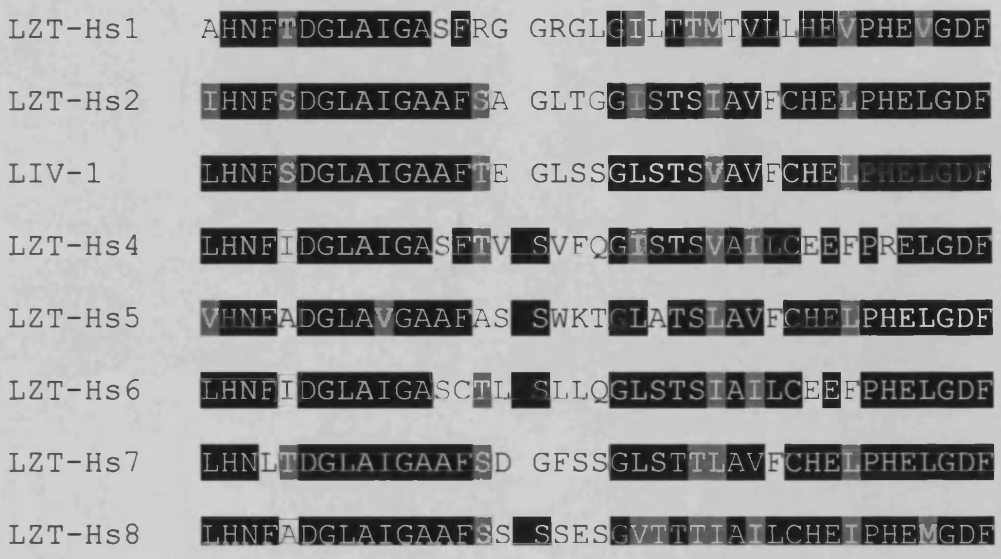

The HNF motif and HEXPHE conserve motif observed in the nine members of LZT subfamily. In the transmembrane domain IV, the histidine, H, residue in LZT-Hs9 gene lost the conserved motif and replaced by aspartic acid, D, residue. In the transmembrane domain V, LZT-Hs4 and LZT-Hs6 genes were observed to possess the glutamic acid, E, residue instead of histidine residue in the conserved motif sequence in contrast to other family members.

Figure 3-4: CPALLY motif in the LZT subfamily

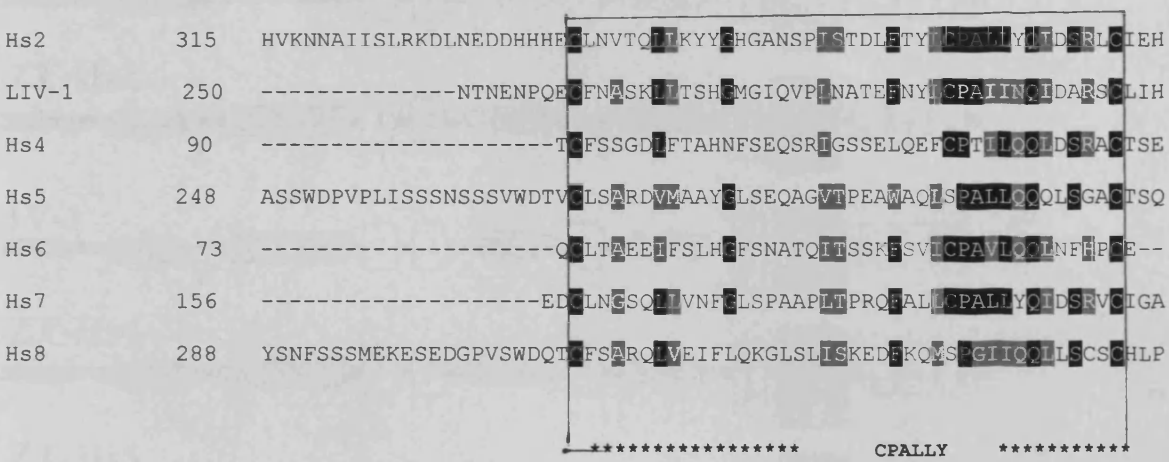

The information extracted from the Boxshade3.2 analysis result and with 50% homology, the black shaded letters are identical residues while the grey letters are complementary residues found within the LZT subfamily. It is obvious that in LZT-Hs1 and LZT-Hs9 their CPALLY motif replaced by other amino acid suggestive of these genes function differently without this motif (not shown).

Figure 3-5: Schematic diagram of LZT subfamily member's tertiary structure

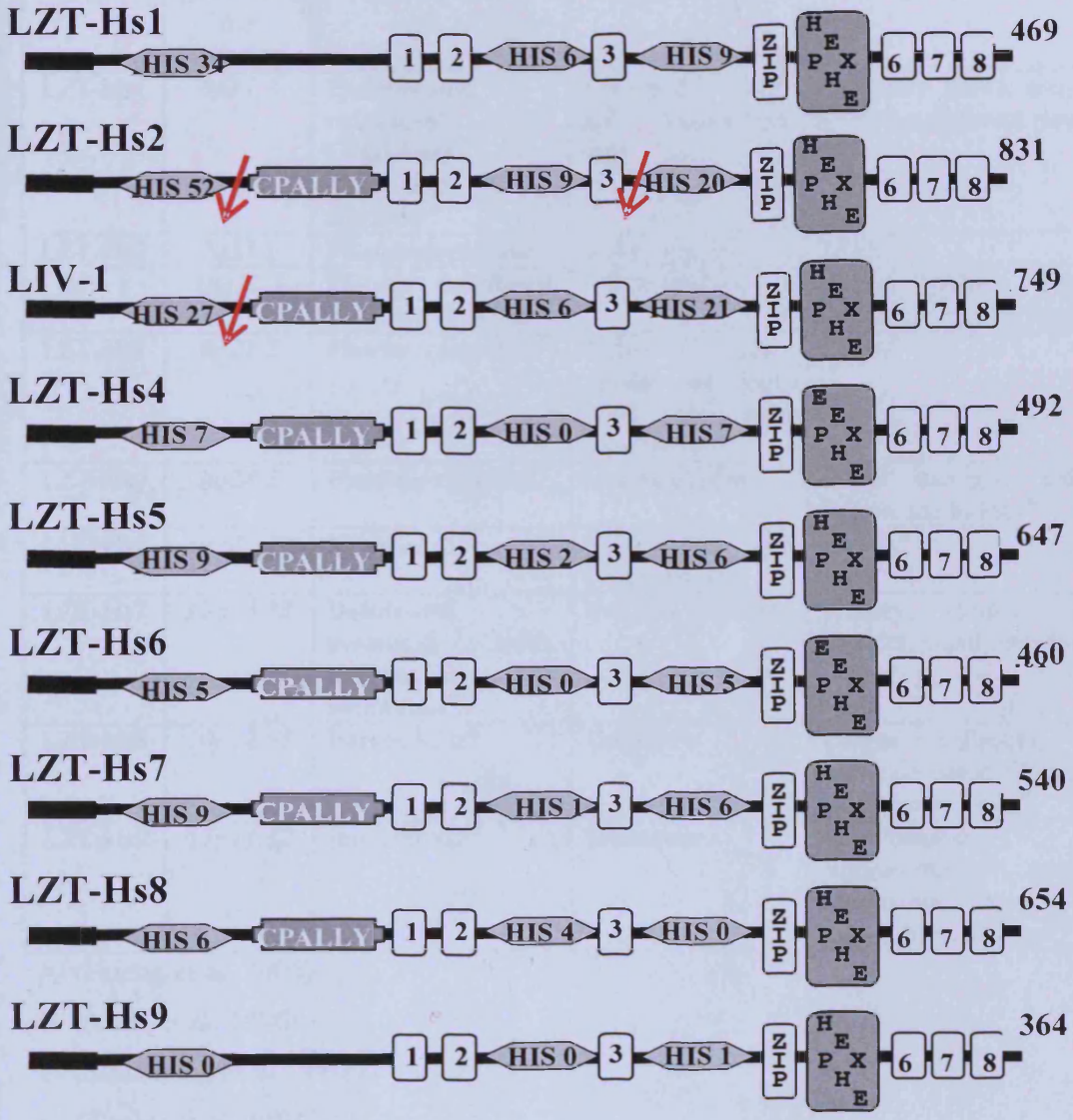

The schematic diagram is a compilation of information from the computer search for each member of the LZT subfamily.

Table 3-5: Summary of LZT subfamily predicted function and localization

LZT	Chromosome location	Location in cells	Known Function	Distribution in tissues
LZT-Hs1	*6p21.3*	Endoplasmic reticulum [H] Golgi body [A] Membrane fraction[C]	Transport zinc and manganese ions	mammary gland, esophagus, lymph node, breast tumor tissue, placenta[B]
LZT-Hs2	*2q33.1*	Plasma membrane	Influx zinc ion	Testis[B]
LIV-1	*18q12.1*	Plasma membrane and lamellipodiae[D]	Influx zinc ion	Breast cancer, pituitary tumor, breast, embryonic stem[B]
LZT-Hs4	*8p21.2*	Plasma membrane[E]	Influx zinc, uptake of iron; bind to non-transferrin	Colon[B]
LZT-Hs5	*8q24.3*	Plasma membrane	Uptake of zinc[F]	Small intestine, stomach, colon, cecum and kidney[B]
LZT-Hs6	*4q22-q24*	Vesicles	Influx zinc and cadmium ions	Cervix[B]
LZT-Hs7	*12q13.13*	Basolateral polarized cells, plasma membrane[G/N]	Remove zinc ion	Kidney, stomach tumor tissue, bladder, small intestine, rectum[B]
LZT-Hs8	*10p12.33*	Intracellular[N]	Unknown	corpus callasum, hippocampus, kidney, tumor tissue, retina, brain, Alzheimer cortex[B]
LZT-Hs9	*11p11.12*	Intracellular[N]	Unknown	glioblastoma multiforme, liposarcoma, squamous cell carcinoma, bone, lung tumour, cervix tumour tissue[B]

A- (Huang et al. 2005)

B- (Ando et al. 1996)

C- (Strausberg et al. 2002)

D- (Taylor et al. 2003)

E- (Taylor et al. 2005)

F- (Kury et al. 2002)

G- (Wang et al. 2004)

H- (Taylor et al. 2004)

N- Demonstrated in next chapter: Engineering LZT-Hs7, LZT-Hs8 and LZT-Hs9 recombinants

Table 3-6: Summary of LZT subfamily glycosylation sites and molecular weight

LIV-1 family gene	N-linked glycosylation located in N-terminal [b]	N-linked glycosylation located intracellular [b]	Predicted molecular weight of the protein (kDalton) [c]
LZT-Hs1	nil	2	49.915
LZT-Hs2	5	5	94.131
LIV-1	4	2	84.282
LZT-Hs4	3	nil	54.059
LZT-Hs5	1	nil	68.421
LZT-Hs6	1	2	49.630
LZT-Hs7	2	1	56.361
LZT-Hs8	5	1	72.805
LZT-Hs9	nil	1	38.352

[b] Based on the search using NetNglyc 1.0 Server

[c] Based on the search using Compute pI/Mw

Table 3-7: Summary of LZT subfamily predicted functional sites

Function sites [d]	Importance of the functional site	LZT family matched to sequence	Nucleotide sites found at
...([S/T])P...	Proline-Directed Kinase phosphorylation site	LZT-Hs2	5 sites (199,245,350,550,588)
MAPK interacting molecules	Carry docking motif to regulate specific interaction MAPK cascade	LZT-Hs1 LIV-1 LZT-Hs6 LZT-Hs7 LZT-Hs8 LZT-Hs9	3 sites (164, 310,377) 1 site (76) 1 site (147) 2 sites (239, 442) 2 sites (502,532, 533) 2 sites (105, 212)

[d] This information was abstracted from the ELM software packages search and below is a schematic representation of the transmembrane domains depicting the MAPK predicted sites. (LZT-Hs4 and LZT-Hs5 predicted sites are not found)

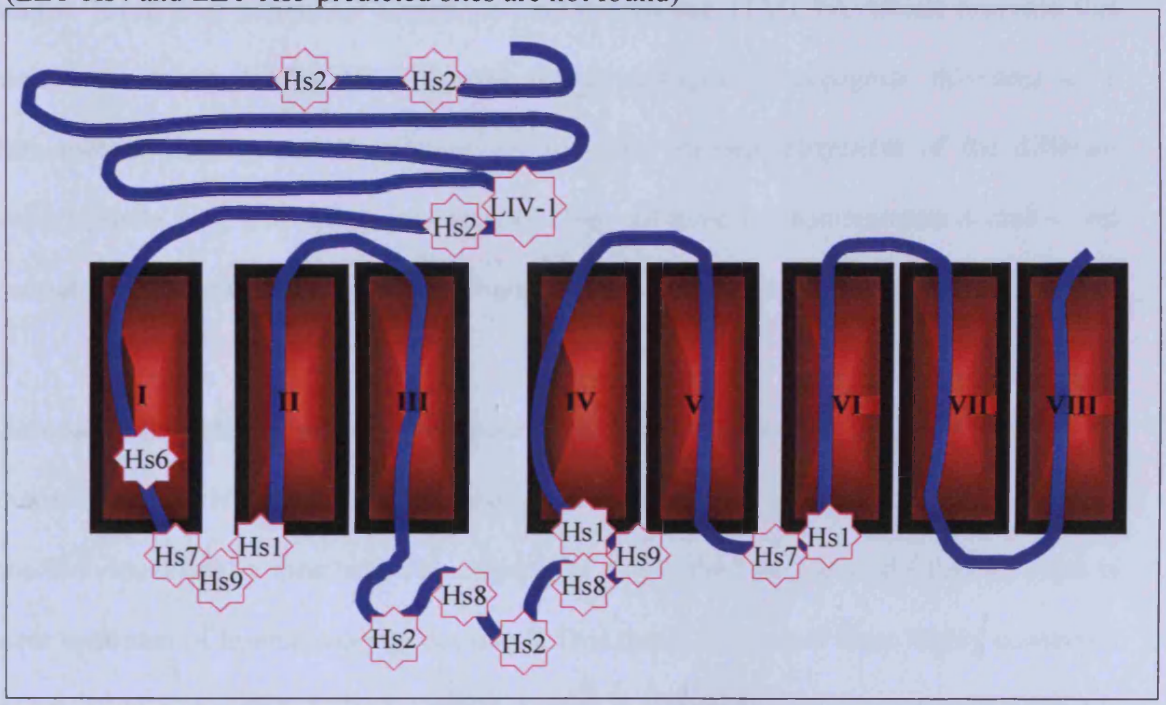

3.7 Discussion

This chapter used several computer prediction softwares to investigate the similarities and differences in the protein sequence of the 9 members of the LZT subfamily. The alignment of the sequences using ClustalW confirmed that these family members have extremely conserved regions that coincide with the transmembrane domains. These proteins are predicted to be zinc influx transporters with a complex transmembrane structure that may provide a pore for zinc to be transported across. It is therefore not surprising that the transmembrane domains are conserved and these would represent the main functional regions of the molecules. The software prediction packages for transmembrane domains can sometimes be erroneous, as their alogorithms do not allow for the presence of any proline residues. There is a conserved proline in transmembrane (TM) IV, which prevents this domain from being recognised. However some packages do recognise this area as a transmembrane domain and in conjunction with the obvious alignment of the different members (Table 3-2), it is valid conclusion that they all have 8 transmembrane domains, and not counting the signal peptide transmembrane domain at the N-terminus end.

Additionally, this alignment of 9 sequences also demonstrates the long and variable N-terminus region. This suggests that this region contains motifs that may regulate the function of the individual family members. An example of this is the motif termed CPALLY, that is present upstream of transmembrane domain I. This motif consists of three highly conserved cysteine residues as well as a single proline residue. It is entirely possible that this motif folds over the pore of the zinc transporter and is able to control the opening and closing of the pore

and hence regulate the transport of zinc across the membrane. Interestingly, there is a fourth cysteine positioned immediately preceding the HEXXH motif in transmembrane IV, which would reside in close proximity to the CPALLY motif in the tertiary structure. Furthermore, there are two exceptions to this. LZT-Hs1 and LZT-Hs9 not only have no CPALLY motif but they also have no cysteine preceding the HEXXH motif. Additionally, LZT-Hs1 is known to reside intracellularly on endoplasmic reticulum membranes and perhaps this data suggests that the CPALLY motif is only important for molecules responsible for zinc influx into the cell.

Furthermore, the computer analysis predicts many N-linked carbohydrate side chains for these family members within the N-terminus region which would be located extracellularly if they were present on the plasma membrane. Again, LZT-Hs1 and LZT-Hs9 are the exception and contain no such predicted side chains. LZT-Hs1 resides in the endoplasmic reticulum and therefore it would not be glycosylated. These data also suggest that LZT-Hs9 would be predicted to also reside intracellularly.

The computer searches had identified 2 out of 9 members of the LZT subfamily to have the PEST sites in their sequences. These sites are suggestive that the proteins undergo post-translational proteolytic processing within the cell. Both LZT-Hs2 and LIV-1 have PEST sites. Recent results in the Tenovus Centre for Cancer laboratories, using 2 different antibodies to LIV-1 (one to the start and another to the end of the N-terminus) have demonstrated that LIV-1 is cleaved at the N-terminus before it relocates to the plasma

membrane. This conclusion was reached as the antibody that detected the epitope near the N-terminus did not recognise the plasma membrane located LIV-1, whereas the second antibody, positioned downstream of the PEST site recognised the LIV-1 positioned on the plasma membrane. As LZT-Hs2 is the other protein with the PEST sites it is predicted that it may also undergo post-translational processing before it would relocates itself to the plasma membrane to transport zinc ions. Interestingly, LZT-Hs2 also had the most homologous sequence to LIV-1 as shown in the phylogenetic tree (Figure 3-2), suggestive that it may be processed in the cell in the same way as LIV-1.

The alignment of the 9 members of the LZT subfamily has revealed a unique motif within the sequences with the sequence HEXPHE. This is in contrast to the ZIP superfamily of zinc transporters, which have a HXXXE motif in transmembrane domain V. In the LZT subfamily, the motif is located in transmembrane V and the pore formation is suggestive of transporting zinc ions across the cell's membrane. Among the 9 members of the LZT subfamily, there are 2 proteins which have been identified that have the first residue, histidine, of the HEXPHE motif, replaced by another residue, glutamic acid, E. This change amino acid residue may be indicative of a preferences for transport of metal ions other than zinc (Liuzzi et al. 2006).

There is also a difference in the amount of histidine rich repeats between the LZT subfamily and to the ZIP superfamily of zinc transporters, that is the former contains seven fold more histidines (Taylor et al. 2003). The ZIP superfamily histidine repeats are only found in

transmembrane III and IV whereas the LZT subfamily has histidine repeats throughtout its sequence (Figure 3-5). It was observed that LZT-Hs2 and LIV-1 genes have the highest number of histidine repeats whilst LZT-Hs9 contains only 1 histidine in the region between transmembrane domains III and IV. A high number of histidines is suggestive of zinc ion coordination in the structure and the presence of only 1 histidine in LZT-Hs9 may imply a role increasing the catalytic activity rather than binding zinc (Little 1977). In contrast, LZT-Hs8 does not contain any histidines residue in the region between transmembrane domains III and IV and this is suggestive of impaired zinc transport activity.

Finally, the mixed charge region, which is located between transmembrane domains III and IV, is possibly involved in the transport mechanism of the zinc ions. Zinc ions are divalent cations and areas of protein of mixed charge are thought to be more reactive and involved in binding of zinc ions. It has been shown that the concentrations of divalent ions are increased near the channel mouth by a weak negative surface potential (Adam 1980). Table 3-4 shows that almost all of the LZT subfamily members have a substantial mixed charged region on the loop between transmembrane domains III and IV, and this might provide the activity needed to bind zinc ions. It is suggested that the divalent zinc ions would act an opposite attraction to allow them to pass through transmembrane domains. Additionally, the residues with high polarity might encourage transport of zinc ions. Interestingly, the potential proline-directed kinase phosphorylation sites in the cytoplasmic region of LZT-Hs2 (2 sites found), and the predicted sites of MAPK cytoplasmic region of LZT-Hs1 (3 sites), LZT-Hs7, LZT-Hs8 and LZT-Hs9 (each protein has 2 sites found in cytosol), were discovered in some

members of the LZT subfamily. Together with the knowledge that MAP kinase pathway is involved in breast cancer progression may suggest an important role of these molecules in cell models.

The analysis of the sequences performed in this chapter has enabled us to confirm that LZT-Hs7, LZT-Hs8 and LZT-Hs9 are indeed members of the LZT subfamily of zinc transporters. At the start of this project, none of these molecules had previously been investigated in cells. It was therefore the intention to clone LZT-Hs7, LZT-Hs8 and LZT-Hs9 into a vector to allow expression in mammalian cells. This would enable these molecules to be characterized for cellular location and zinc transport ability.

Chapter 4

Cloning LZT-Hs7, LZT-Hs8 and LZT-Hs9 recombinants

In this chapter, the sub-cellular distribution of the LZT-Hs7, LZT-Hs8 and LZT-Hs9 proteins was investigated. In addition, the capacity of these proteins to transport zinc ions was investigated. The approach adopted to express these proteins in naïve cells was using the pcDNA/FRT/V5-His TOPO®TA vector. It was therefore necessary to clone LZT-Hs7, LZT-Hs8 and LZT-Hs9 recombinants.

4.1 Positive clones' analysis

LZT-Hs7, LZT-Hs8 and LZT-Hs9 genes were exponentially amplified using the polymerase chain reaction (PCR), which was optimized for each of the genes, Figure 4-1 shows the PCR results for LZT-Hs7, LZT-Hs8, LZT-Hs9 and demonstrates band sizes of approximately 1686, 1962 and 1094 basepairs respectively. These values are in accordance with their predicted sizes. The PCR procedure used two control genes to confirm the PCR technique, which are our 'in-house' LIV-1 gene, and a vector without any gene insertion. Of all the PCR products, only LZT-Hs9 appeared to have two bands instead of a single PCR product. Since it was unclear what the upper band represented, the LZT-Hs9 1094 band was isolated by low melt gel purification. Importantly, the figure also shows the strong signal intensities of all the PCR products which indicates an adequate quantity of DNA has been produced allowing to

proceed to the next procedure, to clone them individually into the pcDNA5/FRT/V5-His-TOPO® TA vector.

This vector was selected to drive expression of the recombinant proteins in mammalian cells by the CMV promoter. The oligonucleotides had been designed to incorporate the relevant gene downstream of the CMV promoter. The 3'- oligonucleotide removed the stop codon from the sequence at the C-terminal end in order that the V5 tag was included on the C-terminal end of the recombinant protein (in the case of LZT-Hs9). This would enable detection of the recombinant protein by Western blot and by immunofluorescence. The other two genes (unlike LZT-Hs9) LZT-Hs7 and LZT-Hs8, had a C-terminal V5 tag that originated from the vector, instead of inserting the sequence in their 3'- oligonucleotide.

Having confirmed the correct genes for LZT-Hs7, LZT-Hs8 and LZT-Hs9, they were cloned into the mentioned vector and *Escherichia coli* was then transformed with the plasmids. The bacteria were then grown and the plasmid purified using an endotoxin free plasmid purification kit to enable expression in mammalian cells by transient transfection. Before the plasmid was purified it was important to check the colonies for the correct gene insertion. This was achieved by PCR using the 5' oligonucleotide for each insert, and a 3' oligonucleotide for BGH, 141 residues downstream of the multiple cloning sites.

4.1.1 LZT-Hs7

As may be seen in Figure 4-2, the PCR procedure confirmed the LZT-Hs7 gene was inserted into the pcDNA5/FRT/V5-His-TOPO® TA vector in the correct orientation and gave a band

of approximately 1827 basepairs in all of the 9 lanes. Although in each instances, the PCR signal was good, indicating an approximately high concentration of product, lanes 2, 3 and 7 show contaminations with double bands or a PCR product of an inappropriately large size. Only clones 1, 4, 5, 6, 8 and 9, therefore, are suitable for making large-scale plasmid preparations to enable the detection of the LZT-Hs7 recombinant protein.

4.1.2 LZT-Hs8

As may be seen in Figure 4-3, the PCR procedure confirmed the LZT-Hs8 gene was inserted into the pcDNA5/FRT/V5-His-TOPO® TA vector in the correct orientation and gave a band of approximately 2103 basepairs in only a lane. There were no bands in lanes 2, 3, 4, 5, 7, 8, 9 and 10, however, lane 6 has a PCR product of an inappropriately large size. Only clone 1, therefore, is suitable for making large-scale plasmid preparations to enable the detection of the LZT-Hs8 recombinant protein.

4.1.3 LZT-Hs9

As may be seen in Figure 4-4, the PCR procedure confirmed the LZT-Hs9 gene was inserted into the pcDNA5/FRT/V5-His-TOPO® TA vector in the correct orientation and gave a band of approximately 1235 basepairs in lanes 14 and 15. Although in each instances, the PCR signal was good, indicating an approximately high concentration of product, lanes 3, 5, 7, 8, 9, 10 and 11 show contaminations with double bands. There were no bands detected in lanes 1, 2, 4, 6, 12 and 13. Only clones 14 and 15, therefore, are suitable for making large-scale plasmid preparations to enable the detection of the LZT-Hs9 recombinant protein.

To summarize, the LZT-Hs7 has six positive recombinant clones, whilst LZT-Hs8 has only one positive recombinant clone and two positive recombinant clones were obtained for LZT-Hs9. Since, any contaminants in the PCR products must be avoided, only the positive recombinant clones were taken forward for large-scale plasmid preparation to enable transfection of mammalian cells and testing for expression of recombinant protein.

4.2 Western blot analysis

This technique allows the identification the recombinant proteins of LZT-Hs7, LZT-Hs8 and LZT-Hs9 by detection of their V5 epitope and Figure 4-5 shows their expression of the 3 LZT family members in CHO cells, following their transfection with the pcDNA5/FRT/V5-His-TOPO® TA vector. Recombinant protein sizes of 63 kDalton, 73 kDalton and 43 kDalton were determined by automated Rf value analysis for LZT-Hs7, LZT-Hs8 and LZT-Hs9, respectively.

The chemiluminescent detection used SuperSignal®Femto Maximum Sensitivity Substrate for LZT-Hs7 and LZT-Hs9 recombinant proteins and SuperSignal®Dura Maximum Sensitivity Substrate for LZT-Hs8. Subsequently, the signals were imaged using AlphaDigiDoc Innotech Imaging system and the Rf value of the recombinant proteins automatically calculated using AlphaDigiDoc computer software for the 3 LZT family members' recombinant proteins sizes.

Figure 4-1 : PCR products of LZT-Hs7, LZT-Hs8 and LZT-Hs9 genes

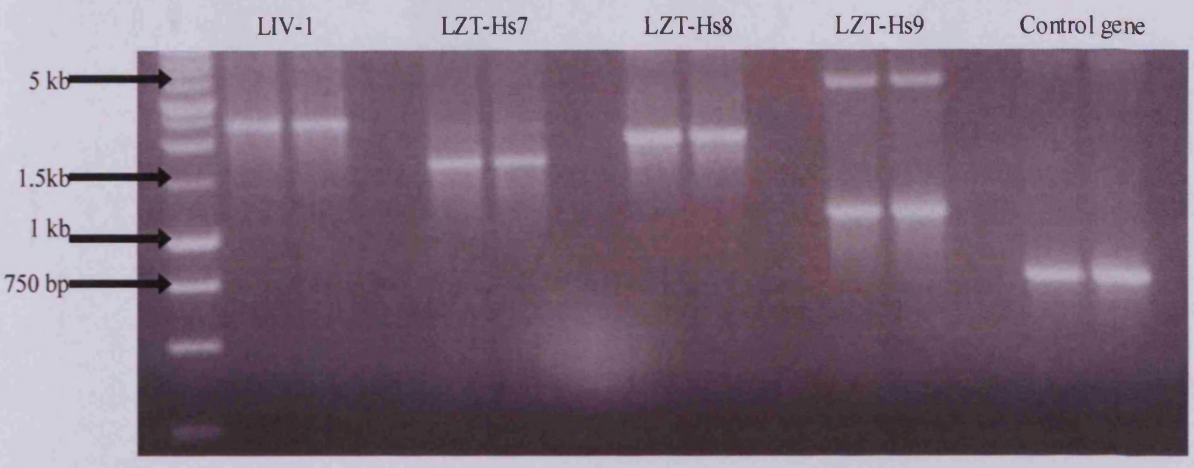

The gel shows PCR products for LIV-1, LZT-Hs7, LZT-Hs8, LZT-Hs9 and the control vector gene in duplicates samples. The band sizes of the LZT family members were approximately 2223 basepairs, 1686 basepairs, 1962 basepairs and 1094 basepairs, respectively. The far left lane is the DNA molecular weight marker ladder.

Figure 4-2: PCR product of LZT-Hs7 transformed colonies for orientation analysis

The gel shows the PCR products of 9 LZT-Hs7 transformed colonies isolated for orientation analysis. The primers used were the forward primer of LZT-Hs7 and the reverse sequencing primer of the vector, BGH, a band size of 1827 basepairs was detected. The far left is the molecular weight marker ladder.

Figure 4-3: PCR product of LZT-Hs8 transformed colonies for orientation analysis

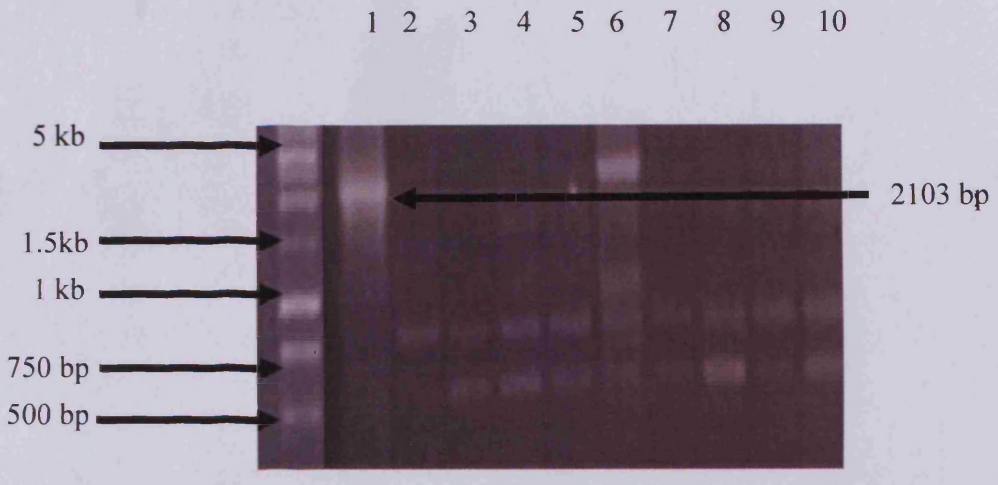

The gel shows PCR products of 10 LZT-Hs8 transformed colonies isolated for the orientation analysis. The primers used were the forward primer of LZT-Hs8 and the reverse sequencing primer of the vector, BGH, a band size of 2103 basepairs was detected only in lane 1. The far left is the molecular weight marker ladder.

Figure 4-4: PCR product of LZT-Hs9 transformed colonies for orientation analysis

The gel is shows PCR products of 15 LZT-Hs9 transformed colonies isolated for orientation analysis. The primers used were the forward primer of LZT-Hs8 and the reverse sequencing primer of the vector, BGH, a band size of 1235 basepairs was detected. The far left is the molecular weight marker ladder.

Figure 4-5: Western blot analysis of the LZT-Hs7, LZT-Hs8 and LZT-Hs9 recombinants to determine their recombinant protein sizes

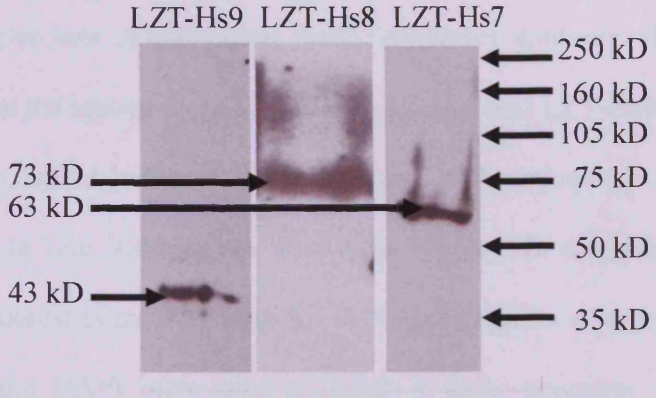

The Western blot membrane shows the LZT-Hs7, LZT-Hs8 and LZT-Hs9 recombinant proteins expressed in CHO cells, following transient transfection. The cells were harvested 24 hours post transfection and 40 µg of protein lysate used as protein sample. The proteins were separated using SDS-Page electrophoresis, transferred onto nitrocellulose membrane and probed with anti-V5 antibody. The LZT-Hs7 protein size is 63 kDalton, LZT-Hs8 protein size is 73 kDalton and LZT-Hs9 protein size is 43 kDalton. The far right lane shows the position of the protein molecular weight markers.

4.3 Immunofluorescence studies

An immunofluorescence technique was used to assess the subcellular distribution of the LZT-Hs7, LZT-Hs8 and LZT-Hs9 in the Chinese Hamster Ovary (CHO) transfected cells. The technique employs two sets of antibodies; firstly, a primary antibody which detects the V5 antibody embedded in the recombinant LZT-Hs7, LZT-Hs8 and LZT-Hs9 fusion proteins ,and secondly, a dye-coupled antibody, Alexa Fluor 488-conjugated antimouse that fluoresces green. Only in one instance, as shown in Figure 9D that Alexa Fluor 594-conjugated antimouse fluoresces red was used for LZT-Hs9 positive recombinant detection. Texas Red Phalloidin and DAPI were used to detect F-actin structures and cell nuclei respectively. Result of this study are shown in Figures 4-6, 4-7 and 4-9, for LZT-Hs7, LZT-Hs8 and LZT-Hs9 recombinant proteins respectively

As may be seen in Figure 4-6A, the LZT-Hs7 recombinant protein is located on the plasma membrane and in the lamellipodiae of transfected CHO cells in non-permeabilised buffer conditions. As expected, the staining of F-actin structures showed red immunofluorescence in all CHO cells as shown in Figure 4-6B, contrasting with the low efficiency of transfection of the recombinant protein as shown in Figure 4-6A and 4-6C. Importantly, overlay of the red and green fluorescence, with DAPI staining shown in blue in Figure 4-6C, revealed that although the recombinant LZT-Hs7 protein was mostly contained within the F-actin filament structures, in some instances it extends beyond it, as shown in Figure 4-6C with a white arrow pointer. Finally, in Figure 4-6D shows more green fluorescence appeared due to LZT-Hs7 positive recombinant proteins, indicating its abundance.

Figure 4-7A shows the expression of the recombinant LZT-Hs8 protein in transfected CHO cells and clearly shows a different staining pattern from LZT-Hs7 in Figure 4-6A. Permeabilisation of the cells did not affect the distribution of LZT-Hs8 recombinant protein, which appears to be present at high levels suggested to be in the endoplasmic reticulum region. Figure 4-8A shows recombinant LZT-Hs8 protein apparently in endoplasmic reticulum in many transfected CHO cells indicating its abundance. Although, LZT-Hs8 appears to be present at high levels in the endoplasmic reticulum of permeabilised cells, it is also present on the plasma membrane of transfected CHO cells of non-permeabilised cells as seen in Figure 4-8B.

Like LZT-Hs8, recombinant LZT-Hs9 protein appears to accumulate in the endoplasmic reticulum of transfected CHO cells in permeabilised conditions as seen in Figure 4-9A and Figure 4-9C, and remains within the outline of the F-actin structures shown in Figure 4-9B and Figure 4-9C. Unlike LZT-Hs8, LZT-Hs9 recombinant protein is not presents on the plasma membrane CHO cells in non-permeabilised conditions (not shown). In another experiment to locate the recombinant LZT-Hs9 protein, a dye-coupled antibody, Alexa Fluor 594-conjugated antimouse that fluoresces red, shows clearly the presents of LZT-Hs9 intracellularly and perinuclear region suggesting it to be in the endoplasmic reticulum region as seen in Figure 4-9D.

Figure 4-6: Expression of LZT-Hs7 recombinant proteins in CHO cells treated in non-permeabilised conditions

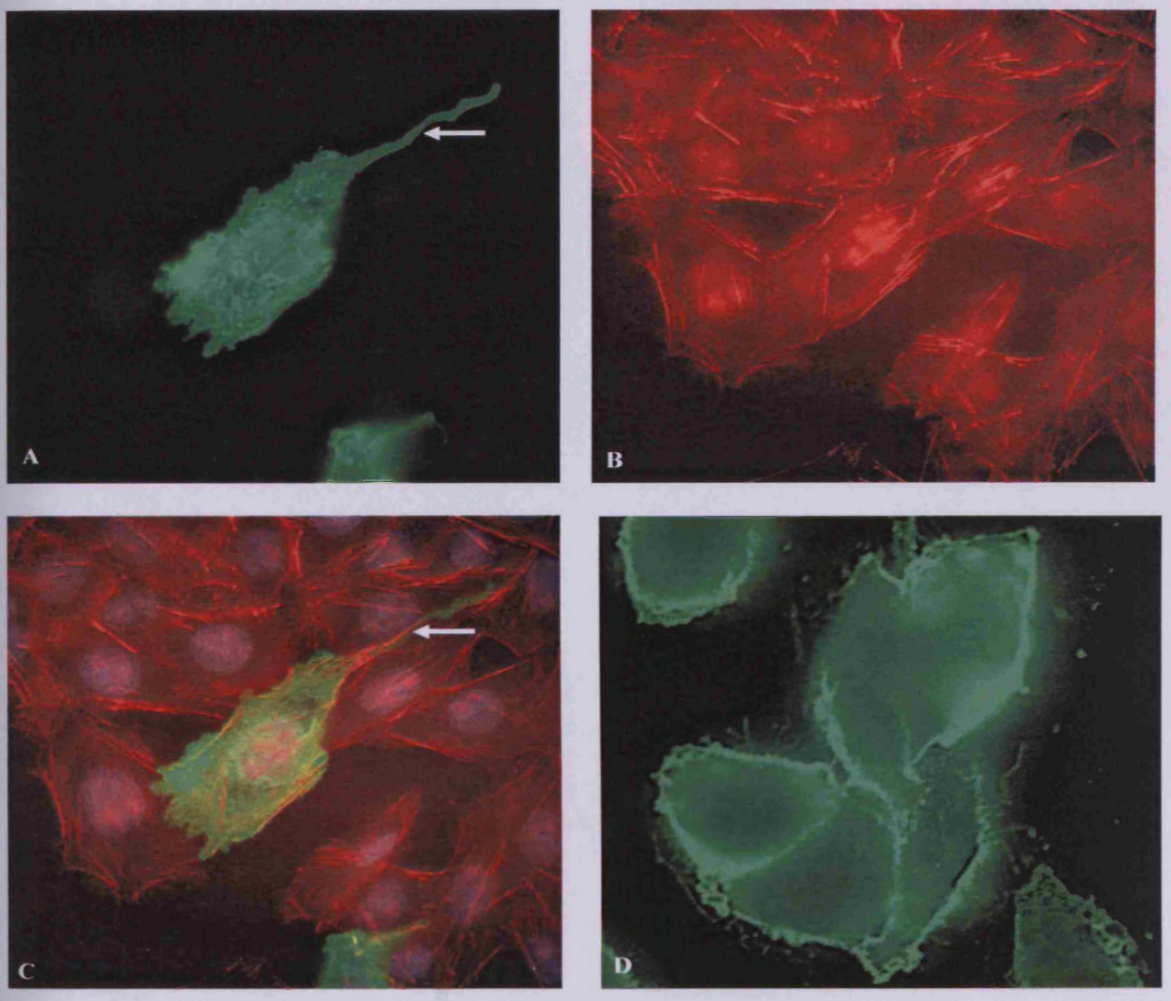

A) LZT-Hs7 recombinant protein probed with anti-V5 antibody and Alexa Fluor 488 with plasma membrane and lamellipodiae staining (white arrows). **B)** F-actin structures stained with Texas Red Phalloidin. **C)** Merged images of LZT-Hs7 positive cells located on lamellipodiae extending beyond F-actin. (white arrow). **D)** Abundance of positive LZT-Hs7 cells with plasma membrane immunostaining.

Figure 4-7: Expression of LZT-Hs8 recombinant proteins in CHO cells in permeabilised conditions

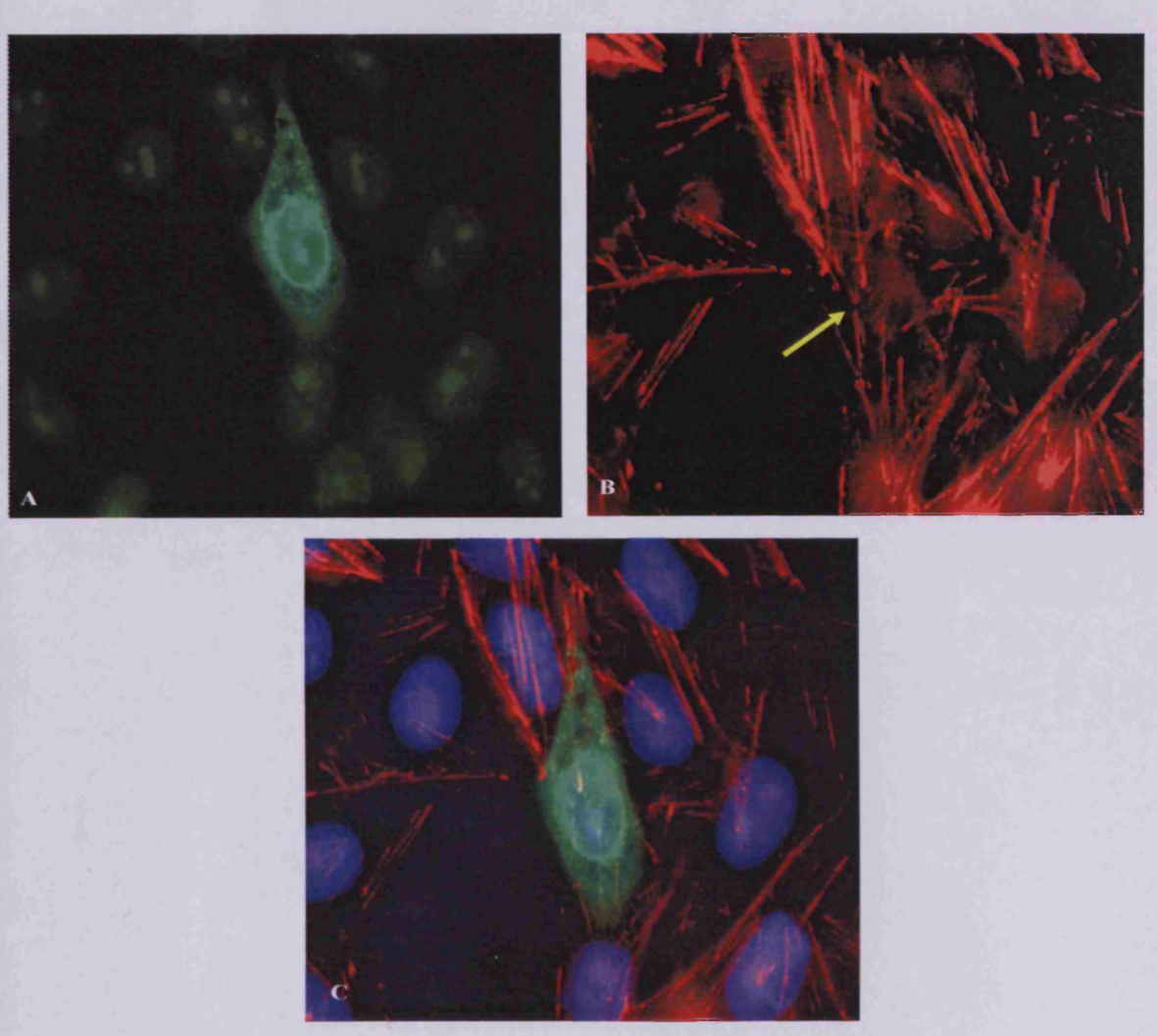

A) LZT-Hs8 recombinant protein probed with anti-V5 antibody and Alexa Fluor 488 with suggestive of intracellular and perinuclear staining. **B)** F-actin structures stained with Texas Red Phalloidin in transfected cell (yellow arrow). **C)** Merged images showing LZT-Hs8 positive cell (located intracellularly) and F-actin staining.

Figure 4-8: Expression of LZT-Hs8 recombinant proteins in CHO cells in permeabilised conditions (A) and non-permeabilised conditions (B)

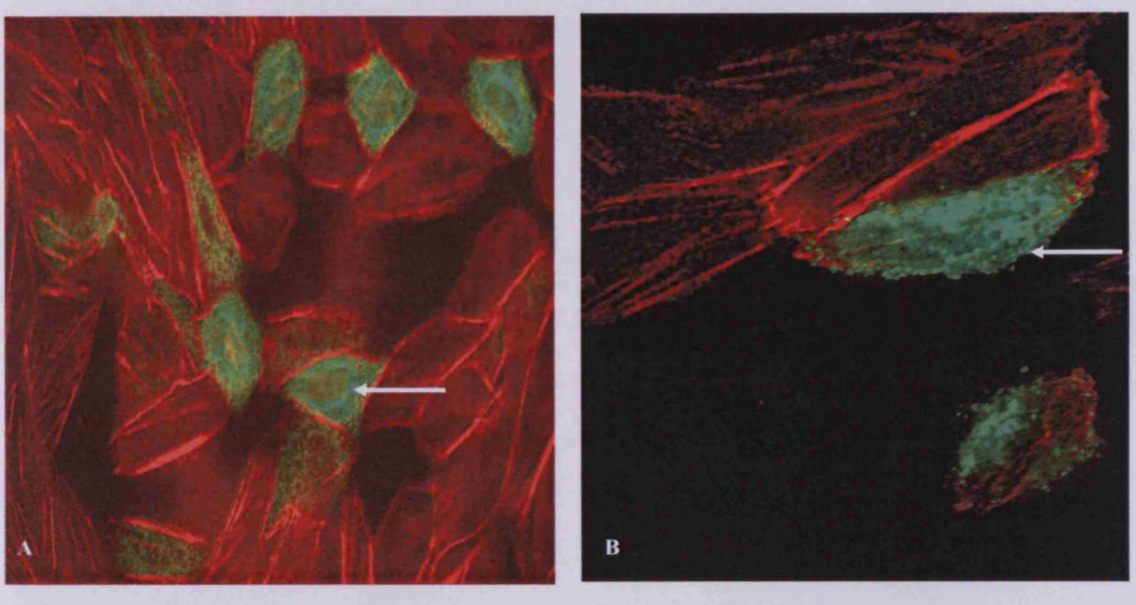

A) Merged images showing LZT-Hs8 recombinant protein detection using Alexa Fluor 488 (fluoresces green) located intracellularly and suggestive of the endoplasmic reticulum staining and appeared to be abundance in transfected cell expressing the LZT-Hs8 in the permeabilised conditions.

B) Merged images showing LZT-Hs8 recombinant protein probed using Alexa Fluor 488 (fluoresces green) located on plasma membrane in non-permeabilised conditions. Not so many transfected cells are the expression LZT-Hs8. In both images, the F-actin structures stained with Texas Red Phalloidin and 1 (an example) LZT-Hs8 positive cell shown with white arrow.

Figure 4-9: Expression of LZT-Hs9 recombinant proteins in CHO cells in non-permeabilised conditions

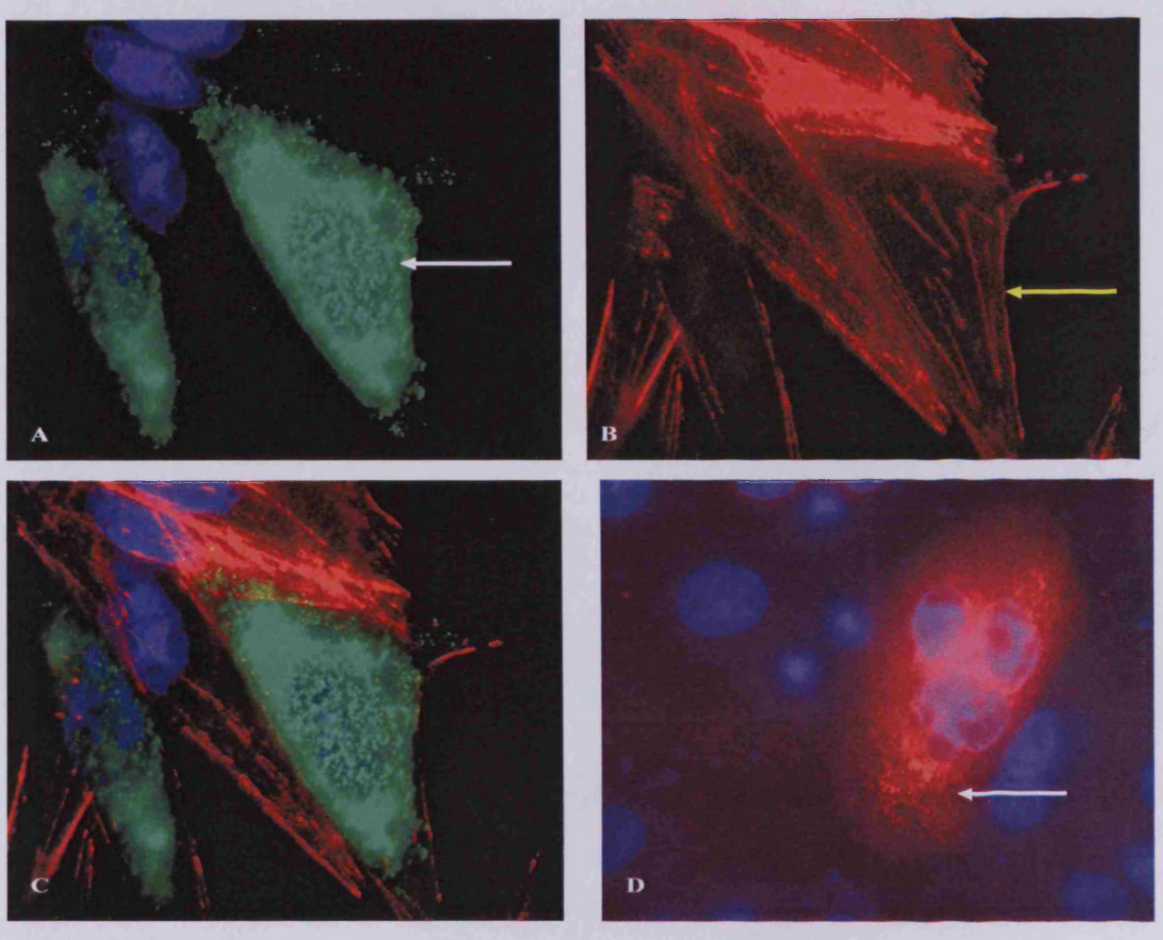

A) LZT-Hs9 recombinant protein probed with anti-V5 antibody and Alexa Fluor 488 showing intracellular staining (white arrow) suggestive of endoplasmic reticulum. **B)** F-actin structures (of same cell) stained with Texas Red Phalloidin. **C)** Merged images of LZT-Hs9 positive cells and F-actin stains. D) LZT-Hs9 recombinant protein stained with Alexa Fluor 594 (white arrow) suggestive of endoplasmic reticulum staining.

4.4 Preliminary zinc analysis transfected tamoxifen resistant cells

Since LZT-Hs7, LZT-Hs8 and LZT-Hs9 are predicted to be zinc influx transporters; an attempt was made to determine whether tamoxifen resistant cells transfected with LZT-Hs7, LZT-Hs8 and LZT-Hs9 had increased intracellular zinc detected by using Newport Green DCF™ diacetate, a zinc sensitive dye. Newport Green DCF™ diacetate fluoresces green in cells on exposure to zinc, the intensity of which corresponds to the level of intracellular zinc. The LZT-Hs7, LZT-Hs8 and LZT-Hs9 recombinant proteins were conjugated with Alexa Fluor 594 antibody that fluoresces red. The cell nuclei were counter stained with DAPI (blue). These multicolour images are shown in Figure 4-10, Figure 4-11 and Figure 4-12 for LZT-Hs7, LZT-Hs8 and LZT-Hs9 recombinant proteins in tamoxifen resistant cells, respectively.

These preliminary experiments did not provide enough evidence for the uptake of zinc in the LZT-Hs7 as expected (Figure 4-10). However, from Figure 4-11, there is a suggestion that the LZT-Hs8 positive cell has decreased intracellular zinc, as evidenced by the decreased green level in that cell (white arrow) as compared to LZT-Hs8 negative cells. This result disagrees with LZT-Hs8 acting as zinc influz transporters because of the reverse effect of zinc exposure shown here. Nevertheless, from Figure 4-12, there is a suggestion that the LZT-Hs9 positive cell has increased intracellular zinc, as evidenced by the increased green level in that cell (white arrow) as compared to LZT-Hs9 negative cells. This result agrees with LZT-Hs9 acting as zinc influz transporters.

Figure 4-10: Expression of LZT-Hs7 recombinant proteins in tamoxifen resistant cells loaded with Newport Green™ diacetate

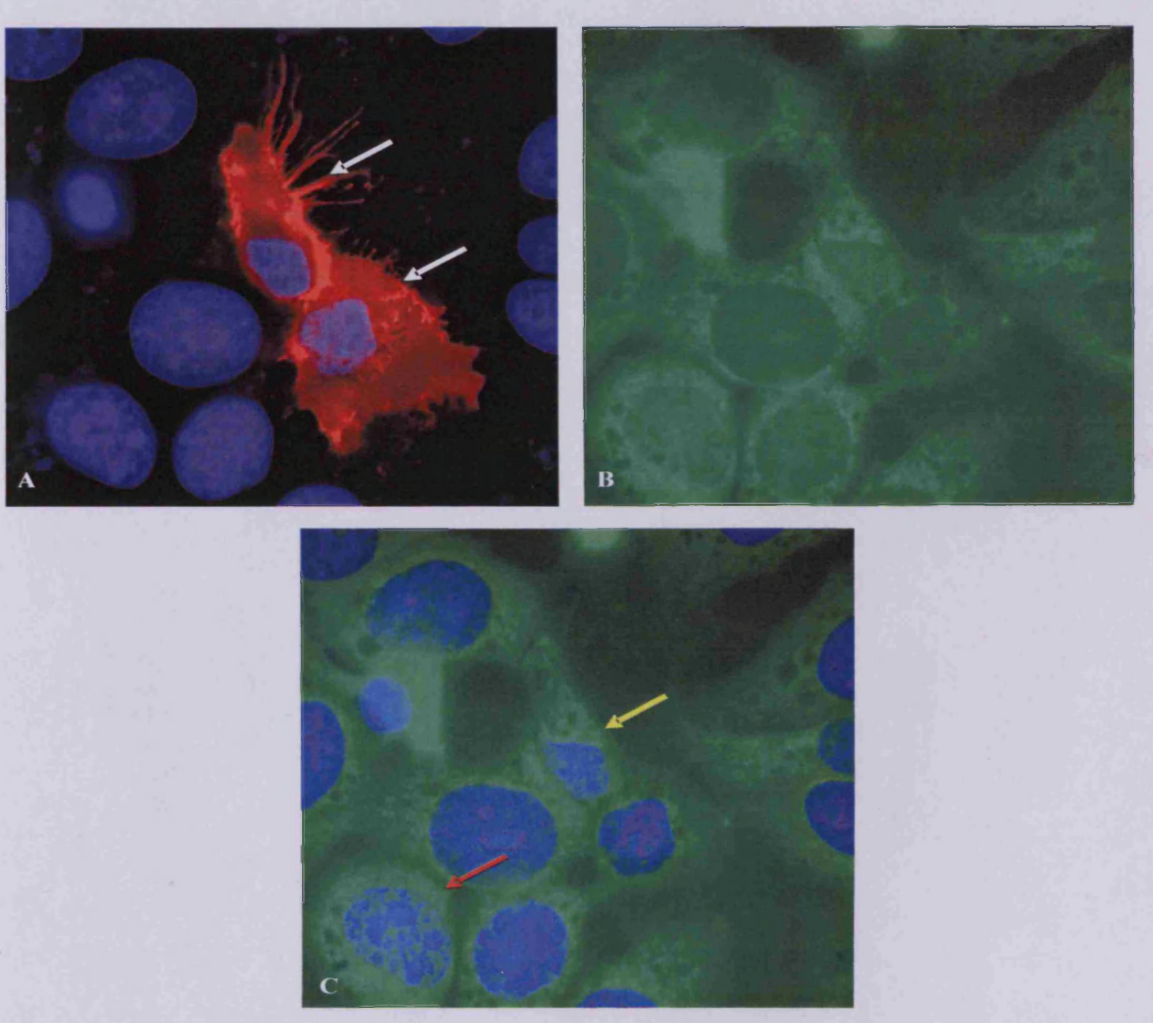

A) LZT-Hs7 positive cells were stained red with anti-V5 antibody and Alexa Fluor 594 with plasma membrane and lamellipodiae staining (white arrows). **B)** The same cells loaded with Newport Green™ diacetate. **C)** The green colour of tranfected (yellow arrow) and untransfected (red arrow) cells was similar.

Figure 4-11: Expression of LZT-Hs8 recombinant proteins in tamoxifen resistant cells loaded with Newport Green™ diacetate

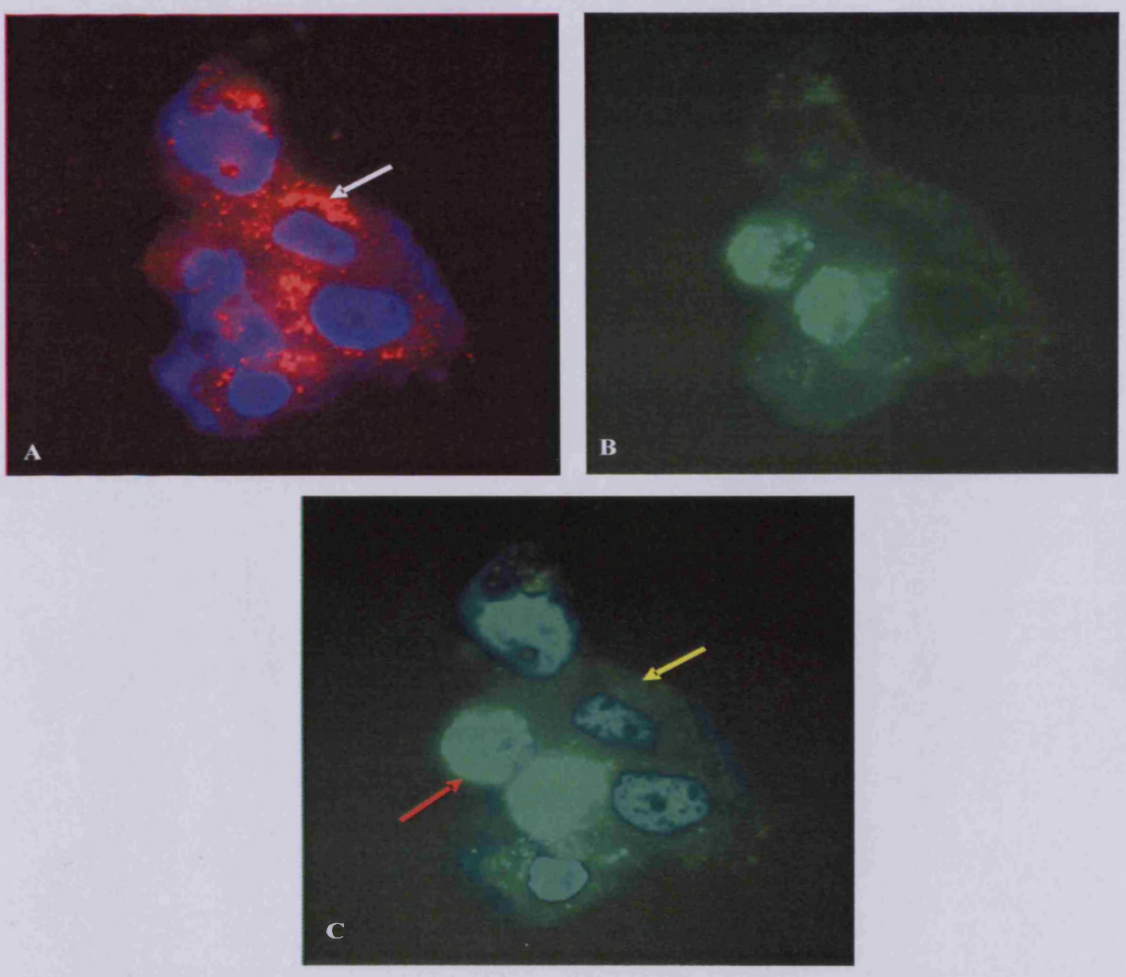

A) LZT-Hs8 positive cells were stained red with anti-V5 antibody and Alexa Fluor 594 with plasma membrane staining (white arrow). **B)** The same cells loaded with Newport Green™ diacetate. **C)** The green color of tranfected cell (yellow arrow) shows less dense as compared to untransfected (red arrow).

Figure 4-12: Expression of LZT-Hs9 recombinant proteins in tamoxifen resistant cells loaded with Newport Green™ diacetate

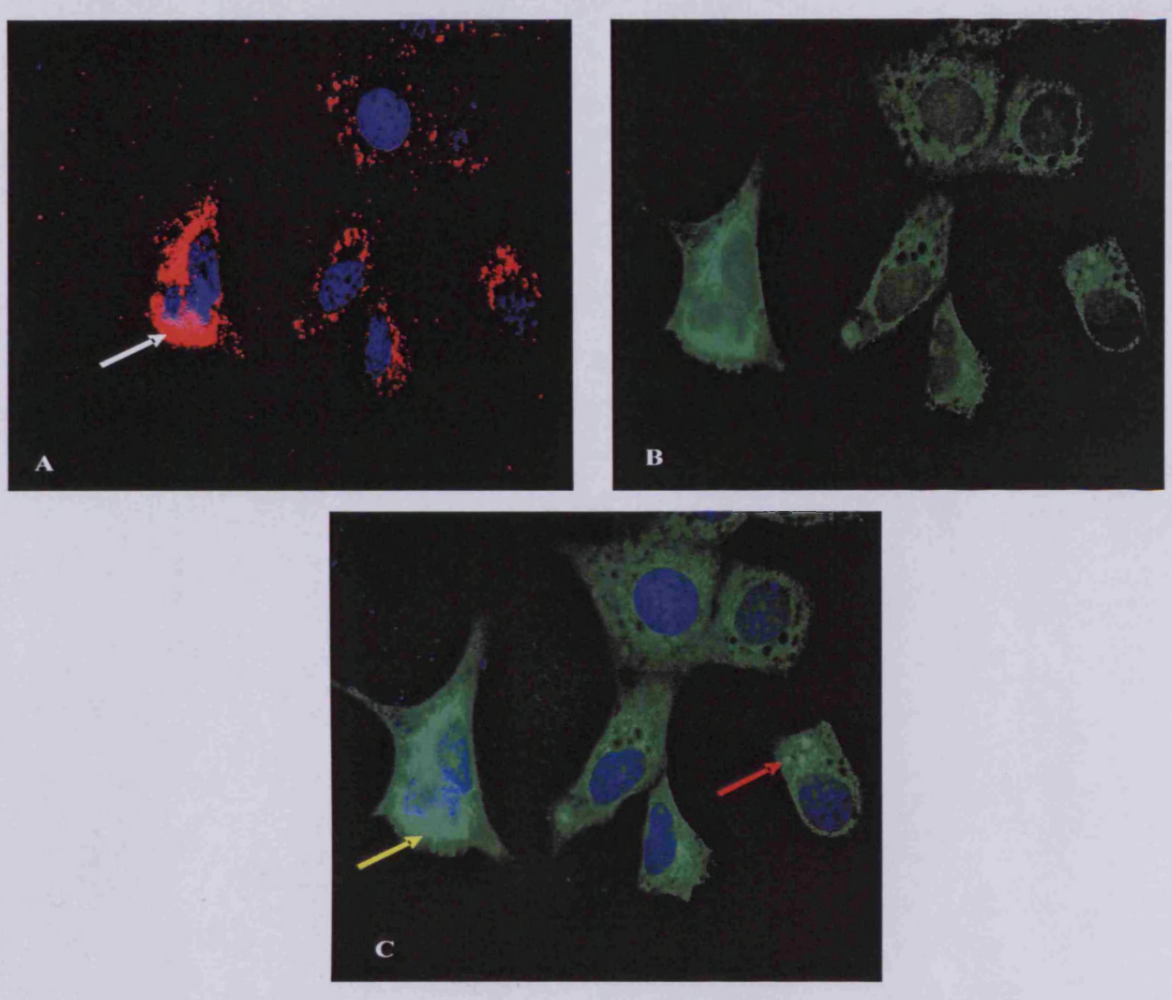

A) LZT-Hs9 positive cells were stained red with anti-V5 antibody and Alexa Fluor 594 with suggestive of endoplasmic reticulum staining (white arrow). **B)** The same cells loaded with Newport Green™ diacetate. **C)** The green colour of tranfected cell (yellow arrow) denser as compared to untransfected (red arrow) and zinc dye accumulated in vesicles (red arrow).

4.5 Discussion

LZT-Hs7, LZT-Hs8 and LZT-Hs9 were successfully cloned into pcDNA5/FRT/V5-His-TOPO® TA vector and this was the first time that LZT-Hs8 and LZT-Hs9 have been cloned and expressed. The recombinant proteins are detected using anti-V5 antibody; nevertheless, the V5 epitope sequence could be inserted in the reverse primers design. However, LZT-Hs9 has the V5 epitope sequence inserted into its reverse primer thus the LZT-Hs9 protein weight will be increased by an insignificant amount of the V5 epitope's of 14 residues long. The LZT-Hs7 and LZT-Hs8 were designed with the V5 epitope from the vector, which adds an approximately 3.6 kDalton (manufacturer instruction) additional weight to the recombinant clones. The actual protein weight obtained for LZT-Hs7, LZT-Hs8 and LZT-Hs9 was 63 kDalton, 73 kDalton and 43 kDalton, respectively.

Protein identification involved separating the mixture of proteins by electrophoresis and transfer to a nylon membrane so that an antibody together with the protein molecular weight markers could visualized the protein band. The ratio of the distance migrated of these proteins compared to the distance migrated by the solvent front, produced the Rf values. The protein molecular weight markers' Rf values are used to make a standard curve and enabling the unknown bands to be checked against the standard curve for estimation of their respective protein weight, although throughout this study, our Rf values were automatically calculated by the AlphaDigiDoc Innotech computer software.

A band of 63 kDalton was obtained for LZT-Hs7 while computer search has predicted the size is 56 kDalton. The LZT-Hs7 recombinant protein was expressed as a fusion protein, with an additional 3.6 kDalton added which incorporated the V5-tag was not inserted at the C-terminal end. The LZT-Hs7 does have two predicted N-linked glycosylation sites on the N-terminus therefore, it is expected that additional protein weight as much as 10 kDalton must be added onto the predicted size, as the N-terminus is located extracellularly. Nevertheless, in another study, LZT-Hs7 recombinant protein showed 2 bands with size of 80 and 70 kDalton (Wang et al. 2004), in contrast another published that LZT-Hs7 produced only 1 band of 61 kDalton (Dufner-Beattie et al. 2003). The latter finding shows similar protein weight estimation as our current study however, there is a 3.4 kDalton weight more, probably due to margin of error for SDS-Page technique or there has been a small glycosylation occurred on the side chain.

A band of 73 kDa was obtained for LZT-Hs8 and computer search has predicted that LZT-Hs8 protein weight is 72.805 kDalton. As in LZT-Hs7, LZT-Hs8 recombinant proteins were expressed as a fusion protein with an additional 3.6 kDalton as the V5-tag at the C-terminal end. Although the computer search has predicted that LZT-Hs8 has 5 N-linked glycosylation sites on the N-terminus, it is not evidenced by the protein weight as LZT-Hs8 produced a band of 73 kDalton. The recombinant protein for LZT-Hs8 have been located on the plasma membrane and therefore it may be expected to be glycosylated as much as 5 to 10 kDalton providing a band approaching 85 kDalton. Although this was not clear, it may suggest

cleavage of the N-terminus before location at the plasma membrane, as observed recently from the LIV-1 protein (Taylor, personal communication).

A band of 43 kDalton was obtained for LZT-Hs9 and the computer search has predicted that LZT-Hs9 protein weight is 38.352 kDalton. Unlike LZT-Hs7 and LZT-Hs8, LZT-Hs9 recombinant protein had the V5-tag inserted at the C-terminal end within the oligonucleotide and not within the multiple cloning sites. This would have added a negligible amount to the recombinant protein, instead of the 3.6 kDalton added to LZT-Hs7 and LZT-Hs8. This gene has been predicted not to have any N-linked glycosylation sites and the LZT-Hs9 is located intracellularly where glycosylation will not occur. Therefore, our estimated LZT-Hs9 protein weight is acceptable due to margin of error for SDS-Page technique.

All three recombinant proteins were successfully expressed in CHO cells. In order to image their cellular location, immunoFluorescence experiments were performed on coverslips and the proteins were fluorescently labelled for detection. These experiments were conducted in both permeabilised and non-permeabilised conditions in order to discover whether they resided on the plasma membrane of the cells or on intracellular membranes. These results demonstrated an intracellular location for all the recombinant proteins and an additional plasma membrane location for LZT-Hs7 and LZT-Hs8 proteins. In the latter, the protein expression was very low level and indeed, it was very difficult to detect positively transfected cells during the experiment. This is a similar result to that observed for LIV-1 protein (Taylor et al. 2003).

The phylogenetic tree (Figure 3-2) showed that LZT-Hs7 clustered with LZT-Hs2 and LIV-1 genes, in the way indicated that these genes probably share a similar subcellular location. LIV-1 is located on the plasma membrane of the cell (Taylor et al. 2003) therefore the other two genes are predicted to be on the plasma membrane. The current study showed LZT-Hs7 is located on the plasma membrane, which is consistent with the prediction.

The phylogenetic tree (Figure 3-2) has linked LZT-Hs8 to LIV-1 gene, indicating both are highly homologous to each other. A recent experiment in the Tenovus laboratories has shown that LIV-1 is cleaved at the N-terminus and then it relocates itself to the plasma membrane. This conclusion was reached as a specific antibody detected an epitope near the N-terminus and did not recognise plasma membrane located LIV-1, however, another antibody detecting an epitope at the end of the N-terminus did recognize LIV-1 on the plsma membrane (Taylor, personal communication). The relocation of LIV-1 protein to the plasma membrane may explain a similar mechanism for LZT-Hs8 recombinant protein and explain the low level present on the plasma membrane

LZT-Hs9 has been shown (Figure 3-2) to be highly homologous to LZT-Hs1 gene, which is suggestive of them sharing similar feature. LZT-Hs1 is located on intracellular membranes that includes the endoplasmic reticulum (Taylor et al. 2004) and from our finding, LZT-Hs9 is also found intracellularly suggested to be located in endoplasmic reticulum region. Like LZT-Hs1, LZT-Hs9 does not have any glycosylation sites within its protein sequence and

secondly, neither of them have a CPALLY motif within their protein sequences suggesting LZT-Hs9 is similar to LZT-Hs1.

These attributes are consistent with other LZT subfamily members for instance LZT-Hs1 located in the endoplasmic reticulum (Taylor et al. 2004), LIV-1 located on the plasma membrane (Taylor et al. 2003) and LZT-Hs4 resides on the plasma membrane (Taylor et al. 2005).

All together, the V5-epitope tag was used successfully to detect all the recombinant proteins in mammalian cells using fluorescent microscopy technique.

A preliminary study was conducted to detect the zinc transport capability in the LZT-Hs7, LZT-Hs8 and LZT-Hs9 recombinant proteins. Unfortunately, it was not possible to show zinc transport capability for LZT-Hs7 as evidenced by a similar level of green dye in transfected and untransfected cells. In contrast, the LZT-Hs7 has been shown by others to carry Zn(II) into the cell (Dufner-Beattie et al. 2003) thus it was expected to observe more green dye in the transfected CHO cells than in the untransfected.

Loading of cells expressing LZT-Hs8 and LZT-Hs9 with Newport Green™ diacetate suggested these two genes are capable of transporting zinc in opposing directions. There is no published work to compare these results to as no others have expressed these genes. The transfected tamoxifen resistant cells expressing LZT-Hs8 has decreased level of zinc as

compared to untransfected cells, suggesting LZT-Hs8 transports zinc from the cytoplasm to outside the cell. Secondly, transfected tamoxifen resistant cells expressing LZT-Hs9 had an increased zinc dye level compared to untransfected cells, indicating the zinc ions were transported from outside the cell into the cytoplasm. Indeed, these controversies from only a preliminary study raised more questions and they now need repeating with a more elaborate experiment design. However, there is increasing evidence in the literature that human ZnT5 variant B, which belongs to a SLC30 zinc transporter family may be able to transport zinc in both directions across membranes (Valentine et al. 2007).

An alternative explanation for the observed results lies in the basic theory that the variable region between transmembrane domains III and IV are involved in zinc ion transport (Guerinot 2000). The variable region has many factors influencing its variability including the mixed charges and high frequency of histidine residues. It was observed that LZT-Hs8 has the smallest amount of mixed charges compared to the other 2 (Table 3-4), and no histidine residues in the variable region suggesting an explaination for inability to transport zinc. However, LZT-Hs7 has a higher frequency of mixed charges than LZT-Hs9 and the former contains 6 histidine residues while the latter has 1 histidine. This would suggest that LZT-Hs7 should be able to transport zinc and therefore needs to be confirmed with other methods and staining techniques.

The second scope of the study was to compare the zinc transport capacity in the cells, in the present of fluorescent dye, aiming at differentiating recombinants of LZT-Hs7, LZT-Hs8 and

LZT-Hs9, to the non-recombinant transfected cells. Caution must be exercised, in the interpretation of these experiments, because it is unclear whether he fixation process altered the zinc levels in these cells. However, the fluorescent labels were Alexa Fluor 594 for labelling the recombinant transfected cells and Newport Green dye for labelling the zinc ion showed that fixed cells had a defined morphological structure and presented fluorescence. Both of the staining characteristics detected only in the dead cells due to the fixation procedure. Other fluorescent stains and methods may be better to consider as a tool to investigate cell's zinc capacity and more importantly, the study must use live cells if the homeostasis of zinc is an active process.

Chapter 5

RNA profiles of the LZT subfamily and siRNA LZT-Hs1 studies

In this chapter, the study shows the expression of the nine LIV-1 family members across breast cancer lines. The study used the PCR technique and the RNA samples, from the wild type MCF-7, the endocrine responsive cells and the resistant derivatives of MCF-7 cells. Subsequently, a preliminary study continued on the LZT-Hs1 gene expression using small interfering RNA technology to show the gene knockdown impact. Another preliminary study is to locate the presence of ERE (estrogen response element) upstream of the gene using Dragon ERE Finder version 2.1.

5.1 Affymetrix Data: LZT subfamily members mRNA expression in responsive and resistant MCF-7 cells

The affymetrix data was taken from a database of previous work held within the Tenovus Centre for Cancer. Table 5-1, summarizes the Affymetrix data derived for the five members of the LZT subfamily of genes represented on the U133A gene chip in response to oestradiol and various anti-hormonal treatments in MCF-7 cells. LZT-Hs1, LZT-Hs4 and LZT-Hs5 had single probes to their genes, while LIV-1 and LZT-Hs6 had 2 and 3 probes respectively. In all but one instance (one of the 3 probe sets for LZT-Hs6), gene expression was deemed to be present in the treated samples. ANOVAs significance testing, however, suggest only Hs6 was

altered by the treatments ($p<0.05$), possibly showing some oestradiol suppression as shown in (Table 5-1). This was evident for the two probes sets called as present.

Table 5-2 summarizes the Affymetrix data derived from the five members of the LZT subfamily of genes in the resistance study. Once again, all genes, except for one probe for LZT-Hs6, were called as present. In contrast to the oestradiol and various anti-hormonal treatment set, Anova significance testing indicated substantial increases in the all of the 5 members of the LZT subfamily in at least one form of resistance ($p<0.05$), with LZT-Hs1 and possibly LZT-Hs4 being raised in all forms of resistance. Interestingly, the expression of the LIV-1 gene appeared to be suppressed in tamoxifen resistant cells.

Table 5-3 shows the Affymetrix probe sets derived for the Anova significant genes in the resistant study. The heat map represents each probe set and shows an elevation of the LZT subfamily gene expression in at least one form of resistance.

Table 5-1 : Affymetrix data for five of the LZT subfamily in response to oestradiol and anti-hormonal treatments

Gene	Number of probes	Present and absent call	Anova significance $p<0.05$	Comment
LZT-Hs1	1	√	X	-
LIV-1	2	√	X	-
LZT-Hs4	1	√	X	-
LZT-Hs5	1	√	X	-
LZT-Hs6	3	2/3 (shown in Table 5-3)	2/3	Possibly suppressed by oestradiol

Table 5-2: Affymetrix data for 5 members of the LZT subfamily in various anti-hormonal resistant cells

Gene	Number of probes	Present and absent call	Anova significance P<0.05	Comment
LZT-Hs1	1	√	√	Elevated in tamoxifen and faslodex resistance, and probably in X-cells
LIV-1	2	√	2/2 (shown in Table 5-3)	Elevated in X-cells and possibly in faslodex resistance. Suppressed in tamoxifen resistance
LZT-Hs4	1	√	√	Elevated in all forms of resistance
LZT-Hs5	1	√	√	Elevated in X-cells
LZT-Hs6	3	2/3	2/3 (shown in Table 5-3)	Elevated forms of resistance, except tamoxifen resistance

Table 5-3: Anova significant probe sets

Gene	Cells	Probeset ID	Heatmap
LZT-Hs6	Oestradiol and anti-hormone treated	209267_s_at	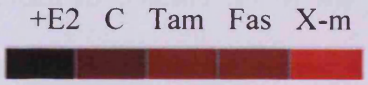
LZT-Hs6	Oestradiol and anti-hormone treated	219869_s_at	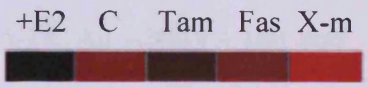
LZT-Hs6	Anti-hormone resistant cells	209267_s_at	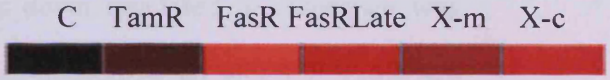
LZT-Hs6	Anti-hormone resistant cells	219869_s_at	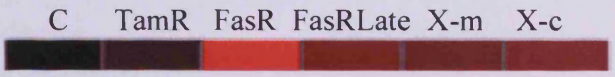
LIV-1	Anti-hormone resistant cells	202088_at	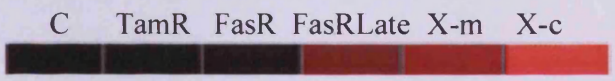
LIV-1	Anti-hormone resistant cells	202089_s_at	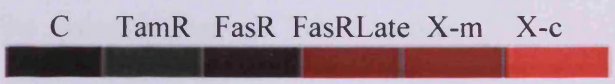

Legend:

TamR:tamoxifen resistant cells, FasR:faslodex resistant cells, FasRLate:faslodex late resistance, X-m: MCF-7 grown in heat inactivated charcoal stripe serum, X-cells:MCF-7 resistant to X medium grown semi-confluence, Tam:tamoxifen, Fas:faslodex, C:control MCF-7 cells, E2:oestradiol

5.2 PCR Data: LZT subfamily members mRNA expression in responsive and resistant MCF-7 cells

In light of the above results demonstrating the differential regulation of a number of LZT subfamily during response and resistance, the study was extended to monitor all of the members of the LZT subfamily in MCF-7 responsive and resistant cells using a semi-quantitative PCR procedure. The 3 PCR sets for each of the LZT family members were converted into histograms and are represented in Figures 5-1 to 5-18. An ANOVA test was performed on each data set to evaluate its significance ($p<0.05$) and these are shown in Table 5-4, pS2, a known oestrogen regulated gene which is down regulated in resistance was examined in the RNA preparations and the data is shown in Figures 5-1 and 5-2. Table 5-5 shows the summary of the LZT family members across all the treatments and in resistance.

5.2.1 pS2

The data presented in Figure 5-1 clearly shows pS2 to be an oestrogen regulated gene with oestradiol promoting the elevation of pS2 mRNA expression versus the untreated oestrogen deprived MCF-7 control cells ($p<0.05$). Of the antihormone treatments employed, only faslodex showed any reduction in pS2 mRNA versus the untreated control. This, however, did not reach statistical significance. Figure 5-2, shows the expressions of pS2 in the various forms of antihormone resistance, with significantly lower levels (versus wild-type cells) being recorded in early and late stage faslodex resistances.

5.2.2 LZT-Hs1

Figure 5-3 shows LZT-Hs1 to be an oestrogen-regulated gene with oestradiol treatment promoting an increase in mRNA expression versus the untreated oestrogen deprived MCF-7

control cells. These data contrast with a lack of an effect of the antihormones. Importantly, LZT-Hs1 mRNA expression was significantly highly increased in all forms of anti-oestrogen resistance ($p<0.05$) and in the cells resistant to oestrogen deprivation ($p<0.003$) (Figure 5-4).

5.2.3 LZT-Hs2

Figure 5-5 shows LZT-Hs2 largely expression is unaltered in MCF-7 cells by the oestradiol and antihormonal treatments and is only slightly suppressed in tamoxifen resistance (Figure 5-6).

5.2.4 LIV-1

Figure 5-7 shows only marginal increases in the expression of LIV-1 gene in oestradiol treated cells (not significant), with some decreases in expression in the presence of faslodex. In comparison to the wild-type cells, only X-cells showed any evidence of increased LIV-1 expression in resistance (Figure 5-8).

5.2.5 LZT-Hs4

Figure 5-9 shows LZT-Hs4 expression to be increased by oestradiol treatment ($p<0.05$) in MCF-7 cells and to be partially suppressed by faslodex (not significant) and X-media ($p<0.012$). Only the faslodex late stage resistance and X-cells showed increases in LZT-Hs4 relative to the wild-type cells with only the former being ANOVA significance ($p<0.05$) (Figure 5-10).

5.2.6 LZT-Hs5

Unfortunately, Hs5 could not be detected in any of the RNA sets at 29 PCR cycles.

5.2.7 LZT-Hs6

As mentioned in the previous Affymetrix section, expression of the LZT-Hs6 gene appeared suppressed by oestradiol treatment (Table 5-1), and this was confirmed by PCR (Figure 5-11). Similarly, the PCR performed on the resistant cells was supportive of the Affymetrix data with increased levels of LZT-Hs6 mRNA being seen in faslodex resistance ($p<0.009$). The remaining forms of anti-hormonal resistant cells show no effect of the treatments. Figure 5-12 shows LZT-Hs6 expression is elevated in faslodex resistance ($p<0.009$), faslodex late stage resistant cells ($p<0.011$) and in X-cells (not significant) in comparison to the wildtype MCF-7 cells.

5.2.8 LZT-Hs7, LZT-Hs8 and LZT-Hs9

These genes were largely unaltered in all treatment groups (Figures 5-13 to 5-18) with very low levels of LZT-Hs9 being observed throughout.

Table 5-5 summarises the above data and illustrates the variability of expression of the 9 LZT subfamily members in individual treatment groups.

Table 5-4 : PCR with ANOVA post-hoc test analysis ($p<0.05$) for LZT family members in treated and resistant cells

Gene	Oestrogen-regulation	Anova significant responses to oestradiol and responsive cells	Anova significant responses to hormone and anti-hormones	Comments
LZT-Hs1	√	-	√	Elevated in oestradiol and every form of resistances
LZT-Hs2	X	-	-	Suppressed in tamoxifen , faslodex , up regulate in FasR late
LIV-1	√	-	-	Suppressed in faslodex
LZT-Hs4	√	√	√	Elevated significantly in oestradiol
LZT-Hs5	-	-	-	Not expressed

LZT-Hs6	**X**	-	√	Suppressed in both tamoxifen and faslodex elevated in the stated resistances
LZT-Hs7	**X**	-	-	Unaltered expression in all cell models
LZT-Hs8	**X**	-	√	Suppressed expression in all cell models
LZT-Hs9	**X**	-	-	With very low expression in all of the RNA sets

Figure 5-1 : Relative mRNA expression of pS2 in oestradiol and anti-hormone treated cells

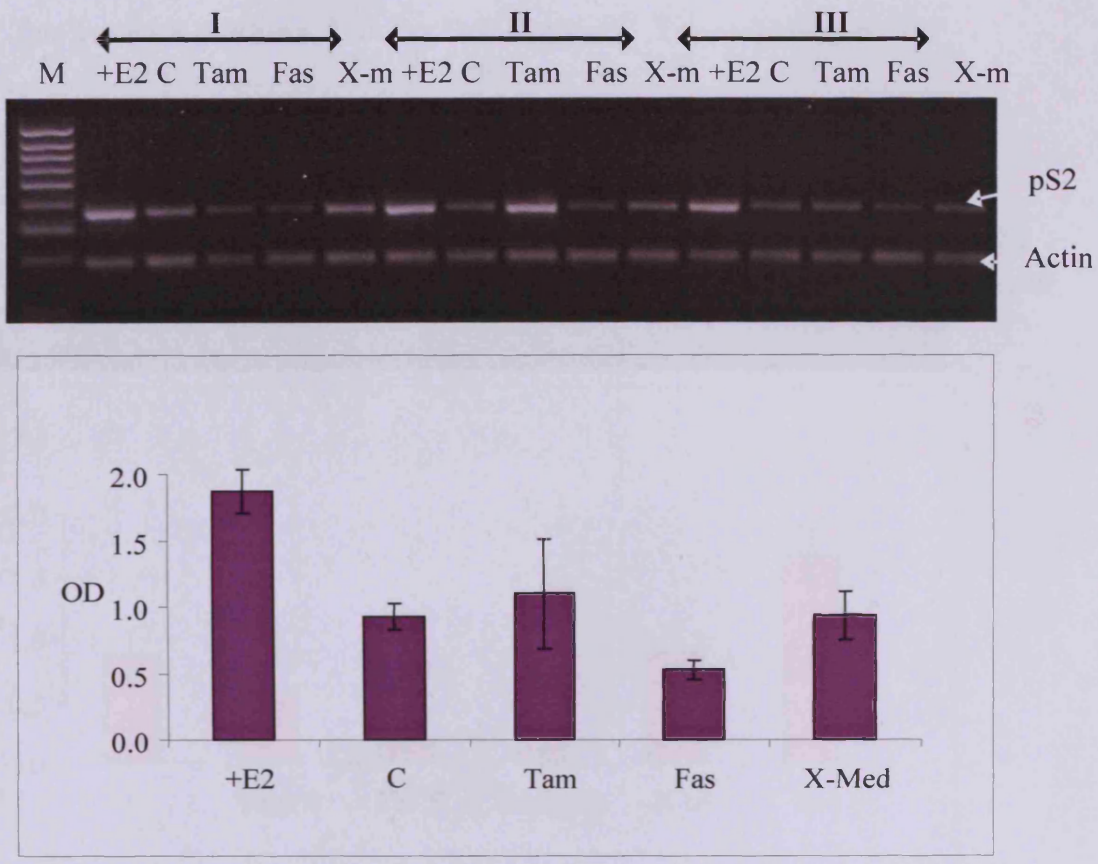

The gel image shows the PCR result of pS2 gene expressions in breast cancer cells. The results are a representative of three mRNA sets. The graph below the gel image is a compilation of the densitometric values from the gel image.

Figure 5-2 : Relative mRNA expression of pS2 in anti-hormone resistant cells

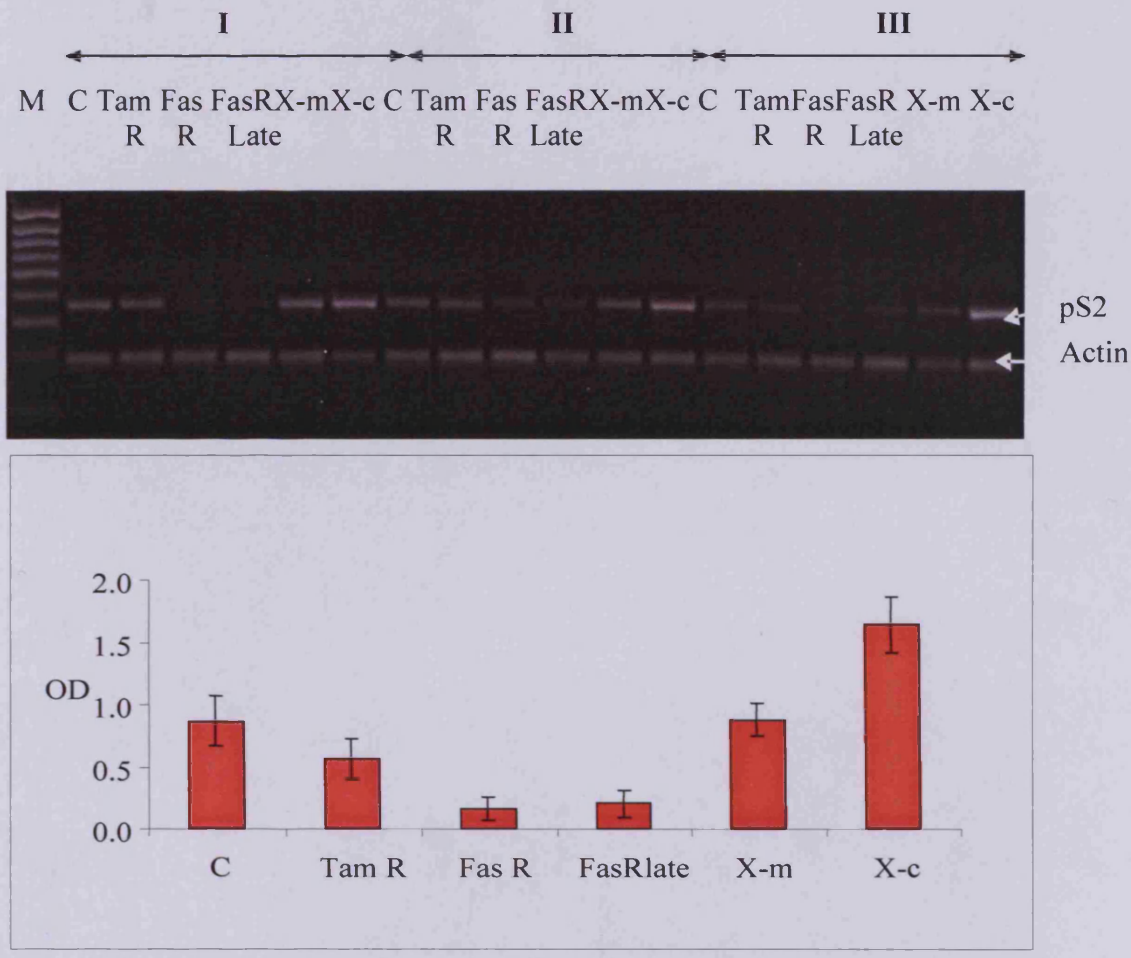

The gel image shows the PCR result of pS2 gene expressions in breast cancer cells. The results are a representative of three mRNA sets. The graph below the gel image is a compilation of the densitometric values from the gel image.

Figure 5-3 : Relative mRNA expression of LZT-Hs1 in oestradiol and anti-hormone treated cells

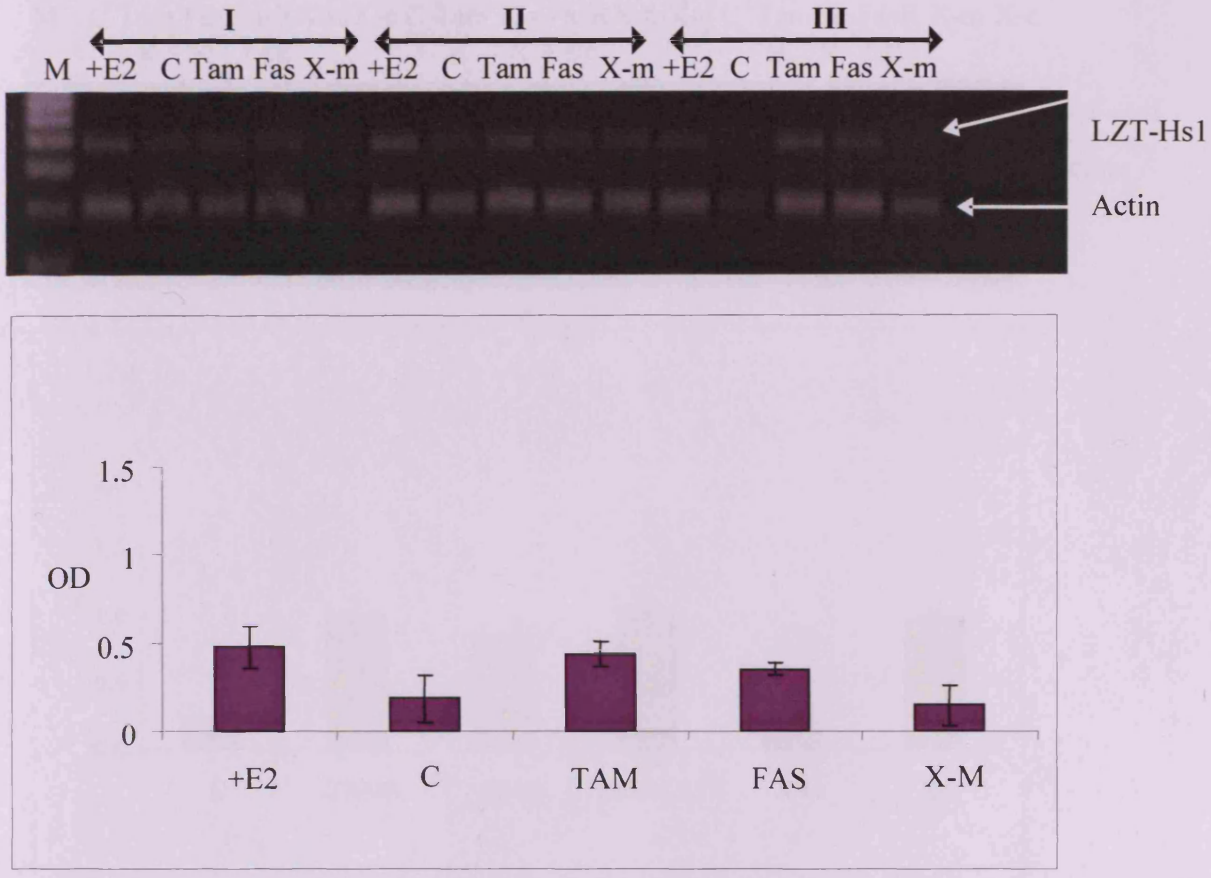

The gel image shows the PCR result of LZT-Hs1 gene expressions in breast cancer cells. The results are a representative of three mRNA sets. The graph below the gel image is a compilation of the densitometric values from the gel image.

Figure 5-4 : Relative mRNA expression of LZT-Hs1 in anti-hormone resistant cells

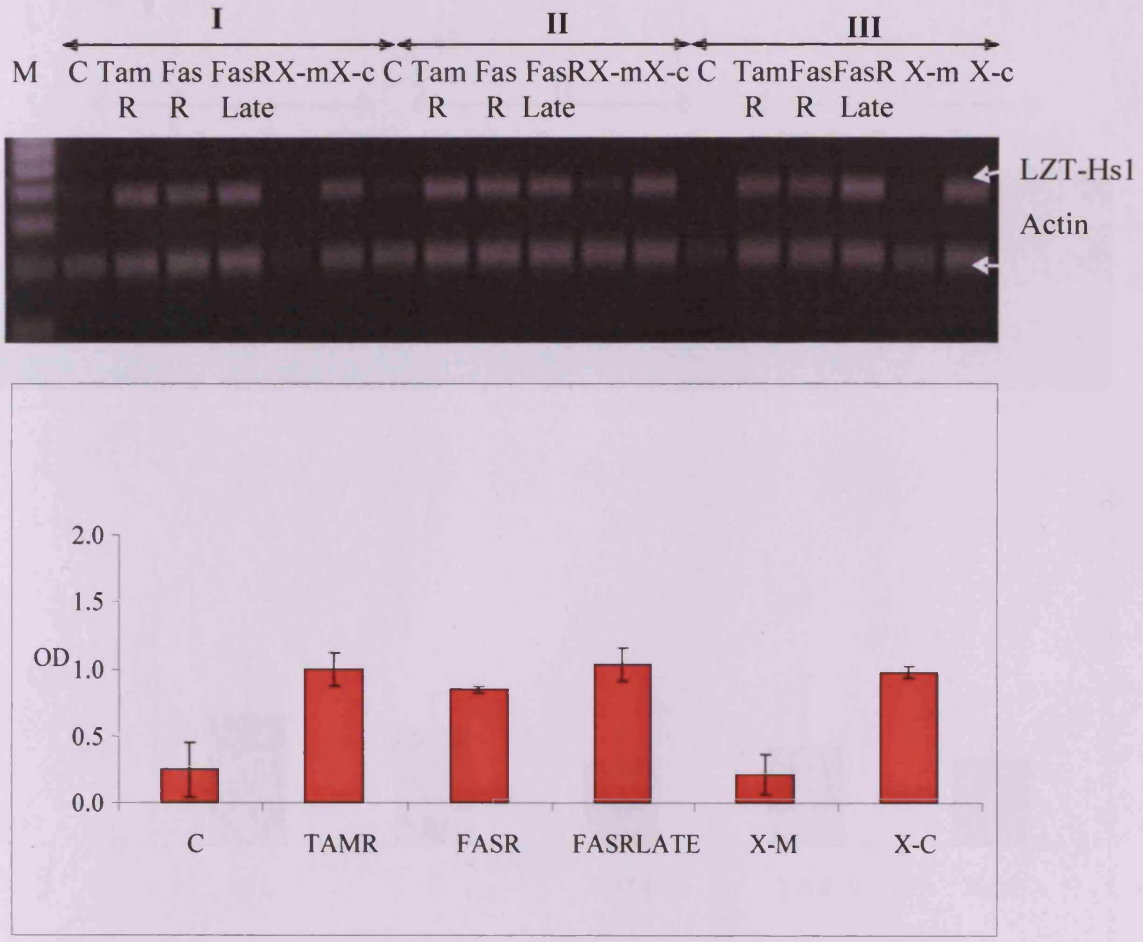

The gel image shows the PCR result of LZT-Hs1 gene expressions in breast cancer cells. The results are a representative of three mRNA sets. The graph below the gel image is a compilation of the densitometric values from the gel image.

Figure 5-5 : Relative mRNA expression of LZT-Hs2 in oestradiol and anti-hormone treated cells

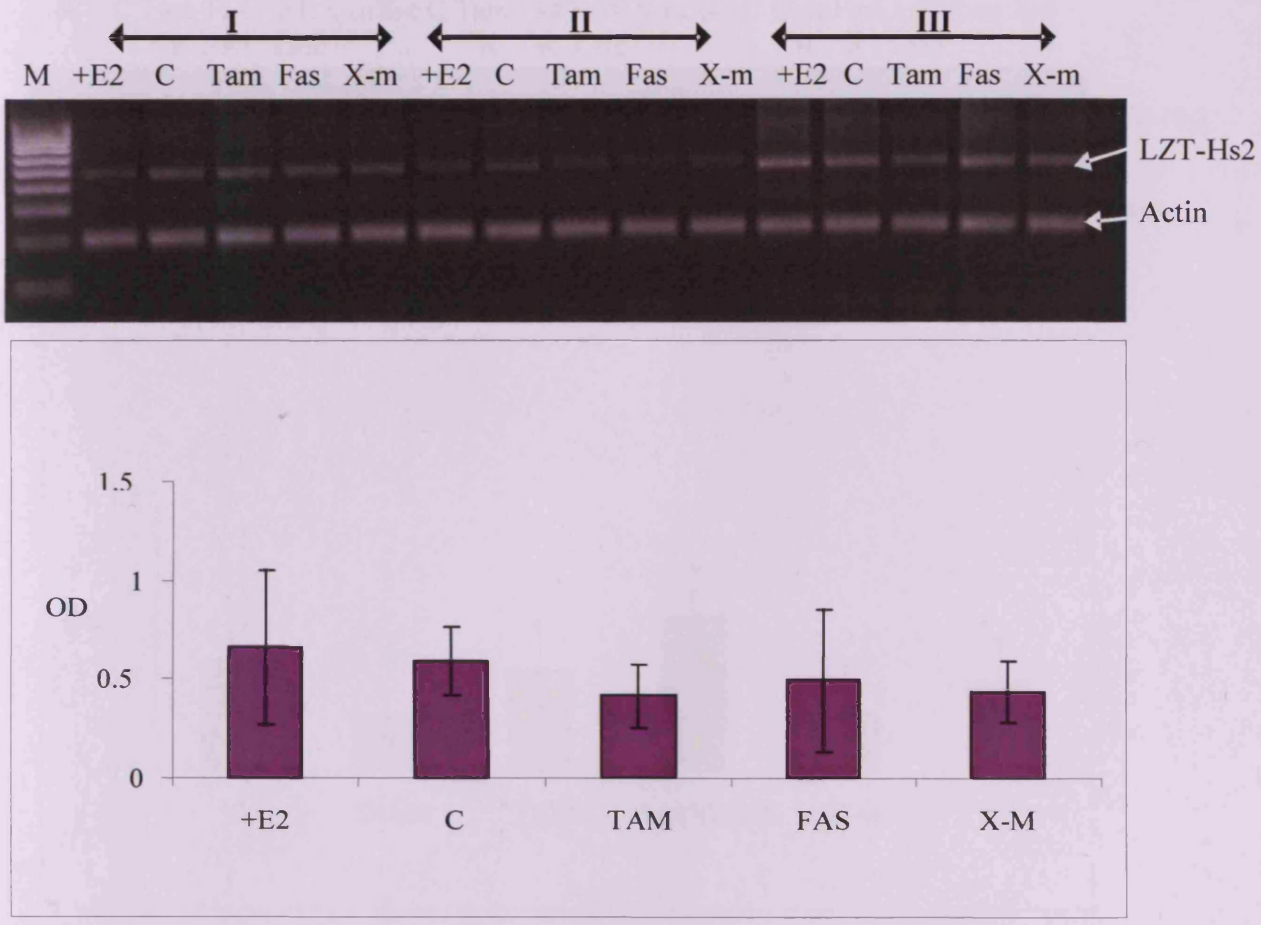

The gel image shows the PCR result of LZT-Hs2 gene expressions in breast cancer cells. The results are a representative of three mRNA sets. The graph below the gel image is a compilation of the densitometric values from the gel image.

Figure 5-6 : Relative mRNA expression of LZT-Hs2 in anti-hormone resistant cells

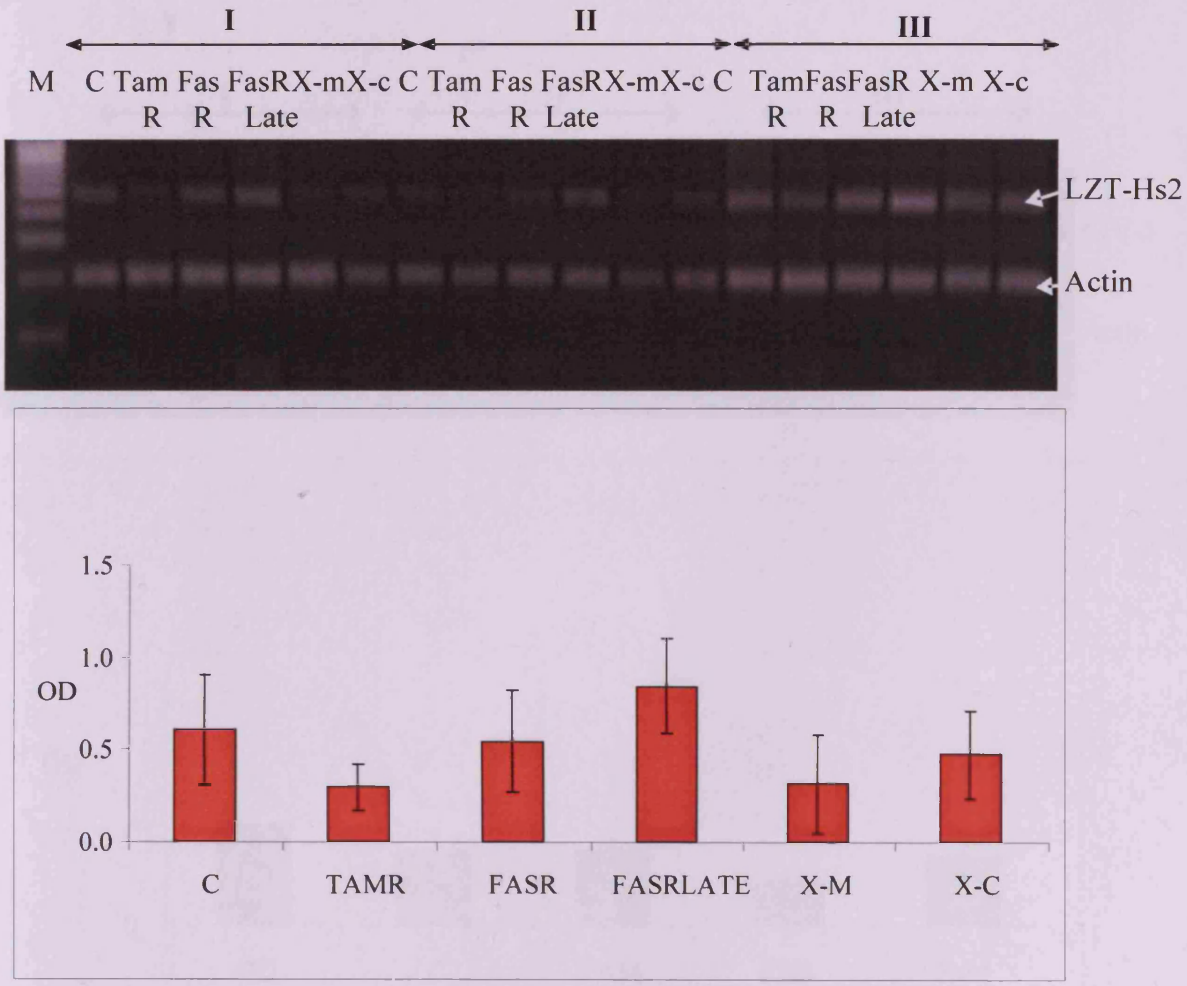

The gel image shows the PCR result of LZT-Hs2 gene expressions in breast cancer cells. The results are a representative of three mRNA sets. The graph below the gel image is a compilation of the densitometric values from the gel image.

Figure 5-7 : Relative mRNA expression of LIV-1 in oestradiol and anti-hormone treated cells

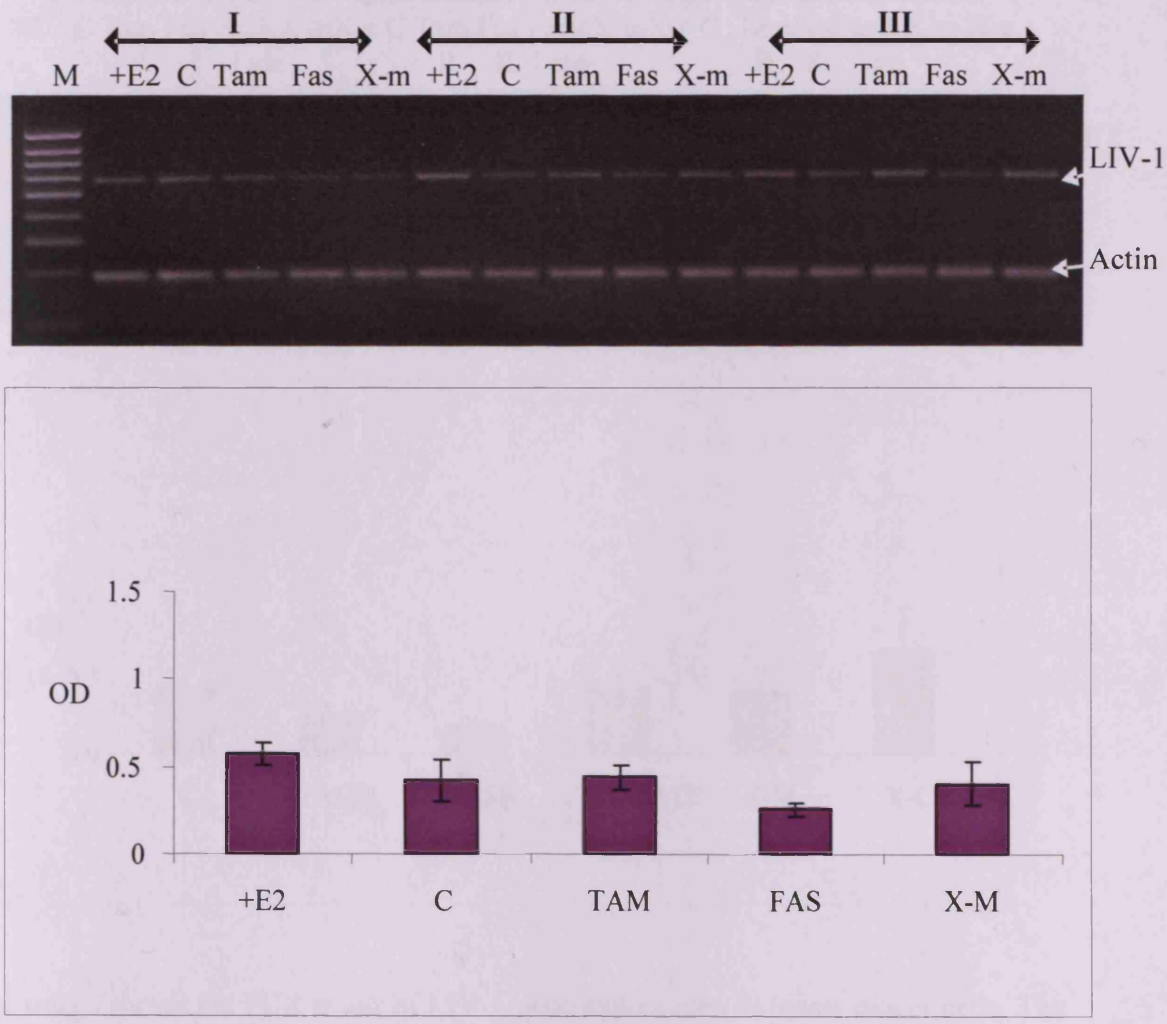

The gel image shows the PCR result of LIV-1 gene expressions in breast cancer cells. The results are a representative of three mRNA sets. The graph below the gel image is a compilation of the densitometric values from the gel image.

Figure 5-8 : Relative mRNA expression of LIV-1 in anti-hormone resistant cells

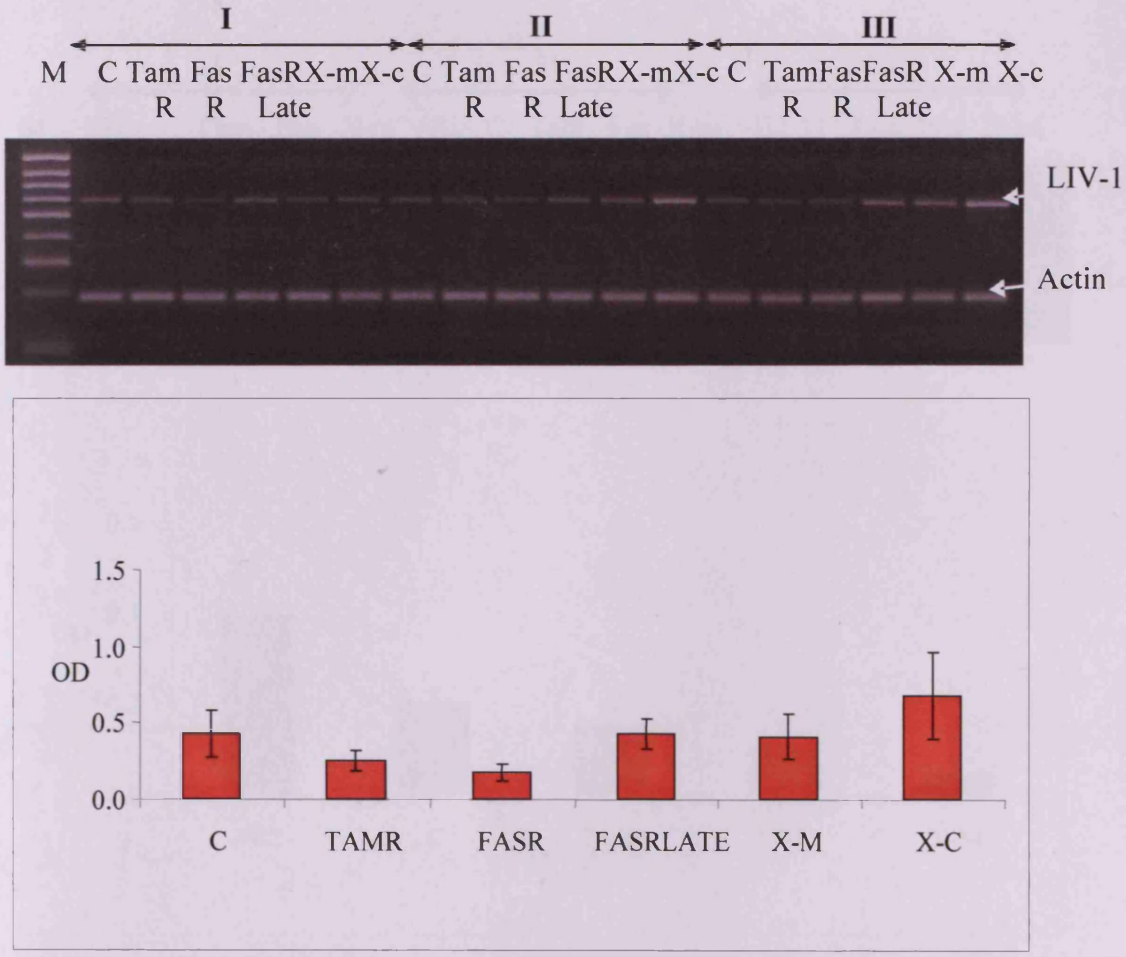

The gel image shows the PCR result of LIV-1 gene expressions in breast cancer cells. The results are a representative of three mRNA sets. The graph below the gel image is a compilation of the densitometric values from the gel image.

Figure 5-9 : Relative mRNA expression of LZT-Hs4 in oestradiol and anti-hormone treated cells

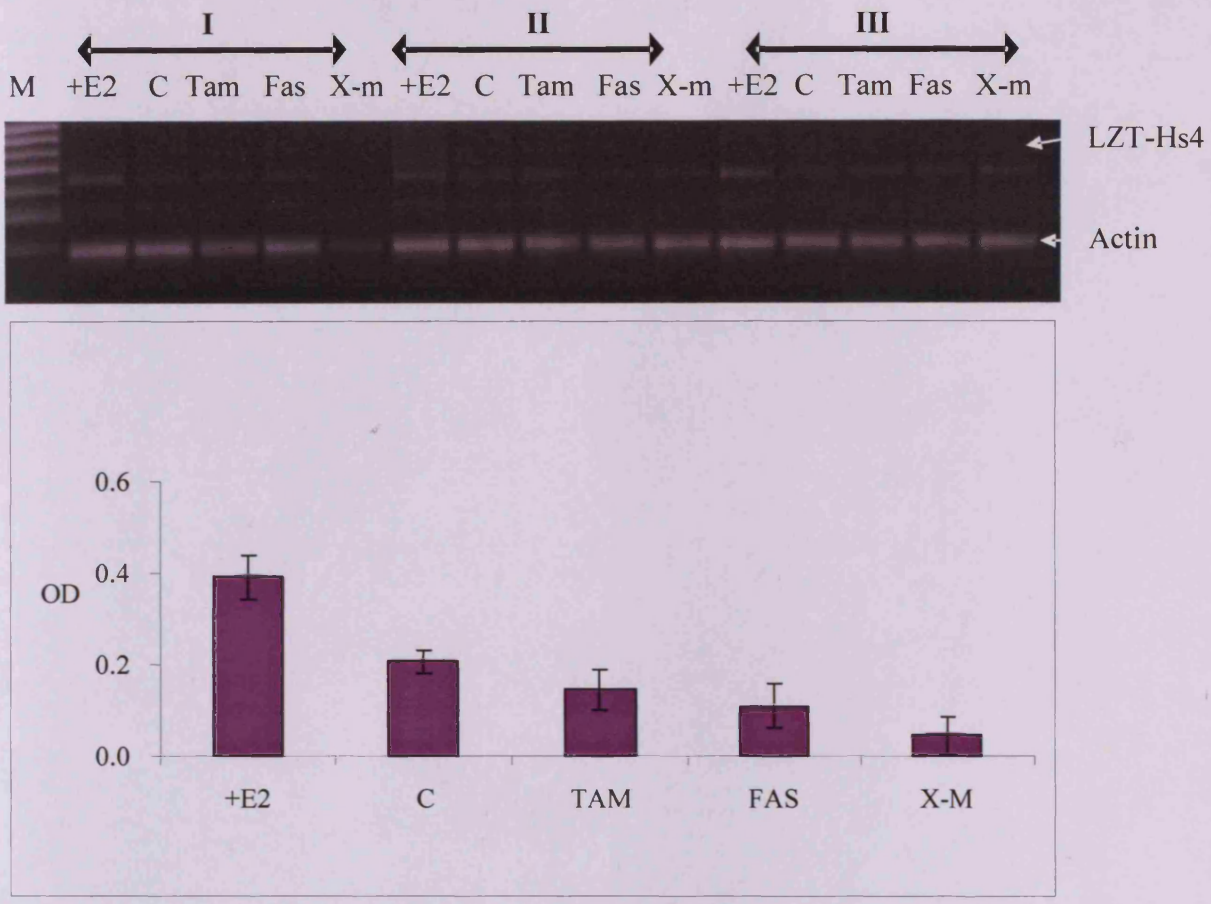

The gel image shows the PCR result of LZT-Hs4 gene expressions in breast cancer cells. The results are a representative of three mRNA sets. The graph below the gel image is a compilation of the densitometric values from the gel image.

Figure 5-10 : Relative mRNA expression of LZT-Hs4 in anti-hormone resistant cells

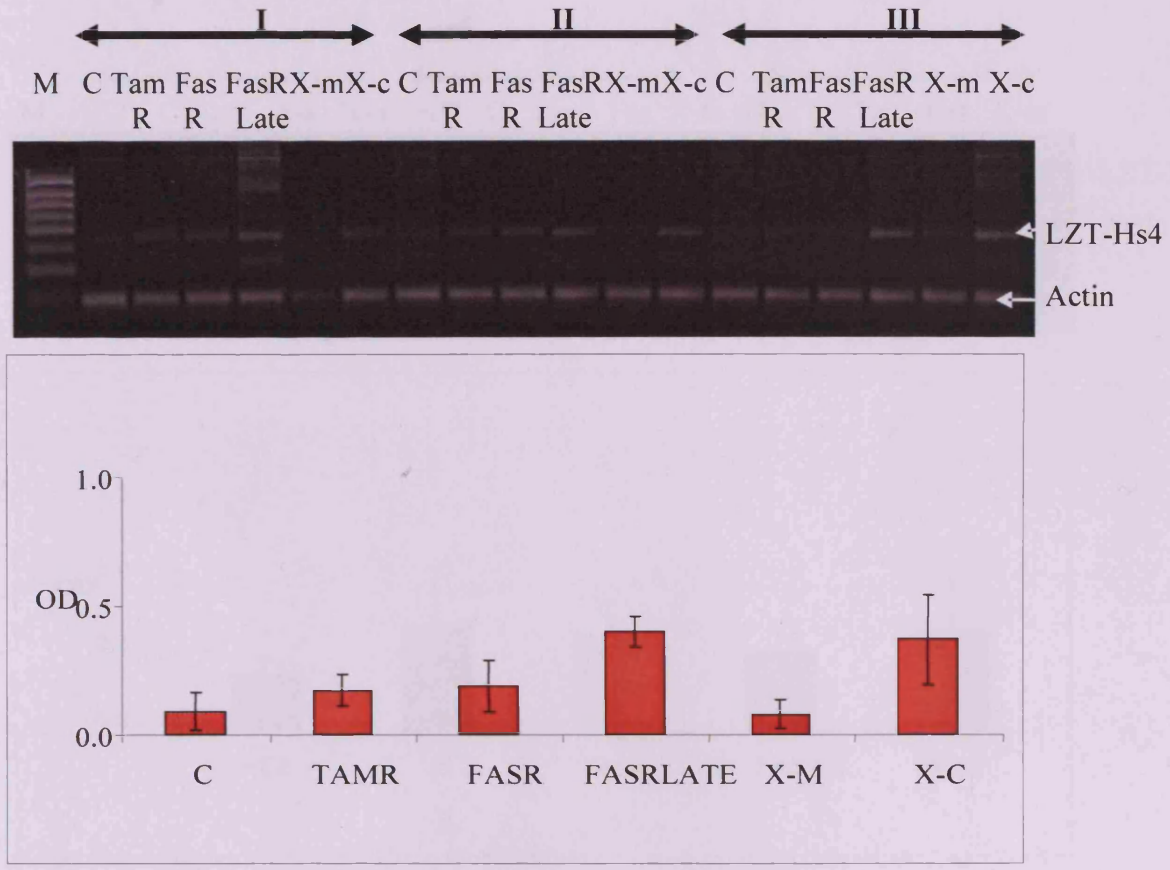

The gel image shows the PCR result of LZT-Hs4 gene expressions in breast cancer cells. The results are a representative of three mRNA sets. The graph below the gel image is a compilation of the densitometric values from the gel image.

Figure 5-11 : Relative mRNA expression of LZT-Hs6 in oestradiol and anti-hormone treated cells

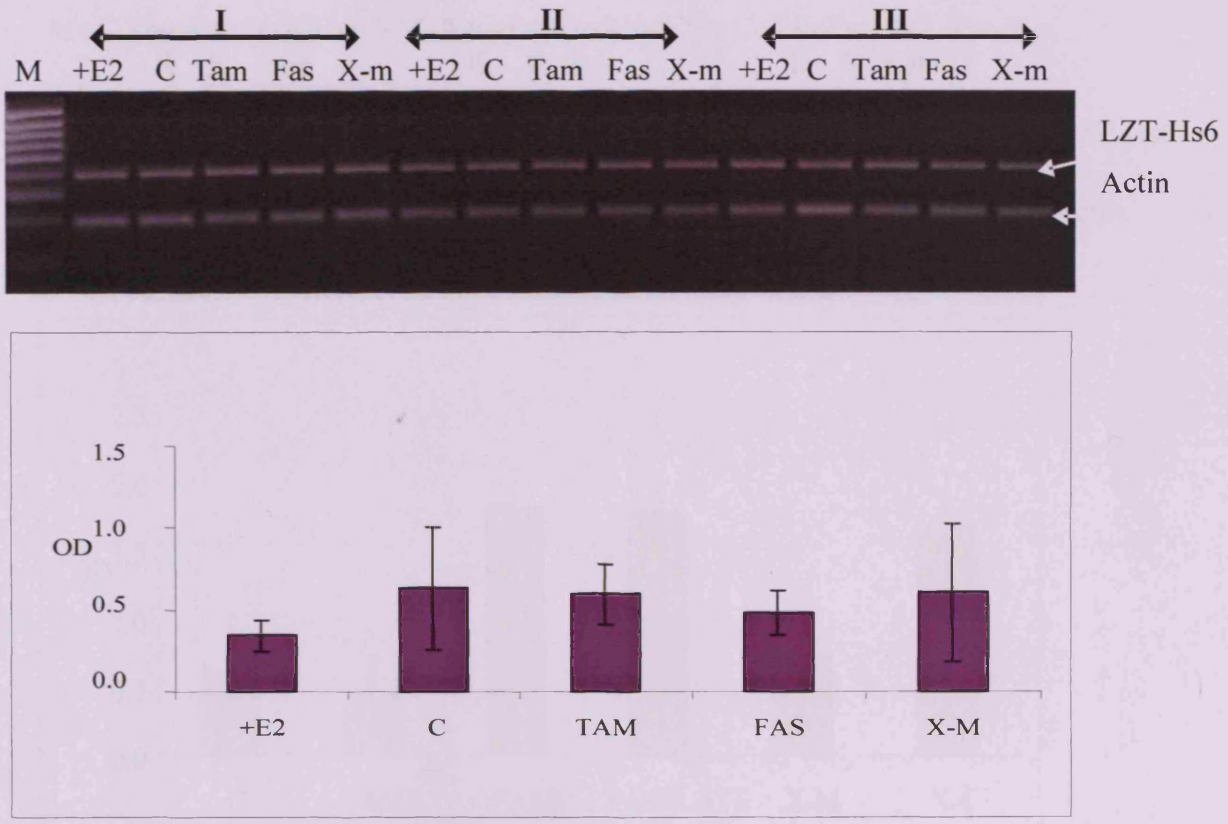

The gel image shows the PCR result of LZT-Hs6 gene expressions in breast cancer cells. The results are a representative of three mRNA sets. The graph below the gel image is a compilation of the densitometric values from the gel image.

Figure 5-12 : Relative mRNA expression of LZT-Hs6 in anti-hormone resistant cells

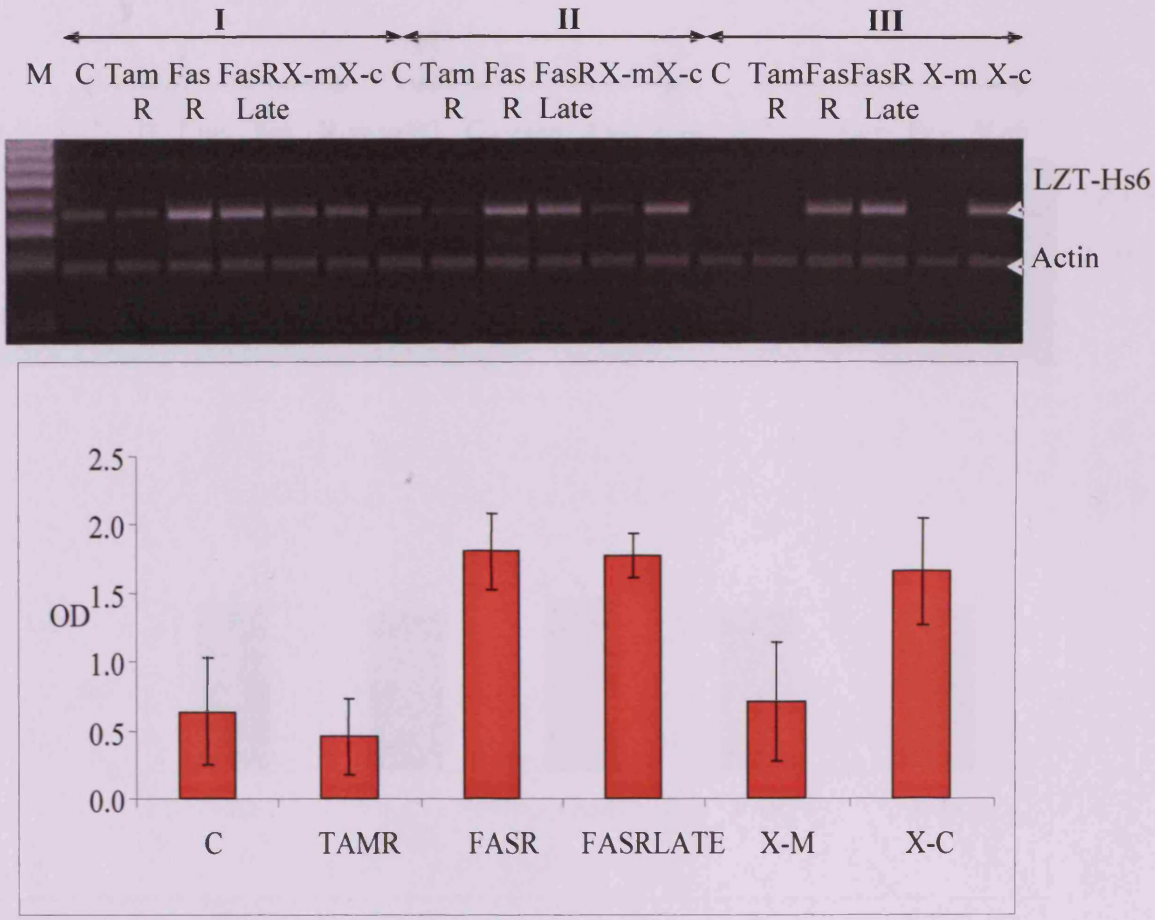

The gel image shows the PCR result of LZT-Hs6 gene expressions in breast cancer cells. The results are a representative of three mRNA sets. The graph below the gel image is a compilation of the densitometric values from the gel image.

Figure 5-13 : Relative mRNA expression of LZT-Hs7 in oestradiol and anti-hormone treated cells

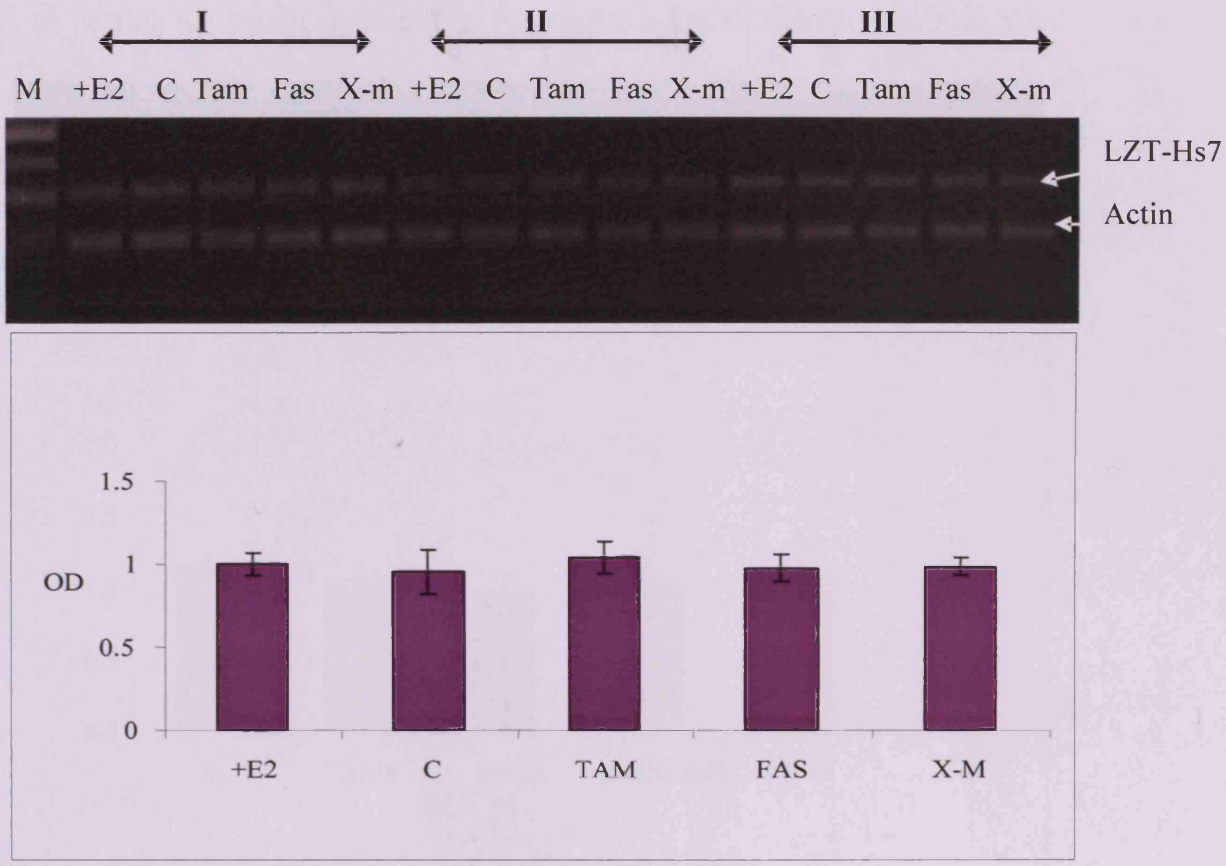

The gel image shows the PCR result of LZT-Hs7 gene expressions in breast cancer cells. The results are a representative of three mRNA sets. The graph below the gel image is a compilation of the densitometric values from the gel image.

Figure 5-14 : Relative mRNA expression of LZT-Hs7 in anti-hormone resistant cells

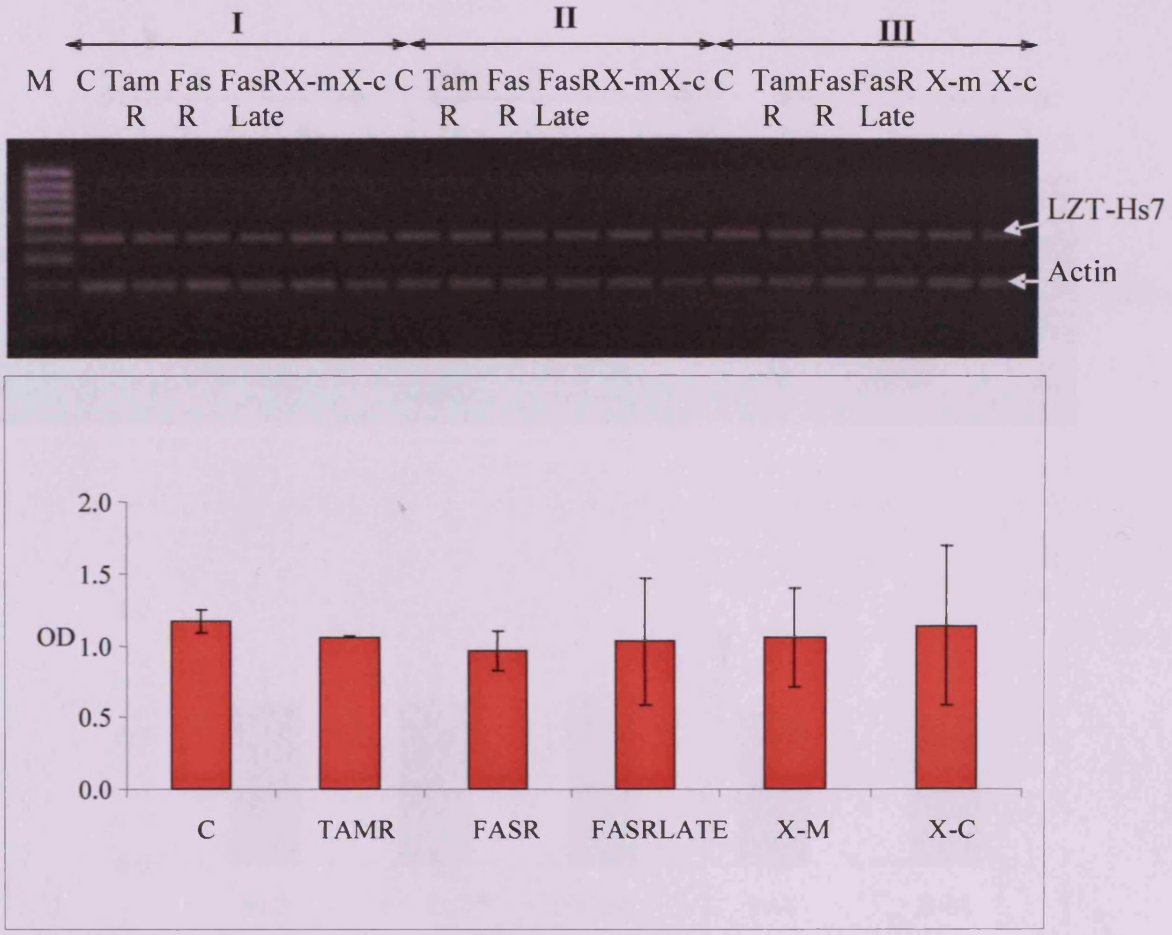

The gel image shows the PCR result of LZT-Hs7 gene expressions in breast cancer cells. The results are a representative of three mRNA sets. The graph below the gel image is a compilation of the densitometric values from the gel image.

Figure 5-15 : Relative mRNA expression of LZT-Hs8 in oestradiol and anti-hormone treated cells

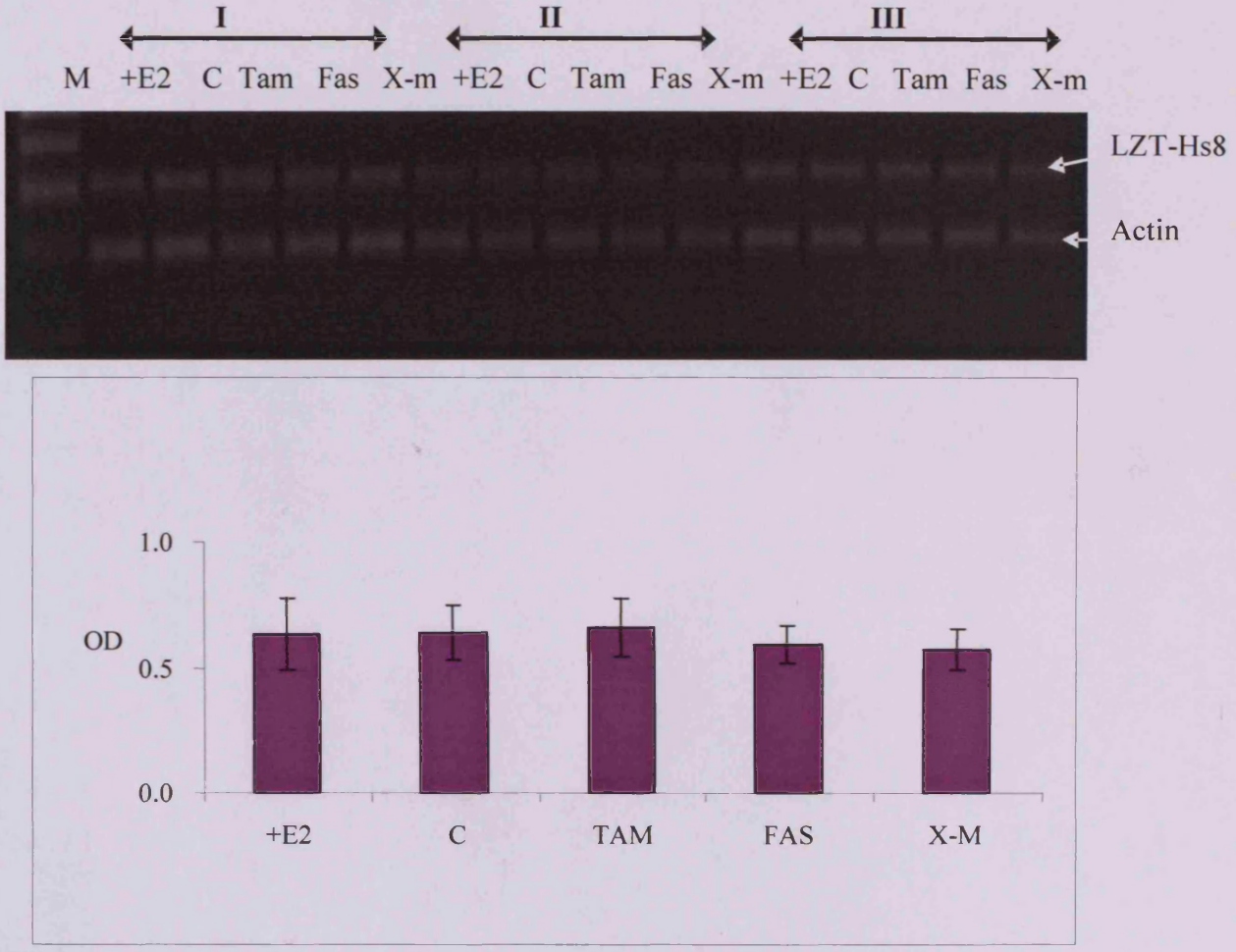

The gel image shows the PCR result of LZT-Hs8 gene expressions in breast cancer cells. The results are a representative of three mRNA sets. The graph below the gel image is a compilation of the densitometric values from the gel image.

Figure 5-16 : Relative mRNA expression of LZT-Hs8 in anti-hormone resistant cells

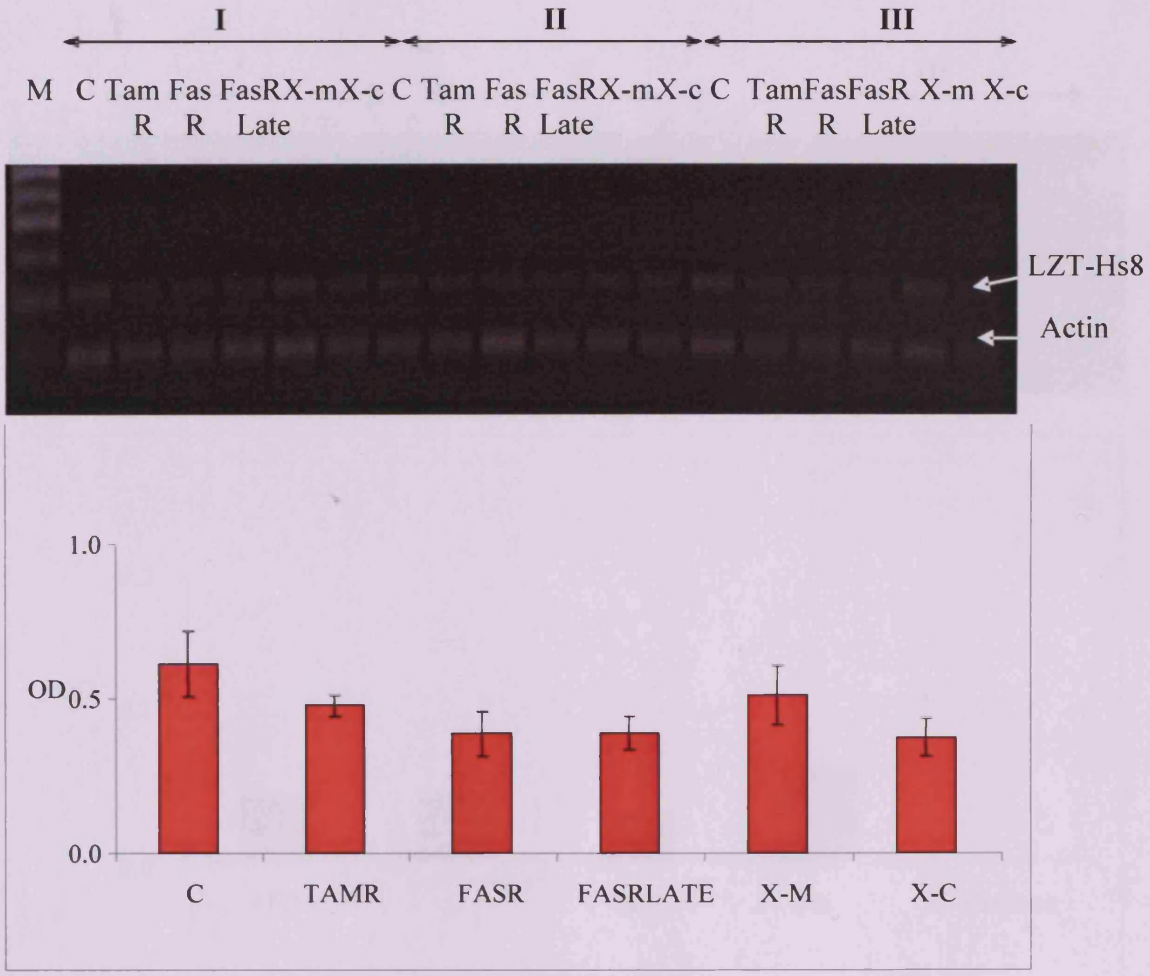

The gel image shows the PCR result of LZT-Hs8 gene expressions in breast cancer cells. The results are a representative of three mRNA sets. The graph below the gel image is a compilation of the densitometric values from the gel image.

Figure 5-17 : Relative mRNA expression of LZT-Hs9 in oestradiol and anti-hormone treated cells

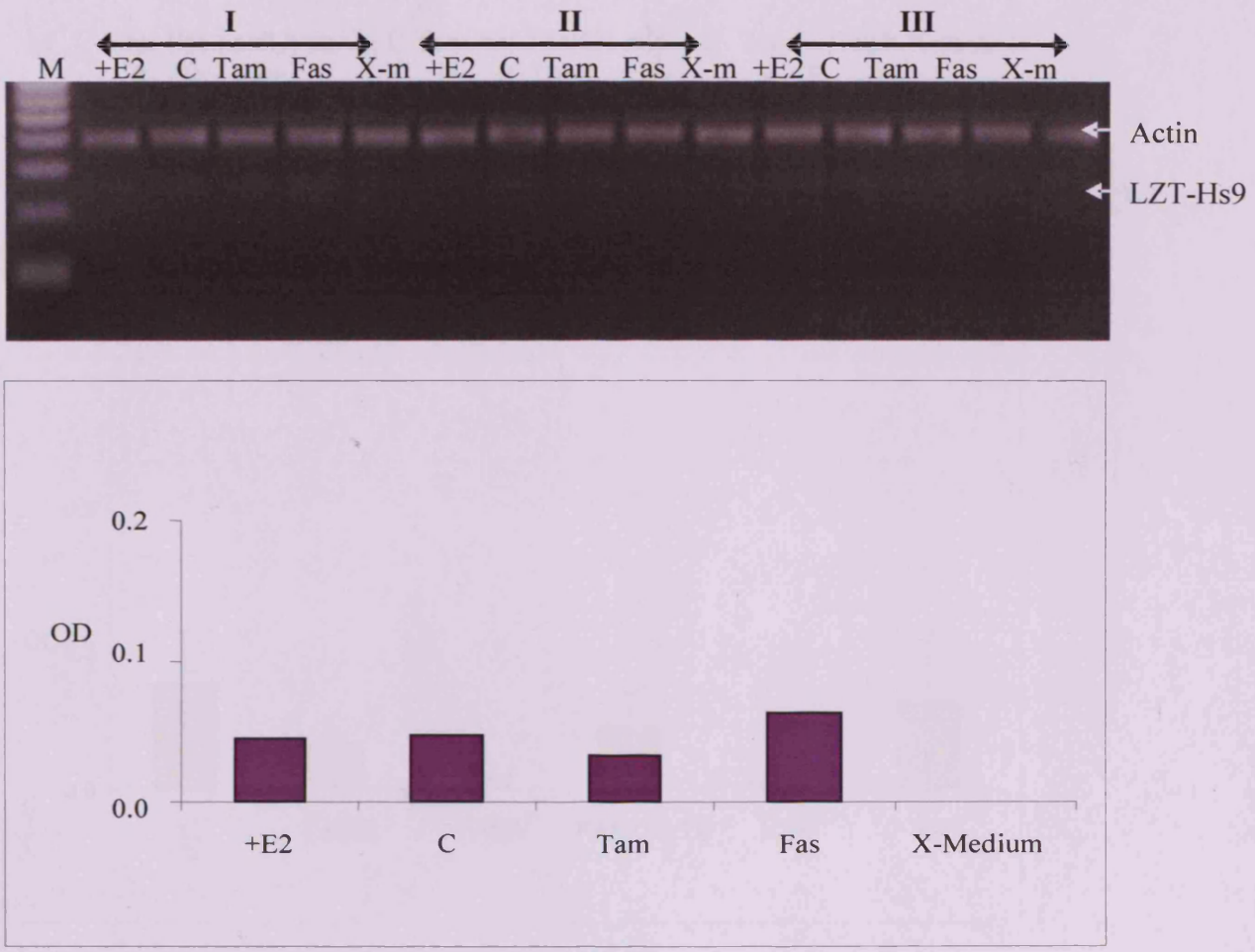

The gel image shows the PCR result of LZT-Hs9 gene expressions in breast cancer cells. The results are a representative of three mRNA sets. The graph below the gel image is a compilation of the densitometric values from the gel image.

Figure 5-18 : Relative mRNA expression of LZT-Hs9 in anti-hormone resistant cells

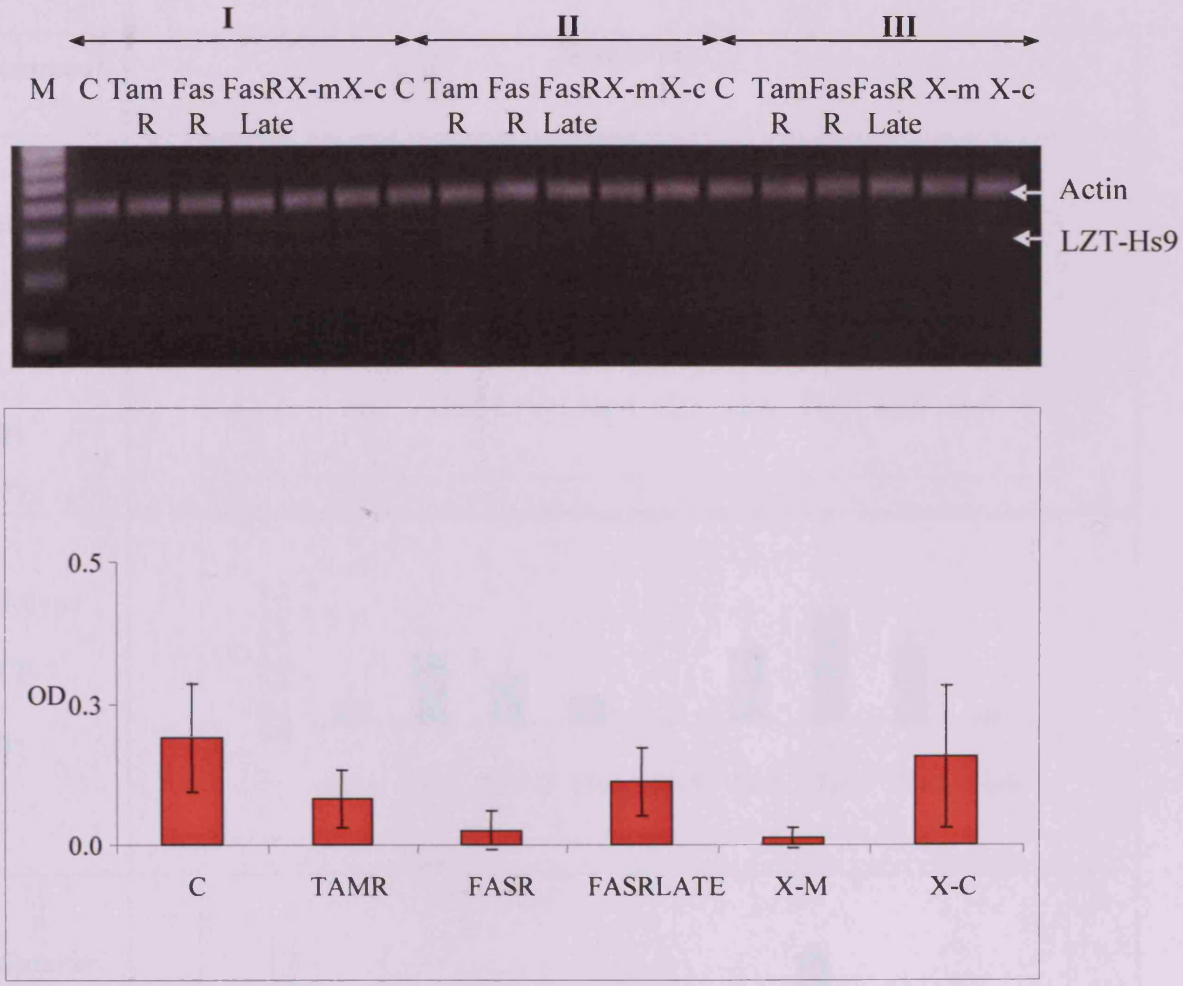

The gel image shows the PCR result of LZT-Hs9 gene expressions in breast cancer cells. The results are a representative of three mRNA sets. The graph below the gel image is a compilation of the densitometric values from the gel image.

Table 5-5 : Summary of the LIV-1 family of genes derived from the PCR data in response and resistance studies

Treatment	Histogram
Oestradiol treated MCF-7 cells	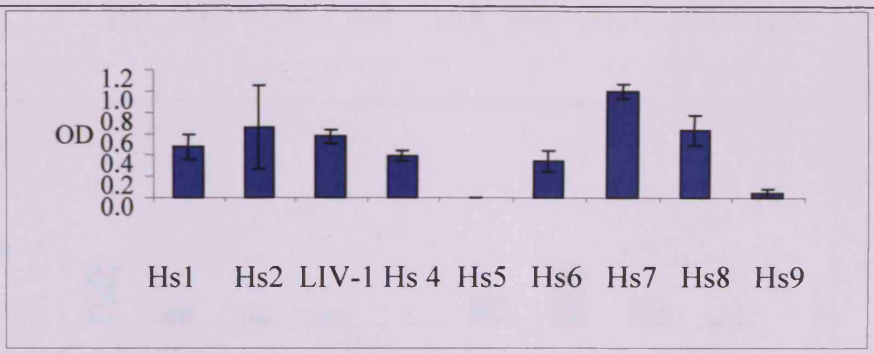
Wildtype MCF-7 cells	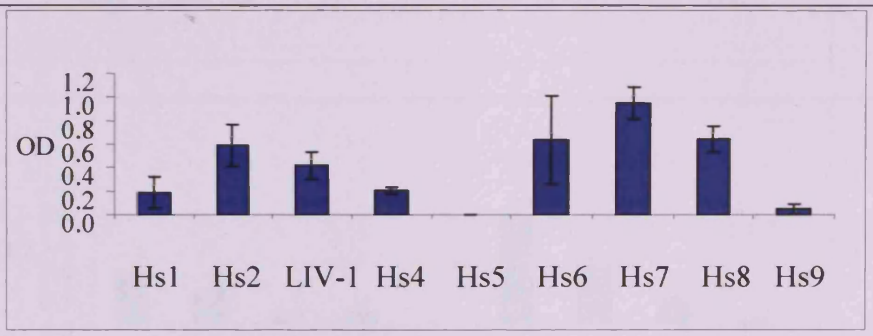
Tamoxifen treated MCF-7 cells	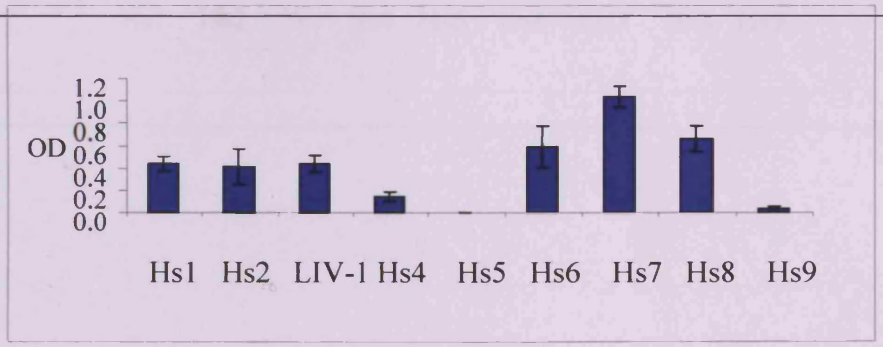

Faslodex treated MCF-7 cells	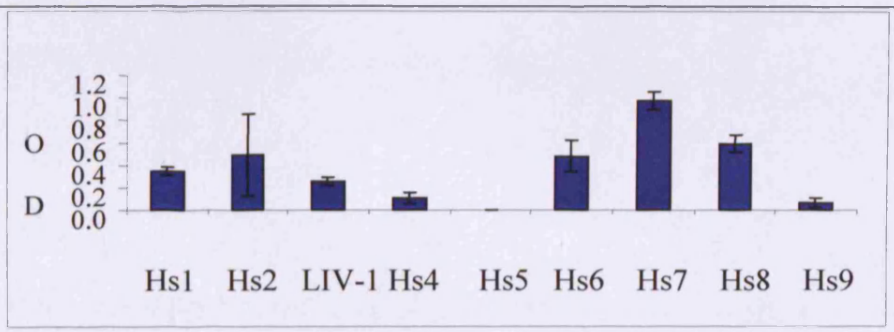
Tamoxifen resistant MCF-7 cells	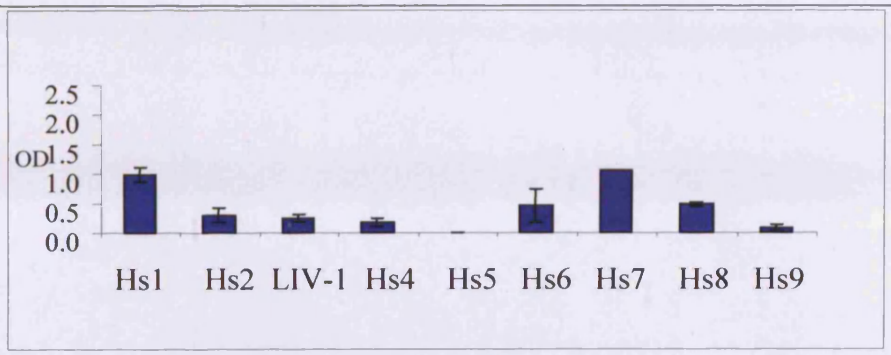
Faslodex resistant MCF-7 cells	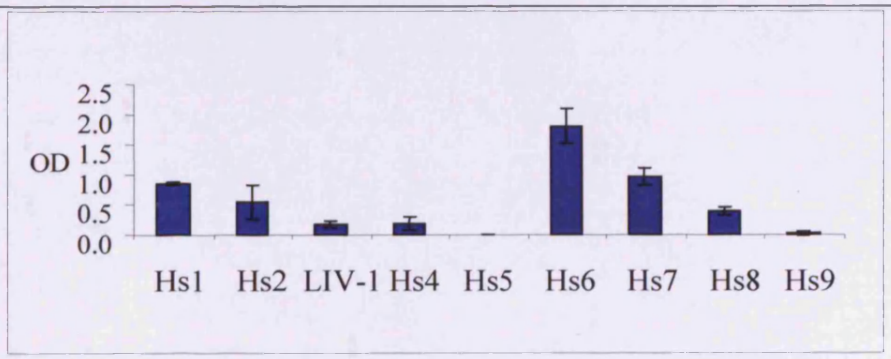

Faslodex late resistant MCF-7 cells	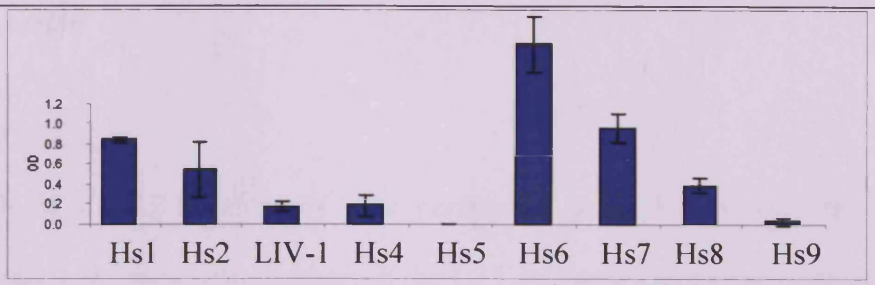
X-medium MCF-7 cells	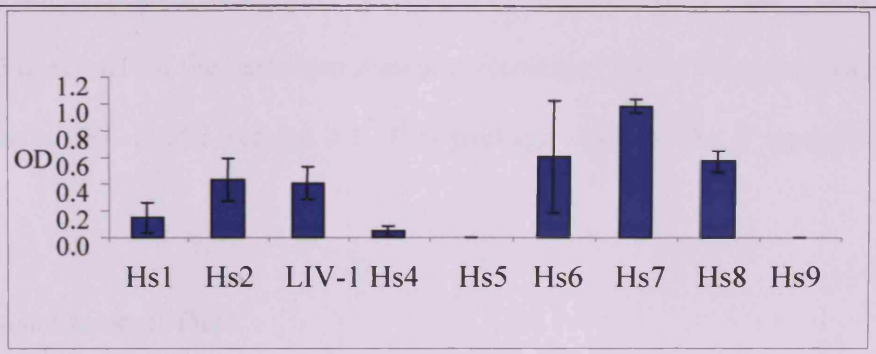
X-cells MCF-7	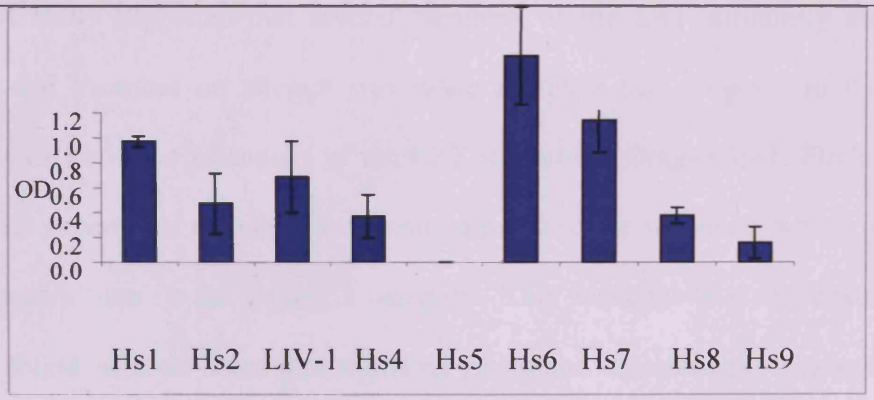

Legend:

Hs1:LZT-Hs1, Hs2:LZT-Hs2, LIV-1:LIV-1, Hs4:LZT-Hs4, Hs5:LZT-Hs5, Hs6:LZT-Hs6, Hs7:LZT-Hs7, Hs8:LZT-Hs8, Hs9:LZT-Hs9

5.3 ERE Promoter search

5.3.1 Ensemble Data

Information for each of the LZT subfamily was performed using Ensemble software packages. In each instance, the accession numbers of the LZT subfamily members were used as an input to select their respective eukaryotic sequences. The sequence of each family member was then used to search for the oestrogen response elements (EREs) via a computer software package, Dragon ERE Finder version 2.1. This package searches the 5' upstream region of the gene.

5.3.2 Estrogen Response Elements Data

Results from the RNA study suggested that several members of the LZT subfamily are oestrogen responsive, and therefore an attempt was made to relate this property to the presence or absence of EREs in the promoters of the LZT subfamily. Dragon ERE Finder version 2.1 uses a model system that contains the minimum palindromic sequence, which is GGTCAnnnTGACC, where 'nnn' is the typical 3 basepairs. This sequence is a consensus sequence that is only found in some oestrogen-regulated genes and therefore the analysis allows the detection of imperfect EREs patterns. These are referred as the 'new patterns', and are potentially functional. Tables 5-6 to 5-14, show the EREs search results for the LZT subfamily and identities of multiple imperfect EREs in each family member. Any nucleotide that changes from the consensus sequence are underlined as indicated in the tables. The tables also include information on the frequency of nucleotides that differ from the consensus palindromic sequence of the ERE. Interestingly, changes occur throughout the LZT family

sequences either in the first half of the consensus sequence (GGTCA) or in the second half of the sequence (TGACC). They were noticeable in both the forward and reverse strands of the DNA.

Observation from Table 5-6 shows imperfect EREs were identified in the LZT-Hs1 promoter, 1 on the forward strand, and 3 on the reverse strand. In all but one instance, 2 nucleotides were changed. Three alterations were seen in the reverse strand of ERE located at nucleotide position -709. Examination of the promoter of LZT-Hs2 produced a broadly similar pattern with 4 imperfect EREs being detected. However, the majority, 75%, contained 3 nucleotide changes. LIV-1 contained 2 imperfect EREs, one with 2 changes and one with 3. Equivalent imperfect EREs were seen throughout the remaining LZT family members and no obvious association was seen between the experimental data any of the oestrogen response of the gene or their expression in resistant cells and their EREs number, location on the forward or reverse strand or the number of nucleotides altered with the EREs sequences.

Table 5-6 : Compilation of ERE sites in LZT-Hs1 both forward and reverse strands

Consensus	G	G	T	C	A	/	T	G	A	C	C	Frequency
F1:+2039	G	C	C	C	A	/	T	G	C	C	C	2
R1: -2875	G	G	T	C	A	/	T	G	A	T	G	2
R2:-709	G	G	T	C	A	/	G	G	C	C	A	3
R3:-64	G	G	C	C	A	/	C	C	A	C	C	2

Altered nucleotides as compared to the consensus sequence are underlined

Table 5-7: Compilation of ERE sites in LZT-Hs2 both forward and reverse strands

Consensus	G	G	T	C	A	/	T	G	A	C	C	Frequency
F1: +2960	G	C	C	C	A	/	T	G	G	C	C	3
F2:+3370	G	G	G	C	A	/	T	A	C	C	C	3
R1:-2148	G	G	C	C	A	/	T	G	A	G	C	2
R2:-3986	G	A	C	C	A	/	T	G	G	C	C	3

Altered nucleotides as compared to the consensus sequence are underlined

Table 5-8 : Compilation of ERE sites in LIV-1 both forward and reverse strands

Consensus	G	G	T	C	A		T	G	A	C	C	Frequency
F1:+3489	T	G	T	G	A		T	G	A	C	C	2
R1:-2623	G	G	A	C	A		A	G	G	C	C	3

Altered nucleotides as compared to the consensus sequence are underlined

Table 5-9: Compilation of ERE sites in LZT-Hs4 both forward and reverse strands

Consensus	G	G	T	C	A		T	G	A	C	C	Frequency
F1:+373	G	A	A	C	A		T	G	A	C	C	2
F2:+1444	G	G	G	C	A		T	G	G	C	T	3
R1:-2043	G	A	C	C	A		T	G	G	C	C	3
R2:-1381	A	G	C	C	A		T	G	C	C	C	3

Altered nucleotides as compared to the consensus sequence are underlined

Table 5-10: Compilation of ERE sites in LZT-Hs5 both forward and reverse strands

Consensus	G	G	T	C	A	/	T	G	A	C	C	Frequency
F1:+358	G	G	C	C	A	/	T	G	G	T	C	3
F2:+910	G	G	C	C	C	/	T	G	G	C	C	3
R1:-1316	G	A	C	C	A	/	T	G	A	C	C	1

Altered nucleotides as compared to the consensus sequence are underlined

Table 5-11: Compilation of ERE sites in LZT-Hs6 both forward and reverse strands

Consensus	G	G	T	C	A	/	T	G	A	C	C	Frequency
F1:+1712	G	G	G	C	A	/	T	G	G	C	T	3
F2:+2334	G	G	C	C	A	/	T	G	C	C	C	2
F3:+5572	G	G	C	C	A	/	T	G	G	T	C	3
R1:-6787	G	A	C	C	A	/	T	G	A	T	C	3

Altered nucleotides as compared to the consensus sequence are underlined

Table 5-12: Compilation of ERE sites in LZT-Hs7 both forward and reverse strands

Consensus	G	G	T	C	A	/	T	G	A	C	C	Frequency
F1:+238	G	A	C	C	A	/	T	G	A	C	C	2
F2:+838	G	G	C	C	A	/	T	G	G	T	C	3
F3:+1390	G	G	C	C	C	/	T	G	G	C	C	2
F4:+1780	G	A	C	C	A	/	T	G	A	C	C	2
R1:-1796	G	A	C	C	A	/	T	G	A	C	C	2
R2:-254	G	A	C	C	A	/	T	G	A	C	C	2

Altered nucleotides as compared to the consensus sequence are underlined

Table 5-13: Compilation of ERE sites in LZT-Hs8 both forward and reverse strands

Consensus	G	G	T	C	A	/	T	G	A	C	C	Frequency
F1:+2167	G	G	T	G	A	/	T	A	A	C	C	2
F2:+3567	A	G	T	C	A	/	T	G	A	C	C	1
R1:-4056	G	G	G	C	A	/	T	C	A	C	C	2
R2:-4717	G	G	T	C	A	/	T	G	G	T	G	2

Altered nucleotides as compared to the consensus sequence are underlined

Table 5-14: Compilation of ERE sites in LZT-Hs9 both forward and reverse strands

Consensus	G	G	T	C	A	/	T	G	A	C	C	Frequency
F1:+744	G	A	G	C	A	/	T	G	G	C	C	2
F2:+2164	G	G	A	C	A	/	T	G	G	C	C	1
R1:-3021	G	G	G	C	A	/	G	G	T	C	T	2
R2:-2180	G	G	A	C	A	/	T	G	G	C	C	2
R3:-463	G	A	C	C	A	/	T	G	G	C	C	3
R4:-374	G	G	A	C	A	/	G	G	G	C	C	3

Altered nucleotides as compared to the consensus sequence are underlined

5.4 siRNA LZT-Hs1

The characterization of LZT subfamily in the Affymetrix search and mRNA profiling revealed that one member of the family LZT-Hs1 gene to be present in increased amounts in several forms of anti-hormone resistance, including tamoxifen resistance. Importantly, the resistant cells have gained an ability to grow in the presence of the anti-hormones, where previous studies have shown an involvement of EGFR and Src signalling. The current section explores the signalling consequences of LZT-Hs1 knockdown with a siRNA technology.

5.4.1 LZT-Hs1 knockdown in tamoxifen resistant cells

Initial experiments showed that the Lipofectamine2000 reagent exhibited some toxicity in the tamoxifen resistant cells (Figure 5-19) and was in itself, able to partially decrease the levels of LZT-Hs1 by approximately 70% at 24 hours post-transfection, and that this effect was also seen in the presence of a scrambled siRNA treated cells. Significantly, this also affected the expression/activation of the other signalling molecules. In light of the inhibitory effects of the Lipofectamine2000, only the actions of the siRNA to LZT-Hs1 over and above the scrambled siRNA are presented.

As may be seen in Figure 5-20, siRNA to LZT-Hs1 promotes an approximately 70% knockdown of LZT-Hs1 mRNA versus the scrambled control cells which was not significantly different as evidenced by the large error bars. One replicate showed a clear knockdown of LZT-Hs1 whereas the other 2 were not so pronounced. However, a successful knockdown of LZT-Hs1 protein was shown in Figure 5-22. No comparable knockdown of

LZT-Hs6 was seen (not significant with large error bars) with the siRNA to LZT-Hs1 (Figure 5-21) treated cells.

Examination of the effects of the siRNA to LZT-Hs1 on LZT-Hs1 protein levels revealed that although the scrambled siRNA treatment in the presence of Lipofectamine2000, considerably reduced LZT-Hs1 protein levels, they were further decreased by the siRNA (Figure 5-22A).

Importantly, examination of EGFR phosphorylation at the tyrosine 1068 (Figure 5-22B) and tyrosine 1173 (Figure 5-22C), showed an appreciable reduction in the levels of phosphorylation at these sites in the presence of the siRNA to LZT-Hs1, together with a comparable reduction in the phosphorylation of c-Src 418 (Figure 5-22D). These data are suggestive of a regulating role of LZT-Hs1 in EGFR/Src signalling and potentially the growth of tamoxifen resistant cells.

Figure 5-19 : Relative mRNA expression of LZT-Hs1 in tamoxifen resistant and siScramble treated cells

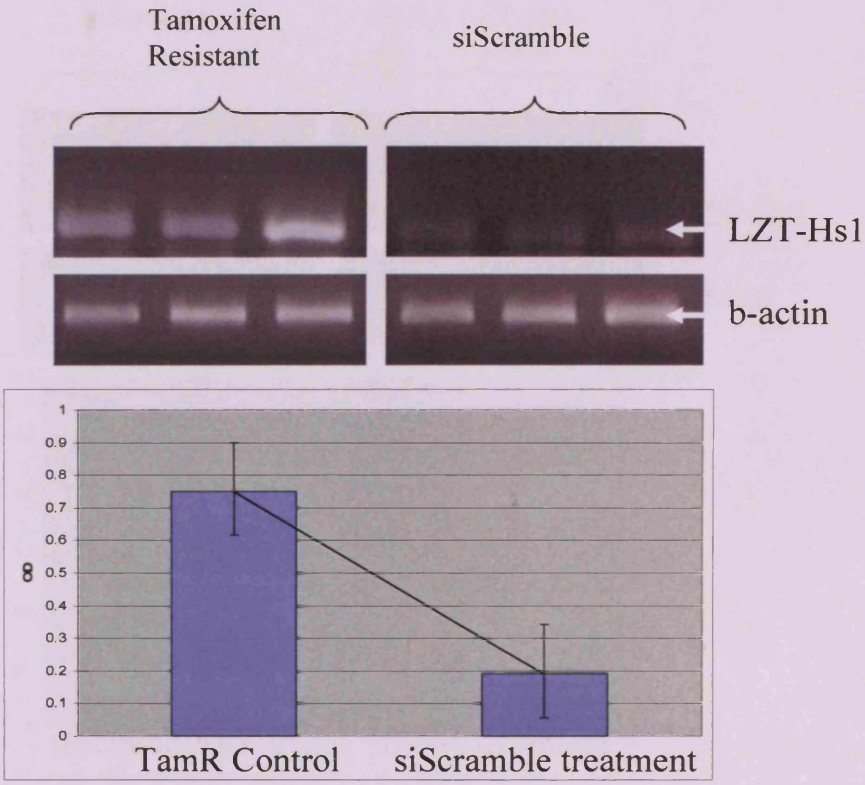

The gel image shows the PCR result of LZT-Hs1 gene expressions in tamoxifen resistant and siScramble treated cells. The results are representative of three mRNA sets. The graph below the gel image is a compilation of the densitometric values from the gel image.

Figure 5-20 : Relative mRNA expression of LZT-Hs1 in tamoxifen resistant and siRNA LZT-Hs1 treated cells

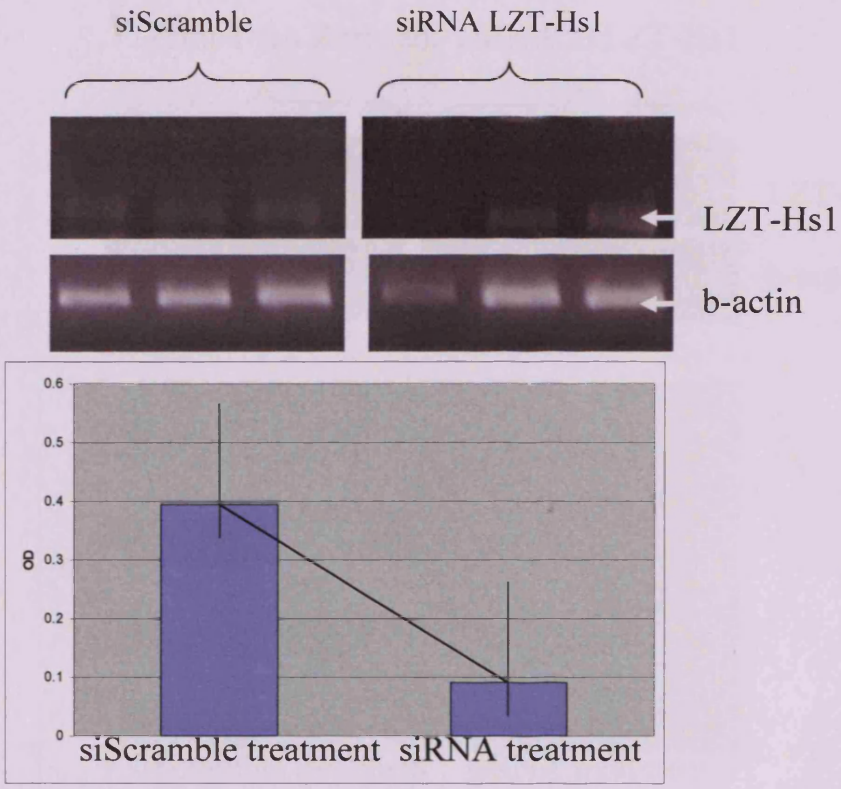

The gel image shows the PCR result of LZT-Hs1 gene expressions in tamoxifen resistant and siScramble treated cells. The results are representative of three mRNA sets. The graph below the gel image is a compilation of the densitometric values from the gel image.

Figure 5-21 : Relative mRNA expression of LZT-Hs1 in siScramble treated and LZT-Hs6 in siRNA LZT-Hs1 cells

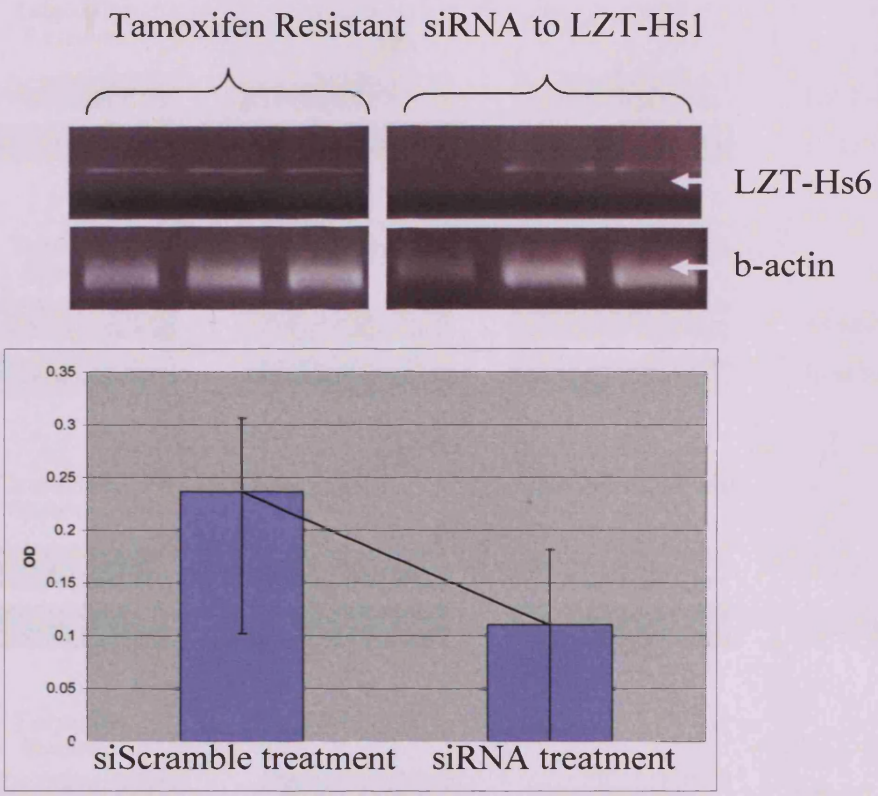

The gel image shows the PCR result of LZT-Hs1 gene expressions in tamoxifen resistant and siScramble treated cells. The results are representative of three mRNA sets. The graph below the gel image is a compilation of the densitometric values from the gel image.

Figure 5-22: Relative protein expression in various cell groups of tamoxifen resistant, siScramble and siRNA LZT-Hs1 treated cells

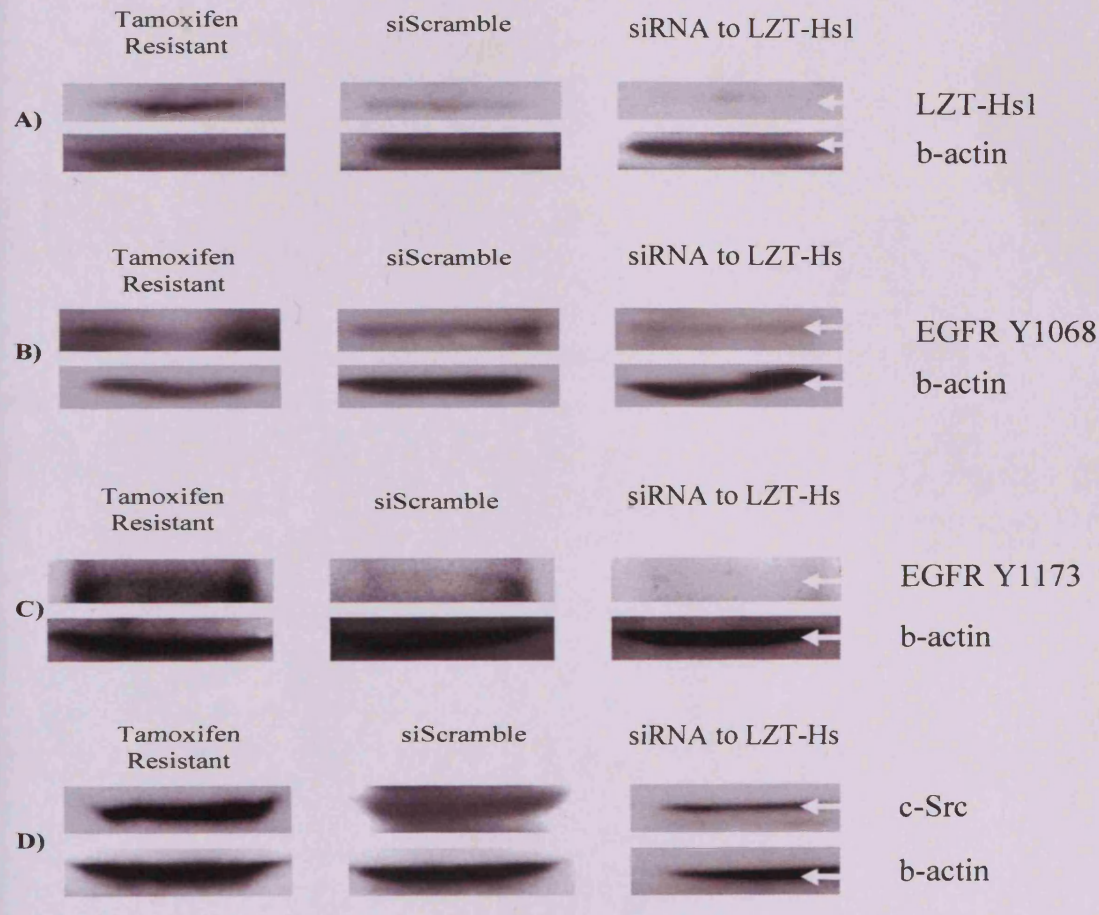

A) LZT-Hs1(56kDalton) protein was reduced after siRNA treatment compared to TamR control and siScramble treatment **B)** EGFRY^{1068} (175kDalton) protein was reduced after siRNA treatment compared to TamR control and siScramble treatment **C)** EGFRY^{1173} (175kDalton) protein was reduced after siRNA treatment compared to TamR control and siScramble treatment **D)** c-Src (60kDalton) protein was reduced after siRNA treatment compared to TamR control and siScramble treatment. In all samples β-Actin is 42kDalton.

5.5 Discussion

The current study is unique in that it represents the first time that the expression of the 9 LZT family members have been examined in breast cancer and anti-hormone resistance. Indeed, while previous studies have invariably looked at the role individual family members might play in normal or pathological condition (Manning et al. 1994; Schaner et al. 2003), we believe that there is considerable merit in trying to unravel the complexities of signaling within this newly identified family of proteins involved in zinc transport. In addition, hopefully in identifying which are most critical to the growth of breast cancer cells we will also determine which are potentially the most appropriate therapeutic targets (Duffy et al. 2000). Excitingly, the initial Affymetrix study, although limited in that only 5 family members were represented on the Affymetrix gene chip, clearly identified that at least one family member showed some regulation by oestrogen at the mRNA level and that several appeared raised in one or more forms of anti-hormone resistance. These results provided the impetus to develop semi-quantitative PCR methods to detect all of the LZT family in our RNA preparations and in turn confirm the appropriateness of the Affymetrix approach as an initial screening procedure.

Initially, the RNA preparations were PCR screened for pS2, a known oestrogen regulated gene, whose levels fall in tamoxifen (Dardes et al. 2002) and faslodex resistance (Hutcheson et al. 2003). Reassuringly, similar patterns were seen using PCR with data indicating that the pS2 gene was elevated by oestradiol however the expression falls significantly in tamoxifen and both early and late stage faslodex resistances.

Examination of the LZT family of genes by PCR identified several important features associated with the Affymetrix data and their differential expression in breast cancer cells. As compared to the Affymetrix data, the current study had shown that the PCR technique gave comparable results for the anti hormone resistance however not for hormone/anti-hormone response. Although the reasons for this are unclear, PCR is a technique where individual primers and assay conditions are designed to maximise the PCR product, whereas an Affymetrix analysis is based on multiple sets of probes some of which may lead to variable results, which are then averaged. This can lead to obscuring modest alterations in our gene expression profiles. In the results, some of the gene expression profiles have histograms with large error bars. As mentioned in Chapter 2 that the RNA samples maybe degraded due to the storage procedure or samples have been kept a long period before the respective RNA expression study started.

Interestingly, several papers have been shown that LZT-Hs5 tissue distribution is specific and restricted to intestinal tissues (Nakano et al. 2003). In contrast, LZT-Hs9 is suggested to be expressed in mammary tumours metastatized to lung tissue (Strausberg et al. 2002) and many other tissue (Figure 3-5) showed widespread distribution, therefore ubiquitously expressed..

In this study, LZT-Hs1 and LZT-Hs4 were shown to be oestrogen regulated, while LIV-1 showed a non-significant trend in this direction. Since the oestrogen regulation of the full

LZT family has not been examined previously, no literature comparisons can be made. With respect to the LIV-1 gene, several studies have previously shown it to be increased in expression by oestradiol (El-Tanani and Green 1996) confirmed by Affymetrix and additionally, its expression in clinical breast cancer specimens has been linked to oestrogen receptors (El-Tanani and Green 1997).

In light of the limited literature in this area, an attempt was made to evaluate the effects of oestradiol on the expression of the LZT family and investigate the presence of oestrogen response elements (EREs) in their promoter. Using Dragon ERE Finder 2.0, imperfect EREs were located in the promoters of all of the family members, in both the forward and reverse strands. This analysis, however, did not detect any sequences corresponding to the consensus sequence GGTCA nnn TGACC, and it is unclear how many alterations are allowed before oestrogen receptor (ER)-ERE binding activity is lost. Certainly, it has been suggested that two alterations can lead to either gain or loss of ERE activity (Bajic et al. 2003), and in many instances through out the LZT family members, as many as 3 alterations were detected. Significantly, oestrogen receptor activity is not necessarily wholly directed through EREs and, as previously stated, can operate through interactions with other nuclear transcription factors (NTFs) for example Sp1 and AP-1, and through the oestradiol binding to plasma membrane associated oestrogen receptor with direct induction of signal transduction pathways.

Interestingly, in the tamoxifen resistance model, increased activity of epidermal growth factor receptor (EGFR) has been directly linked to tumour cell growth with the EGFR selective tyrosine kinase inhibitor (TKI), gefitinib, promoting exclusive growth inhibition.

Subsequently, experiments by our group (Taylor et al. 2005), have shown tamoxifen resistant cells have increased levels of intracellular zinc, and that exposure of the cells to exogenous zinc is able to facilitate EGFR signalling via a Src dependent mechanism. Increases in zinc transporter levels might therefore promote the increased zinc levels in tamoxifen resistant cells and thus aid EGFR growth signaling.

Although 4 of the LZT family members were altered in expression across multiple forms of anti-hormone resistance, (LZT-Hs1, LZT-Hs4 and LZT-Hs6), only LZT-Hs1 was elevated in the tamoxifen resistance model. Consequently, to further study the relevance of zinc transporter and their involvement in anti-hormone resistance, we specifically targeted the LZT-Hs1 in the tamoxifen resistance model with an siRNA and investigated its effect on EGFR signalling. Encouragingly, even as only a preliminary study and set against a background of Lipofectamine2000 that induced cell toxicity, was able to demonstrate some knockdown of LZT-Hs1 mRNA and protein which produced a reduction in the phosphorylation of the EGFR at two tyrosine sites (Y^{1068} and Y^{1173}), and the levels of activated c-Src 418 and subsequent experiments in the Tenovus laboratories have confirmed this (Taylor, personal communication).

All together, these data imply an important role for zinc transporters in the growth of breast cancer cells and specifically the acquisition of endocrine resistance.

Chapter 6

Discussion

6.1 General discussion

The work performed in this thesis is unique in that it represents the first occasion that an attempt has been made to assess the relevance of the LIV-1 family to a disease state. Thus, although individual family members are increasingly being examined in multiple species (Strausberg et al. 2002), tissues (Strausberg et al. 2002) and in various diseases states (Manning et al. 1994; Nakano et al. 2003), less is known about how they might collectively act in cells and influence the disease process.

As such, this thesis has examined a few different areas, firstly, the similarity or dissimilarity of predicted secondary protein structures within the 9 family members of the LZT family. Secondly, successfully characterized the properties of LZT-Hs7, LZT-Hs8 and LZT-Hs9, where 2 gene have not been previously examined in the literature. Thirdly, analysed the oestrogen regulation of the LZT family members and their expression in endocrine resistance and finally, observed the cellular affects of LZT-Hs1 knockdown by siRNA as this gene shows clear up-regulation in several forms of anti-hormone resistance.

In this thesis, the expression of the different members of LZT subfamily has been examined in endocrine responsive and anti-hormone resistant breast cancer cells. Of particular significance is the absent or low expression of two family members in breast cancer cells,

LZT-Hs5 and LZT-Hs9, respectively. It has previously been reported that the LZT-Hs5 gene expression in tissues is restricted to the developing and mature intestine and is centrally involved in the pathogenesis of acrodermatitis enteropathica thus proving its specific tissue distribution (Huang et al. 2005). In contrast, LZT-Hs9 has been suggested to be expressed widely in many tissues such as in glioblastoma multiforme, liposarcoma, squamous cell carcinoma, bone, lung tumour, pituitary, neuroblastoma, kidney tumour and cervix tumour tissue (Strausberg et al. 2002), although there is no data available for breast tissue. As a consequence of the low expression displayed in the current study and they are excluded from the model.

An attempt has been made to assign the remaining 7 members of the LZT family to a subcellular location, with computer predictions, immunolocalisation studies and reference to the literature. These are suggesting that LIV-1 (Taylor et al. 2003), LZT-Hs4 ((Taylor et al. 2005) and LZT-Hs7 (Wang et al. 2004) are present on the cell's plasma membrane, whilst LZT-Hs1 is present in the endoplasmic reticulum (Taylor et al. 2004) and the Golgi body (Huang et al. 2005). For the first time, our current study showed that LZT-Hs8 and LZT-Hs9 genes are present in the endoplasmic reticulum in permeabilised cells; however, LZT-Hs8 is also present on the plasma membrane in unpermeabilised cells, albeit with low abundance. Significantly, in the present study LZT-Hs7 showed no evidence of zinc handling capacity which is in direct contrast to previous results showing LZT-Hs7 capable of transporting zinc. In conclusion, LZT-Hs8 and LZT-Hs9 showed evidence of zinc activity with each of them are suggested to act differently, one as efflux and the other as influx, respectively.

Among the LZT subfamily genes that are up regulated in one or multiple forms of acquired anti-hormone resistance are LZT-Hs1, LZT-Hs4 and LZT-Hs6. Furthermore, only LZT-Hs2 and LZT-Hs7 are unaltered in endocrine responsive and resistant breast cancer cells. LZT-Hs2 has been shown to have widespread tissue distribution and interestingly, it is involved in metastatis to the lymph nodes in breast cancer (Strausberg et al. 2002). However, LZT-Hs7 is commonly expressed in other tissues such as stomach tumour tissue or liver tumour tissue (Strausberg et al. 2002) and not commonly found in breast cancer tissue. This observed tissue distribution readily explains the reason for the unaltered expression across breast cancer cells Of LZT-Hs2 and LZT-Hs7. Figures 6-1 to 6-4 attempt to summarise what has been discovered about the remaining 5 members of the LZT subfamily in the endocrine responsive and anti-hormone resistant breast cancer cells.

Based on the model we can suggest a few interesting characters or properties of the LZT family in breast cancer. Firstly, each individual LZT family members are performing their respective cellular functions in differing compartments of the cell. In the cell, LZT-Hs1 is located in the endoplasmic reticulum and Golgi body whilst LZT-Hs2, LIV-1 and LZT-Hs4 and LZT-Hs7 are located on the plasma membrane, LZT-Hs8 located on plasma membrane however LZT-Hs9 in endoplasmic reticulum, and LZT-Hs6 on vesicle membranes. Although they appeared to be located in different sub-cellular compartment, their ability to transport zinc ions should be into the cytoplasm transporting zinc ions from either outside the cell or intracellular stores. Therefore, at any moment in time, the cytoplasmic zinc concentration will in part be a function of the levels of these zinc transporters.

In endocrine responsive and resistant breast cancer, zinc handling may be restricted primarily to 4 members of the LZT family, LZT-Hs1, LIV-1, LZT-Hs4 and LZT-Hs6. Some of the genes in this group appear to be oestrogen regulated while others are constitutively expressed in the cell. Those genes that are constitutively expressed may maintain the cell's basal cellular functions such as normal growth activity and cell survival processes. Whereas those genes that are oestrogen regulated enable the oestrogen-mediated responses to occur, such as additional/abnormal growth of the cell (Figure 6-1).

Figure 6-1 illustrates a model showing which LIV-1 family members have evidence of oestrogen regulation in the endocrine responsive MCF-7 cells, specifically, LZT-Hs1 located in the endoplasmic reticulum, LIV-1 and LZT-Hs4 that are located on the plasma membrane.

Of these 5 members of the LZT family that have been identified, only LZT-Hs1, LIV-1 and LZT-Hs4 show evidences of oestrogen regulation and might therefore contribute to the altered behaviour of hormone and anti-hormone treated breast cancer cells. In the latter instance, when the cells become resistant to anti-hormone treatment, LZT-Hs6 appeared to be up regulated, adding to the already 3 existing genes. It is postulated that since LZT-Hs2, LZT-Hs7, LZT-Hs8 and LZT-Hs9 are constitutively or poorly expressed, they may perform basal zinc handling, and not being reactive to external stimuli. Figure 6-3 shows genes that appeared to be increased in tamoxifen resistant cells are LZT-Hs1 and LZT-Hs4, and interestingly, these two genes (alongside with LIV-1 and LZT-Hs6) also appeared up regulated in prolonged oestrogen deprived breast cancer cells (Figure 6-2). LZT-Hs1 and

LZT-Hs4 genes together with additional, LZT-Hs6, are increased in another resistant state, faslodex resistant cells (Figure 6-4). It is believed that this will provide a growth advantage to the resistant cells possibly through the activation of growth factor signalling. This principle was proven by our preliminary study of siRNA to LZT-Hs1 in the tamoxifen resistant cells, which was able to reduce activation of the EGFR and Src pathways, as this is the dominant pathway of tamoxifen resistant cells.

6.2 Exciting things to do in the future

This study poses a series of questions about involvement of the LZT family in resistant tissues after endocrine treatment. The siRNA to LZT-Hs1 study implied that LZT-Hs1 was able to activate epidermal growth factor receptor. However, this should be further investigated for instance, to determine the affect on the EGFR Y^{845} site or if LZT-Hs1 also affects the activation of other growth factors such as insulin growth factor receptor, as these two receptors often cross-talk in many forms of resistance. Additionally, it would be useful to determine is siRNA knockdown of LZT-Hs1 would affect the growth and invasiveness of the resistant cells. Clear understanding of the mechanism of action of LZT-Hs1 may provide evidence of its ability to be a therapeutic candidate for an inhibitory compound.

LZT-Hs1, LZT-Hs4 and LZT-Hs6 recombinant clones are available to study the over-expression of the LZT family in responsive cells. These genes have been found to be elevated in resistant cells however if we could deliberately over-express them in responsive cells, this could determine if alone they are able to create a resistant phenotype. This individual

phenotypic feature would therefore be a marker to differentiate which tumour cells have the capability to become resistant to anti-hormone therapies.

As we have already cloned most of the above genes, their expression may be manipulated by mutation technology within the sequences that are of interest. This study would determine which region on the sequence was important for transport of zinc ions. Some of the regions of interest are the CPALLY motif, HEXPHE region and transmembrane domain III and IV. If they were mutated, this study could help us understand the zinc transport system of the zinc influx transporters, LZT subfamily. The mutations may additionally affect the cell morphology and would show, which is the most appropriate region for the design of inhibitory compounds, could have a role in the treatment of anti-hormone resistant breast cancer.

Figure 6-1: A cell diagram illuatrate the LZT subfamily involvement in oestrogen regulation

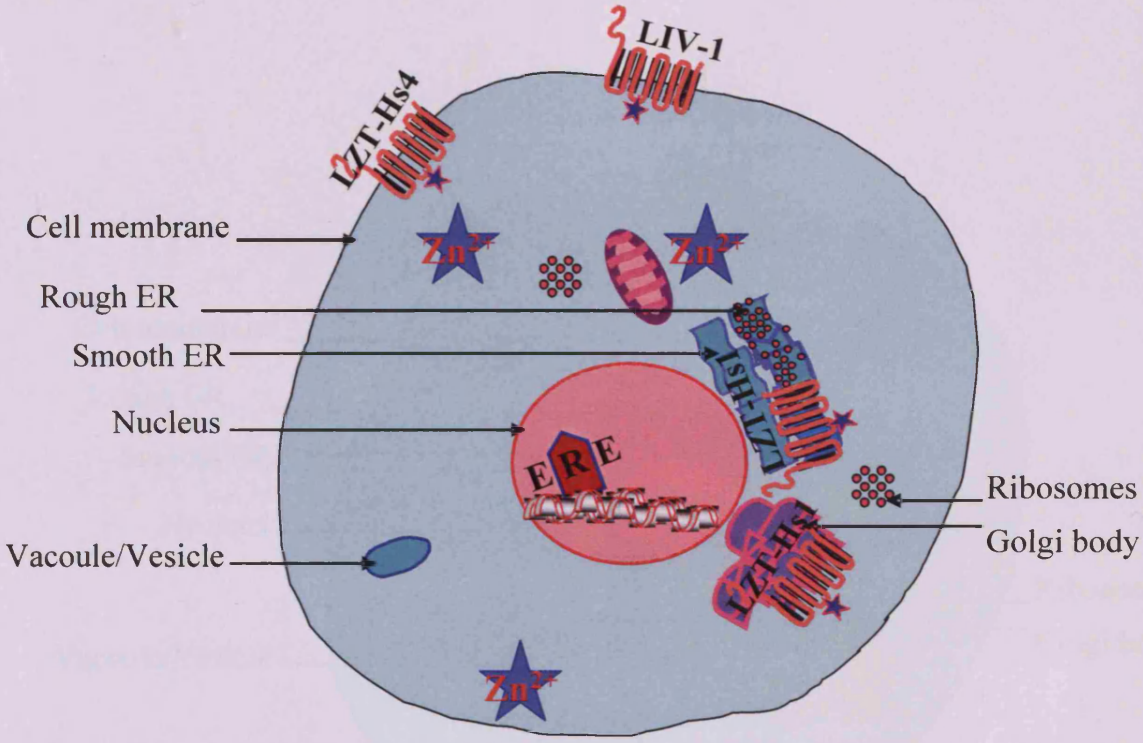

The MCF-7 cells under oestradiol stimulus appeared to up-regulate some members of the LZT subfamily; they are LIV-1 and LZT-Hs4, which are located on the plasma membrane and LZT-Hs1, located in the endoplasmic reticulum region. In the schematic diagram of LZT subfamily protein shows zinc located at the predicted binding site between transmembrane III and IV.

Figure 6-2 : A cell diagram illustrates the LZT subfamily involvement in prolonged oestrogen deprivation cells

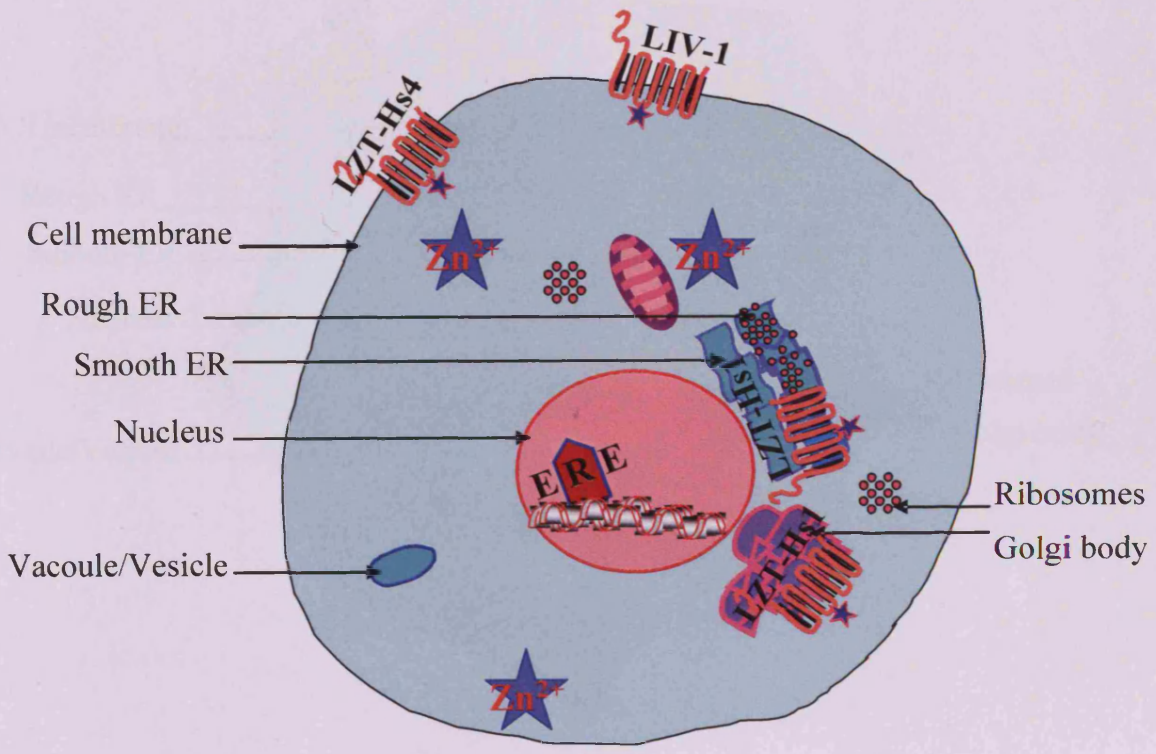

The MCF-7 cells under prolonged oestrogen deprivation condition appeared to up-regulate some members of the LZT subfamily; they are LZT-Hs1 and LZT-Hs4 significantly shown in our study data however, LIV-1 gene is expressed but not significant.

Figure 6-3 : A cell diagram illustrates the LZT subfamily involvement in tamoxifen resistant cells

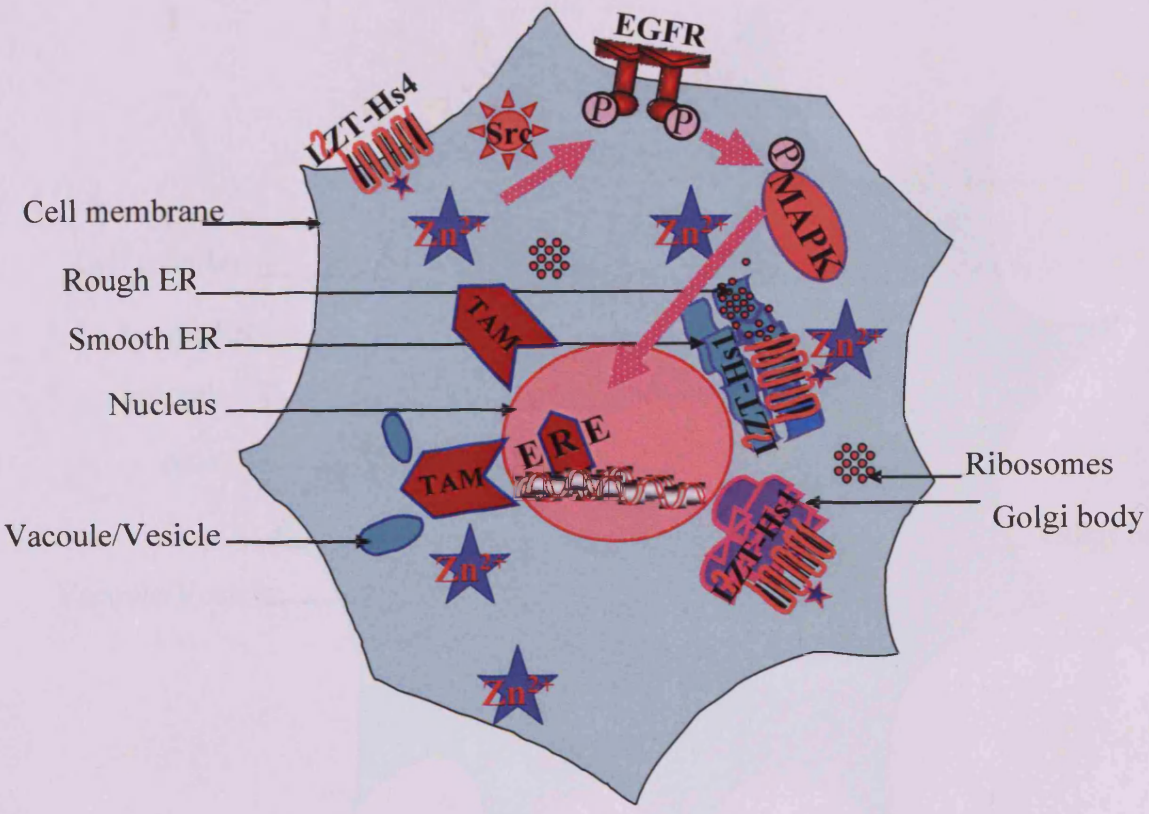

The MCF-7 cells under tamoxifen resistant condition appeared to up-regulate some members of the LZT subfamily; they LZT-Hs1 and LZT-Hs4 only. It is suggested that the LZT subfamily proteins involved are promoting abnormal growth via EGFR/Src pathway, shown by cell rough edges.

Figure 6-4 : A cell diagram illustrates the LZT subfamily involvement in faslodex resistant cells

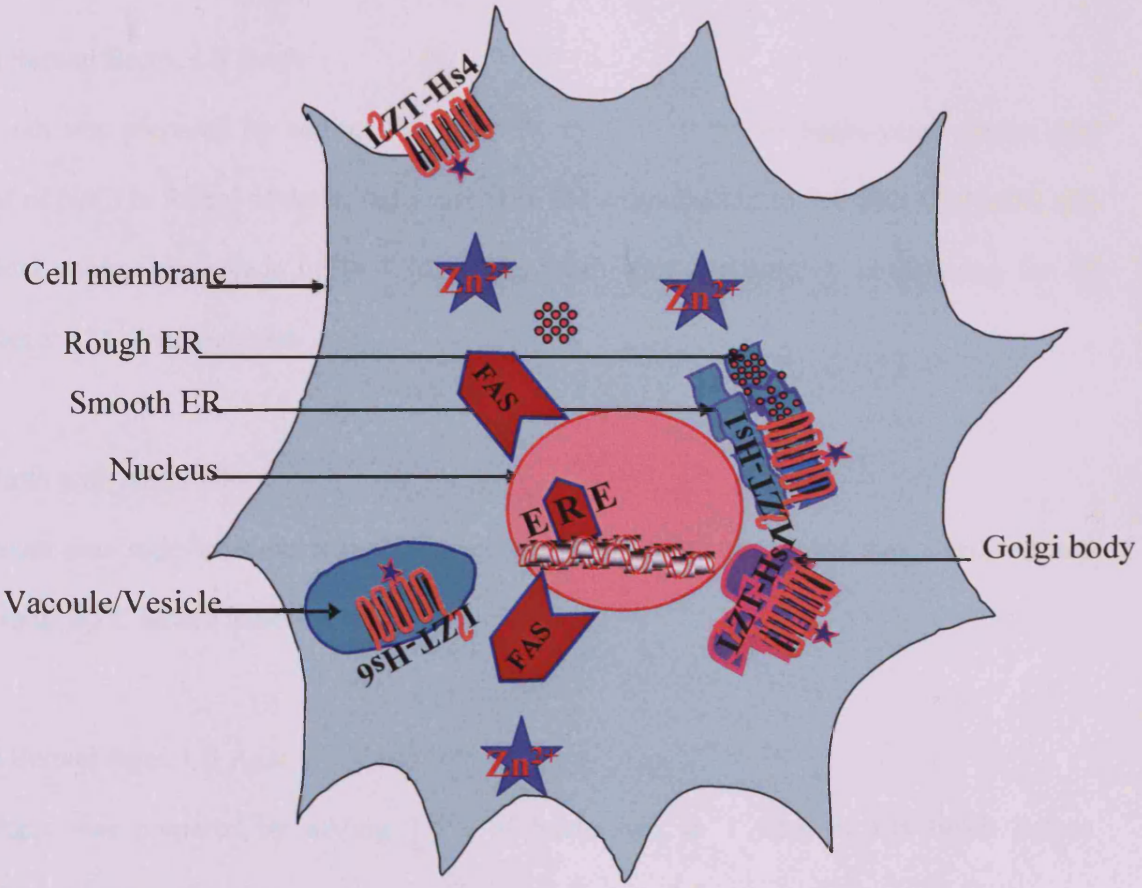

The MCF-7 cells under faslodex resistant condition appeared to up-regulate some members of the LZT subfamily; they are LZT-Hs1, LZT-Hs4 and LZT-Hs6. The cell is progressing aggressively under resistant condition showing aggressive phenotype cell with membranes pointing outward to invasion.

Appendix A

Molecular Biology

Luria Bertani Broth, LB Broth

LB broth was prepared by adding 1% of bacto-tryptone, 0.5% of bacto-yeast extract and 0.17M of NaCl in 950ml of deionised water. The pH was adjusted to 7.4 with 1N NaOH and the final volume was made up to 1 litre. The broth was sterilised by autoclaving for 40 minutes at 121^0C temperature.

LB Broth with Ampicillin

LB broth was supplemented with 100µg/ml ampicillin after the broth was sterilised and lukewarm, 55^0C before antibiotic addition.

Luria Bertani Agar, LB Agar

LB Agar was prepared by adding 1.5% of bacto-agar in 1 litre of LB broth before sterilisation by autoclaving.

Antibiotic Ampicillin

Ampicillin was kept as 100X concentrated stock solutions in sterilised deionized water, and sterilised by filtration through 0.2µM filter. The antibiotics were aliquot and kept in -20^0C to avoid degradation and frequent freeze-thawing process. For the purpose of selection media, 100µg/ml of Ampicillin was added to the sterilised media prior to using the media.

Tris/Acetate buffered EDTA, TAE Buffer

TAE buffer is used in the agarose gel electrophoresis procedure and the 50X concentration buffer was made of 242g of Trizma® base, 57.1ml of glacial acetic acid and 18.2g of EDTA into 1 Liter of deionised water.

DNA loading buffer

DNA loading buffer is used to load DNA samples into agarose gel and the 5X concentration buffer was made of 5ml glycerol, 200µl of 50X TAE buffer, 1ml of saturated bromophenol blue and 1 ml of 10% solution of xylene cyanol and the volume was adjusted to 10ml with deionized water. The buffer was aliquot and stored at -20^{0}C.

PCR Buffer

The PCR buffer is used in PCR mixture and 10X concentration buffer was made of 4ml 0.5M Tris-HCl (pH 8.3), 10ml of 1M KCl, 300µl 1M $MgCl_2$, 100µl of 2% gelatine and 5.6ml sterile nuclease free water and the volume was adjust to 20ml with deionized water. The buffer was aliquot and stored at -20^{0}C.

0.5M Tris-HCl with pH 8.3

This Tris-HCl buffer was used in preparing the PCR buffer and the 0.5M Tris-HCl was made of 6.05g Trizma® base which was dissolved in 80ml of sterile nuclease free water. Concentrated HCl acid was used to correct the pH to 8.3 and the volume was adjusted to 100ml with nuclease free water. This solution was sterilised by autoclaving and stored at room temperature.

Appendix B

Protein Biochemistry

10% Sodium dodecyl sulphate, SDS

10% of SDS solution was made by adding 10g SDS in 90ml of sterile nuclease free water and left overnight to dissolve without stirring or shaking. Then adjust the volume to 100ml and stored the solution at room temperature.

Phosphate Buffer Solution-Tween, PBS-T

1X PBS-T is used in the dilution of antibody for binding purpose and as washing buffer in the immunoblotting procedure. 10X concentrated PBS-T buffer was made up of 3.9g Na_2HPO_4, 10.7g NaH_2PO_4 and 85g NaCl dissolved in and adjust the volume to 1L with distilled water. 10ml of Tween 20 was added to have 0.01% final concentration of PBS-T and the solution was stored at room temperature. Further dilution to prepare 1X PBS-T solution is using distilled water.

Protein sample buffer

Protein sample buffer is used to add to protein samples in the SDS-PAGE procedure. The protein sample buffer was made up of 0.02M Tris-HCl pH 8.0, 0.002M EDTA, 2% SDS (v/v), 10% 2-Mercaptoethanol (v/v), 20% glycerol, 2.5% bromophenol blue (v/v), 200µl of Tris-HCl with pH8.0, 4ml glycerol, 500µl of saturated bromophenol blue were added into a sterile universal and in a fume cupboard, add 2ml of 2-Mercaptoethanol was added into.

Finally, the volume was adjusted to 20ml with nuclease free water. The buffer was aliquot and stored at -20^{0}C.

2M Tris-HCl with pH 8.0

To prepare stock solution of 2M Tris-HCl, for preparing other Tris containing buffers, was made up of 242.2g Trizma® base dissolve in 850ml of deionized water. Concentrated HCl acid was used to correct the pH to 8.0 and the volume was adjusted to 1L with deionized water. The solution was sterilized by autoclaving and stored at room temperature.

0.5M Ethylenediamine tetra-acetic acid, EDTA

To prepare stock solution of 0.5M EDTA, for preparing other EDTA containing buffers, was made up of 93.05g EDTA-$NA_2{\cdot}2H_2O$ dissolve in 300ml of deionized water and 10N NaOH solution was used to correct pH to 8.0 and the volume was adjusted to 500ml with deionized water. The solution was sterilized by autoclaving and stored at room temperature.

10N NaOH

To prepare stock solution of 10N NaOH, for preparing other NaOH containing buffers, was made up of 40g NaOH dissolve in 90ml of sterile nuclease free water. The volume was adjusted to 100ml with sterile nuclease free water and store at room temperature.

5X SDS-PAGE Running Buffer (0.05M Tris, 0.384M glycine, 1% SDS)

1X SDS-PAGE running buffer is used as the electrophoresis buffer for running the gels in SDS-PAGE procedure. 5X concentrated SDS-PAGE running buffer was made up of 30.2g Trizma® base and 144g glycine dissolve in 600ml deionized water. Then 100ml of 10% SDS solution was added and adjust the volume to 1L using deionized water and the solution was stored at room temperature. Further dilution to prepare 1X SDS-PAGE solution is using deionized water.

10X SDS-PAGE Transfer Buffer (25mM, 192mM, 0.1% SDS)

1X SDS-PAGE transfer buffer is used as the electrophoresis buffer for western transfer of protein to be immobilized on PVDF membranes. 10X concentrated SDS-PAGE transfer buffer was made up of 30g Trizma® base and 143.5g glycine dissolve in 500ml deionized water. Then 100ml of 10% SDS solution was added and adjust the volume to 800ml using deionized water and the solution was stored at room temperature. Further dilution to prepare 1X SDS-PAGE transfer buffer, 100ml of the 10X SDS-PAGE as stock solution, was diluted into 700ml deionized water and was added with 200ml methanol.

Appendix C

DNA and Protein Marker

DNA Molecular Weight Marker

1 Kilobase (kb) DNA

In the 1 kb DNA has 13 DNA fragments in range of 250 kb, 253 kb, 500 kb, 750 kb, 1 kb, 1.5 kb, 2 kb, 2.5 kb, 3 kb, 4 kb, 5 kb, 6 kb, 8 kb and 10 kb in sizes.1 kb to 10 kb with exact 1 kb increments. On an EtBr stained gel, only the 1 kb and 3 kb fragments have increased intensities relative to other fragments which each has approximately 25ng/µl of DNA. To load the ladder in a convenient volume is 5ul in a lane.

Hyperladder IV

Hyperladder IV has 9 DNA fragments in range of 100 bp and 200 bp which both fragments has 20ng amount of DNA, 300 bp and 400 bp with each both fragments has 40ng amount of DNA, 500 bp and 600 bp each has 60ng amount of DNA, 700 bp and 800 bp each has 80ng amount of DNA and 1 kb size fragment with 100ng amount of DNA. The DNA amount in the each fragments help to accurately quantify the sample on the stained EtBr gels. To load the ladder in a convenient volume is 5µl in a lane.

Protein Molecular Weight Marker

Full range Rainbow™ coloured protein molecular weight marker

The full range Rainbow™ coloured protein molecular weight marker has 10 protein bands that are in these sequence; 10 kD, 15 kD, 30 kD, 35 kD, 50 kD, 75 kD, 105 kD, 160 kD and 250 kD. To load the ladder in a convenient volume is 10 µl in a lane.

Appendix D

Abbreviation

ANOVA	analysis of variance
ATP	adenosine triphosphate
cDNA	Complementary or copy DNA
DNA	deoxyribonucleic acid
dNTP	Deoxynucleotide triphosphate
EDTA	ethylenediaminetetraacetic acid
kb	kilo base
mRNA	messenger RNA
RCF	relative centrifugal field
r.p.m	revolutions per minute
RNA	ribonucleic acid
RT	reverse transcriptase
RT-PCR	reverse transcription polymerase chain reaction
siRNA	small interfering RNA

Appendix E

Publication

'The emerging role of the LIV-1 subfamily of zinc transporters in breast cancer'

The Emerging Role of the LIV-1 Subfamily of Zinc Transporters in Breast Cancer

Kathryn M Taylor,[1] Helen E Morgan,[1] Kathryn Smart,[1] Normawati M Zahari,[1] Sara Pumford,[1] Ian O Ellis,[2] John F R Robertson,[3] and Robert I Nicholson[1]

[1]Tenovus Centre for Cancer Research, Welsh School of Pharmacy, Cardiff University, Cardiff, United Kingdom; Departments of [2]Histopathology and [3]Surgery, University of Nottingham, City Hospital, Nottingham, United Kingdom

Zinc transporter LIV-1 (SLC39A6) is estrogen regulated and present in increased amounts in estrogen receptor–positive breast cancer as well as in tumors that spread to the lymph nodes. The LIV-1 subfamily of ZIP zinc transporters consists of nine human sequences that share considerable homology across transmembrane domains. Many of these sequences have been shown to transport zinc and/or other ions across cell membranes. Increasingly, studies have implicated members of the LIV-1 transporter subfamily in a variety of diseases. We review these studies and report our own investigations of the role in breast cancer of the nine LIV-1 zinc transporters. We have documented the response of these transporters to estrogen and antiestrogens, and also their presence in our models of resistance to antiestrogens. Resistance to antiestrogen drugs such as tamoxifen and fulvestrant often occurs in advanced breast cancer. In these models we observed differential expression of individual LIV-1 family members, which may be related to their observed variable tissue expression. We were unable detect ZIP4, which is known to be expressed in the intestine. HKE4/SLC39A7 had elevated expression in both antiestrogen-resistant cell lines, and ZIP8 had elevated expression in fulvestrant-resistant cells. In addition, we investigated the expression of the nine LIV-1 family members in a clinical breast cancer series. Although a number of different LIV-1 family members showed some association with growth factor receptors, LIV-1 was solely associated with estrogen receptor and a variety of growth factors commonly associated with clinical breast cancer. HKE4, however, did show an association with the marker of cell proliferation Ki67 the spread of breast cancer to lymph nodes.

Online address: http://www.molmed.org
doi: 10.2119/2007-00040.Taylor

INTRODUCTION TO THE LIV-1 FAMILY OF ZINC TRANSPORTERS

Zinc Transporter Families

Zinc is an essential ion in cells; without it cells cannot sustain life. Zinc is a cofactor for more than 300 enzymes, representing more than 50 different enzyme classes, and is essential for cell growth (1). Zinc is involved in protein, nucleic acid, carbohydrate, and lipid metabolism, as well as in the control of gene transcription, differentiation, development, and growth (2). Zinc deficiency can be detrimental, causing stunted growth and serious metabolic disorders (3), while excess zinc can be toxic to cells (4). Cellular levels of zinc are tightly regulated by specific zinc transporter proteins, of which there are two known families. These two families have opposing action on zinc transport. The ZnT family (SLC30A) (previously termed CDF for cation diffusion facilitator) of zinc transporters (5) transport zinc out of cells or into intracellular compartments from the cytoplasm, whereas the ZIP family (for Zrt-, Irt-like Proteins) (SLC39A) of zinc transporters (6) transport zinc into the cell cytoplasm from either outside the cell or from intracellular compartments. Although these two families are termed zinc transporters, evidence shows that some members are able to transport other divalent cations such as iron, cadmium, copper, and manganese as well as zinc. The exact molecular mechanism for such transport is still unknown, however. The ZnT family contains nine human sequences, and the ZIP family contains 14 human sequences (7). Increasing evidence implicates various members of the SLC39A family of ZIP transporters in disease states and suggests that aberrant expression of zinc transporters leads to uncontrolled growth such that occurring in cancer. Thus any molecules controlling cellular zinc levels are worthy of investigation.

Address correspondence and reprint requests to *Kathryn M Taylor, Tenovus Centre for Cancer Research, Welsh School of Pharmacy, Cardiff University, Redwood Building, King Edward VIIth Avenue, Cardiff, CF10 3XF, UK. Phone: +442920 875226; Fax: +442920 875152; Email: Taylorkm@cardiff.ac.uk.*
Submitted April 23, 2007; Accepted for publication June 22, 2007.

The LIV-1 Family of ZIP Transporters

More than 100 SLC39A sequences have been identified, originating from more than 12 species (7,8). The 14 human members of the SLC39A family have

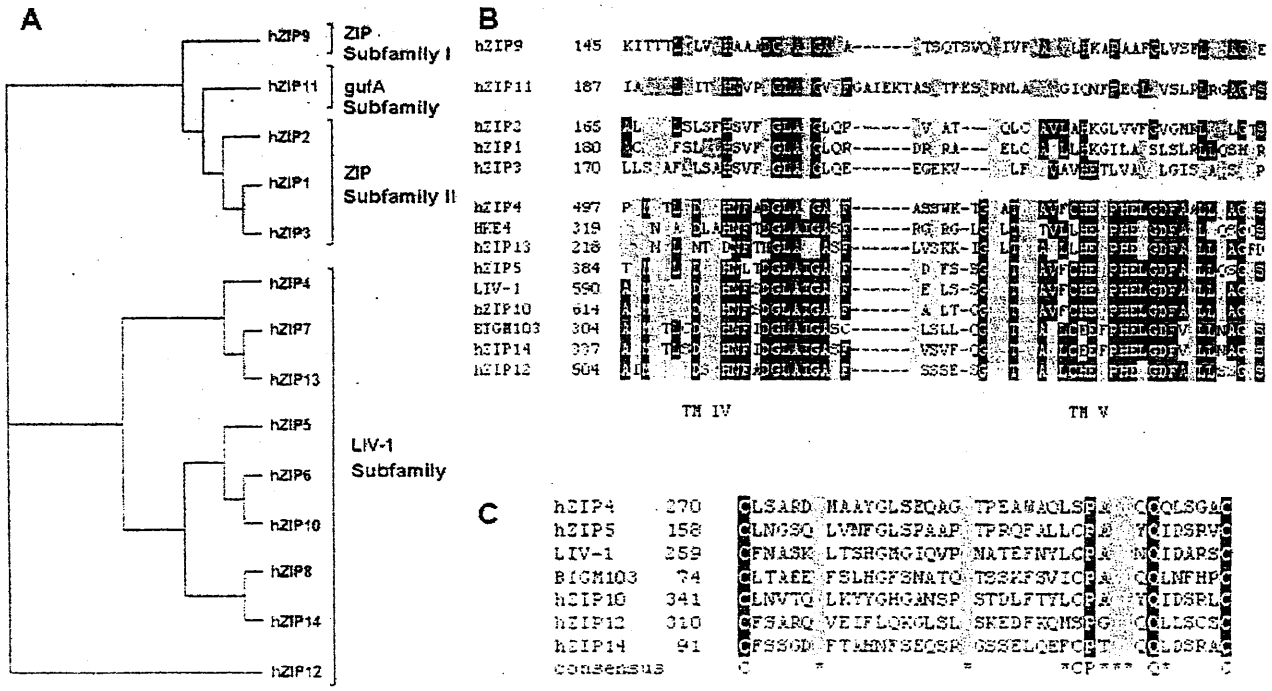

Figure 1. Phylogenetic tree and alignment of the human members of the ZIP superfamily of zinc transporters. (A) This phylogenetic tree was drawn using ClustalW and treeview software. (B) This alignment demonstrating the highly conserved motif in TM V for the LIV-1 family was performed using ClustalW and shaded using Boxshade software. Black shading represents at least 50% identity, gray shading represents at least 50% complementary residues. (C) This alignment demonstrating the CPALLY motif directly upstream of TM I was performed using ClustalW and shaded using Boxshade software. Black shading represents at least 50% identity, gray shading represents at least 50% complementary residues.

been divided into four separate groups (Figure 1A), nine of which are in the LIV-1 subfamily (7). Importantly, the LIV-1 subfamily is a highly conserved group of eight transmembrane domain proteins that are mainly situated on the plasma membrane and transport zinc into cells. At least one SLC39A sequence, however, member HKE4 (SLC39A7/ZIP7), exists on intracellular membranes and transports zinc into the cytosol (9). All of the SLC39A LIV-1 family members contain the consensus sequence present in other ZIP transporters, located in the region of transmembrane domains IV and V, and a histidine-rich motif (of the form HXHXH, where H is histidine and X is any amino acid) thought to be important in zinc transport, located on the long intracellular loop between TM III and IV, immediately preceding TM IV (10). The LIV-1 family sequences also contain a highly conserved potential metalloprotease motif, which closely resembles the active site motif of matrix metalloproteases and is situated in transmembrane domain V (Figure 1B), and considerably increased histidine residues on the N-terminus and extracellular loop between TM II and III (7). For example, ZIP10 has 49 histidines in the extracellular N-terminus, nine on the first extracellular loop between TM II and III and 20 on the intracellular loop between TM III and IV. Interestingly, two of the LIV-1 family sequences, ZIP14 and BIGM103/ZIP8, have the initial H of the HEXXH motif in TM V replaced with an E, which may suggest an ability to transport ions other than zinc. Furthermore, ZIP8 has been demonstrated to transport cadmium in the testis (11), and ZIP14 mediates non–transferrin-bound iron uptake into hepatocytes (12).

The Properties of the LIV-1 Family of ZIP Transporters

Current information about the various members of the LIV-1 subfamily, including clarification of the names of each sequence, is documented in Table 1. Most sequences have widespread tissue distribution, as judged by the EST sequences in the GenBank, whereas ZIP4, ZIP5, and ZIP12 appear to be more tissue specific. Most of the LIV-1 family proteins reside on the plasma membrane of cells, a characteristic consistent with a role as a zinc influx transporter. This role has been demonstrated for ZIP4 (13), ZIP5 (14), LIV-1 (15), and ZIP14 (16,17), but not for HKE4, which has been observed on the endoplasmic

Table 1. Nomenclature and Known Function of LIV-1 Family Members.

Human gene name	Protein name	Other names	Cell location	Tissue distribution	Transport function	Disease link	Chromosome	Accession number
SLC39A4	ZIP4	LZT-Hs5	PM	Small intestine, stomach, colon, cecum, kidney	Zinc uptake	Acrodermatitis enteropathica (35-37)	8q24.3	NM_017767
SLC39A5	ZIP5	LZT-Hs7	Basolateral surface of polarized cells	Kidney, liver, spleen, colon, stomach, pancreas	Zinc removal		12q13.13	NM_173596
SLC39A6	LIV-1, ZIP6	LZT-Hs3	PM	Widespread	Zinc influx	Breast cancer (21-22),	18q12.1	NM_012319
SLC39A7	HKE4, ZIP7	LZT-Hs1	ER and Golgi	widespread	Zinc and manganese bidirectional? (20)	Tamoxifen resistance in breast cancer	6p21.3	NM_006979
SLC39A8	BIGM103, ZIP8	LZT-Hs6	Vesicles	Widespread	Cadmium influx (11), Zinc influx	Faslodex resistance in breast cancer	4q22-q24	NM_022154
SLC39A10	ZIP10	LZT-Hs2	PM	Widespread	Zinc influx		2q33.1	NM_020342
SLC39A12	ZIP12	LZT-Hs8		Brain, lung, testis, retina		Asthma (32)	10p12.33	NM_152725
SLC39A13	ZIP13	LZT-Hs9		Widespread			11p11.12	NM_152264
SLC39A14	ZIP14	LZT-Hs4	PM	Widespread	Zinc influx, non-transferrin-bound iron uptake (12)	Asthma (32), inflammation mediated by IL-6 (31)	8p21.2	NM_015359

PM, plasma membrane.

reticulum (9) and golgi (18) membranes, or BIGM103/ZIP8, which has been observed on intracellular vesicles such as lysosomes and endosomes (19).

Because of membrane topology, location on intracellular membranes is presumed to enable ion transport from intracellular compartments to the cytoplasm. However, the yeast equivalent of HKE4, Yke4p, has recently been shown to balance the zinc level between the cytosol and the secretory pathway by transporting zinc in either direction across membranes, depending on the zinc status of the cells (20). This observation is interesting and may explain the presence in the LIV-1 family sequences of additional histidine-rich regions positioned on the side of the membrane opposing that of the other ZIP transporters.

We have previously observed a conserved motif, which we termed CPALLY, immediately preceding the first TM domain (Figure 1C). This motif does not occur in HKE4, which is not present on the plasma membrane, or ZIP13, which is grouped with ZIP7 in the phylogenetic tree and thus may also reside on intracellular membranes. This CPALLY motif contains three conserved cysteines, which usually form disulfide bonds with other cysteine residues. Furthermore, all of the human LIV-1 family members, except HKE4 and ZIP13, have a conserved cysteine immediately preceding their HEXXH motif in TM V. This motif may be involved in binding to this additional cysteine, thus closing the pore and regulating the movement of zinc across the membrane.

Normal Tissue Expression of LIV-1 Family Members

The normal tissue expression of the different members of the LIV-1 family shows considerable variation, which may indicate their diverse roles in different tissues (Table 1). ZIP4 is present in the intestine and kidney (21), particularly the duodenum and jejunum, which are crucial sites of zinc absorption. ZIP5 is expressed in kidney, liver, pancreas, and intestine, particularly the basolateral membrane of the adult and developing mouse intestine (22). LIV-1 has widespread distribution but is not appreciably present in heart and intestine and is primarily increased in hormonally controlled tissues (15). HKE4 (9), ZIP14 (17), and ZIP13 are ubiquitously expressed, appearing in many tissues. ZIP12 is ex-

pressed in brain, lung, testis, and retina, and ZIP10 is predominantly expressed in brain and spinal cord (data obtained from expression array in the HUGO database).

The LIV-1 Family of ZIP Transporters and Disease States

The first member of the LIV-1 family to be linked to disease was LIV-1 itself, which was shown to be estrogen regulated and present in increased amounts in estrogen-receptor–positive breast cancers that spread to the lymph nodes (23,24). More recently, this association of LIV-1 with estrogen receptors has been substantiated by larger scale analysis of breast cancer specimens. These studies have shown that LIV-1 is such a reliable marker of estrogen-receptor–positive cancers (25,26) that it is one of the genes used routinely to distinguish the luminal A type of clinical breast cancer (27,28). Furthermore, in zebrafish embryos, LIV-1 was shown to be the downstream target of the transcription factor STAT3, which has a proven role in the development of cancer (29). This work also found that LIV-1 was essential for the nuclear localization of the transcription factor Snail, which plays a major role in the epithelial-to-mesenchymal switch because of its ability to down regulate the expression of genes associated with cell adhesion. This finding suggests that LIV-1 could form a link between cancer and normal development (30) and raises the question of whether any other LIV-1 family members have a similar role. Interestingly, the expression of two other LIV-1 family sequences, ZIP4 and ZIP5, has been observed in the developing mouse intestine (22) and the *Drosophila* LIV-1 family member called fear of intimacy (FOI) has been shown to be essential for gonad development (31). Another LIV-1 family member, ZIP14, is substantially increased during the zinc-dependant differentiation of adipocytes (16) and is regulated by IL-6, a mechanism that requires STAT3 signaling (32).

Additionally, the LIV-1 family of zinc transporters has been implicated in other disease states. For example, increases in expression of the zinc transporters LIV-1, ZIP12, and ZIP14 have been observed during acute inflammation in the airway and asthma and have been suggested to promote an increase in zinc uptake, which can reduce inflammation (33). The zinc content in brains of individuals with schizophrenia is lower than that of individuals with other cerebral diseases (34), and a role for the ZIP12 gene has been demonstrated by observation of mutations in ZIP12 in a small group of schizophrenic patients. Significantly, brain zinc content was maintained in rats fed a zinc-deficient diet by a compensatory rise in LIV-1 expression in the brain (35). The ZIP4 gene has been demonstrated to be mutated in the zinc deficiency disorder acrodermatitis enteropathica (21,36), and the observed mutations were shown to disrupt the molecule in areas thought important for zinc transport (37).

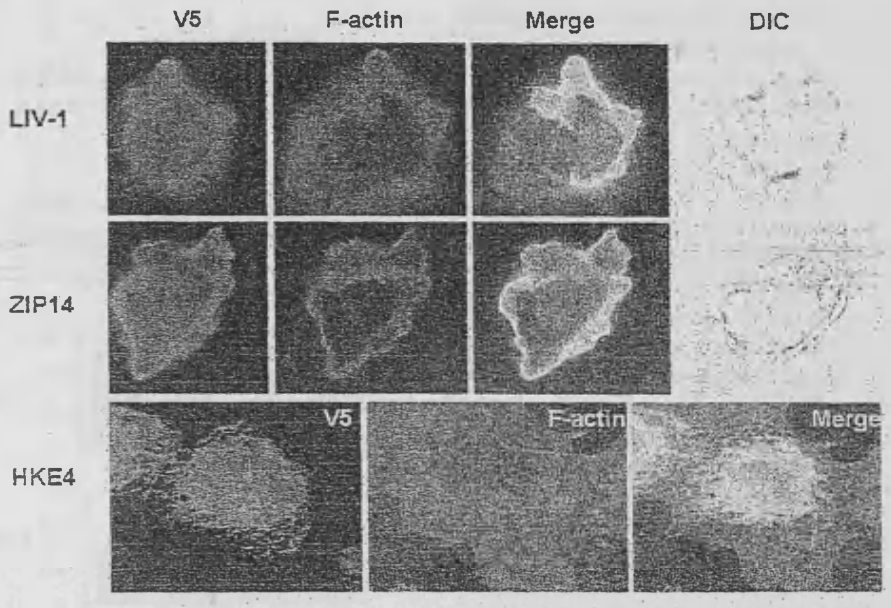

Figure 2. Cellular location of three human LIV-1 family members in MCF-7 cells. MCF-7 cells expressing recombinant HKE4, LIV-1, or ZIP14 were imaged using a mouse anti-V5 antibody (Invitrogen) conjugated to Alexa Fluor 488 (green) and assembled onto slides using Vectorshield with DAPI (Vector Laboratories). All cells were incubated with Texas red phalloidin to stain F-Actin filaments red. Coverslips were viewed on a Leica RPE automatic microscope using a 63x oil immersion lens. The fluorescent superimposed images were acquired using a multiple bandpass filter set appropriate for DAPI, fluorescein, and Texas Red as well as bright field for differential interference contrast imaging.

INVESTIGATION OF THE LIV-1 FAMILY OF ZIP TRANSPORTERS IN BREAST CANCER.

The increase of scientific literature implicating ZIP transporters in a variety of diseases has led to our recent investigation of the relevance of the expression of the nine family members of the LIV-1 family of ZIP transporters in breast cancer. Because LIV-1 itself is known to be regulated by estrogen, we initially investigated the response of these nine LIV-1 family members to short-term treatment with estrogen and antiestrogens. We then followed up with investigation of these nine LIV-1 family members in our cell-line models of longer-term treatment, which have developed resistance to antiestrogens, as well as expression in breast cancer samples. These results are detailed below.

In addition, we transiently transfected MCF-7 cells with constructs for three LIV-1 family members with a

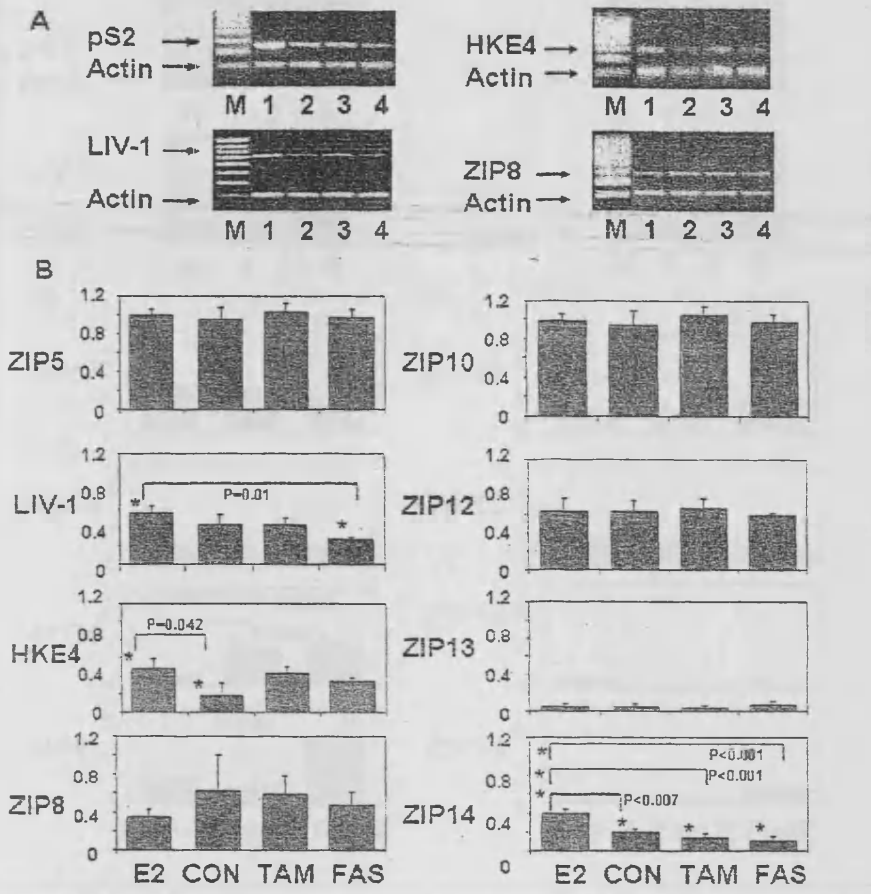

Figure 3. Comparison of the effect of antihormones on the RNA expression of the nine human LIV-1 family members. MCF-7 cells were treated with 4-hydroxytamoxifen (TAM), fulvestrant (FAS), or oestradiol (E2) for seven days in serum growth factor–free DCCM medium before total RNA was extracted, reverse transcribed to cDNA, and PCR performed for individual ZIPs. All data were normalized to individual β-actin levels. The upper panel shows representative agarose gels of pS2, LIV-1, HKE4, and ZIP8 in MCF-7 treated with oestradiol (lane 1), untreated (lane 2), treated with Tamoxifen (lane 3), or treated with Fulvestrant (lane 4). M represents size markers. Lower panel shows mean ± SEM densitometric values of 8 genes, comparing their expression levels in MCF-7 cells untreated (CON), or treated with oestradiol (E2), Tamoxifen (TAM), or Fulvestrant (FAS). Statistically significant results are indicated with asterisks, and the relevant *P* value is given. ZIP4 was undetectable.

C-terminal V5 tag to confirm the same cellular location as previously observed in Chinese hamster ovary cells (9,15,16). Figure 2 shows plasma membrane staining for both LIV-1 and ZIP14 (green) in unpermeabilized MCF-7 cells as determined by colocalization with F-actin filaments (red) and association with the outside of the cell, observed by DIC imaging. In contrast, HKE4 stains intracellular compartments in permeabilized MCF-7 cells, such as the endoplasmic reticulum (green), as evidenced by perinuclear staining and an equal meshlike appearance throughout the cell interior, yet clearly does not reach the cell extremities, which were stained by F-actin (red).

The Response of the LIV-1 Family of ZIP Transporters to Antiestrogens

Because of the similarity between the sequences of the nine LIV-1 family members, we investigated whether any of the other LIV-1 family members were also estrogen-regulated and/or expressed in breast cancer cells. To achieve this we compared the RNA expression of all nine members of the LIV-1 family of ZIP transporters in the estrogen-receptor–positive MCF-7 breast cancer cell line that had been exposed to estrogen, the partial antiestrogen tamoxifen ,or the pure antiestrogen fulvestrant for 10 days. Cells were harvested, RNA was prepared, RT-PCR was performed, and DNA for individual genes was amplified by PCR in the presence of actin, to allow normalization of the results (Figure 3). To verify the profile of the samples, we first investigated the expression of the estrogen-regulated gene pS2, which was characterized by elevation in response to estrogen, little response to tamoxifen, and reduced expression in response to fulvestrant (see Figure 3A). We observed differential expression of all nine LIV-1 family members, both in the amount of RNA present and in the response to different treatments (see Figure 3B). We show representative gels of the three LIV-1 family members with the largest response (see Figure 3A). ZIP4 was undetectable in all samples, a finding that may reflect its known expression in the intestine and kidney (21). The levels of ZIP5, 10, 12, and 13 did not change across the treatments, and all were expressed at relatively low levels, at which ZIP5, ZIP10, and ZIP12 required an increased number of PCR cycles compared with the other LIV-1 family members. LIV-1 and ZIP14 appeared to be estrogen regulated, showing an increased response to estrogen and reduced response to tamoxifen or fulvestrant, which was statistically significant (see Figure 3). Although HKE4 was also significantly increased in response to estrogen treatment, it was also increased, to a lesser extent, in response to both tamoxifen and fulvestrant. ZIP8 showed a slight decrease in response to

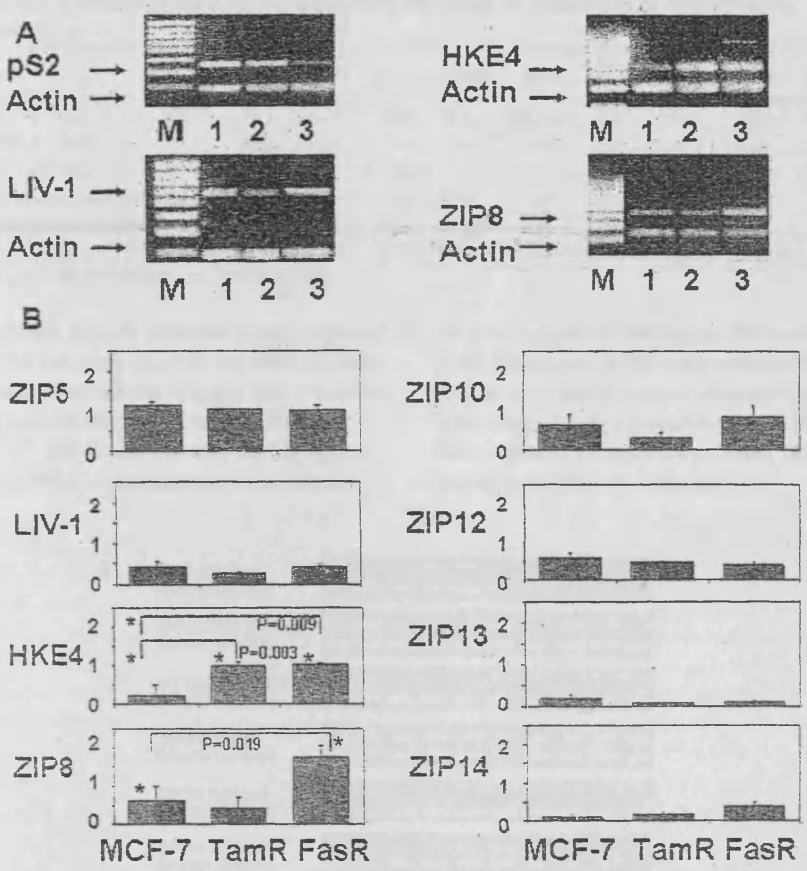

Figure 4. Comparison of RNA expression of the nine human LIV-1 family members in antihormone-resistant MCF-7 cells. The expression of different ZIPs in tamoxifen (TamR)- and fulvestrant (FasR)-resistant MCF-7 cells was compared with wild-type MCF-7 cells. RNA was extracted and reverse transcribed to cDNA. The upper panel shows representative gels of pS2, LIV-1, HKE4, and ZIP8 in MCF-7 (lane 1), TamR (lane 2) and FasR (lane 3) cell lines. M represents size markers. Lower panel shows mean ± SEM densitometric values of 8 genes comparing their expression levels in MCF-7, TamR, and FasR cells. Statistically significant results are indicated with asterisks, and the relevant *P* value is given. ZIP4 was undetectable.

estrogen, which was not significant presumably due to the large error bars.

The observed changes in the SLC39A-family mRNA levels reported here are anticipated to be reflected in the production of the individual proteins, but this possibility has not been examined across the SLC39A family because of the absence of available antibodies. However, recent results in our laboratory with two new antibodies to endogenous LIV-1 and HKE4 suggest that this relationship exists, because both LIV-1 and HKE4 proteins were increased by estrogen treatment, and LIV-1 was decreased with both tamoxifen and faslodex treatments whereas HKE4 was unchanged, mirroring the results that we observed at the mRNA level.

The LIV-1 Family of ZIP Transporters in Antiestrogen Resistance

Although estrogen-receptor–positive breast cancers are routinely treated clinically with antihormones such as tamoxifen or fulvestrant, with time the tumors develop resistance to these agents, leading to subsequent regrowth, usually with an altered and more aggressive phenotype (38). To better understand the mechanisms underlying the occurrence of resistance, we have developed a unique panel of antiestrogen responsive and resistant cell lines derived from the estrogen-receptor–positive human breast cancer cell line MCF-7 (39,40). We have investigated the expression of all nine human LIV-1 family members in both our tamoxifen (TamR)- and fulvestrant (FasR)-resistant cell lines and compared them to the wild-type MCF-7 cells (Figure 4) in an effort to examine any potential role that individual LIV-1 family members may play in the development of antihormone-resistant breast cancer. These antihormone-resistant cell lines are able to grow in the presence of antiestrogens by efficiently utilizing signaling pathways such as epidermal growth factor receptor (EGFR) (39,40), Src (41), Insulin-like growth factor receptor 1 (IGF1-R) (42), and c-Met (43), which allows them to exhibit a more aggressive phenotype (44). Cells were harvested, RNA prepared, RT-PCR performed, and DNA for individual genes was amplified by PCR in the presence of actin, to allow normalization of the results. The cell samples were first characterized for pS2 levels, and showed the expected decrease in the FasR cells (45). Representative gels are given for the three LIV-1 family members that appeared most altered, LIV-1, HKE4, and ZIP8. ZIP4 levels were again undetectable, and the levels of ZIP5, ZIP10, ZIP12, and ZIP13 were relatively low, with ZIP5, ZIP10, and ZIP12 again requiring an increased number of PCR cycles. Levels of ZIP5, ZIP12, and ZIP13 did not change, and the levels of LIV-1, ZIP12, and ZIP13 were either unchanged or reduced in the resistant cell lines. ZIP14, although present in low amounts, was increased in the resistant cells, and ZIP10 was decreased in TamR cells. Only HKE4 and ZIP8 produced statistically significant changes, with HKE4

Table 2. Summary of LIV-1 Family Expression Response to Treatments or Antihormone Resistance

Cells	ZIP4	ZIP5	LIV-1	HKE4	ZIP8	ZIP10	ZIP12	ZIP13	ZIP14
MCF-7 + E2	ND	—	Up	Up	Down	—	—	—	Up
MCF-7 + TAM	ND	—	—	—	—	—	—	—	Down
MCF-7 + FAS	ND	—	Down	—	—	—	—	—	Down
Tamoxifen-resistant cells	ND	—	—	Up	—	—	—	—	—
Fulvestrant-resistant cells	ND	—	—	Up	Up	—	—	—	—

ND, not determined; —, no change.

elevated in both resistant states, whereas ZIP8 was considerably elevated in FasR cells. These results suggest that a number of LIV-1 family members (ZIP4, ZIP5, LIV-1, ZIP10, ZIP12, and ZIP13) appear unaltered or decreased by the acquisition of endocrine resistance. However, both HKE4 and ZIP8 were elevated in one or both antihormone-resistant cell lines, suggesting a possible role in the development of resistance. These results are summarized in Table 2.

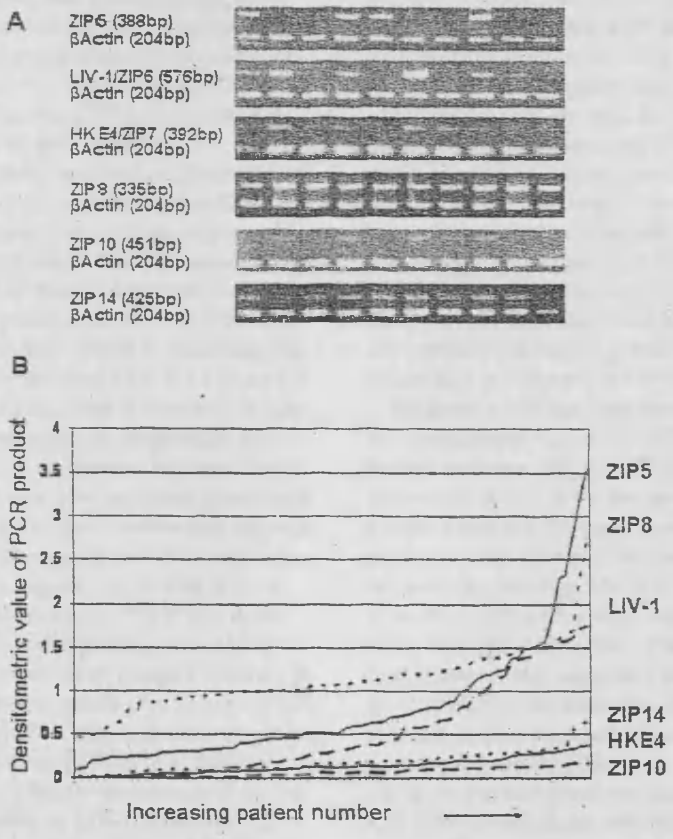

Figure 5. Comparison of the expression of LIV-1 family members in a series of samples from breast cancer patients. (A) representative results from 10 patient tumor samples amplified with gene specific primers for ZIP5, HKE4, ZIP10, LIV-1, ZIP8, ZIP14, and β-actin. (B) distribution of the densitometric values for ZIP5, HKE4, ZIP10, LIV-1, ZIP8, and ZIP14 in the patient samples, with no correction for the number of PCR cycles.

We have previously demonstrated that our TamR cells have increased intracellular zinc levels (46; Taylor et al, unpublished results), increased EGFR (39), Src (41), and IGF1-R (42) signaling as well as increased growth and invasion (41). Interestingly, treatment of these cells with 20 μM zinc can activate EGFR, Src, and IGF1-R signaling as well as growth and invasion (46; Taylor et al, unpublished results). Furthermore, we have demonstrated a role for HKE4 in the development of the aggressive phenotype in TamR cells by using siRNA for HKE4 which prevented the observed zinc-induced activation of signaling pathways (Taylor et al, unpublished results). Whether ZIP8 has a similar role in the FasR cells needs to be investigated. We have, however, not examined whether these transporters have the ability to transport metals other than zinc or whether these pathways can be stimulated by other metals.

LIV-1 FAMILY OF ZIP TRANSPORTERS IN BREAST CANCER SAMPLES

LIV-1 is an estrogen-regulated gene that has been implicated in estrogen-receptor–positive breast cancer and the subsequent spread to the regional lymph nodes (23–26), and more recently it has been used as a reliable marker of luminal A type clinical breast cancer (27,28). We therefore investigated whether any other LIV-1 family members also had a positive association with breast cancer. For this analysis we used a series of tumor samples from 74 patients presenting with primary breast cancer to the Breast Cancer Unit, City Hospital, Nottingham, between 1987 and 1989. For sample analysis we used the same PCR conditions described in Figure 3. The expression of three LIV-1 family members, ZIP4, ZIP12, and ZIP13, was undetectable in these samples, and examples of the expression levels of the remaining six LIV-1 family members are documented in Figure 5 for 10 patients. The graph depicting the variation of each LIV-1 family member with increasing patient number (see Figure 5) demonstrates that LIV-1 and ZIP5 show the most heter-

Table 3. Statistical Analysis of LIV-1 Family Members with Indicators of Breast Cancer Progression

	ZIP5	LIV-1	HKE4	ZIP8	ZIP10	ZIP14
ER	0.009 (+)	< 0.001 (+)	NS	0.04 (-)	0.033 (+)	NS
EGFR	NS	< 0.001 (-)	NS	NS	NS	NS
ErbB2[a]	NS	NS	NS	0.027 (-)	NS	NS
ErbB3[a]	NS	< 0.001 (+)	0.001 (+)	NS	< 0.001 (+)	NS
ErbB4	NS	0.028 (+)	NS	NS	NS	NS
IGF1-R	NS	0.02 (+)	NS	NS	NS	NS
STAT3[a]	NS	0.007(+)	0.031(+)	NS	< 0.001(+)	0.004 (+)
Ki 67	NS	NS	0.026 (+)	NS	NS	NS
Grade	NS	0.007 (-)	NS	NS	NS	NS

Comparative analysis of densitometric data assumed statistical significance was assumed if $P < 0.05$. NS, not significant. [a]Spearman's correlation test.

ogeneity, with samples varying from low to medium and high values. However, it is noteworthy that ZIP5 required an increased number of PCR cycles, suggesting low levels in the breast cancer samples. In contrast, the distribution of HKE4, ZIP8, ZIP10, and ZIP14 across the samples showed little variation.

Comparative analysis of densitometric data was performed using the SPSS (version 10) statistical analysis package using either a two-sided Mann-Whitney U test with the previously described cut off values or a Spearman rank correlation test where indicated (Table 3). Statistical significance was assumed if $P < 0.05$ and is shown for a number of common indicators of breast cancer progression and grade. LIV-1 has previously been identified as an estrogen-regulated gene and a prognostic marker of endocrine response (23,24). Here we confirm this association ($P < 0.001$, Figure 6A) as well as an inverse relationship to EGFR ($P < 0.001$, Figure 6B) and a positive association with two other erbB receptor tyrosine kinase members, erbB3 ($P = .001$, $r = 0.414$) and erbB4 ($P = .028$), and another growth factor receptor, IGF1-R ($P = .02$). No other LIV-1 family member exhibits the same profile as LIV-1; however, ZIP5 ($P = .009$, see Figure 6A) and ZIP10 ($P = .033$) both show a positive association with estrogen receptor (ER), although the distribution of ZIP10 in Figure 5B suggests that ZIP10 may be of less clinical relevance. No other LIV-1 family member has an association with EGFR or ErbB4; however, HKE4 ($P = .001$) and ZIP10 ($P < 0.001$) both show a positive association with ErbB3. ZIP8 behaves differently from other LIV-1 family members and shows a negative association with both ER ($P = .04$) and ErbB2 ($P = .027$). This negative association with ER was also suggested in response of MCF-7 cells to estrogen treatment (see Figure 3) but was not statistically significant. These results together suggest that the different LIV-1 family members may transport zinc, but their activation may be regulated differently, allowing them variation of function in different cell types.

Recently, LIV-1 has been shown to be the downstream target of STAT3 in zebrafish embryos (29), and ZIP14 is regulated by IL-6 (32), a mechanism that uses STAT3 signaling. We have observed a positive correlation in these breast cancer samples between STAT3 and LIV-1 ($P = .007$), ZIP14 ($P = .004$), HKE4 ($P = .031$), and ZIP10 ($P = .001$). This observation is interesting, especially because the level of STAT3 has been well documented to be associated with breast cancer progression (47).

We next investigated the association of LIV-1 family members with histological grade. LIV-1 was the only family member associated with grade and was highly expressed in low histological grade tumors ($P = .007$, see Figure 6C). The only other observed relationship between any other LIV-1 family members was a positive association of HKE4 with the well-known proliferation marker Ki67 ($P = .026$) and those cancers with increased lymph node involvement ($P = .036$). Although this patient group was small, this latter result was an interesting observation which had previously been documented for LIV-1 (23) and may support a role of HKE4 in proliferating and metastatic tumors.

It appears from this small patient series that LIV-1 is the LIV-1 family member most associated with endocrine response in breast cancer, although HKE4 does have some association with factors suggestive of aggressive behavior such as increased proliferation and lymph node involvement. However, ZIP5 and ZIP10 also appear to be regulated by estrogen within the breast cancer samples, but due to their apparent low levels of expression may not have any useful clinical relevance. Some LIV-1 family members show an association with members of the erbB growth factor family as well as STAT3, an association that may be suggestive of their mechanism of action. Clearly, ZIP5 and ZIP8 are not regulated in the same way. The observed diversity of expression within this LIV-1 family may be indicative of the different role that each molecule has in a variety of different tissues. Zinc has a vital role in cellular processes, and deregulated expression of zinc transporters could have dramatic consequences in the regulation of zinc, which in its turn could be pivotal in the initiation or progression of breast cancer. Investigations to decipher such actions and assess zinc transporters as novel therapeutic targets are currently underway.

ACKNOWLEDGMENTS

The authors wish to thank the Tenovus cancer charity for funding and Mrs Lynne Farrow for help with the statistical analysis.

APPENDIX

Materials and Methods

Cell culture. MCF-7 cells were grown in the presence of 4-hydroxytamoxifen (10^{-7} M), fulvestrant (10^{-7} M), or estradiol (10^{-9}M) for seven days in serum growth-

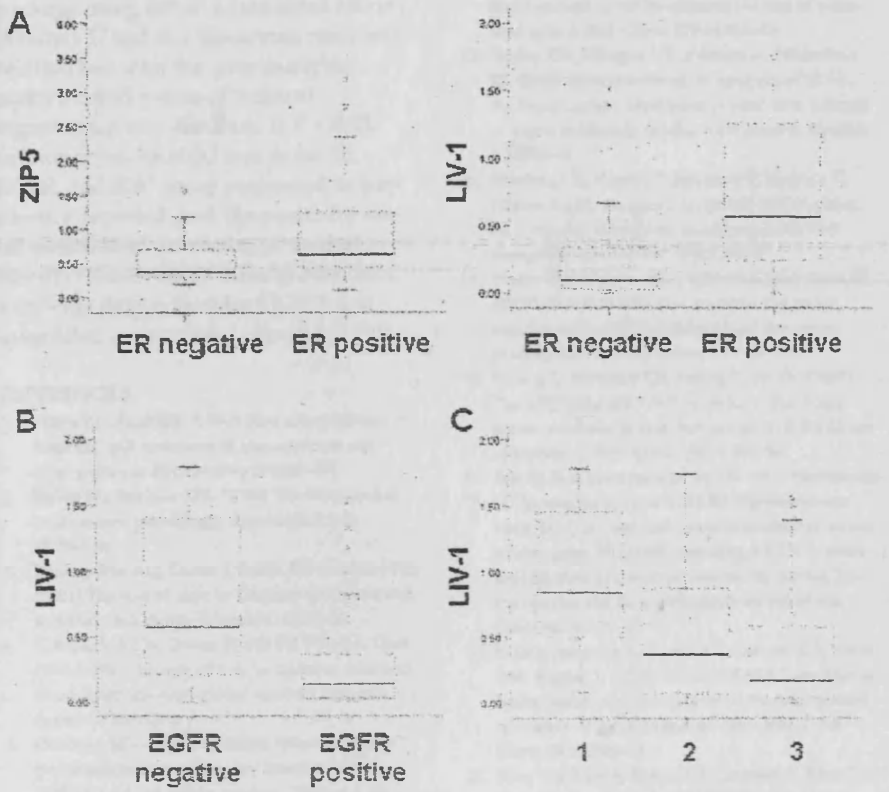

Figure 6. Comparison of the expression of LIV-1 and/or ZIP5 with ER, EGFR and grade in a series of breast cancer samples. (A) shows the positive correlation of both LIV-1 and ZIP5 with estrogen receptor (ER). (B) shows the reverse relationship of LIV-1 with EGFR. (C) shows the decreasing levels of LIV-1 with worsening grade.

factor–free DCCM medium [Biosynergy (Europe), Cambridge, UK]. The production of TamR- and FasR-resistant MCF-7 cells has been described previously (40). The two antiestrogen-resistant cell lines were grown for four days before being transferred into phenol-red/steroid-free, serum growth-factor–free DCCM medium for 24 h prior to harvest.

RNA extraction and RT-PCR. Total RNA was extracted and reverse transcribed to cDNA using random hexamers as previously described (48). The following PCR primers (MWG Biotech) were used to detect the ZIP genes: ZIP4 5′-CCCATCACCA TGGCGTCCCTGG-3′ 5′-GGTGCC CTCG GGGTTGCTGA GG-3′ 330 bp, ZIP5 5′- GGGTGACCTG GAA GAGTCAA –3′ 5′- CAGCAA GGGC CGTAGTAGAC-3′ 388 bp, LIV-1 5′-GTC TAACAG C TCTAGGAGGC-3′ 5′-CACCAATTGC TAGGCCATCG-3′ 576bp, HKE4 5′-ATC GCTCTCT ACTTCAGATC -3′ 5′-CTCTTCTGAA CCCCTC TTG-3′ 392 bp, ZIP8 5′-CCCATCACCA TGGCCCCGGG TCGCGCG-3′ 5′-GGGTGA AAGT TCAATT GCTG TAA-3′ 335 bp, ZIP10 5′-TTGGCAGTTC AA-GAGG GAAAG-3′ 5′-CGA TTATGCT CATACTGT-3′ 451 bp, ZIP12 5′-AAACTTGCCT TCCCCAGACT-3′ 5′- TGAGTGAGAG GCCCTTCTGT-3′ 297 bp, ZIP13 5′-CCCATCACCA TGG CGGGCCC AAG-3′ 5′-GGGAATGACA AGCAACGGGA A-3′ 242 bp, ZIP14 5′-TGCTTGGCTT ATGGAGAACC-3′ 5′-GAGATGACGG TCA CACAGAGG-3′ 425 bp, β-Actin (NM_001101) 5′-GGAGCAATGA TCTTGATC TT-3′ 5′-CCTTCC TGGG CATGGAGTCCT-3′. PCR parameters were optimized accordingly from the previously described protocol (48) using 29 cycles for ZIP4, LIV-1, HKE4, ZIP8, ZIP13, and ZIP14; 31 cycles for ZIP10 and ZIP12; and 33 cycles for ZIP5. All data were normalized with respect to individual β-actin levels and statistical analysis (one-way ANOVA with post hoc Dunnett test) was performed.

Fluorescent microscopy. Recombinant proteins for LIV-1 (15), HKE4 (9), and ZIP14 (17) were engineered in vector pcDNA3.1/V5-His-TOPO to provide a C-terminal V5 tag as previously described. MCF-7 cells were seeded on coverslips for 24 h before transfection with lipofectamine 2000 as described previously (15), and after 16–24 h were prepared for fluorescence microscopy by fixing with 4% formaldehyde, permeabilizing with 0.4% saponin if required, and blocking with 10% normal goat serum before incubating with a mouse anti-V5 antibody (1/2000, Invitrogen) conjugated to Alexa Fluor (1/2000) 594 (red) or 488 (green), and then assembled onto slides using Vectorshield with DAPI (Vector Laboratories). All coverslips were viewed on a Leica RPE automatic microscope using a 63x oil immersion lens. The fluorescent superimposed images were acquired using a multiple bandpass filter set appropriate for DAPI, fluorescein, and Texas Red as well as bright field for differential interference contrast (DIC) imaging.

Tumor samples. Tumor samples were from 74 patients presenting with primary breast cancer to the Breast Cancer Unit, City Hospital, Nottingham, between 1987 and 1989. The samples were snap frozen in liquid nitrogen and stored at –70°C. Clinical and pathological data was provided, and that which was used in the study is presented in Table 2. Total RNA was extracted from each breast tumor sample as previously described (48). RNA was extracted and reverse transcribed to cDNA as described above.

Statistical analysis. Comparative analysis of densitometric data from the breast cancer samples was performed using the SPSS (version 10) statistical analysis

package using either a two-sided Mann-Whitney U test or a Spearman rank correlation test with the previously described cutoff values. Statistical significance was assumed if $P < 0.05$. Immunocytochemical assays for ER, EGFR, and Ki67 were performed as previously reported and the positivity cutoff points used for statistical analysis (49–51). The levels of other growth factors were determined by RT-PCR and quantified as described previously (52).

REFERENCES

1. Vallee BL, Auld DS. (1990) Zinc coordination, function, and structure of zinc enzymes and other proteins. *Biochemistry* 29:5647–59.
2. Vallee BL, Falchuk KH. (1993) The biochemical basis of zinc physiology. *Physiological Rev.* 73:79–118.
3. Truong-Tran AQ, Carter J, Ruffin RE, Zalewski PD. (2001) The role of zinc in Caspase activation and apoptotic cell death. *Biometals* 14:315–30.
4. Koh JY, Suh SW, Gwag BJ, He YY, Hsu CY, Choi DW. (1996) The role of zinc in selective neuronal death after transient global cerebral ischemia. *Science* 272:1013–6
5. Palmiter RD, Huang L. (2004) Efflux and compartmentalization of zinc by members of the SLC30 family of solute carriers. *Pflugers Arch.* 447:744–51.
6. Eide DJ. (2004) The SLC39 family of metal ion transporters. *Pflugers Arch.* 447:796–800.
7. Taylor KM, Nicholson RI. (2003) The LZT proteins; the new LIV-1 subfamily of ZIP zinc transporters. *BBA Biomembranes* 1611:16–30.
8. Gaither LA, Eide DJ. (2001) Eukaryotic zinc transporters and their regulation. *Biometals* 14: 251–70.
9. Taylor KM, Morgan HE, Johnson A, Nicholson RI. (2003) Structure-function analysis of HKE4, a member of the new LIV-1 subfamily of zinc transporters. *Biochem. J.* 377:131–9.
10. Guerinot ML. (2000) The ZIP family of metal transporters. *Biochim. Biophys. Acta.* 1465:190–8.
11. Dalton TP, He L, Wang B, et al. (2005) Identification of mouse SLC39A8 as the transporter responsible for cadmium-induced toxicity in the testis. *Proc. Natl. Acad. Sci. U S A* 102: 3401–6.
12. Liuzzi JP, Aydemir F, Nam H, Knutson MD, Cousins RJ. (2006) Zip14 (Slc39a14) mediates non-transferrin-bound iron uptake into cells. *Proc. Natl. Acad. Sci. U S A.* 103:13612–7.
13. Kim BE, Wang F, Dufner-Beattie J, Andrews GK, Eide DJ, Petris MJ. (2004) Zn2+-stimulated endocytosis of the mZIP4 zinc transporter regulates its location at the plasma membrane. *J. Biol. Chem.* 279:4523–30.
14. Wang F, Kim BE, Petris MJ, Eide DJ. (2004) The mammalian Zip5 protein is a zinc transporter that localizes to the basolateral surface of polarized cells. *J. Biol. Chem.* 279:51433–41.
15. Taylor KM, Morgan HE, Johnson A, Nicholson RI. (2003) Structure-function analysis of LIV-1, the breast cancer associated protein that belongs to a new subfamily of zinc transporters. *Biochem. J.* 375:51–9.
16. Tominaga K, Kagata T, Johmura Y, Hishida T, Nishizuka M, Imagawa M. (2005) SLC39A14, a LZT protein, is induced in adipogenesis and transports zinc. *FEBS J.* 272:1590–9.
17. Taylor KM, Morgan HE, Johnson A, Nicholson RI. (2005) Structure-function analysis of a novel member of the LIV-1 subfamily of zinc transporters, ZIP14. *FEBS Letters* 579:427–32.
18. Huang L, Kirschke CP, Zhang Y, Yu YY. (2005) The ZIP7 gene (Slc39a7) encodes a zinc transporter involved in zinc homeostasis of the Golgi apparatus. *J. Biol. Chem.* 280:15456–63.
19. Begum NA, Kobayashi M, Moriwaki Y, Matsumoto M, Toyoshima K, Seya T. (2002) Mycobacterium bovis BCG cell wall and lipopolysaccharide induce a novel gene, BIGM103, encoding a 7-TM protein: identification of a new protein family having Zn-transporter and Zn-metalloprotease signatures. *Genomics.* 80:630–45.
20. Kumanfasrovics A, Poruk KE, Osborn KA, Ward DM, Kaplan J. (2006) YKE4 (YIL023C) encodes a bidirectional zinc transporter in the endoplasmic reticulum of Saccharomyces cerevisiae. *J Biol Chem.* 281:22566–74.
21. Kury S, Dreno B, Bezieau S, Giraudet S, Kharfi M, Kamoun R, Moisan JP. (2002) Identification of SLC39A4, a gene involved in acrodermatitis enteropathica. *Nat. Genet.* 31:239–40.
22. Huang ZL, Dufner-Beattie J, Andrews GK. (2006) Expression and regulation of SLC39A family zinc transporters in the developing mouse intestine. *Dev. Biol.* 295:571–9.
23. Manning DL, Robertson JFR, Ellis IO, et al. (1994) Estrogen-regulated genes in breast-cancer: association of pliv1 with lymph-node involvement *Eur. J. Cancer* 30A;675.
24. Manning DL, McClelland RA, Knowlden JM, et al. (1995) Differential expression of estrogen-regulated genes in breast-cancer. *Acta Oncologica* 34:641–6.
25. Tozlu S, Girault I, Vacher S, et al. (2006) Identification of novel genes that co-cluster with estrogen receptor alpha in breast tumor biopsy specimens, using a large-scale real-time reverse transcription-PCR approach. *Endocr. Relat. Cancer* 13:1109–20.
26. Schneider J, Ruschhaupt M, Buness A, et al. (2006) Identification and meta-analysis of a small gene expression signature for the diagnosis of estrogen receptor status in invasive ductal breast cancer. *Int. J. Cancer* 119:2974–9.
27. Chung CH, Bernard PS, Perou CM. (2002) Molecular portraits and the family tree of cancer *Nat. Genet.* 32:533–40.
28. Perou CM, Sorlie T, Eisen MB, et al. (2000) Molecular portraits of human breast tumours. *Nature* 406:747–52.
29. Yamashita S, Miyagi C, Fukada T, Kagara N, Che YS, Hirano T. (2004) Zinc transporter LIVI controls epithelial-mesenchymal transition in zebrafish gastrula organizer. *Nature* 429:298–302.
30. Taylor KM, Hiscox S, Nicholson RI. (2004) Zinc transporter LIV-1: a link between cellular development and cancer progression. *Trends Endocrinol. Metab.* 15:461–3.
31. Mathews WR, Ong D, Milutinovich AB, Van Doren M. (2006) Zinc transport activity of Fear of Intimacy is essential for proper gonad morphogenesis and DE-cadherin expression. *Development* 133:1143–53.
32. Liuzzi JP, Lichten LA, Rivera S, et. al. (2005) Interleukin-6 regulates the zinc transporter Zip14 in liver and contributes to the hypozincemia of the acute-phase response. *Proc. Natl. Acad. Sci. U S A* 102:6843–8.
33. Lang CJ, Murgia C, Leong M, et al. (2006) Anti-inflammatory effects of zinc and alterations in zinc transporter mRNA in mouse models of allergic inflammation. *Am. J. Physiol. Lung Cell. Mol. Physiol.* In press.
34. Bly M. (2006) Examination of the zinc transporter gene, SLC39A12. *Schizophr. Res.* 81:321–2.
35. Chowanadisai W, Kelleher SL, Lonnerdal B. (2005) Zinc deficiency is associated with increased brain zinc import and LIV-1 expression and decreased ZnT-1 expression in neonatal rats. *J. Nutr.* 135:1002–7.
36. Wang K, Zhou B, Kuo YM, Zemansky J, Gitschier J. (2002) A novel member of a zinc transporter family is defective in acrodermatitis enteropathica. *Am. J. Hum. Genet.* 71:66–73.
37. Wang F, Kim BE, Dufner-Beattie J, Petris MJ, Andrews G, Eide DJ. (2004) Acrodermatitis enteropathica mutations affect transport activity, localization and zinc-responsive trafficking of the mouse ZIP4 zinc transporter. *Hum. Mol. Genet.* 13:563–71.
38. Nicholson RI, Johnston SR. (2005) Endocrine therapy: current benefits and limitations. *Breast Cancer Res. Treat.* 93(Suppl 1):S3–10.
39. Knowlden JM, Hutcheson IR, Jones HE, et al. (2003) Elevated levels of EGFR/c-erbB2 heterodimers mediate an autocrine growth regulatory pathway in Tamoxifen-resistant MCF-7 cells. *Endocrinology* 144:1032–44.
40. McClelland RA, Barrow D, Madden TA, et al. (2001) Enhanced epidermal growth factor receptor signaling in MCF7 breast cancer cells after long-term culture in the presence of the pure antiestrogen ICI 182,780 (Faslodex) *Endocrinology* 142:2776–88.
41. Hiscox S, Morgan L, Green TP, Barrow D, Gee J, Nicholson RI. (2006) Elevated Src activity promotes cellular invasion and motility in tamoxifen resistant breast cancer cells. *Breast Cancer Res. Treat.* 97:263–74.
42. Knowlden JM, Hutcheson IR, Barrow D, Gee JM, Nicholson RI. (2005) Insulin-like growth factor-I receptor signaling in tamoxifen-resistant breast cancer: a supporting role to the epidermal growth factor receptor. *Endocrinology* 6:4609–18.

43. Hiscox S, Jordan NJ, Jiang W, Harper M, McClelland R, Smith C, Nicholson RI. (2006) Chronic exposure to fulvestrant promotes over-expression of the c-Met receptor in breast cancer cells: implications for tumor-stroma interactions. *Endocr. Relat. Cancer* 13:1085–99.
44. Hiscox S, Morgan L, Barrow D, Dutkowski C, Wakeling A, Nicholson, RI. (2004) Tamoxifen resistance in breast cancer cells is accompanied by an enhanced motile and invasive phenotype: inhibition by gefitinib ('Iressa', ZD1839). *Clin. Exp. Metastasis* 21:201–12.
45. Kuske B, Naughton C, Moore K, et. al. (2006) Endocrine therapy resistance can be associated with high estrogen receptor {alpha} (ER{alpha}) expression and reduced ER{alpha} phosphorylation in breast cancer models. *Endocr. Relat. Cancer* 13:1121–33.
46. Taylor KM, Vichova P, Hiscox S, Nicholson RI. (2005) Zinc-dependant stimulation of Src, EGFR and IGFR signaling pathways in tamoxifen-resistant breast cancer and the role of zinc transporters. *Breast Cancer Res. Treat.* 94:S162
47. Gamero AM, Young HA, Wiltrout RH. (2004) Inactivation of Stat3 in tumor cells: releasing a brake on immune responses against cancer? *Cancer Cell* 5:111–2.
48. Knowlden JM, Gee JM, Bryant S, et. al. (1997) Use of reverse transcription-polymerase chain reaction methodology to detect estrogen-regulated gene expression in small breast cancer specimens. *Clin. Cancer Res.* 3:2165–72.
49. Nicholson RI, McClelland RA, Gee JM, et al. (1994) Epidermal growth factor receptor expression in breast cancer: association with response to endocrine therapy. *Breast Cancer Res. Treat.* 29: 117–25.
50. Snead DR, Bell JA, Dixon AR, Nicholson RI, Elston CW, Blamey RW, Ellis IO. (1993) Methodology of immunohistological detection of oestrogen receptor in human breast carcinoma in formalin-fixed, paraffin-embedded tissue: a comparison with frozen section methodology. *Histopathology* 23:233–8.
51. van Dierendonck JH, Keijzer R, van de Velde CJ, Cornelisse CJ. (1989) Nuclear distribution of the Ki-67 antigen during the cell cycle: comparison with growth fraction in human breast cancer cells. *Cancer Res.* 49:2999–3006.
52. Knowlden JM, Gee JM, Seery LT, Farrow L, Gullick WJ, Ellis IO, Blamey RW, Robertson JF, Nicholson RI. (1998) c-erbB3 and c-erbB4 expression is a feature of the endocrine responsive phenotype in clinical breast cancer. *Oncogene* 17:1949–57.

Appendix F

Poster Presentation and Certificate of Attendance

20th EORTC-NCI-AACR Symposium on 'Molecular targets and Cancer Therapeutics'

Geneva, Switzerland, 21-24 October 2008

THEIR ROLE IN BREAST CANCER.

NORMAWATI MOHAMAD ZAHARI, Kathryn M. Taylor and Robert I. Nicholson

Tenovus Centre for Cancer Research, Welsh School of Pharmacy, King Edward VII Avenue, Cardiff University, Cathays Park, Cardiff, CF10 3XF, UK. email: mohamadzahariN@cardiff.ac.uk

INTRODUCTION

- Zinc participates in reactions of cellular metabolism attributed to body physiologic. Zinc-dependant enzyme and protein reactions needed zinc for catalyst or structural functions, directing desired growth.
- Exclusively, zinc and enzymes are essential for synthesis of DNA and RNA, whilst zinc induces monocytes to produce IL-1 and IL-6.
- Zinc absorption in cells by diffusion mechanism and protein-mediated processes. The latter involves proteins from two family of genes namely the solute-linked carrier (SLC), SLC30/ZnT and SLC39/ZIP. LIV-1 family of protein is a new subfamily of ZIP, zinc Transporters family hence the term LZT is created.
- Each of LIV-1 family of protein are called LZT-Hs1(SLC39A7), LZT-Hs2(SLC39A10), LIV-1(SLC39A6), LZT-Hs4(SLC39A14), LZT-Hs5(SLC39A4), LZT-Hs6(SLC39A8), LZT-Hs7(SLC39A5), LZT-Hs8(SLC39A12) and LZT-Hs9(SLC39A13). In brackets are equivalents names of their human gene, Hs for *Homo sapiens*.
- It was reported that pLIV-1 predominantly expressed in the estrogen receptor tumours and lymph mode-positive patients.
- This is the first occasion showed relevance of LIV-1 family members to a disease state using breast cancer cell lines (shown) and clinical isolates (not shown). Uniquely, LZT-Hs7, LZT-Hs8 and LZT-Hs9 positives clones were tested for their zinc capacity.

MATERIALS AND METHODS

RNA EXPERIMENT

1. RNA extractions of breast cancer cell lines and clinical isolates were available from the RNA/DNA bank in TCCR.
2. Primers pairs were designed and PCR programs optimization to the LIV-1 family members, respectively.
3. Electrophoresis gels were analysed converted into statistical data and graphs representation as shown.

DNA EXPERIMENT

1. LZT-Hs7, LZT-Hs8 and LZT-Hs9 were cloned into pcDNA5/FRT/V5-His-TOPO® TA vector. Earlier, the genes were unsuccessful to be cloned into neither pcDNA3.1 Directional TOPO® and pEF5/FRT/V5 Directional TOPO®.
2. Stringent analysis were done for positive clones before these procedures: Western blot, immunohistochemistry (fluorescence microscope and fluorescent antibodies) and zinc detection using 50µM Newport Green™ Diacetate, discharged directly on cells for 30 minutes incubation at 37°C

RESULTS

RNA EXPERIMENT

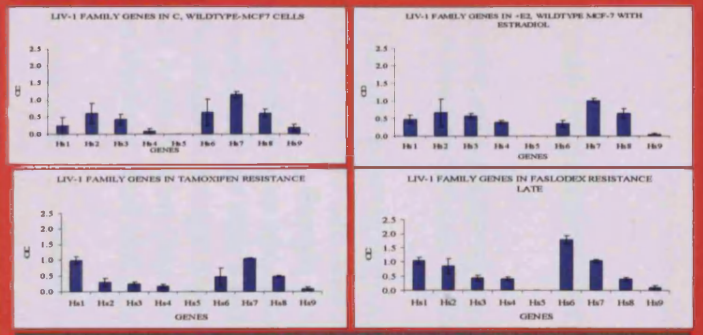

LZT-Hs1 has increased expression in Tamoxifen resistant cells. LIV-1 shows a reduction in signal intensities in both Tamoxifen and Faslodex resistant cells. LZT-Hs6 showed increased expression in Faslodex Late resistant cells. LZT-Hs5 gene expression was undetected in all cell lines.

DNA EXPERIMENT

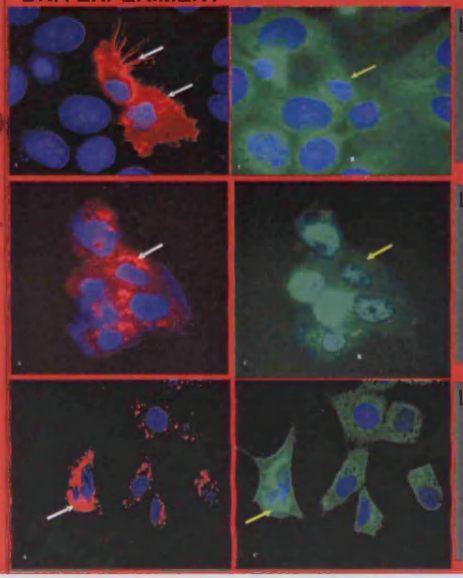

LZT-Hs7 recombinant with Alexa Fluor 594 (red stain) and localised with green fluoresce of Newport Green™ Diacetate.

LZT-Hs8 recombinant with Alexa Fluor 594 (red stain) and localised with green fluoresce of Newport Green™ Diacetate but almost undetected.

LZT-Hs9 recombinant with Alexa Fluor 594 (red stain) and localised with green fluoresce of Newport Green™ Diacetate, seems to be in enclosed structure.

CONCLUSION

1. LZT-Hs1 is up-regulated in Tamoxifen resistant breast cancer cells.
2. LZT-Hs6 is up-regulated in Faslodex Late resistant breast cancer cells.
3. All LIV-1 family members expressed differentially in both the breast cancer cell lines and clinical isolates except LZT-Hs5 is undetected in neither models.
4. LZT-Hs7 protein size is 63 kDalton, LZT-Hs8 is 73 kDalton and LZT-Hs9 is 43 kDalton.
5. Recombinant protein of LZT-Hs7 localizes on the plasma membrane whilst LZT-Hs8 and LZT-Hs9 are located in the endoplasmic reticulum, interestingly, LZT-Hs8 is also found on the plasma membrane with minimal expression.
6. Preliminary work in zinc capacity, all recombinants have green fluoresce of Newport Green Diacetate™ dye in their respective protein locations and Tamoxifen resistant cells, with attention to LZT-Hs8 expression, is not easily seen as others, comparatively.
7. It is intriguing to study the LIV-1 family of proteins, individually and collectively, their functions and involvement in signalling pathways or growth hormone of a disease, i.e breast cancer; or as a supplement treatment for zinc deficiency and homeostasis.

REFERENCES

1. Liuzzi, J.P and Cousin,R.J.(2004)."Mammalian zinc transporters." *Annual Review of Nutrition*,pp:151-172.
2. Maifra, D and Cozzolino, S.M.F.(2004)."The importance of zinc in human nutrition." *Rev.Nutr.,Campinas*,17(1):79-87.
3. Manning et al.(1994)."Oestrogen-regulated gene in breast cancer: Association of pLIV-1 lymph mode involvement." *European Journal of Cancer Part A: General Topics*,30(5):675-678.
4. Taylor K.M., et al.(2003)."Structure-function analysis of LIV-1, the breast cancer-associated protein that belongs to a new subfamily of zinc transporters." *Biochemical Journal*,375(1):51-59.
5. Kathryn M. Taylor, Helen E. Morgan, **Normawati M. Zahari**, Sara P, Ian O. Ellis, John F.R. Robertson and Robert I. Nicholson.(2007)."The emerging role of the LIV-1 subfamily of zinc transporters in breast cancer." *Mol. Med*, 13(7-8):396-406.

Acknowledgements

CARDIFF UNIVERSITY
PRIFYSGOL CAERDYDD
UNIVERSITI MALAYA
tenovus
the cancer charity

CERTIFICATE OF ATTENDANCE

26 Nov 2008 - 22:20

This is to certifty that

Normawati Mohamad Zahari - United Kingdom

has attended the **20th EORTC-NCI-AACR Symposium on 'Molecular Targets and Cancer Therapeutics'** organised in Geneva, Switzerland from 21 to 24 October 2008.

The scientific programme of the **20th EORTC-NCI-AACR Symposium on 'Molecular Targets and Cancer Therapeutics'** has been reviewed and approved by the Accreditation Council of Oncology in Europe (ACOE).

ACOE is a multidisciplinary body of full time specialists practising in the field of oncology and are all recognized for their experience in their field.

It acknowledges the quality of the scientific programme and its educational value. ACOE accreditation ha been endorsed by the European Accreditation Council of Continuing Medical Education (EACCME) - as institution of the European Union of Medical Specialists (UEMS).

The **20th EORTC-NCI-AACR Symposium on 'Molecular Targets and Cancer Therapeutics'** has beer designated for a maximum of

19 European CME Credits (ECMEC'S). These credits are also recognized as Physician's Recognition Award (AMA PRA Category 1 credits) by the American Medical Association[1].

The above mentioned participant has earned .... out of 19 ECMEC's at this event.

(1 ECMEC per full educational hour attended with a maximum of 6 ECMEC's for a full day and 3 ECMEC's for a half day.

This conference operates an honour system. Each medical specialist should claim only those hours credit that he/she actually spent in the educational activity.

References

Addo, S. et al. 2002. A phase I trial to assess the pharmacology of the new oestrogen receptor antagonist fulvestrant on the endometrium in healthy postmenopausal volunteers. *British Journal of Cancer* 87(12), pp. 1354-1359.

Aebi, S. et al. 2000. Is chemotherapy alone adequate for young women with oestrogen-receptor-positive breast cancer? *Lancet* 355(9218), pp. 1869-1874.

Andersen, J. 1992. Determination of estrogen receptors in paraffin-embedded tissue: Techniques and the value in breast cancer treatment. *Acta Oncologica* 31(6), pp. 611-627.

Ando, A. et al. 1996. cDNA cloning of the human homologues of the mouse Ke4 and Ke6 genes at the centromeric end of the human MHC region. *Genomics* 35(3), pp. 600-602.

Anne M. Bowcock, et al. 1999. *The Breast Cancer, Molecular Genetics, Pathogenesis, and Therapeutics*. Humana Press, Totowa, New Jersey.

Attardi, B. et al. 1980. Monkey pituitary oestrogen receptors and the biphasic action of oestradiol on gonadotropin secretion. *Nature* 285(5762), pp. 252-254.

Bajic, V. B. et al. 2003. Dragon ERE Finder version 2: A tool for accurate detection and analysis of estrogen response elements in vertebrate genomes. *Nucleic Acids Research* 31(13), pp. 3605-3607.

Beato, M. and Klug, J. 2000. Steroid hormone receptors: An update. *Human Reproduction Update* 6(3), pp. 225-236.

Begum, N. A. et al. 2002. Mycobacterium bovis BCG cell wall and lipopolysaccharide induce a novel gene, BIGM103, encoding a 7-TM protein: Identification of a new protein family having Zn-transporter and Zn-metalloprotease signatures. *Genomics* 80(6), pp. 630-645.

Benassayag, C. et al. 1999. Estrogen receptors (ERα/ERβ) in normal and pathological growth of the human myometrium: Pregnancy and leiomyoma. *American Journal of Physiology - Endocrinology and Metabolism* 276(6 39-6).

Bergink, E. W. 1980. Oestriol receptor interactions: their biological importance and therapeutic implications. *Acta Endocrinologica* 94(Suppl. 233), pp. 9-16.

Bierich, J. R. et al. 1982. Stunted growth with more or less normal appearance. *European Journal of Pediatrics* 139(4), pp. 214-238.

Boonyaratanakornkit, V. and Edwards, D. P. 2004. Receptor mechanisms of rapid extranuclear signalling initiated by steroid hormones. *Essays in Biochemistry* 40, pp. 105-120.

Booth, M. et al. 1989. Risk factors for ovarian cancer: A case-control study. *British Journal of Cancer* 60(4), pp. 592-598.

Bossche, H. V. et al. 1994. Aromatase inhibitors - Mechanisms for non-steroidal inhibitors. *Breast Cancer Research and Treatment* 30(1), pp. 43-55.

Braunsberg, H. 1977. Oestrogen receptors in relation to human breast cancer. *Ricerca in Clinica e in Laboratorio* 7(1), pp. 47-74.

Britton, D. J. et al. 2006. Bidirectional cross talk between ERα and EGFR signalling pathways regulates tamoxifen-resistant growth. *Breast Cancer Research and Treatment* 96(2), pp. 131-146.

Burger, H. G. 1996. The endocrinology of the menopause. *Maturitas* 23(2), pp. 129-136.

Cerillo, G. et al. 1998. The oestrogen receptor regulates NFkB and AP-1 activity in a cell-specific manner. *Journal of Steroid Biochemistry and Molecular Biology* 67(2), pp. 79-88.

Chappell, S. A. et al. 2000. Expression of oestrogen receptor alpha variants in non-malignant breast and early invasive breast carcinomas. *Journal of Pathology* 192(2), pp. 159-165.

Chen, S. et al. 2006. What do we know about the mechanisms of aromatase inhibitor resistance? *Journal of Steroid Biochemistry and Molecular Biology* 102(1-5 SPEC. ISS.), pp. 232-240.

Combs, D. W. 1995. Recent developments in aromatase inhibitors. *Expert Opinion on Therapeutic Patents* 5(6), pp. 529-533.

Cui, X. et al. 2006. Epidermal growth factor induces insulin receptor substrate-2 in breast cancer cells via c-Jun NH2-terminal kinase/activator protein-1 signaling to regulate cell migration. *Cancer Research* 66(10), pp. 5304-5313.

Dalton, T. P. et al. 2005. Identification of mouse SLC39A8 as the transporter responsible for cadmium-induced toxicity in the testis. *Proceedings of the National Academy of Sciences of the United States of America* 102(9), pp. 3401-3406.

Dardes, R. C. et al. 2002. Regulation of estrogen target genes and growth by selective estrogen-receptor modulators in endometrial cancer cells. *Gynecologic Oncology* 85(3), pp. 498-506.

Davis, T. E. and Carbone, P. P. 1978. Drug treatment of breast cancer. *Drugs* 16(5), pp. 441-464.

Dowsett, M. 1996. Endocrine resistance in advanced breast cancer. *Acta Oncologica* 35(SUPPL. 5), pp. 91-95.

Dowsett, M. 1998. Theoretical considerations for the ideal aromatase inhibitor. *Breast Cancer Research and Treatment* 49(SUPPL. 1).

Dowsett, M. et al. 1996a. Oestrogen formation in breast: Clinical and biological importance. *Journal of Endocrinology* 150(SUPPL.).

Dowsett, M. et al. 1996b. The control and biological importance of intratumoural aromatase in breast cancer. *Journal of Steroid Biochemistry and Molecular Biology* 56(1-6), pp. 145-150.

Dowsett, M. et al. 2005. Biological characteristics of the pure antiestrogen fulvestrant: Overcoming endocrine resistance. *Breast Cancer Research and Treatment* 93(SUPPL. 4).

Duffy, M. J. et al. 2000. Metalloproteinases: Role in breast carcinogenesis, invasion and metastasis. *Breast Cancer Research* 2(4), pp. 252-257.

Dufner-Beattie, J. et al. 2004. The adaptive response to dietary zinc in mice involves the differential cellular localization and zinc regulation of the zinc transporters ZIP4 and ZIP5. *Journal of Biological Chemistry* 279(47), pp. 49082-49090.

Dufner-Beattie, J. et al. 2003. The acrodermatitis enteropathica gene ZIP4 encodes a tissue-specific, zinc-regulated zinc transporter in mice. *Journal of Biological Chemistry* 278(35), pp. 33474-33481.

Eccles, S. A. 2001. The role of c-erbB-2/HER2/neu in breast cancer progression and metastasis. *Journal of Mammary Gland Biology and Neoplasia* 6(4), pp. 393-406.

Eddy, S. R. 1995. Multiple alignment using hidden Markov models. *Proceedings / . International Conference on Intelligent Systems for Molecular Biology ; ISMB. International Conference on Intelligent Systems for Molecular Biology* 3, pp. 114-120.

Eide, D. J. 2004. The SLC39 family of metal ion transporters. *Pflugers Archiv European Journal of Physiology* 447(5), pp. 796-800.

El-Tanani, M. K. K. and Green, C. D. 1996. Insulin/IGF-1 modulation of the expression of two estrogen-induced genes in MCF-7 cells. *Molecular and Cellular Endocrinology* 121(1), pp. 29-35.

El-Tanani, M. K. K. and Green, C. D. 1997. Interaction between estradiol and growth factors in the regulation of specific gene expression in MCF-7 human breast cancer cells. *Journal of Steroid Biochemistry and Molecular Biology* 60(5-6), pp. 269-276.

Elkak, A. E. and Mokbel, K. 2001. Pure antiestrogens and breast cancer. *Current Medical Research and Opinion* 17(4), pp. 282-289.

Emanuelsson, O. et al. 2007. Locating proteins in the cell using TargetP, SignalP and related tools. *Nat. Protocols* 2(4), pp. 953-971.

Espie, M. 1998. Treatment of breast cancer. *Le traitement du cancer du sein* 27(26), pp. 1332-1335.

Evans, T. R. J. 1994. Clinical applications of new aromatase inhibitors. *Critical Reviews in Oncology/Hematology* 16(2), pp. 129-143.

Favoni, R. E. and De Cupis, A. 1998. Steroidal and nonsteroidal oestrogen antagonists in breast cancer: Basic and clinical appraisal. *Trends in Pharmacological Sciences* 19(10), pp. 406-415.

Flőtotto, T. et al. 2001. Hormones and hormone antagonists: Mechanisms of action in carcinogenesis of endometrial and breast cancer. *Hormone and Metabolic Research* 33(8), pp. 451-457.

Friedlander, M. and Thewes, B. 2003. Counting the costs of treatment: The reproductive and gynaecological consequences of adjuvant therapy in young women with breast cancer. *Internal Medicine Journal* 33(8), pp. 372-379.

Gaither, L. A. and Eide, D. J. 2001. Eukaryotic zinc transporters and their regulation. *BioMetals* 14(3-4), pp. 251-270.

Gee, J. M. W. et al. 2000. Biological and clinical associations of c-jun activation in human breast cancer. *International Journal of Cancer* 86(3), pp. 177-186.

Girdler, F. et al. 2001. ERα and ERαβ expression in tamoxifen-treated breast tumours. *Breast Cancer Research and Treatment* 69(3), p. 293.

Godden, J. et al. 1992. The response of breast cancer cells to steroid and peptide growth factors. *Anticancer Research* 12(5), pp. 1683-1688.

Guerinot, M. L. 2000. The ZIP family of metal transporters. *Biochimica et Biophysica Acta - Biomembranes* 1465(1-2), pp. 190-198.

Gwinn, M. L. et al. 1990. Pregnancy, breast feeding, and oral contraceptives and the risk of epithelial ovarian cancer. *Journal of Clinical Epidemiology* 43(6), pp. 559-568.

Hagen, M. L. et al. 2004. The molecular mechanisms of oestrogens. Basic aspects. *Østrogeners molekylære virkemekanismer. Basale aspekter* 166(13), pp. 1216-1220.

Happerfield, L. C. et al. 1997. The localization of the insulin-like growth factor receptor 1 (IGFR-1) in benign and malignant breast tissue. *Journal of Pathology* 183(4), pp. 412-417.

Harris, A. L. et al. 1983. Endocrine effects of low dose aminoglutethimide alone in advanced postmenopausal breast cancer. *British Journal of Cancer* 47(5), pp. 621-627.

Hart, S. et al. 2005. GPCR-induced migration of breast carcinoma cells depends on both EGFR signal transactivation and EGFR-independent pathways. *Biological Chemistry* 386(9), pp. 845-855.

Hermenegildo, C. and Cano, A. 2000. Pure anti-oestrogens. *Human Reproduction Update* 6(3), pp. 237-243.

Hirokawa, T. et al. 1998. SOSUI: classification and secondary structure prediction system for membrane proteins. *Bioinformatics* 14(4), pp. 378-379.

Hiscox, S. et al. 2004. Tamoxifen resistance in breast cancer cells is accompanied by an enhanced motile and invasive phenotype: Inhibition by gefitinib ('Iressa', ZD1839). *Clinical and Experimental Metastasis* 21(3), pp. 201-212.

Hofmann, K. and Stoffel, W. 1993. TMbase - A database of membrane spanning proteins segments. *Biol. Chem* 374(166).

Horne, G. M. et al. 1988. Relationships between oestrogen receptor, epidermal growth factor receptor, ER-D5, and P24 oestrogen regulated protein in human breast cancer. *Journal of Pathology* 155(2), pp. 143-150.

Howell, A. 2006. Pure oestrogen antagonists for the treatment of advanced breast cancer. *Endocrine-Related Cancer* 13(3), pp. 689-706.

Howell, A. et al. 1998. The primary use of endocrine therapies. *Recent results in cancer research. Fortschritte der Krebsforschung. Progres dans les recherches sur le cancer* 152, pp. 227-244.

Howell, A. et al. 1996. New Endocrine Therapies for Breast Cancer. *European Journal of Cancer* 32(4), pp. 576-588.

Howell, A. et al. 2004. Comparison of fulvestrant versus tamoxifen for the treatment of advanced breast cancer in postmenopausal women previously untreated with endocrine therapy: A multinational, double-blind, randomized trial. *Journal of Clinical Oncology* 22(9), pp. 1605-1613.

Huang, L. et al. 2005. The ZIP7 gene (Slc39a7) encodes a zinc transporter involved in zinc homeostasis of the Golgi apparatus. *Journal of Biological Chemistry* 280(15), pp. 15456-15463.

Hutcheson, I. R. et al. 2003. Oestrogen receptor-mediated modulation of the EGFR/MAPK pathway in tamoxifen-resistant MCF-7 cells. *Breast Cancer Research and Treatment* 81(1), pp. 81-93.

Hutton, J. D. et al. 1979. Steroid endocrinology after the menopause: a review. *Journal of the Royal Society of Medicine* 72(11), pp. 835-841.

Iino, Y. et al. 1997. Mechanism of acquired antiestrogen resistance and its management in breast cancer. *Nippon rinsho. Japanese journal of clinical medicine* 55(5), pp. 1149-1154.

Ikeda, M. et al. 2002. Transmembrane topology prediction methods: A re-assessment and improvement by a consensus method using a dataset of experimentally- characterized transmembrane topologies. *In Silico Biology* 2(1), pp. 19-33.

Jarzabek, K. et al. 2005. Distinct mRNA, protein expression patterns and distribution of oestrogen receptors α and β in human primary breast cancer: Correlation with proliferation marker Ki-67 and clinicopathological factors. *European Journal of Cancer* 41(18), pp. 2924-2934.

Jirström, K. et al. 2005. Pathology parameters and adjuvant tamoxifen response in a randomised premenopausal breast cancer trial. *Journal of Clinical Pathology* 58(11), pp. 1135-1142.

Johnston, S. R. D. 1997. Acquired tamoxifen resistance in human breast cancer - Potential mechanisms and clinical implications. *Anti-Cancer Drugs* 8(10), pp. 911-930.

Jordan, S. J. et al. 2003. Risk factors for epithelial ovarian cancer. *Cancer Forum* 27(3), pp. 148-151.

Kato, S. et al. 2000. Molecular mechanism of a cross-talk between oestrogen and growth factor signalling pathways. *Genes to Cells* 5(8), pp. 593-601.

Katzenellenbogen, B. S. et al. 2000. Estrogen receptors: Selective ligands, partners, and distinctive pharmacology. *Recent Progress in Hormone Research* 55, pp. 163-195.

Keeling, J. W. et al. 2000. Oestrogen receptor alpha in female fetal, infant, and child mammary tissue. *Journal of Pathology* 191(4), pp. 449-451.

Keir, H. M. 1980. Fundamental aspects of oestrogens: intracellular receptors and gene activation. *Scottish Medical Journal* 25(2), pp. 135-140.

Kimmick, G. and Muss, H. B. 1995. Current status of endocrine therapy for metastatic breast cancer. *ONCOLOGY* 9(9).

Kiss, A. L. et al. 2006. Oestrogen-mediated tyrosine phosphorylation of caveolin-1 and its effect on the oestrogen receptor localisation: An in vivo study. *Molecular and Cellular Endocrinology* 245(1-2), pp. 128-137.

Knecht, D. A. and Luck, D. N. 1977. Synthesis and processing of ribosomal RNA by the uterus of the ovariectomised adult rat during early oestrogen action. *Nature* 266(5602), pp. 563-564.

Knoop, A. S. et al. 2001. Value of epidermal growth factor receptor, HER2, p53, and steroid receptors in predicting the efficacy of tamoxifen in high-risk postmenopausal breast cancer patients. *Journal of Clinical Oncology* 19(14), pp. 3376-3384.

Knowlden, J. M. et al. 1997. Use of reverse transcription-polymerase chain reaction methodology to detect estrogen-regulated gene expression in small breast cancer specimens. *Clinical Cancer Research* 3(11), pp. 2165-2172.

Knowlden, J. M. et al. 2000. A possible divergent role for the oestrogen receptor alpha and beta subtypes in clinical breast cancer. *International Journal of Cancer* 86(3), pp. 209-212.

Knowlden, J. M. et al. 2005. Insulin-like growth factor-I receptor signaling in tamoxifen-resistant breast cancer: A supporting role to the epidermal growth factor receptor. *Endocrinology* 146(11), pp. 4609-4618.

Knowlden, J. M. et al. 2003. Elevated levels of epidermal growth factor receptor/c-erbB2 heterodimers mediate an autocrine growth regulatory pathway in tamoxifen-resistant MCF-7 cells. *Endocrinology* 144(3), pp. 1032-1044.

Koga, M. et al. 1990. Differential effects of phorbol ester on epidermal growth factor receptors in estrogen receptor-positive and -negative breast cancer cell lines. *Cancer Research* 50(16), pp. 4849-4855.

Koohi, M. K. et al. 2005. Transcriptional activation of the oxytocin promoter by oestrogens uses a novel non-classical mechanism of oestrogen receptor action. *Journal of Neuroendocrinology* 17(4), pp. 197-207.

Krishna Murthy, A. S. et al. 1973. Biochemical studies on liver tumors of children. *Archives of Pathology and Laboratory Medicine* 96(1), pp. 48-52.

Kristensen, V. N. and Børresen-Dale, A. L. 2000. Molecular epidemiology of breast cancer: Genetic variation in steroid hormone metabolism. *Mutation Research - Reviews in Mutation Research* 462(2-3), pp. 323-333.

Krulik, M. 1994. Adjuvant therapy of early node negative breast cancer. *LES TRAITEMENTS ADJUVANTS DU CANCER DU SEIN PRECOCE SANS ATTEINTE GANGLIONNAIRE* 15(3), pp. 210-215.

Ku?ry, S. et al. 2002. Identification of SLC39A4, a gene involved in acrodermatitis enteropathica. *Nature Genetics* 31(3), pp. 239-240.

Kuiper, G. G. J. M. et al. 1997. Comparison of the ligand binding specificity and transcript tissue distribution of estrogen receptors and ? and ? *Endocrinology* 138(3), pp. 863-870.

Kushner, P. J. et al. 2000. Oestrogen receptor function at classical and alternative response elements. *Novartis Foundation Symposium* 230, pp. 20-32.

Larionov, A. A. et al. 2002. Local uptake and synthesis of oestrone in normal and malignant postmenopausal breast tissues. *Journal of Steroid Biochemistry and Molecular Biology* 81(1), pp. 57-64.

Lazier, C. B. and Haggarty, A. J. 1979. A high-affinity oestrogen-binding protein in cockerel liver cytosol. *Biochemical Journal* 180(2), pp. 347-353.

Leake, R. 1997. Prediction of hormone sensitivity - The receptor years and onwards. *Endocrine-Related Cancer* 4(3), pp. 289-296.

Leary, A. and Dowsett, M. 2006. Combination therapy with aromatase inhibitors: The next era of breast cancer treatment? *British Journal of Cancer* 95(6), pp. 661-666.

Legha, S. S. and Blumenschein, G. R. 1982. Systemic therapy of metastatic breast cancer: A review of the current trends. *Oncology* 39(3), pp. 140-145.

Leygue, E. et al. 1999. Oestrogen receptor-α variant mRNA expression in primary human breast tumours and matched lymph node metastases. *British Journal of Cancer* 79(5-6), pp. 978-983.

Liao, S. 1975. Cellular receptors and mechanisms of action of steroid hormones. *International Review of Cytology* Vol.41, pp. 87-172.

Liuzzi, J. P. et al. 2006. Zip14 (Slc39a14) mediates non-transferrin-bound iron uptake into cells. *Proceedings of the National Academy of Sciences of the United States of America* 103(37), pp. 13612-13617.

Liuzzi, J. P. and Cousins, R. J. 2004. Mammalian zinc transporters. *Annual Review of Nutrition* 24, pp. 151-172.

Liuzzi, J. P. et al. 2005. Interleukin-6 regulates the zinc transporter Zip14 in liver and contributes to the hypozincemia of the acute-phase response. *Proceedings of the National Academy of Sciences of the United States of America* 102(19), pp. 6843-6848.

Long, B. J. et al. 1998. The steroidal antiestrogen ICI 182,780 is an inhibitor of cellular aromatase activity. *Journal of Steroid Biochemistry and Molecular Biology* 67(4), pp. 293-304.

Love, R. R. and Philips, J. 2002. Oophorectomy for breast cancer: History revisited. *Journal of the National Cancer Institute* 94(19), pp. 1433-1434.

Lucisano, A. et al. 1984. Ovarian and peripheral plasma levels of progestogens, androgens and oestrogens in post-menopausal women. *Maturitas* 6(1), pp. 45-53.

Luttrell, L. M. et al. 1996. Role of c-Src tyrosine kinase in G protein-coupled receptor- and G subunit-mediated activation of mitogen-activated protein kinases. *Journal of Biological Chemistry* 271(32), pp. 19443-19450.

Macaskill, E. J. and Dixon, J. M. 2007. Neoadjuvant use of endocrine therapy in breast cancer. *Breast Journal* 13(3), pp. 243-250.

Macaulay, V. M. et al. 1994. Biological effects of stable overexpression of aromatase in human hormone-dependent breast cancer cells. *British Journal of Cancer* 69(1), pp. 77-83.

Mahfoudi, A. et al. 1995. Specific mutations in the estrogen receptor change the properties of antiestrogens to full agonists. *Proceedings of the National Academy of Sciences of the United States of America* 92(10), pp. 4206-4210.

Manning, D. L. et al. 1994. Oestrogen-regulated genes in breast cancer: Association of pLIV1 with lymph node involvement. *European Journal of Cancer Part A: General Topics* 30(5), pp. 675-678.

Marino, M. et al. 2006. Estrogen signaling multiple pathways to impact gene transcription. *Current Genomics* 7(8), pp. 497-508.

Marsigliante, S. et al. 1992. Transcriptionally active non-ligand binding oestrogen receptors in breast cancer. *Cancer Letters* 66(3), pp. 183-191.

Marsigliante, S. et al. 1995. Multiple isoforms of the oestrogen receptor in endometrial cancer. *Journal of Molecular Endocrinology* 14(3), pp. 365-374.

Marsigliante, S. et al. 1996. Human larynx expresses isoforms of the oestrogen receptor. *Cancer Letters* 99(2), pp. 191-196.

Mauriac, L. et al. 2003. Fulvestrant (Faslodex) versus anastrozole for the second-line treatment of advanced breast cancer in subgroups of postmenopausal women with visceral and non-visceral metastases: Combined results from two multicentre trials. *European Journal of Cancer* 39(9), pp. 1228-1233.

McClelland, R. A. et al. 2001. Enhanced epidermal growth factor receptor signaling in MCF7 breast cancer cells after long-term culture in the presence of the pure antiestrogen ICI 182,780 (Faslodex). *Endocrinology* 142(7), pp. 2776-2788.

McClelland, R. A. et al. 1998. Oestrogen-regulated genes in breast cancer: Association of pLIV1 with response to endocrine therapy. *British Journal of Cancer* 77(10), pp. 1653-1656.

McDonnell, D. P. et al. 1993. The mechanism of action of steroid hormones: A new twist to an old tale. *Journal of Clinical Pharmacology* 33(12), pp. 1165-1172.

McGuire, W. L. et al. 1975. Steroids and human breast cancer. *Journal of Steroid Biochemistry* 6(5), pp. 723-727.

McInerney, E. M. and Katzenellenbogen, B. S. 1996. Different regions in activation function-1 of the human estrogen receptor required for antiestrogen- and estradiol-dependent transcription activation. *Journal of Biological Chemistry* 271(39), pp. 24172-24178.

McKeage, K. et al. 2004. Fulvestrant: A review of its use in hormone receptor-positive metastatic breast cancer in postmenopausal women with disease progression following antiestrogen therapy. *Drugs* 64(6), pp. 633-648.

Michalides, R. et al. 1996. A clinicopathological study on overexpression of cyclin D1 and of p53 in a series of 248 patients with operable breast cancer. *British Journal of Cancer* 73(6), pp. 728-734.

Michlmayr, G. et al. 1981. Encouraging results with cytostatic therapy in metastasizing breast cancer. *ERFOLGE DER ZYTOSTATISCHEN THERAPIE BEIM METASTASIERENDEN MAMMAKARZINOM* 93(6), pp. 205-208.

Miller, W. R. 1987. Fundamental research leading to improved endocrine therapy for breast cancer. *Journal of Steroid Biochemistry* 27(1-3), pp. 477-485.

Miller, W. R. et al. 2005. Growth factor signalling in clinical breast cancer and its impact on response to conventional therapies: The Edinburgh experience. *Endocrine-Related Cancer* 12(SUPPL. 1).

Miller, W. R. et al. 1985. Growth of human breast cancer cells inhibited by a luteinizing hormone-releasing hormone agonist. *Nature* 313(5999), pp. 231-233.

Miller, W. R. and Sharpe, R. M. 1998. Environmental oestrogens and human reproductive cancers. *Endocrine-Related Cancer* 5(2), pp. 69-96.

Müller, G. and Frick, W. 1999. Signalling via caveolin: Involvement in the cross-talk between phosphoinositolglgcans and insulin. *Cellular and Molecular Life Sciences* 56(11-12), pp. 945-970.

Murphy, L. C. and Watson, P. H. 2006. Is oestrogen receptor-α a predictor of endocrine therapy responsiveness in human breast cancer? *Endocrine-Related Cancer* 13(2), pp. 327-334.

Nakamura, M. 1965. Cytological and histological studies on the pancreatic islets of a diabetic strain of the mouse. *Zeitschrift für Zellforschung und Mikroskopische Anatomie* 65(3), pp. 340-349.

Nakano, A. et al. 2003. Novel SLC39A4 mutations in acrodermatitis enteropathica. *Journal of Investigative Dermatology* 120(6), pp. 963-966.

Nardon, E. et al. 2003. Insulin-like growth factor system gene expression in women with type 2 diabetes and breast cancer. *Journal of Clinical Pathology* 56(8), pp. 599-604.

Nicholson, R. I. et al. 1993. Relationship between EGF-R, c-erbB-2 protein expression and Ki67 immunostaining in breast cancer and hormone sensitivity. *European Journal of Cancer Part A: General Topics* 29(7), pp. 1018-1023.

Nicholson, R. I. et al. 1994. Epidermal growth factor receptor expression in breast cancer: Association with response to endocrine therapy. *Breast Cancer Research and Treatment* 29(1), pp. 117-125.

Nicholson, S. et al. 1989. Expression of epidermal growth factor receptors associated with lack of response to endocrine therapy in recurrent breast cancer. *Lancet* 1(8631), pp. 182-185.

Nio, Y. et al. 1999. DNA synthesis in freshly separated human breast cancer cells assessed by tritiated thymidine incorporation assay: relationship to the long-term outcome of patients. *British Journal of Surgery* 86(11), pp. 1463-1469.

Nyholm, H. C. J. et al. 1993. Plasma oestrogens in postmenopausal women with endometrial cancer. *British Journal of Obstetrics and Gynaecology* 100(12), pp. 1115-1119.

Osborne, C. K. et al. 2004. Fulvestrant: An oestrogen receptor antagonist with a novel mechanism of action. *British Journal of Cancer* 90(SUPPL. 1).

Parker, M. G. 1990. Mechanisms of action of steroid receptors in the regulation of gene transcription. *Journal of Reproduction and Fertility* 88(2), pp. 717-720.

Parker, M. G. 1998. Transcriptional activation by oestrogen receptors. *Biochemical Society Symposium* 63, pp. 45-50.

Parr, C. et al. 2004. The Hepatocyte Growth Factor Regulatory Factors in Human Breast Cancer. *Clinical Cancer Research* 10(1 I), pp. 202-211.

Patterson, J. et al. 1982. The biology and physiology of 'nolvadex' (tamoxifen) in the treatment of breast cancer. *Breast Cancer Research and Treatment* 2(4), pp. 363-374.

Paulsen, I. T. and Saier Jr, M. H. 1997. A novel family of ubiquitous heavy metal ion transport proteins. *Journal of Membrane Biology* 156(2), pp. 99-103.

Pfeiffer, C. C. et al. 1974. Treatment of pyroluric schizophrenia (Malvaria) with large doses of pyridoxine and a dietary supplement of zinc. *Journal of Orthomolecular Psychiatry* 3(4), pp. 292-300.

Piquer, J. et al. 1991. Correlations of female steroid hormone receptors with histologic features in meningiomas. *Acta Neurochirurgica* 110(1-2), pp. 38-43.

Platet, N. et al. 2004. Estrogens and their receptors in breast cancer progression: A dual role in cancer proliferation and invasion. *Critical Reviews in Oncology/Hematology* 51(1), pp. 55-67.

Poortman, J. et al. 1983. Subcellular distribution of androgens and oestrogens in target tissue. *Journal of Steroid Biochemistry* 19(1 C), pp. 939-945.

Prat, J. et al. 2007. Endometrial carcinoma: Pathology and genetics. *Pathology* 39(1), pp. 72-87.

Pritchard, K. I. and Sutherland, D. J. A. 1989. The use of endocrine therapy. *Hematology/Oncology Clinics of North America* 3(4), pp. 765-805.

Puntervoll, P. et al. 2003. ELM server: A new resource for investigating short functional sites in modular eukaryotic proteins. *Nucleic Acids Research* 31(13), pp. 3625-3630.

Rechsteiner, M. and Rogers, S. W. 1996. PEST sequences and regulation by proteolysis. *Trends in Biochemical Sciences* 21(7), pp. 267-271.

Reed, M. J. and Purohit, A. 1996. The oestrogen status of postmenopausal women. *Journal of Clinical Ligand Assay* 19(1 SUPPL. 1), pp. 137-143.

Robertson, J. F. R. et al. 2007. Effects of fulvestrant 250 mg in premenopausal women with oestrogen receptor-positive primary breast cancer. *European Journal of Cancer* 43(1), pp. 64-70.

Rochefort, H. 1995. Oestrogen- and anti-oestrogen-regulated genes in human breast cancer. *Ciba Foundation symposium* 191, pp. 254-265; discussion 265.

Rochefort, H. and Borgna, J. L. 1981. Differences between oestrogen receptor activation by oestrogen and antioestrogen. *Nature* 292(5820), pp. 257-259.

Sabbah, M. et al. 1996. The 90 kDa heat-shock protein (hsp90) modulates the binding of the oestrogen receptor to its cognate DNA. *Biochemical Journal* 314(1), pp. 205-213.

Sainsbury, J. R. C. et al. 1987. Epidermal-growth-factor receptor status as predictor of early recurrence of and death from breast cancer. *Lancet* 1(8547), pp. 1398-1402.

Sainsbury, J. R. C. et al. 1985. Epidermal-growth-factor receptors and oestrogen receptors in human breast cancer. *Lancet* 1(8425), pp. 364-366.

Salmi, A. et al. 1998. The effect of intrauterine levonorgestrel use on the expression of c-JUN, oestrogen receptors, progesterone receptors and Ki-67 in human endometrium. *Molecular Human Reproduction* 4(12), pp. 1110-1115.

Samet, J. M. et al. 2003. Mechanisms of Zn^{2+}-induced signal initiation through the epidermal growth factor receptor. *Toxicology and Applied Pharmacology* 191(1), pp. 86-93.

Santen, R. J. et al. 1982. Aminoglutethimide as treatment of postmenopausal women with advanced breast carcinoma. *Annals of Internal Medicine* 96(1), pp. 94-101.

Sasano, H. and Ozaki, M. 1997. Aromatase expression and its localization in human breast cancer. *Journal of Steroid Biochemistry and Molecular Biology* 61(3-6), pp. 293-298.

Schally, A. V. et al. 1984. Potential use of analogs of luteinizing hormone-releasing hormones in the treatment of hormone-sensitive neoplasms. *Cancer Treatment Reports* 68(1), pp. 281-289.

Schaner, M. E. et al. 2003. Gene Expression Patterns in Ovarian Carcinomas. *Molecular Biology of the Cell* 14(11), pp. 4376-4386.

Schwabe, J. W. R. et al. 1993. DNA recognition by the oestrogen receptor: From solution to the crystal. *Structure* 1(3), pp. 187-204.

Scobie, G. A. et al. 2002. Human oestrogen receptors: differential expression of ERalpha and beta and the identification of ERbeta variants. *Steroids* 67(12), pp. 985-992.

Shibata, H. et al. 1997. Role of Co-activators and Co-repressors in the Mechanism of Steroid/Thyroid Receptor Action. *Recent Progress in Hormone Research* 52, pp. 141-164.

Shin, I. et al. 2006. ErbB receptor signaling and therapeutic resistance to aromatase inhibitors. *Clinical Cancer Research* 12(3 II).

Skliris, G. P. et al. 2006. Expression of oestrogen receptor-α in oestrogen receptor-α negative human breast tumours. *British Journal of Cancer* 95(5), pp. 616-626.

Sluyser, M. and Kassenaar, A. A. H. 1975. Mechanism of androgen action at the cellular level. *PHARMACOL.THER.SER.B.* 1(2), pp. 179-188.

Smith, R. G. and Schwartz, R. J. 1979. Isolation and purification of a hen nuclear oestrogen receptor and its effects on transcription of chick chromatin. *Biochemical Journal* 184(2), pp. 331-343.

Song, M. R. et al. 1998. Differential modulation of transcriptional activity of oestrogen receptors by direct protein-protein interactions with retinoid receptors. *Biochemical Journal* 336(3), pp. 711-717.

Sonobe, H. et al. 1998. Malignant granular cell tumor: Report of a case and review of the literature. *Pathology Research and Practice* 194(7), pp. 507-516.

Sormunen, R. T. et al. 1999. Immunolocalization of the fodrin, E-cadherin, and β-catenin adhesion complex in infiltrating ductal carcinoma of the breast - Comparison with an in vitro model. *Journal of Pathology* 187(4), pp. 416-423.

Spies, C. M. et al. 2006. Membrane glucocorticoid receptors are down regulated by glucocorticoids in patients with systemic lupus erythematosus and use a caveolin-1-independent expression pathway. *Annals of the Rheumatic Diseases* 65(9), pp. 1139-1146.

Strausberg, R. L. et al. 2002. Generation and initial analysis of more than 15,000 full-length human and mouse cDNA sequences. *Proceedings of the National Academy of Sciences of the United States of America* 99(26), pp. 16899-16903.

Suh, S. W. et al. 2000. Evidence that synaptically-released zinc contributes to neuronal injury after traumatic brain injury. *Brain Research* 852(2), pp. 268-273.

Sutherland, R. L. et al. 1980. High-affinity anti-oestrogen binding site distinct from the oestrogen receptor. *Nature* 288(5788), pp. 273-275.

Tan, S. H. and Wolff, A. C. 2007. Luteinizing hormone-releasing hormone agonists in premenopausal hormone receptor-positive breast cancer. *Clinical Breast Cancer* 7(6), pp. 455-464.

Tanaka, N. et al. 2000. The receptor for advanced glycation end products is induced by the glycation products themselves and tumor necrosis factor-α through nuclear factor-αB, and by 17α-Estradiol through sp-1 in human vascular endothelial cells. *Journal of Biological Chemistry* 275(33), pp. 25781-25790.

Taylor, K. M. et al. 2003. Structure-function analysis of LIV-1, the breast cancer-associated protein that belongs to a new subfamily of zinc transporters. *Biochemical Journal* 375(1), pp. 51-59.

Taylor, K. M. et al. 2004. Structure-function analysis of HKE4, a member of the new LIV-1 subfamily of zinc transporters. *Biochemical Journal* 377(1), pp. 131-139.

Taylor, K. M. et al. 2005. Structure-function analysis of a novel member of the LIV-1 subfamily of zinc transporters, ZIP14. *FEBS Letters* 579(2), pp. 427-432.

Taylor, K. M. and Nicholson, R. I. 2003. The LZT proteins; The LIV-1 subfamily of zinc transporters. *Biochimica et Biophysica Acta - Biomembranes* 1611(1-2), pp. 16-30.

Tominaga, K. et al. 2005. SLC39A14, a LZT protein, is induced in adipogenesis and transports zinc. *FEBS Journal* 272(7), pp. 1590-1599.

Umekita, Y. et al. 1992. Immunohistochemical studies on oncogene products (EGF-R, c-erbB-2) and growth factors (EGF, TGF-α) in human breast cancer: Their relationship to oestrogen receptor status, histological grade, mitotic index and nodal status. *Virchows Archiv - A Pathological Anatomy and Histopathology* 420(4), pp. 345-351.

Valentine, R. A. et al. 2007. ZnT5 variant B is a bidirectional zinc transporter and mediates zinc uptake in human intestinal Caco-2 cells. *The Journal of biological chemistry* 282(19), pp. 14389-14393.

Wang, F. et al. 2004. The mammalian Zip5 protein is a zinc transporter that localizes to the basolateral surface of polarized cells. *Journal of Biological Chemistry* 279(49), pp. 51433-51441.

Wilkinson, M. L. et al. 1983. A new sex-steroid binding protein in foetal liver. *IRCS Medical Science* 11(12), pp. 1123-1124.

Wilson, D. W. et al. 1984. Quantitative aspects of the E2 receptor assay for human breast tumour cytosol using dextran-coated charcoal. *British Journal of Cancer* 50(4), pp. 493-499.

Wu, C. W. et al. 1977. Subunit location of the intrinsic divalent metal ions in RNA polymerase from Escherichia coli. *Biochemistry* 16(25), pp. 5449-5454.

Wu, W. et al. 2002. Src-dependent phosphorylation of the epidermal growth factor receptor on tyrosine 845 is required for zinc-induced Ras activation. *Journal of Biological Chemistry* 277(27), pp. 24252-24257.

Zidan, J. et al. 2002. Treating relapsed epithelial ovarian cancer with luteinizing hormone-releasing agonist (Goserelin) after failure of chemotherapy. *Israel Medical Association Journal* 4(8), pp. 597-599.